Studies of Fluorescence Detection of Nucleic Acid Sequences.

A thesis submitted to the University of Manchester
for the degree of Doctor of Philosophy in the Faculty of Medicine,
Dentistry, Nursing and Pharmacy.

2003

Hannah Elizabeth Savage
B.Sc (Hons)

School of Pharmacy and Pharmaceutical Sciences

Table of Contents

Figures

Tables

Abstract

Studies on the human genome have yielded much information about the underlying causes of genetic diseases. Highly sensitive, specific assays are thus required to analyse patient-derived genetic samples. One such technique to improve the sensitivity and specificity of hybridisation assays is the use of split-probe oligo systems. In these systems two probe oligos bind in a contiguously to the target sequence to be detected, in doing so they may bring together groups, which can interact causing a detectable signal, in the present case fluorescence. This study describes various novel excimer split-probes and the first examples of exciplex split-probe fluorescence detectors. The excimer and exciplex split-probe systems were able to signal the presence of their complementary DNA or RNA target by the appearance of a broad excimer/ exciplex fluorescence band. This signal was greatly red-shifted from the fluorescence band seen for the individual probe oligos, and thus had a very small background. Excimer/ exciplex emission seen from the split-probe systems was found to be greatest in the presence of specific solvent additives, known to cause structural changes in DNA duplexes. This, along with results from studies using an RNA target complementary to the DNA exci-probes, and LNA probes complementary to a DNA target suggested that structural properties of the tandem duplex formed by the split-probes and target may affect excimer/ exciplex fluorescence.

Split-probe systems were tested using two linker types to attach the exciplex partners to the probe oligos, one a short linker of several methylene groups and the other a longer peptide linker of five amino acids. Both types of system resulted in excimer/ exciplex emission showing that there is scope for the use of different linkers in the split-probe systems.

Split-probe exciplex systems were found to emit in the presence of betaine and sulfolane additives, used in PCR to increase yield and specificity, and so may lend themselves to real-time monitoring of PCR reactions. In addition, the excimer and the exciplex split-probe systems were sensitive to single nucleotide polymorphisms, giving no excimer/ exciplex signal in the presence of a SNP located at a particular position along the target. Therefore, with careful probe design split-probe systems sensitive to SNPs could be used in routine genetic analysis. This thesis also shows it is possible to incorporate LNA technology into split-probe exciplex systems giving probes with greater affinity to target sequences, further increasing specificity and sensitivity.

Abbreviations

A	Adenosine
Ala	Alanine
AUC	Area under the curve
Boc	t-Butyloxycarbonyl
bp	Base pair(s)
C	Cytidine
CD	Circular Dichroism
$CDCl_2$	D_1-chloroform
D2O	Deuterium oxide
dA	Deoxyadenosine
dC	Deoxycytidine
DCM	Dichloromethane
ddNT	Dideoxynucleotides
DEA	Diethylaniline
DEPC	Diethylpyrocarbonate
dG	Deoxyguanosine
DMAP	Dimethylaminopyridine
DMF	Dimethylformamide
DMSO	Dimethyl sulfoxide
dT	Deoxthymidine
dUTP	Deoxyuridine triphosphate
DVT	Deep vein thrombosis
FRET	Fluorescence resonance energy transfer
G	Guanosine
Gly	Glycine
I_E/I_M	Ratio of Excimer/exciplex fluorescence to monomer (LES) Fluorescence.
HPLC	High performance liquid chromatography
HRP	Horseradish peroxidase
LES	Localyl excited state
LNA	Locked nucleic acid
Me_4Si	Tetramethylsilane
MeOD	D_4-methanol
mRNA	Messenger RNA
NMR	Nuclear magnetic resonance
PCR	Polymerase chain reaction
SNP	Single nucleotide polymorphism
ssLNA	Single stranded locked nucleic acid
T	Thymidine
tBu	*Tert*-butyl

TFA	Trifluoroacetic acid
TFE	2,2,2-Trifluoroethanol
TLC	Thin layer chromatography
Tm	Melting temperature
Tris	Tris(hydroxymethyl)methylamine
UV	Ultra violet
Nap	Naphthalene

Declaration

No portion of this work referred to in this thesis has been submitted in support of an application for another degree or qualification of this or any other university or other institute of learning.

Copyright Declaration

Acknowledgements

I would firstly like to thank my supervisor, Prof. K. T. Douglas, for his invaluable help and guidance throughout the course of my thesis.

I am also very grateful to Dr. Elena Bichenkova for all her help and advice on the synthesis, fluorescence studies and interpretation of results. I would also like to thank Dr. Ali Sardarian for the modification of the exci-partners for attachment to oligonucleotides and for his patient help with chemical synthesis.

I would like to thank everyone else who has help me along the way, including all the members of the group past and present. I would particularly like to thank Candelaria Rogert for helping me out with the modification and HPLC of the oligonucleotides, and for letting me use her oligos when my supplies were running low. I also wish to say a special thank you to Dr. Virginia McNally for helping me to keep my sanity (just), and to all of my friends back home for listening to me and putting up with my moaning.

And last, but definitely not least, I would like to thank my Mum and Dad for their constant support.

To Mum and Dad

1. Introduction.

1 Introduction.

1.1 Why is the detection of DNA sequences important?

Now that sequencing of the human genome is almost finished, with completion expected at the end of 2003 [1], much information on the underlying genetic causes of many inherited and acquired diseases has been made available. Many genetic diseases have been found to be the result of a change of a single base pair. These alterations, termed single nucleotide polymorphisms (SNP), may cause changes in the amino acid sequence of important proteins. Some SNPs on the other hand may not cause a change in protein expression, but may be close on the chromosome to other unknown deleterious mutations, and can thus serve as genetic markers for these.

One example of a disease-causing SNP is the G-A transition at position 20210 in the 3'-untranslated region of the prothrombin or Factor II gene. Prothrombin is the precursor of the serine protease thrombin, which catalyses the last reaction in the blood clotting cascade, converting fibrinogen to fibrin [2]. Prothrombin is key in the balance between pro-coagulation and anti-coagulation [3]. The presence of the mutation causes an upregulation of 3'-end processing leading to increased mRNA. This in turn leads to an increase in protein synthesis and prothrombin plasma concentration [4]. The mutation occurs in only 2.3% of the Caucasian population, but in 6% of patients with deep vein thrombosis (DVT) and 18% of those patients with a family history of DVT. The presence of the mutation was also found to increase the risk of myocardial infarction in young women four-fold: this risk was elevated in the presence of other risk factors (for example, smoking, hypertension, diabetes or obesity). Therefore, methods sensitive to single base pair mutations for the rapid screening of patients' samples to detect these and other disease-causing mutations will be important in their prevention and treatment. Hybridisation analysis, where a short probe oligonucleotide (15-20 base pairs) bearing some kind of label is used to identify a DNA or RNA sequence by hybridising to complementary base pairs [5], is one of the most powerful tools for the detection of genetic sequences.

1.2 Hybridisation

In order to detect specific sequences in a complex genome such as that of humans (the haploid genome contains 3×10^9 base pairs) such methods of hybridisation analysis must be highly sensitive and selective. The probe oligo used must be able to discriminate

between the desired sequence and all other sequences, which may differ from the target by only one base pair, especially in the detection of SNPs. A probe of 20 base pairs has a high probability of occurring only once in the human genome, and a probe of this length will be very selective for the desired target. Shorter sequences have a possibility of occurring more than once in the genome and could thereby produce false positive results.

Once a suitable probe sequence has been chosen, a label must be applied to this so that hybridisation to the target can be detected. The type of label chosen determines the sensitivity of the assay. Therefore, the label should be, amongst other criteria set out below, detectable at a low concentration and give low background signals in the absence of the target.

1.3 Labelling strategies.

Other criteria that make a label suitable for use in DNA analysis are:

- The label should be easily attached to DNA
- It should be stable during storage and under hybridisation conditions
- The presence of the label should not interfere with hybridisation
- The signal should ideally change upon hybridisation so that separation of bound and unbound probes is unnecessary.
- The label and method of detection should be compatible with automated analysis so that high throughput screening of a large number of samples can be achieved.

Although no label fulfils all these criteria, the many suitable labelling strategies available can be divided into direct and indirect labels.

1.3.1 Indirect labels.

Indirect labels are not attached covalently to the DNA probe. The simplest method uses a specific antibody that binds to duplex DNA; the DNA-antibody complex can then be detected using a second labelled antibody, which binds to the first. Alternatively, a hapten can be attached to the nucleic acid probe; the hapten can then be detected using a specific, labelled binding protein. One such widely used example of this is the very strong interaction between biotin and the egg white protein avidin, or its bacterial relative streptavidin from *Streptomyces*. Modifying a biologically active molecule (e.g. an oligonucleotide) with biotin often causes little change in the biological or physicochemical properties of either molecule [6-8]. Biotin can be incorporated into a growing DNA chain by the use of a biotinylated nucleotide phosphate, commonly dUTP. Alternatively, biotin can

be introduced at the 5' or the 3' termini [9]. Reporter groups, for example fluorophores, can be attached to avidin without affecting its affinity for biotin. In typical assays using this type of label, such as that shown in Figure 1.1, the biotin-carrying oligo (H) is allowed to bind to the target molecule (M) (e.g. the complementary oligonucleotide), which is usually immobilised on a solid support. The complex is then incubated with the labelled avidin molecule and the signal is allowed to develop. Anti-avidin antibodies possessing a fluorophore and a biotin arm that can bind to avidin can additionally be used. This can be repeated several times to give a sandwich of detection layers (Figure 1.1), thereby amplifying the signal [10].

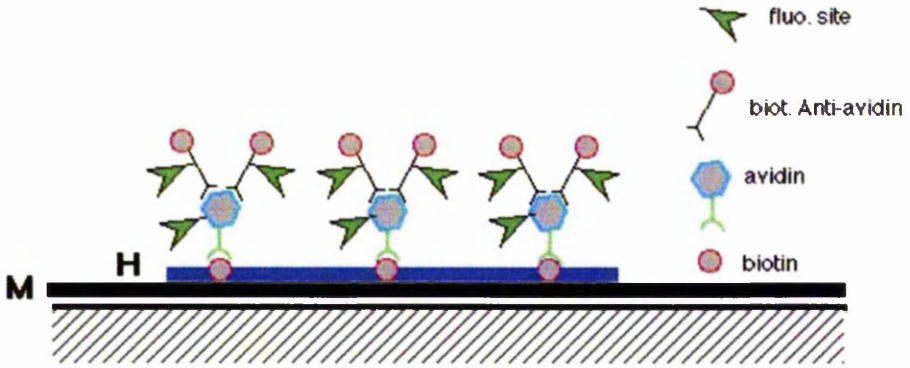

Figure 1.1: Schematic diagram of how a sandwich of detection layers can be built up for a biotin: avidin-based hybridisation assay.

The assay can alternatively be performed in solution, but the final complex must still be captured on to a solid phase coated with an anti-avidin tag molecule, which binds to avidin without disrupting the complex.

Disadvantages of using indirect labelling methods include the extra steps of incubation with labelled avidin or antibody, and the removal of these unbound conjugates. In many of these assays immobilisation of the target or the probe is necessary, requiring extra procedures. In these cases non-specific binding of the labelled conjugate to the solid support can give rise to high background signals [11].

1.3.2 Direct labels.

Direct labels are attached directly *via* a covalent bond to the oligonucleotide probe. The first direct label was based on the radioactive (^{32}P) isotope attached as the terminal 5'-phosphate, but it had a very short shelf life due to the short half life of ^{32}P (14.2 days). This, along with the possible health hazards associated with the preparation and use of the

probes and the problems of disposal of radioactive waste, has limited their routine use and commercialisation [11].

Other direct labels include enzyme labels, where enzymes such as horseradish peroxidase or alkaline phosphatase, are attached covalently to the probe oligo. After hybridisation of the probe to the target the label is detected by the addition of a chromogenic substrate, which reacts with the enzyme to give a coloured product [12].

Alternatively a chemiluminescent compound, for example isoluminol or acridium, can be attached to the oligo probe. Such compounds emit light after chemical reactions or processing by enzymes such as horseradish peroxidase and alkaline phosphatase, due to their chemi-excitation during reaction: they then emit this excess energy as chemiluminescence [13].

Many fluorescent dye molecules are commercially available and can be attached at various positions to the oligo probe. Some such fluorescent labelling strategies will be described in this introduction. Unlike other types of label that give signals which are independent of the hybridisation state of the probe, the fluorescence of some dye molecules depends on their environment. This means that the fluorescent signal may be modulated on duplex formation. Therefore no separation of bound and unbound probes is required, however, this also means that there is usually a background fluorescence.

Labels that are independent of the hybridisation state require hybridisation strategies that allow separation of bound and unbound probe. This is usually achieved by attaching the probe or target sequence to a solid support so that unbound species can be washed away. These assays are termed heterogenous assays.

1.4 Heterogenous assays

Many current heterogeneous hybridisation techniques use a solid support, usually a membrane of nitrocellulose or nylon, to immobilise the DNA or RNA strand containing the target sequence. These sequences are then exposed to their complementary probes and hybridisation is allowed. The membrane is then washed to remove unbound probe, as signals generated from the probes are independent of their hybridisation state. The amount of probe bound is then measured by detection of the label (Figure 1.2) [5;14]. One such assay developed using a locked nucleic acid (LNA) probe will now be described as LNA-based probes are used later in the study described in this thesis.

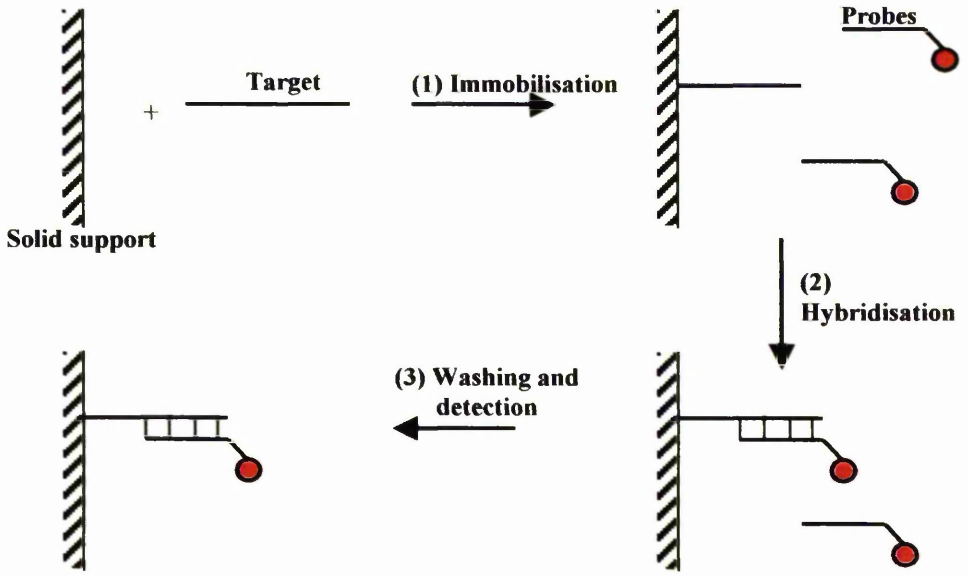

Figure 1.2: Steps required in heterogenous assays using a solid support. (1) Immobilisation of target to the solid support, (2) hybridisation of the probes to the target, (3) washing to remove unbound probes and detection of bound probes.

1.4.1 Heterogenous assays using Locked Nucleic Acid (LNA) based probes.

Locked nucleic acids (LNA) are nucleic acid mimics capable of binding strongly to DNA or RNA. LNA monomers contain a 2'-O, 4'-C-methylene linked bicyclic ribofuranyl nucleoside (Figure 1.3) locked into a C3'-endo (Figure 1.4) conformation (N-type) normally seen in RNA [15]. They follow Watson-Crick base-pairing with LNA: LNA hybrids showing the most stable Watson-Crick base-pairing system yet developed [16].

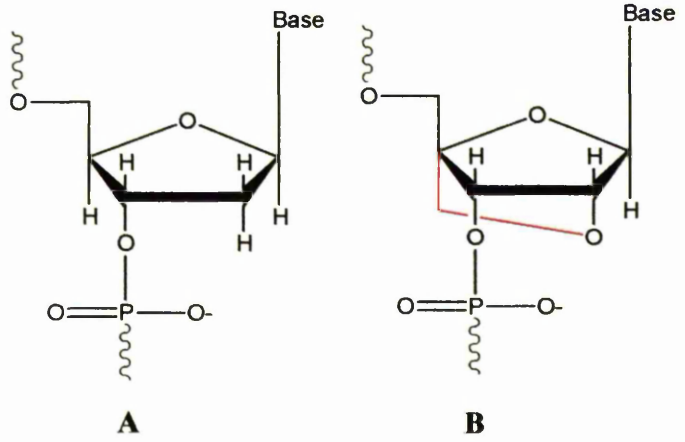

Figure 1.3: (A) DNA nucleotide. (B) LNA nucleotide with the 2'-O, 4'-C-methylene link shown in red.

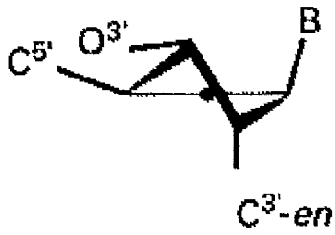

Figure 1.4: Diagrammatic representation of the C3'-endo (N-type) conformation of the sugar ring adopted by LNA monomers [17]. The 2'-O, 4'-C-methylene link is not shown for simplicity.

The incorporation of LNA monomers into DNA increases the melting temperature (T_m) by +3 to +9 °C per ring modification. The LNA monomers, locked in the N-type conformation, have been shown to affect the conformation of their neighbouring deoxyribonucleotides in single-stranded LNA. From NMR studies nucleotides flanking the LNA monomer were seen to have equal populations of N- and S-type conformers. A nucleotide between two LNA monomers is found predominantly in the N-type conformation [18]. However, these conformational effects are very local and in LNA: DNA duplexes the nucleotides base-paired to the LNA nucleotides remain in the S-type conformation commonly seen in DNA. The greater affinity of ssLNA toward complementary DNA and RNA is possibly a result of the locked nucleotides suppressing backbone motions and organising the backbone of the ssLNA. The effect of this is to pre-organise ssDNA for duplex formation. This would lead to a smaller change in backbone entropy (ΔS_r) on duplex formation [18]. Improved nucleobase stacking is thought to also explain the stabilising effect of LNA. The introduction of an abasic LNA monomer into DNA resulted in a value of T_m identical to the same sequence with an abasic DNA monomer in place of the LNA. However, the presence of a normal LNA monomer vastly increased the T_m relative to the corresponding DNA sequence [15]. These properties and others, including biological stability towards nucleases and the lack of detectable toxicity [16] make LNA very attractive in biological research for both antisense drug development and in the field of DNA diagnostics.

Several LNA-based capture probes have so far been developed. One of these includes an assay for genotyping the $ApoB_{R3500Q}$ mutation. This autosomal dominant disorder, caused by a single nucleotide mutation coding for amino acid 3500 (arg to gln), results in a predisposition to coronary heart disease in affected patients. As cholesterol concentrations in the serum of these individuals is in the normal range, the only reliable method for susceptibility is genotyping. [19]. An assay has been developed using allele-

specific LNA capture probes complementary to the site of the ApoB SNP (Figure 1.5). These probes were immobilised onto a solid support and biotinylated fragments of the patient's DNA, amplified by PCR, allowed to hybridise to the capture probes [19]. Binding was visualised using horseradish peroxidase (HRP)-conjugated streptavidin and a chromogen, ortho-phenylenediamine. This chromogen is oxidised in the presence of HRP to give a water-soluble brown product with an absorption maximum of 402 nm [12]. The assay was found to be very specific, giving no detectable signal in the presence of a single base-mismatched target, and was in 100% concordance with DNA sequencing techniques.

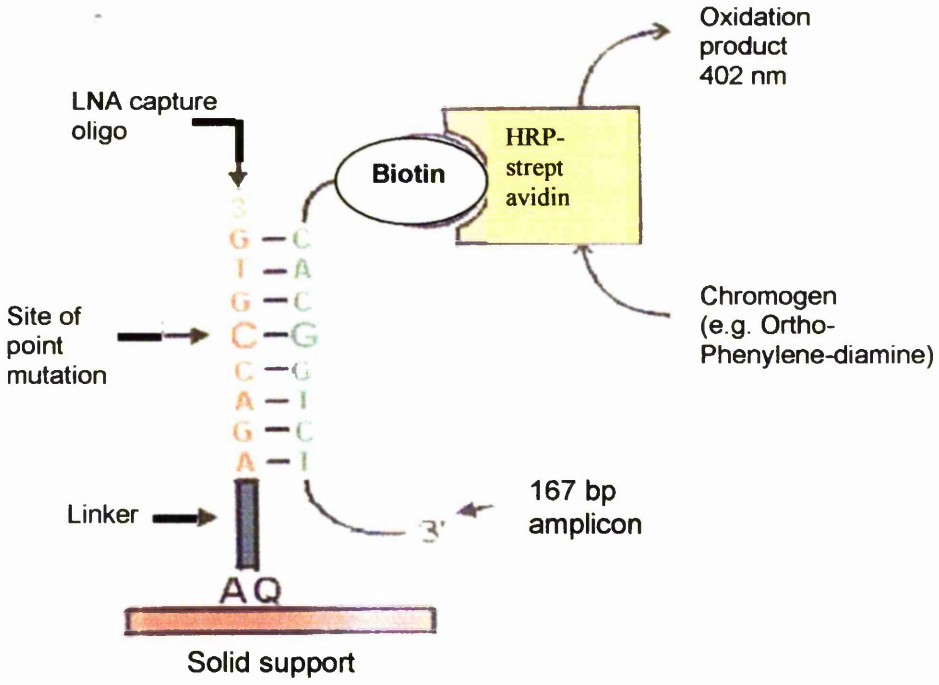

Figure 1.5: Diagram of the use of LNA capture probes to detect PCR amplicons. Denatured biotinylated amplicons are hybridised in wells containing wild type or mutant capture probes. Amplicons only hybridise to perfectly matching LNA capture probes. Bound target is complexed with Horseradish Peroxidase (HRP) conjugated to streptavidin and visualised by reaction with a chromogen.

A similar method, again using allele-specific LNA capture probes, has been used for the detection of a mutation in the gene coding for coagulation factor V (Leiden mutation), which involves a G-A transition at position 1691 of the factor V gene. Carriers have an increased risk of venous thromboembolism, with heterozygotes having a 3.5- to 7-fold increased risk and homozygotes an 80-fold higher risk than those without the mutation. Using the LNA capture probes much smaller probes could be used than with strictly DNA-based probes. The use of shorter probes improves their mismatch readout potential. This

technique was shown to distinguish well between complementary and single base mismatch sequences and was in complete agreement with DNA sequencing [20].

The problem with these and other heterogenous assays is that the immobilisation and washing processes introduce extra steps, which can be time-consuming, laborious and difficult to autonomate. This, along with background signals generated from non-specific binding of probes to the solid support, makes these assays undesirable and expensive for routine use in clinical situations. Therefore, simpler assays are needed that eliminate some of these extra steps, for example assays in which hybridisation and detection take place in one phase without the need for separation. Such homogeneous assays are now briefly covered.

1.5 Homogeneous assays.

The signal generated by the label used in homogenous assays must depend on the hybridisation state of the probe oligo. Ideally the signal from the label should change or become detectable on hybridisation of the probes to the target. Certain fluorescent labels are suitable for this purpose as their fluorescence can depend on the environmental changes brought about by hybridisation, resulting in a change in one or more fluorescent properties such as quantum yield, lifetime or energy transfer.

1.6 Probes based on energy transfer.

1.6.1 Energy transfer.

Electronic energy transfer quenches emission of a fluorescent molecule M by transfer of excitation energy to a quenching moiety, Q. The fluorescence of Q may increase if Q is a fluorescent molecule, or the transferred energy may be dissipated in other ways. The simplest energy transfer process is radiative energy transfer, which involves the emission of a photon from M* which is reabsorbed by Q. For this type of transfer to occur the emission spectrum of M must overlap with the excitation spectrum of Q. This mechanism does not involve any interaction between M and Q. On the other hand, non-radiative energy transfer requires interaction between M and Q. Electron energy transfer involves the transfer of the excited electron to the lowest unoccupied molecular orbital of the quencher with simultaneous transfer of an electron from the highest occupied molecular orbital of Q into the corresponding molecular orbital of M. This mechanism requires that M and Q are close enough so that overlap of the electron orbitals can take place (6-20Å) [21] Coulombic energy transfer, also known as fluorescence resonance energy

transfer (FRET), occurs over longer distances (20-100 Å) by long-range dipole-dipole coupling. For efficient energy transfer the donor and acceptor must be in resonance that is the fluorescence spectrum of the donor must overlap with the absorption spectrum of the acceptor [5]. Energy transfer leads to a decrease in fluorescence lifetime of the donor due to the additional decay pathway to the acceptor. The rate of energy transfer (K_{ET}) depends on the distance between the centres of the two fluorophores, following the Förster equation **(1)** [22].

$$K_{ET} = 1/\tau_D \, (R_0/R)^6 \qquad (1)$$

where τ_D is the fluorescence lifetime of the donor in the absence of the acceptor, R_0 the critical transfer distance at which the energy transfer rate is equal to the intrinsic rate of decay, and R is the distance between the centres of the fluorophores [23]. In addition the transition dipoles of the donor and the acceptor must be oriented favourably to one another, or have a certain degree of rapid rotational freedom. In this way, by using two suitable fluorophores which bind to a macromolecule, FRET can be used as a spectroscopic ruler over the distance range 10-60 Å [22]. Some examples of fluorescent probes for hybridisation-based analyses, which use the properties of energy transfer, Molecular Beacons, Scorpions and the Taqman probes, are described below.

1.6.2 Molecular Beacons.

Molecular Beacons, for solution-based fluorescent assays consist of a single-stranded nucleic acid with a stem and loop structure. The loop is complementary to the target (Figure 1.6). The arm sequences on either side of the loop sequence are unrelated to the target sequence and complementary to each other, so that they are able to form a stem. A fluorescent moiety is attached to one arm and a quenching moiety to the other. In the absence of the target stem formation keeps these two molecules together, so that the fluorescence of the fluorophore is quenched (FRET). The energy transferred from the fluorophore to the quencher is dissipated as heat, not fluorescence. On encountering the target, the probe preferentially hybridises to it due to the formation of a longer, more stable sequence. Therefore, the probe undergoes a spontaneous conformational change, which forces the fluorescent and the quenching moieties apart (see Figure 1.6). The fluorophore is no longer quenched, and fluorescence increases by approximately 25-fold [24].

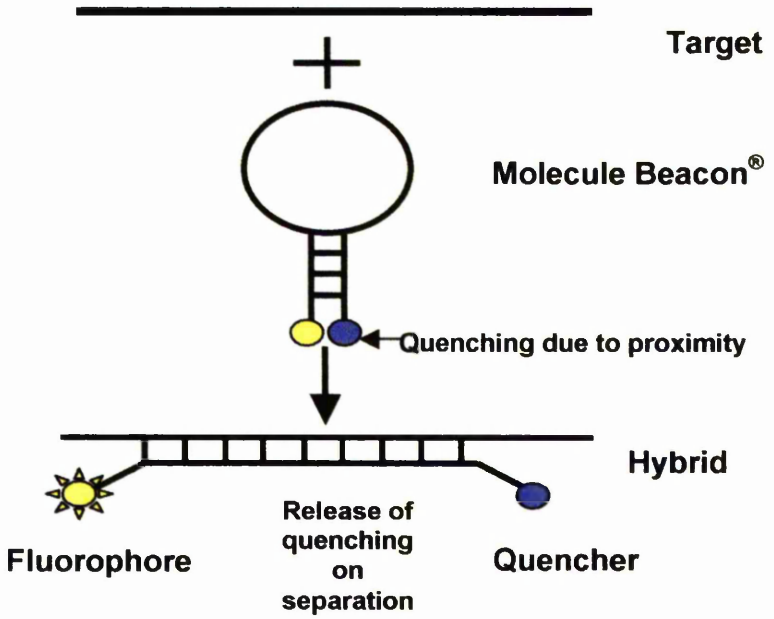

Figure 1.6: Schematic representation of the mode of action of Molecular Beacons®.

Molecular Beacon technology has been improved by the development of wavelength-shifting Molecular Beacons. These are based on the structure of Figure 1.6, but with one arm bearing two fluorophores, one a harvester and the other an emitter, which are separated by several nucleotide bases. When the probe is in the stem-loop conformation the fluorescence of the harvester, which absorbs optimally at the wavelength range available, is quenched by the quencher. On binding to the target the harvester and the quencher are separated and energy absorbed by the harvester is channelled by FRET to the emitter. This then fluoresces at a longer wavelength. In doing so the background fluorescence from any unquenched harvester is decreased. This approach overcomes the limitation of conventional Molecular Beacons where optimal emission is only a few nanometers longer than the excitation wavelength so that a portion of the excitation light can reach the detector, limiting sensitivity [25].

Smart Probes [26] are similar to Molecular Beacons, but have only one dye molecule (a rhodamine or oxamine derivative) attached to an arm sequence of cytosines (Figure 1.7). In the absence of the target the probe forms a stem and loop structure and guanosine bases of the complementary arm sequence quench the fluorescence of this dye molecule, by photo-induced electron-transfer from ground-state guanosine to excited dye. This occurs preferentially from guanosine bases, as the oxidation potential of guanosine is lower than those of the other bases. On hybridisation of the probe to target the dye is separated from the guanosine arm and fluorescence increases six-fold. This technique reduces the

background present for Molecular Beacons that may arise from inefficient labelling where only the dye molecule is incorporated, or due to photo-destruction of the quencher reducing its ability to quench the dye.

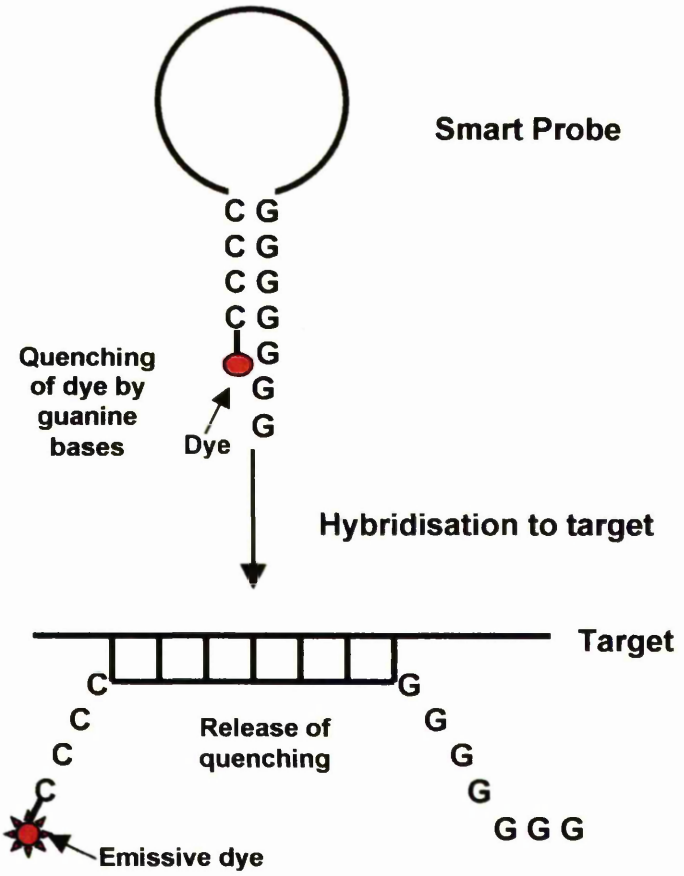

Figure 1.7: Schematic representation of the mode of action of Smart Probes.

1.6.3 Scorpions

Scorpion probes are similar to Molecular Beacons, having a loop complementary to the target sequence and a stem holding a fluorophore and a quencher in close proximity so that fluorescence is quenched in the absence of the target. In addition to the quencher the 3'-end is attached to a PCR primer *via* a linker that prevents 5'-extension. When the primer has been extended by PCR, after denaturation, the loop strand preferentially binds to the target. This separates the fluorophore and quencher, thus producing a fluorescent signal (Figure 1.8) [27].

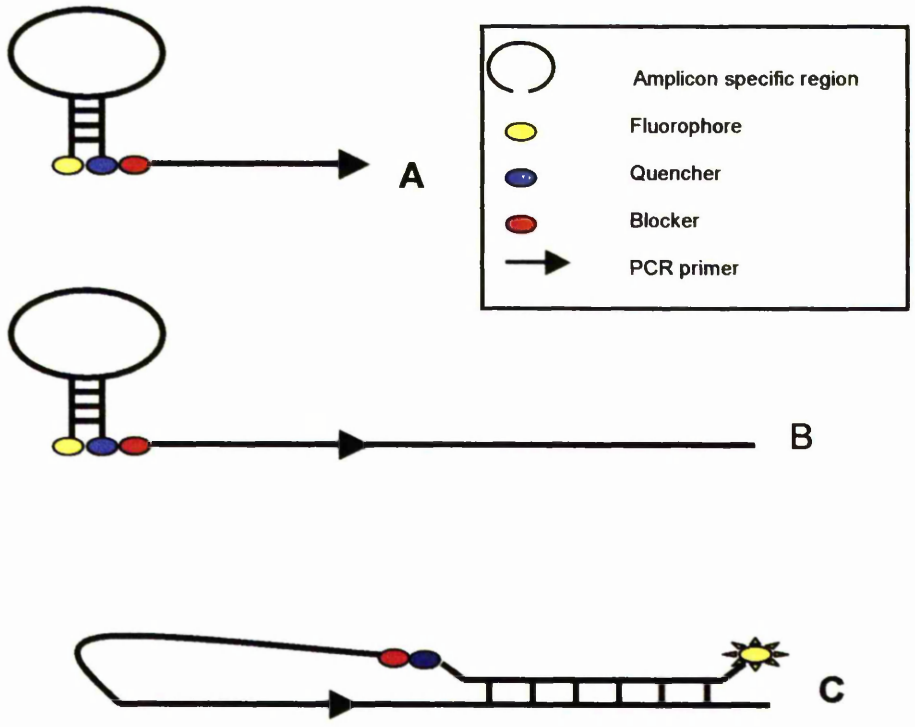

Figure 1.8: Detection of PCR products with Scorpions. (A) Scorpion primer carrying a 5'-extension comprising a probe, a pair of self-complementary stem sequences and a fluorophore-quencher pair. The blocker group prevents 5'-extension. (B) After PCR extension from the primer, the target region is attached to the same strand as the probe. (C) Following a second round of denaturation and annealing, when the probe hybridises to target, the fluorophore is no longer in close contact with the quencher and so fluorescence is detected.

1.6.4 Taqman probes.

The Taqman probe (Figure 1.9), first described by Holland *et al.* [28], was developed for use in PCR to detect product formation, and uses the inherent 5', 3'- exonuclease activity of the DNA polymerase from *Thermus aquaticus* (Taq polymerase) used in PCR primer extension. This DNA polymerase in addition to its polymerase activity also cleaves 5'-terminal nucleotides in double-stranded DNA to release mono- and oligo-nucleotides. The probe oligo is designed to bind to a specific target sequence of the template DNA, and is labelled with ^{32}P on its 5'-terminus. During amplification of the template, resulting in primer extension, the 5'-3' exonuclease activity of Taq polymerase degrades the probe, releasing the label on smaller fragments, which are easily differentiated from the undegraded probe. In this way simultaneous target amplification and generation of target specific signal is achieved.

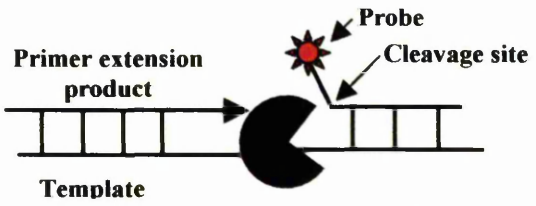

Figure 1.9: Diagramatic representation of the 5'-3' exonuclease cleavage of a 5'-labelled oligonucleotide Taqman probe to generate labelled fragments [28].

The Taqman probe has been improved by the use of a dual-labelled fluorogenic probe [29], with a reporter dye attached to the 5'-terminus and a quencher attached to the 3'-terminus. When the probe is intact, fluorescence of the dye is quenched by the quencher. After binding to the target sequence, the probe is degraded by the Taq polymerase during primer extension, which releases dye from the quencher resulting in an increase in fluorescence. This system can be used in conjunction with a sequence detector allowing the detection of a fluorescent signal continuously so reactions can be monitored in real-time.

As these probes are linear, with no secondary structure, they have a fairly high background signal because of inefficient quenching due to the distance between quencher and dye. Therefore, a further improvement was proposed by Kong *et al.* [30] by combining the Taqman probe with Molecular Beacons. The probe consists of a stem and loop structure, as used for Molecular Beacons, that brings dye and quencher together, making quenching more efficient, thereby reducing background fluorescence. The loop and the 5'-arm are complementary to the target sequence of the template. On hybridisation not only are the dye and quencher separated, which increases fluorescence, but the 5'-3' exonuclease activity of Taq during primer extension hydrolyses the probe between the two. The dye and the quencher are no longer attached to the same oligo and therefore fluorescence greatly increases. This probe gives a greatly enhanced fluorescent signal and a smaller background signal.

Some fluorescent dyes undergo changes in their fluorescence spectrum due to changes in their environment. Thus, the spectrum of such molecules attached to a probe oligo may change on hybridisation of the probe with the target and thus they could be used as hybridisation probes. Some examples are now described.

1.7 Probes based on changes in emission spectra.

Some dyes, such as pyrene and fluorescein (Figure 1.10), when attached to a probe oligonucleotide undergo fluorescence quenching or an increase in fluorescence intensity on hybridisation of the probe to the target.

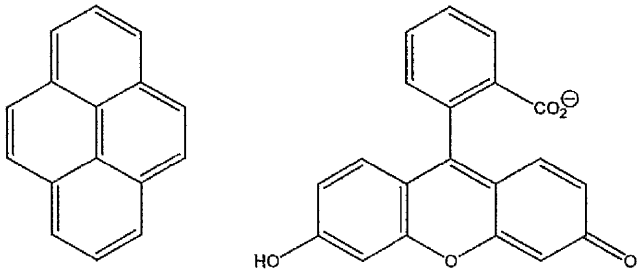

Pyrene Fluorescein

Figure 1.10: Structures of pyrene and fluorescein.

Pyrene attached *via* ethylenediamine linkers to the N (4) position of cytosine residues in a poly (C) chain (< 5% labelled) showed a four-fold decrease in intensity on hybridisation to a poly (I) strand [31]. The decrease in fluorescence was found to be proportional to the amount of base pairing. These changes were attributed to environmental changes resulting from probe hybridisation. It was thought that before hybridisation the pyrene moiety was located in the hydrophobic plaits of the randomly folded poly (C) chain. On hybridisation pyrene was expelled outwards from the helix due to steric hindrance into a more hydrophilic environment, causing the fluorescence efficiency and the lifetime to decrease. When natural DNA sequences were labelled in the same way fluorescence was seen to drop by 30%, which was less than the decrease seen for the poly (C) sequence, possibly due to secondary structure present in the natural DNA. Pyrene groups in these areas will not undergo an environmental change on hybridisation to the complementary strand [32].

Natural DNA labelled with fluorescein attached to the N (4) of cytosine residues showed a 17% decrease in fluorescein fluorescence on hybridisation to the complementary strand. This decrease was possibly due to a change in the monoanion: dianion ratio (carboxylic function pK_a <5, phenol function pK_a 6.4 [33]). This could be caused by a modification in the apparent pK_a of the conjugated fluorescein when it is in duplex structure due to the increased negative charge density of the phosphate backbone [34]. The

decrease in fluorescence, however, was small and photo-bleaching of fluorescein was also found to be a problem.

Telser *et al.* [35] also reported only a small change in the fluorescence intensity of fluorescein-labelled oligos on hybridisation when fluorescein was attached either to thymidine *via* a 7- atom linker arm attached to the pyrimidine ring at C5, or to a cytosine *via* a 4-atom linker to N (4). In this study the fluorescence emission when fluorescein was attached to single-stranded DNA was slightly red-shifted compared to that of free fluorescein. On duplex formation between target and probe the emission maximum shifted back to that of free fluorescein. This shift of emission maximum was thought to be due to aromatic stacking of fluorescein with the nucleobases in ssDNA, removed on duplex formation.

Pyrene derivatives attached in a similar way resulted in much greater changes in the emission spectrum on hybridisation of labelled ssDNA to its complement, namely a four-fold decrease in quantum yield on duplex formation. This was thought to be due to pyrene intercalating into the double-stranded structure. Some polyaromatic compounds such as pyrene can intercalate into B-DNA between adjacent bases pairs (type I binding). In addition groove binding to the exterior of the duplex is also possible for pyrene (type II binding) [36;37].

Pyrene has also been attached to the 5'-terminus of RNA probe oligos [38;39], and on duplex formation with complementary RNA the fluorescence intensity was seen to increase significantly. These probes were sensitive to mismatches, giving no enhancement of fluorescence when a mismatch between the target and the probe was present near the 5'-pyrene modification site. However, if the mismatch occurred more than three base pairs away from the position of the pyrene modification it could not be detected.

The detectable signal indicating binding of the probe to the target in the cases described above is the change in emission intensity at one wavelength. The problem with this is that this change is monitored against a large background fluorescence, which greatly reduces the sensitivity of such probes. Therefore, other fluorescent methods are required to reduce this background, and increase sensitivity. One fluorescent phenomenon, which has been exploited for use in hybridisation probes is the highly red-shifted excimer fluorescence seen for some aromatic dye molecules, and excimers are now discussed.

1.8 Excimer- and Exciplex-based probes.

1.8.1 Excimers

An **excimer** is an **exci**ted state dimer (MM*) in which both molecules (M) are the same. It is formed between one molecule in an excited singlet state (M*) and the other in the ground state (M) as shown in Figure 1.11 [21].

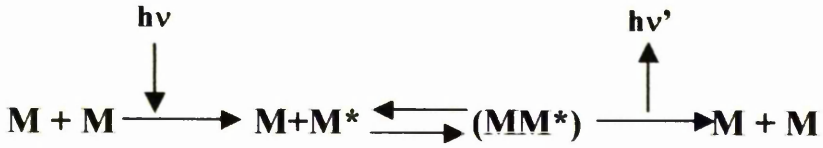

Figure 1.11: The formation and fate of an excimer (MM)*.

The newly formed species (MM*) has its own electronic and geometric structure, vibrational and rotational levels and its own reactivity. This dimer can emit fluorescence. The fluorescence of singlet excimers is seen as a broad structureless band at longer wavelengths than normal monomer emission [21]. Emission occurs at longer wavelengths as the electronically excited dimer is stabilised, whilst the ground state is mutually repulsive (see Figure 1.13). The energy level diagram of Figure 1.12 [40] describes the situation. The two electrons in Ψ_b gain -2ΔE, the electron raised to Ψ_a gains +ΔE and the excited electron in Ψ_a* gains -ΔE, the overall stabilization is -2ΔE. In the ground state dimer there would be another electron in Ψ_a instead of Ψa*, off-setting the gain in energy. Therefore the ground state dimer is not stable.

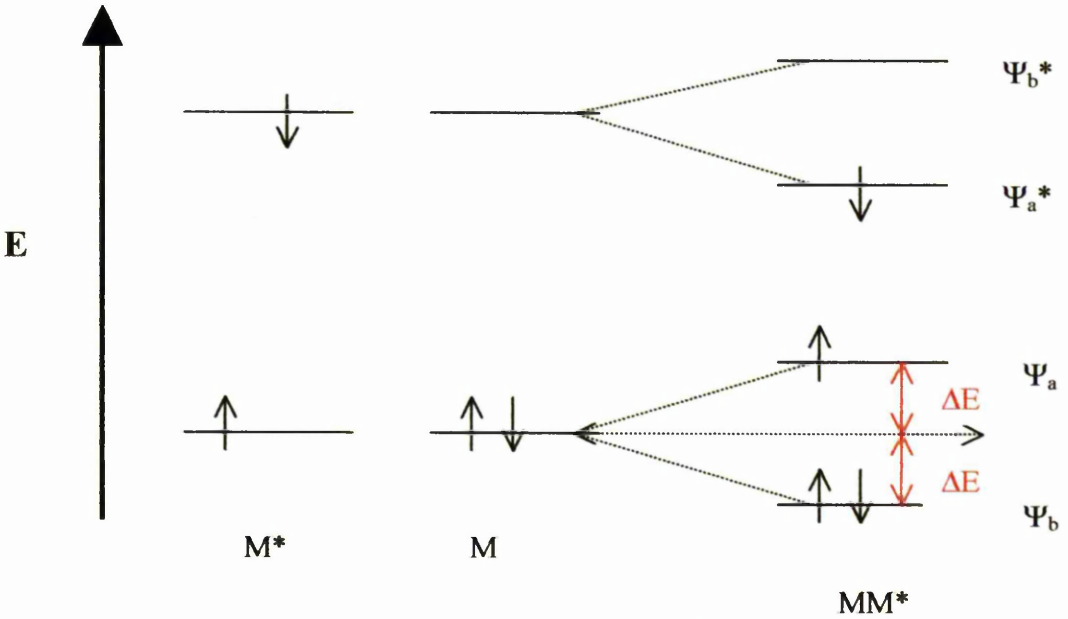

Figure 1.12: Energy level diagram of an excimer [40].

The lack of structure in the excimer fluorescence band is due to the fact that the dimer does not exist in the ground state: it is a repulsive state with only a small degree of Van der Waals' stabilisation, and so there are no corresponding vibrational levels in this state. Transitions occur to the lower repulsive energy surface as shown in Figure1.13 [21]. The excimer will have many levels associated with low frequency vibrations, but these will overlap, and so it is impossible to distinguish any vibronic structure in the excimer band. The monomer emission remains structured, on the other hand, due to transitions from the lowest vibrational level of the first excited state to different vibrational levels in the ground state [41].

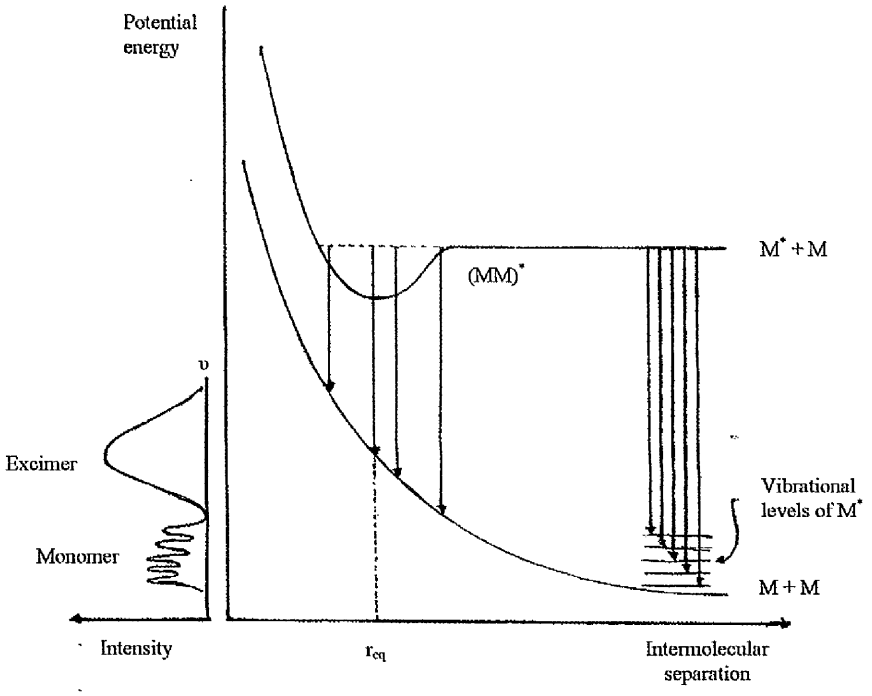

Figure 1.13: Intermolecular potential energy curves for monomer and excimer. Diagram taken from Gilbert & Baggott [21].

An example of a molecule that forms an excimer on excitation of a crystal or a sufficiently concentrated solution is pyrene. The excimer binding energy for pyrene is 39.3 $KJmol^{-1}$, which is higher than typical Van der Waals forces [21]. The entropy change associated with pyrene excimer formation is $-73.6\ JK^{-1}mol^{-1}$, indicating that the excimer structure is fairly ordered. These data compare well with those of pyrene crystals [42], which also show excimer fluorescence, suggesting that pyrene molecules in solution adopt a similar structure to crystalline pyrene. The pyrene molecules in these crystals are arranged in sandwich pairs with the distance between monomers being 3.53 Å. (Figure 1.14.)

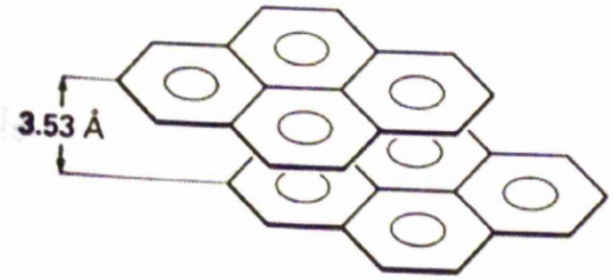

Figure 1.14: The sandwich structure adopted by pyrene excimers. Diagram taken from Gilbert and Baggott [21].

The emission spectrum of a pyrene excimer in solution is shown in Figure 1.15. Emission from free excited pyrene (M*) still present is termed the locally excited state, and is reduced since its concentration is reduced due to excimer formation. Therefore, excimer formation is a type of emission quenching.

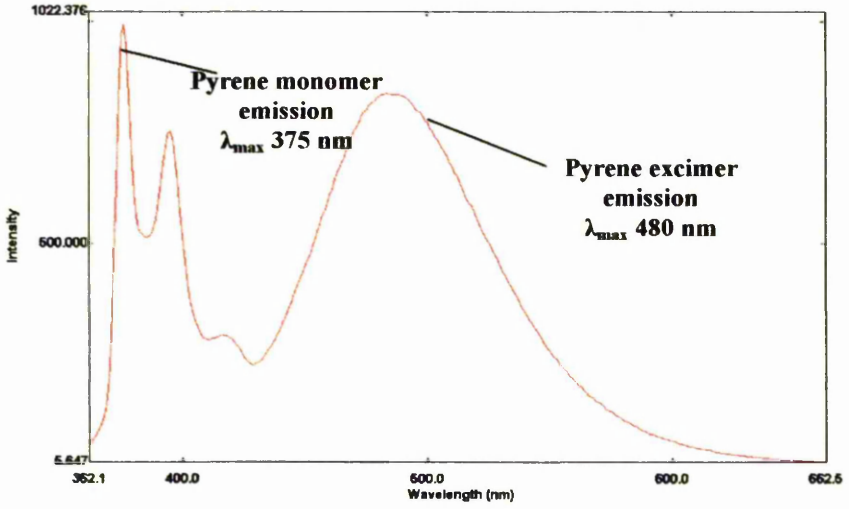

Figure 1.15: Emission spectra of pyrene showing both the monomer and the red-shifted excimer band.

Excimers show very large Stokes shifts, i.e. the difference between the λ_{max} of absorbed and emitted light. The Stokes shift is much larger than for many dyes currently in use, see Table 1.1. In cases where dyes have small Stokes shifts the excitation and the emission spectra overlap, and not all the emitted light can be detected as a proportion is mixed with the excitation beam. This leads to a decrease in sensitivity from the need to use filters to detect only emitted light.

Table 1.1: Stokes shifts of some commercially available dyes compared to that of the pyrene excimer (www.probes.com).

Dye	λ_{max} of Absorption (nm)	λ_{max} of Emission (nm)	Stokes shift (nm)
Pyrene monomer	340	375	35
Pyrene excimer	346	480	**134**
BODIPY FL	505	513	8
Fluorescein	492	520	28
Rhodamine Green	504	532	28
TAMRA	565	580	15
ROX	585	605	20
Texas Red	583	603	20

1.8.2 Exciplexes

It is also possible to see a similar unstructured, red-shifted emission from excited complexes composed of two different partners, M and Q. For such **excited complexes**, called **exciplexes,** the process may be written as in Figure 1.16. A molecule M becomes electronically excited and forms a complex with a different molecule Q, which is in its ground state. As for excimers, emission from this excited complex occurs at longer wavelengths due to stabilisation of the exciplex.

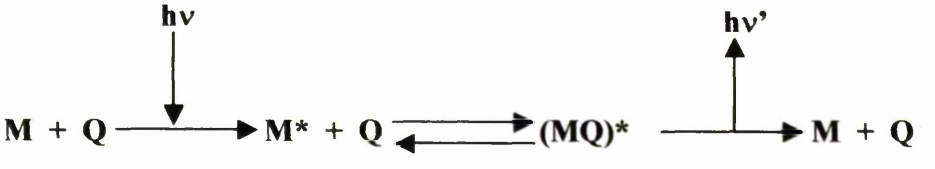

Figure 1.16: The formation and emission of an exciplex.

Unlike excimer emission, exciplex emission is very sensitive to solvent polarity and the redox properties of the monomers. This suggests that electron transfer may be involved, as the orbitals of the exciplex partners do not coincide, as do those of the excimer. One of the components acts as an electron acceptor and the other as an electron donor, forming a complex with a dipolar nature, $(M^{+}Q^{-})^{*}$ or $(M^{-}Q^{+})^{*}$. The dipolar nature of the exciplex depends on the solvent polarity. It becomes more dipolar as solvent polarity increases until complete electron transfer occurs to form solvated radical ions (M^{-}+Q^{+}) or

($M^{\cdot+}$+$Q^{\cdot-}$). In this way intermolecular exciplexes are not usually seen to emit in solvents as polar as acetonitrile (ε 35.9) [43-45].

However, several intramolecular exciplexes, in which the exci-partners are held close together emit in solvents as polar as acetonitrile [46;47], and in a few cases in solvents more polar than acetonitrile [48]. These intramolecular exciplexes consist of either an aromatic donor and acceptor linked by a short flexible polymethylene chain, or an aromatic compound substituted with an aliphatic amine. This aliphatic amine acts as a donor and the aromatic group as an acceptor [49]. As the donor and acceptor are linked, quenching *via* ionic dissociation, the dominant pathway for intermolecular exciplexes, does not occur. Instead the intramolecular exciplex undergoes structural changes from a compact, folded structure to a looser geometry on going to more polar solvents. This increases the distance between the donor and the acceptor. The change in structure causes an increase in the radiationless transition probability, which leads to quenching [47-50]. The structures of intermolecular exciplexes are also less rigid in polar solvents than those in non-polar solvents or than those of excimers. The geometry of these exciplexes also becomes looser on changing to polar solvents due to solvation of the partners [51]. Again this increases the radiationless transition probability resulting in a decrease in fluorescence decay and fluorescence yield. In very polar solvents the spectrum of a pyrene and diethylaniline (DEA) exciplex is identical to that of the separate ion pairs Py^{-} DEA^{+} [43], indicating that in very polar solvents the exciplex becomes a solvated ion pair [44] or completely dissociated ions [43;52 51].

It is thought that excimer and exciplex emission is not strictly dependent on the geometry of the two fluorophores relative to one another [47;53;54]. For excimer emission, fluorescence may occur from various configurations and the excimer energies lie between the zero point energies of the donor and acceptor molecules. These cover a range of energies, which include all the possible configurations. If no steric hindrance is present, the excimer will adopt a sandwich structure, this conformation giving the maximum fluorescence.

Naphthalkylamines can form intramolecular exciplexes between the amine and the aromatic ring system. Short methylene chains linking these two groups restrict possible conformations that the exciplex is allowed to adopt [53]. However, exciplex emission is still seen for linker lengths as short as two methylene groups. This emission is not as intense as that seen from napthylamines with longer methylene linkers as the interaction between the donor and the acceptor is not as strong due to the restricted geometry. The less demanding geometrical requirements of these intramolecular exciplexes was thought to be due to the

small size of the amine nitrogen. However, similar results were obtained for an aromatic amine donor (e.g. dimethylaniline) linked *via* a methylene chain to an aromatic hydrocarbon acceptor (e.g. anthracene) [55]. These two moieties were joined by chains of varying length, from one to three methylene groups. Again exciplex emission was seen for the intramolecular exciplex joined by one and two methylene groups where the partners were unable to form a parallel sandwich structure. The longer linkers resulted in exciplex emission at longer wavelengths, due to more favourable orbital overlap. Exciplex stability is thought to be a function of orbital stability [56]. These data suggest that a sandwich structure may be favourable, but not necessary.

Further evidence of the geometry of exciplexes came from studies of intermolecular exciplexes between naphthalene-conjugated dienes and pyrene [54]. For naphthalene-conjugated diene exciplexes it was observed that k_q, the rate of quenching of naphthalene fluorescence by conjugated dienes, was influenced by the presence of substituent groups, suggesting that the optimum geometry was a sandwich structure. Experiments with pyrene: dimethylaniline exciplexes and pyrene: t-butyl-substituted dimethylaniline exciplexes (^{t}butyl groups prevent the formation of the sandwich configuration) showed that the fluorescence quenching rate of ^{t}Bu-substituted dimethylaniline was just as efficient as unsubstituted dimethylaniline. This would not occur if exciplexes adopted only a sandwich configuration. It was suggested that ^{t}Bu-substituted dimethylaniline formed a localised pair geometry, see Figure 1.17. If M and Q are both π electron systems a sandwich arrangement is favourable. However, if this is not sterically feasible then localised interactions will dictate the optimum geometry [54].

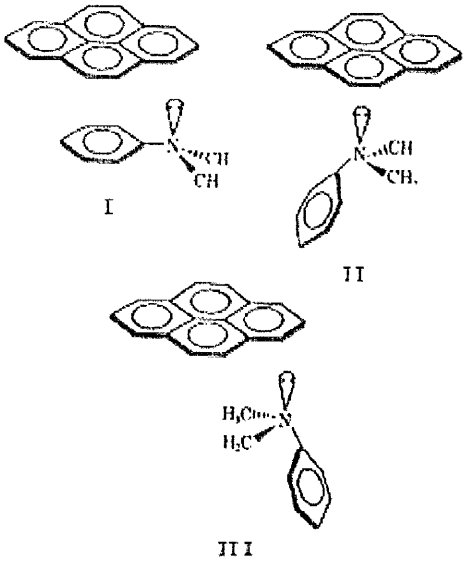

Figure 1.17: Structure I shows the favoured sandwich structure adopted for an exciplex. Structures II and II show localised pair geometries adopted if steric effects prevent the formation of the sandwich geometry. Diagram taken from Taylor *et al.* [54].

1.8.3 Excimer-based oligonucleotide probes.

There are several examples in the literature where oligonucleotides have been substituted with multiple pyrene moieties able to form excimers with each other (λ_{max} 480 nm). The change in the ratio of the intensity of the excimer band relative to the monomer band (I_E/I_M) on addition of complementary strands, or a general change in fluorescence intensity is used as an indication of binding. Tong *et al* [57] attached 1 to 5 pyrene groups to a polyamide *via* lysine residues and the polyamide was attached to the 3'-terminus of the oligonucleotide. Monomer and excimer bands were seen for the individual probes, the I_E/I_M increasing as the number of pyrene groups increased. On binding to complementary DNA excimer fluorescence increased 2-fold, indicating that in the single-stranded probes stacking may occur between the bases and the pyrene moieties causing quenching of the excimer band. On binding this interaction is removed and the pyrene residues are free for excimer formation.

A *bis*-pyrene moiety (*bis*-(2-1-pyreneyl)ethylamine) was attached to the 5'-terminus of an oligo probe *via* a 6-bond linker group [58], and the free label showed a strong excimer band and a weaker monomer band. When the label was attached to the oligo the excimer band disappeared, possibly due to pyrene interacting with the nucleobases. On duplex formation this interaction is prevented and the excimer band re-appeared. Lewis *et al* [59] on the other hand observed a decrease in the excimer emission of a *bis*-pyrenyl moiety

on probe binding, when they attached a *bis*-pyrenyl alcohol to the 5'-phosphate group of a probe oligo, the I_E/I_M ratio decreasing from 0.8 to 0.27 on binding of the probe to complementary DNA.

Bis-pyrenylated probes have also been found to be sensitive to the secondary structure of mRNA [60]. Two pyrene residues (pyrenemethylamine) were attached to the 5'-phosphate of an oligo probe, and binding of this probe to target mRNA at single-stranded regions resulted in minor changes in the excimer fluorescence. However, binding of the probe to double-stranded regions caused excimer fluorescence to be quenched as a result of pyrene interacting with the double-stranded structure. An increase in excimer fluorescence was seen when the complementary region of the mRNA was a stem and loop junction.

Pyrene moieties have also been incorporated at internal sites in the oligo strand as pseudonucleotides [61] where in a 3-carbon chain mimics the sugar and pyrene acts as a pseudo-base. Two such pyrene pseudo-bases were incorporated into an oligo. These were separated by several nucleotides, so that on hybridisation to the target a loop was formed bringing the pyrene groups together. This caused a 4-fold increase in monomer emission, but excimer emission was unchanged. Pyrene moieties have also been incorporated internally *via* glycerol linkers at adjacent positions between the phosphate groups of the backbone, maintaining the 3-carbon internucleotide separation [62]. On hybridisation of these probes to their complements the I_E/I_M value increased from 0.72 to 2.56.

Although excimer-based probes have potential for use in hybridisation assays due to the greatly red-shifted excimer emission, most of the excimer-based probes described here show both excimer and monomer bands in the absence of the target. Upon hybridisation a change in excimer fluorescence intensity or in the I_E/I_M value is seen. These probes, like those described above for use in homogenous assays, thus can have large background signals, which reduces their sensitivity. It would therefore be desirable to develop a novel type of probe system that could be used in homogeneous assays, but which would have a low background in the absence of the target sequence. This thesis suggests such a system, namely the use of a split-probe system. Consequently, some discussion now follows of various uses of split-oligonucleotide systems in general, along with examples of their use as probes.

1.9 Split-oligo systems.

A split-oligo system consists of two or more short probe oligos, each complementary to different sequences in the same target strand. The oligos may be

complementary to adjacent sites, binding contiguously to the target sequence as shown in Figure 1.18.

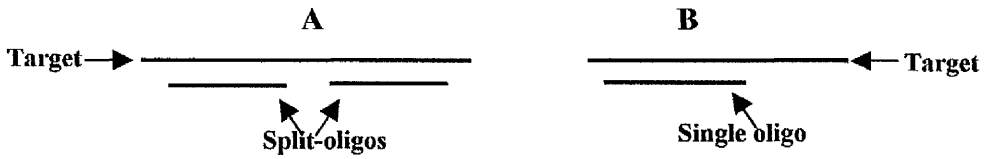

Figure 1.18: Schematic diagram of hybridisation of (A) a split-oligo system and (B) a normal single oligo system.

Split-oligo systems have been used for increasing capture efficiency of probes, for the specific photo-modification of oligonucleotides and as detector systems. These uses of split-oligonucleotide systems are described below.

1.10 Using split-oligo systems to increase capture efficiency of oligo probes.

Cooperative interactions are known to occur between oligonucleotides bound to adjacent sites of a target sequence [63;64]. These interactions are largely due to base stacking interactions between the bases at the duplex junction. The cooperative interactions result in enhanced equilibrium binding constants. In fact, the free energy afforded by hybridisation at contiguous sites was found to be between –1.4 and –2.4 Kcal/mol [65]. Cooperativity was also shown to exist in the presence of modifying groups at the 5'- and 3'-junctions of the contiguously bound oligos [66]. Also discrimination of mismatches at the junctions was found to be higher in these tandem complexes compared to ordinary duplexes bearing a terminal mismatch. This feature of the tandem duplexes could potentially be exploited in the hybridisation analysis of SNPs.

The use of a second contiguous binding short oligo has been successfully used to increase the sensitivity of capture probes by up to 25-fold due to cooperative interactions between the two short oligos [67;68]. Capture probes are short oligo probes, complementary to the target strand. These are immobilised on to a solid support, which can either be a chip or a magnetic bead. In this method the target sequence is pre-hybridised with another short oligo of 11 nucleotides (or more) before hybridisation with the capture probe. This oligo binds to the target sequence in an adjacent position to the binding site of the capture probe. After this pre-hybridisation step, the target and probe module are allowed to hybridise to the capture probe (Figure 1.19). Increased capture was seen in the presence of the pre-hybridised module, especially if there was no gap between this and the capture probe. This increased capture may have been due to the pre-hybridised module opening up any

secondary structure of the target, and also the effect of increased base stacking interactions between the adjacently positioned pre-hybridised module and the capture probe oligo. The pre-hybridisation step increased capture of the Hepatitis C virus, which is known to form a stable stem and loop structure in the highly conserved 5'-nontranslated region, by up to 25-fold, and the technique was in 95% correlation with current commercial tests of equal sensitivity. The technique has also been used for the purification of PCR products [69].

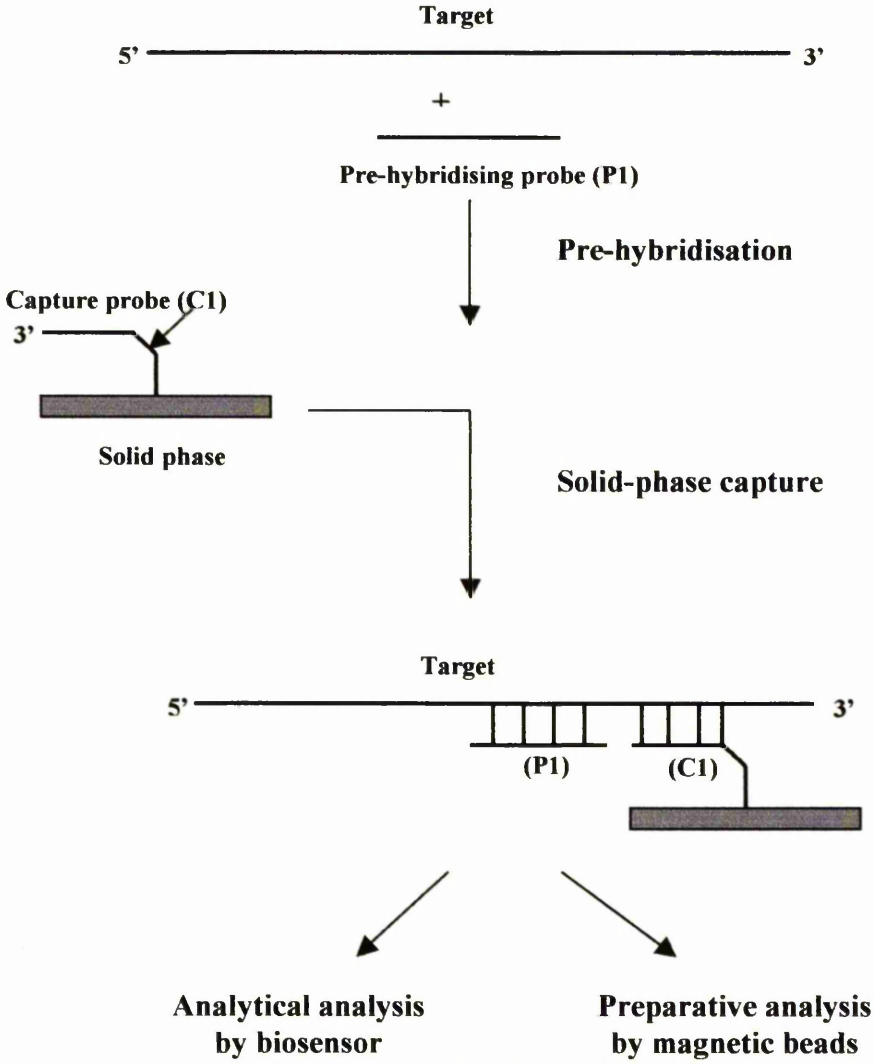

Figure1.19: Schematic representation of the oligonucleotide-assisted capture method. The oligo module (P1) is initially pre-hybridised to the target, and this complex is captured on the immobilised capture probe. Detection of the capture on a chip surface is analysed by biosensor, while capture onto magnetic beads allows detection by PCR.

1.11 Split-probe systems that improve photo-modification of DNA.

Split-probe systems have also been developed to enable the specific photo-modification of DNA [70-74]. Chemical modification of nucleic acids has been important in studying gene expression and for the design of biologically active gene-addressed

substances. The process involves the binding of an affinity reagent to a specific target sequence, on binding to the target the reagent is activated and brings about a modification of some kind. Affinity reagents, however, can bind non-specifically to other cellular components if used in biological systems. Therefore, the use of photo-reactive derivatives is desirable as they are inactive in the dark, but can be easily activated at the target. Perfluoroazide derivatives can undergo photo-dissociation resulting predominantly in singlet nitrene species, which are highly reactive. Reaction of these with ssDNA is by electrophilic addition at the N(7) position of guanosine bases. Perfluoroazide derivatives, however, lack photo-reactivity in the visible region and so their application in complex biological systems is restricted as the UV light required to activate them destroys proteins and nucleic acids [72]. Consequently a binary or split-probe system was developed [73;74] using two oligos, complementary to adjacent sequences in the target. The 5'-terminus of one was labelled with a photo-sensitising group (S), either anthracene or pyrene, and the 3'-terminus of the other was labelled with a photo-reactive perfluoroazide group (R). On binding of the two probes, S and R are brought together (Figure 1.20).

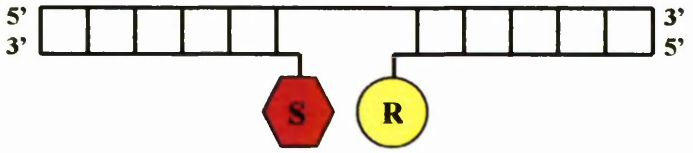

Figure 1.20: Diagram of the split-probe system for specific photo-modification of oligonucleotides. Where S represents the photo-sensitising group, and R the photo-reactive group

The groups were chosen so that the energy of the transition between the lowest vibrational levels of the ground state and the first electronically excited state in the sensitiser was greater than in the reagent. The emission spectrum of the sensitiser also had to overlap with the absorption spectrum of the reagent. On irradiation with near-UV light after correct binding, energy is absorbed by the sensitiser and transferred by singlet-singlet energy transfer to the azido group. This leads to an excited state azide group, yielding a singlet nitrene, which reacts with spatially close guanosine bases in the target as previously described. This method of photo-cross linking was found to be 300 times faster and 90 times more specific than reaction in the absence of a sensitiser (direct modification). A similar system using perylene as a sensitiser, which could be activated by visible light was found to be 3000 times faster than direct modification, and gave yields of 98-99 % [71].

1.12 Using Split-Oligos systems as detectors.

For a detector system based on a split-oligo approach at least one of the probe oligos must carry a label that changes its signal or becomes detectable only on the correct binding of all the probe components to the specific target site and any subsequent modification steps (e.g. ligation, immobilisation). Using such a split-probe detection system could potentially reduce the length of the probe sequence required. As mentioned earlier, a probe of at least 20 nucleotides is required to uniquely detect a sequence in the human genome. However, it is possible for stable duplexes to form between oligos of 12-13 nucleotides in length under physiological conditions (37 °C). Therefore, it is feasible for probes of 20 nucleotides to form non-perfect complexes to non-target regions. In such a split-probe system shorter oligo probes can be used. Any non-specific binding of only one probe will not result in a signal. The use of shorter probes would also be desirable for a detection system to be used *in vivo* as shorter probes will have fewer problems with cellular uptake. Several approaches have been described in the literature, some of which are described below.

1.12.1 Split-Probe detector systems involving the ligation of two or more probes.

Several such detector systems have been described which use template-directed ligation of two or more short oligo probes. In one example two oligos were used, one labelled with biotin and the other with ^{32}P [75;76]. The probes bound contiguously to the target and a ligase enzyme was used to join them. After ligation the oligonucleotide duplex was allowed to bind to streptavidin immobilised onto a solid support and detected by autoradiography (Figure 1.21). Fluorescently labelled probes could be used in place of ^{32}P for safer handling. This method was able to discriminate between two alleles of the human β globin gene, β_A and β_S (sickle cell gene), which differ by a single nucleotide.

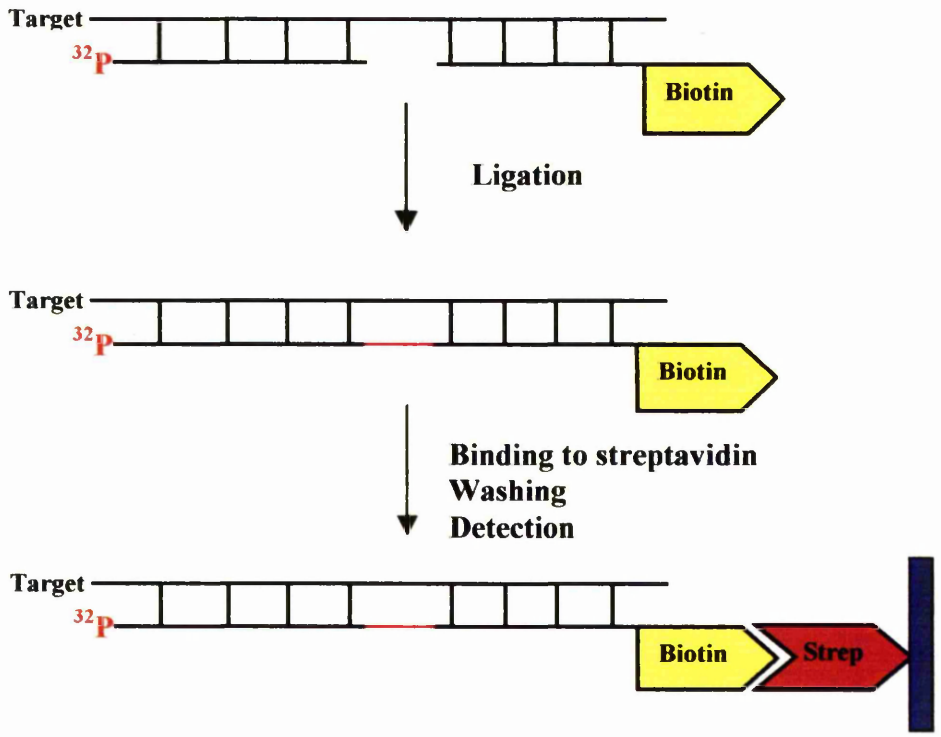

Figure 1.21: Diagram of the detection of target oligo *via* hybridisation of oligo probes, one labelled with biotin and the other with ^{32}P, to adjacent positions of the target. The ligase then joins the correctly bound probe oligo. The radioactively labelled probes are then immobilised and detected by autoradiography only if they have been ligated to the biotinylated probe that can be bound to streptavidin on a solid support [75;76].

Cruickshank *et al.* [77] proposed using chemical ligation of the two probes instead of enzymatic ligation. In this case one probe oligo also had a photoreactive functional group attached to the oligo so that on correct binding it would be positioned at the junction site of the two oligo probes. This system is capable of forming a covalent bond between the two probes on photo-activation. Possible photo-reactive groups include benzo-alpha-pyrones (coumarins) (Figure 1.22).

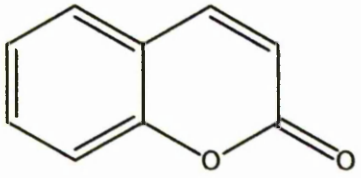

Figure 1.22: Structure of benzo-alpha-pyrone (a coumarin), a photoreactive group capable of forming a covalent bond between two probe oligos on irradiation.

It is also possible to join the two oligos, one bearing a 5'-phosphate group at the nick site, by chemical ligation with cyanogen bromide in the presence of a tertiary amine [78-80].

Cyanogen bromide activates the phosphate group to reaction with hydroxyl groups of the other adjacent oligo, thereby joining the two. This method of ligation proceeded very quickly (~3 minutes) with no by-product formation.

A similar ligation method [81] (Figure 1.23) uses a biotinylated probe, made by the template-dependent ligation of three short oligos (two 8-mers and one 4-mer), one carrying a biotin moiety. The probes bound in adjacent positions along the target sequence and were joined by enzymatic ligation. The ligated probe: target duplex was then immobilised onto a membrane by UV irradiation. The membrane was then washed, the ligated 20-mer probe became complexed tightly to the target and was retained. However, short unligated probe fragments not held as tightly to the immobilised target were washed away. The retained, biotinylated probe was then visualised by staining with a streptavidin-chromophore conjugate. This technique was found to be specific, as no signal from the unligated products was detected and it was sensitive to single-base mutations, as these also gave no signal. Again, however, undesirable extra steps of ligation, immobilisation and staining are still required.

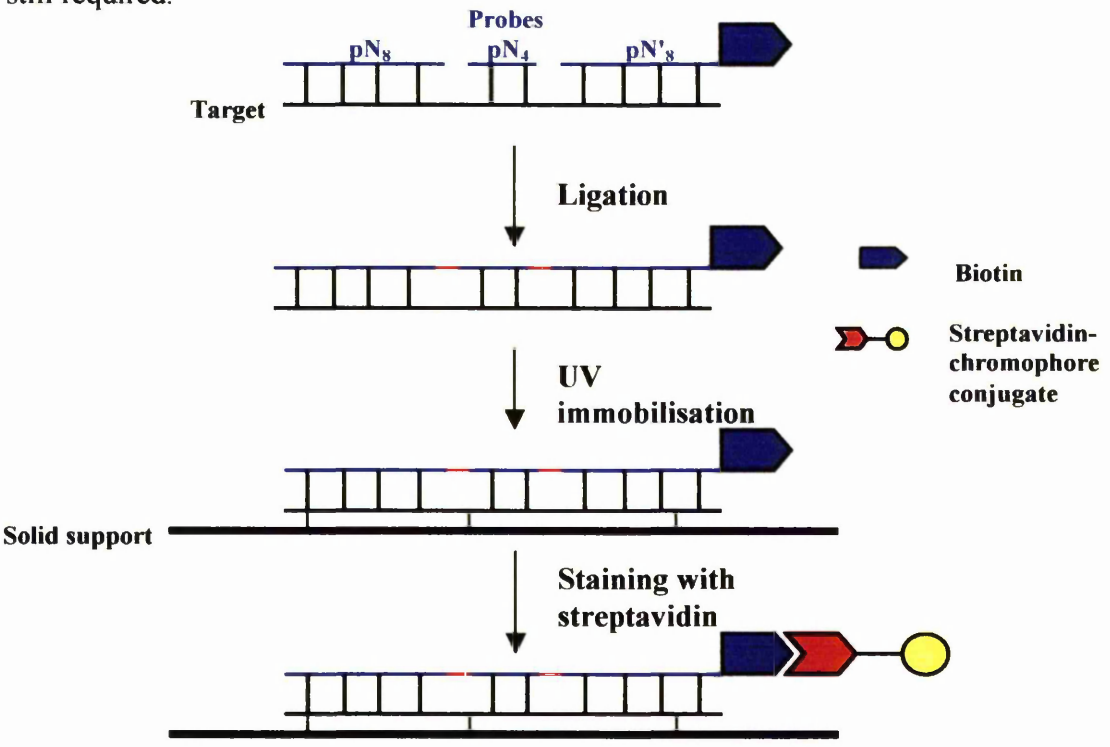

Figure 1.23: Formation and detection of a DNA-probe complex *via* ligation of the pN_8 + pN_4 + pN'_8 tandem on the DNA template (target), UV immobilisation of the complex onto a solid support and visualisation with the streptavidin-chromophore conjugate [81].

A homogeneous DNA detection method similar to the template-directed ligation methods described above has been developed [82;83] (Figure 1.24) for use in conjunction with

PCR amplification to detect genotypes. It is based on template-directed dye terminator incorporation (TDI) similar to the ligation methods. After amplification of DNA containing a SNP, a primer probe bearing fluorescein conjugated to its 3'-terminus is added to the target, along with dideoxynucleotides (ddNTs). These bear one of two different dye molecules, one specific for the wild type and one specific for the mutant target. These dyes can undergo FRET with the fluorescein dye if incorporated into the primer sequence. The primer binds to the target in the position adjacent to the SNP, and the dye-carrying ddNTs are then incorporated in to the primer. The one incorporated depends on the genotype of the sample. On excitation at the fluorescein excitation wavelength, energy is transferred by FRET to the other dye, which has been incorporated into the primer, and quenching of the fluorescein fluorescence occurs, accompanied by an increase of fluorescence of the incorporated dye. In this way the mutational status of the sample can be determined by analysing the fluorescence intensity of the three dye molecules.

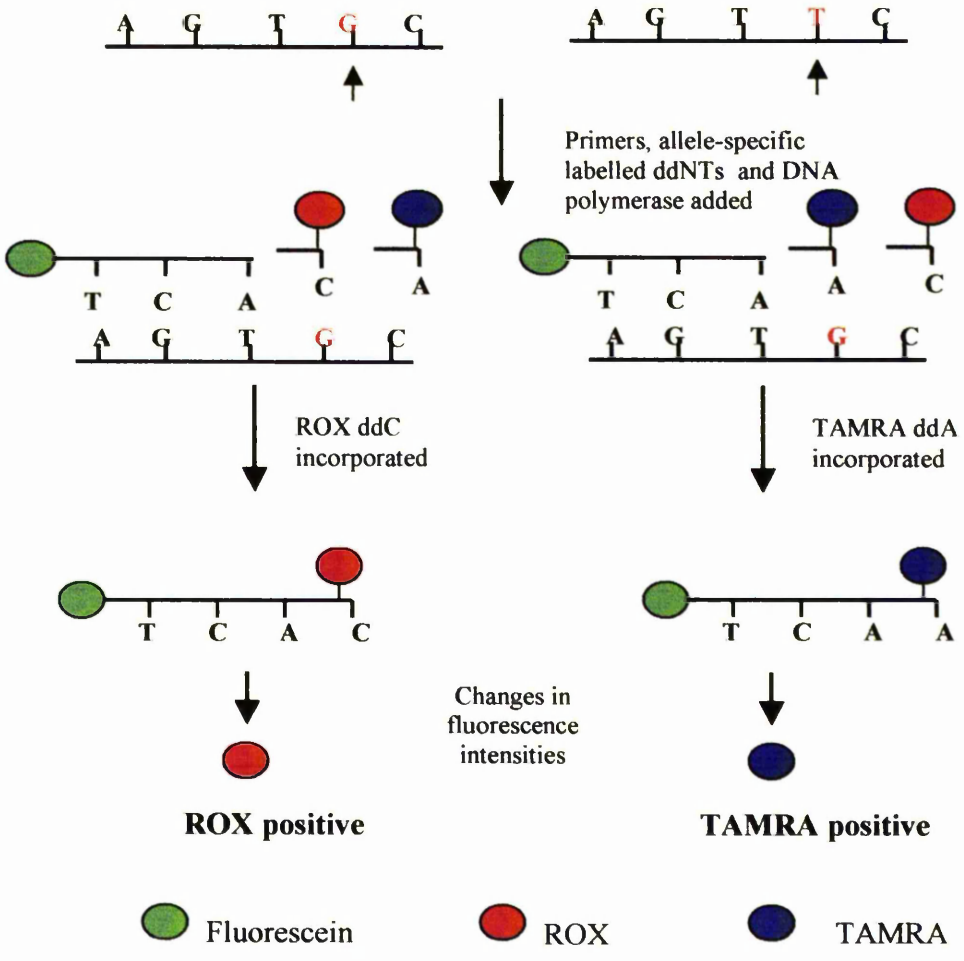

Figure 1.24: DNA detection using template-directed dye terminator incorporation (TDI)

This method has been further developed [84] using two dye-labelled oligos, one bearing fluorescein as before, which binds to the target adjacent to the SNP. A second probe then binds directly adjacent to it. There are two variations of this probe, one specific for the wild-type sequence and one for the mutant. Each is labelled with a different dye, which can undergo FRET with fluorescein. After binding of the probes to the target they are ligated enzymatically, the fluorescence intensities of all the dyes are monitored, and the mutational status of the sample determined as above. This method involves only a two-stage protocol that can be designed to fit into standard PCR protocols. Many other split-probe detection systems have been described which do not require these extra ligation steps. Such systems, described below, involve both heterogeneous and homogeneous assay techniques and a variety of detection methods.

1.12.2 Heterogeouous Split-probe detection systems

1.12.2.1 Split-oligo systems using nanoparticles.

One heterogenous split-oligo detector system uses oligonucleotide-functionalised gold nanoparticles [85;86], small particles of gold about 13 nm in diameter. The nanoparticles can be functionalised with oligonucleotides labelled with Raman dyes. Each nanoparticle can hold around 110 oligos. The assay developed using these (Figure 1.25) involves a capture probe of about 15 nucleotides, which is bound to the surface of a solid support. The capture probe is first allowed to hybridise to the target sequence (~30 nucleotides). The chip is then treated with a solution containing the functionalised nanoparticles. The oligonucleotides bound to the gold surface hybridise to the target in an adjacent position to the capture probe oligo. The chip is then treated with a silver enhancing solution containing Ag(I) ions. The gold nanoparticles promote the reduction of Ag(I) and this initiates silver deposition. The deposition of silver enhances the Raman scattering of the dye and therefore a specific signal is detected in the presence of the target. Other Raman dyes can be used enabling multiplex detection. Multiplex studies on sequences from Hepatitis A Virus, Hepatitis B virus, HIV, Ebola virus, Smallpox virus and *Bacillium anthracis* showed that no cross hybridisation occurred between the targets and the different targets could be differentiated easily by the Raman scattering pattern.

It was also possible to detect SNPs by using two different nanoparticle probes, each functionalised with oligos specific for different genotypes. To distinguish between the SNPs, however, additional washes were required with buffer at a higher temperature or salt concentration, which causes dissociation of imperfectly matched duplexes.

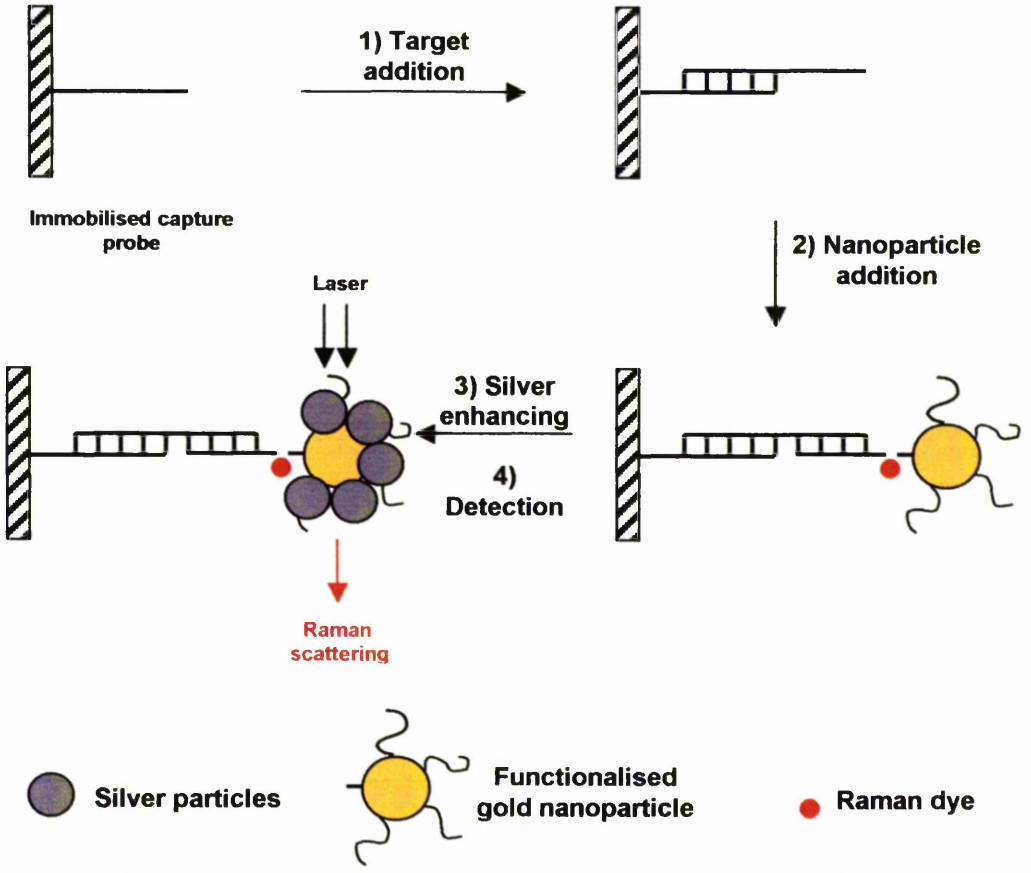

Figure 1.25: Schematic diagram of the nanoparticle split-oligo assay [85;86].

A similar nanoparticle split-oligo system has been developed that uses electrical detection instead of Raman scattering [87]. In these assays microelectrodes are prepared where the gaps between the electrodes are about 20 μm. The capture oligo probes are immobilised on to the chip surface in these gaps. The target is allowed to hybridise to the capture probes and the microelectrode array is then treated with the oligonucleotide-functionalised gold nanoparticles. These hybridise to the target as before in an adjacent position to the capture probe. The split-oligo system is then treated with the silver enhancing solution. Silver is deposited in the presence of the gold nanoparticles filling the gaps between the electrodes, thereby completing the circuit. Measured resistance then indicates the presence of the target (in the absence of the target there is no current).

1.12.2.2 Triplex-forming split-probe systems.

Another heterogenous split-probe detection system, based on triplex formation, has been developed to increase the specificity and sensitivity of target [88]. The target (A in Figure 1.26) is immobilised on a solid support. One or two short oligo probes, C, are then

allowed to hybridise to the target *via* normal Watson-Crick base pairing. In the case of two C probes these bind in adjacent positions to the target so that no gap occurs between them. The final probe oligo, B, which possesses a reporter group and is capable of triplex formation, is then allowed to bind *via* Hoogsteen binding to the duplex (A:C). Oligo B will only bind once C has correctly bound to the target and in the case of two C probes, B only binds if the C probes bind in adjacent positions with no gaps between them (Figure 1.26). If, instead of C, a fourth oligo, D, is used which binds to the target so that there is a gap between probe oligos C and D, then B is unable to bind. Therefore, this method can, with careful probe design, be successfully used to detect mismatches. However, laborious immobilising and washing steps are still required and triplex formation is only realistically achievable for a limited number of sequences.

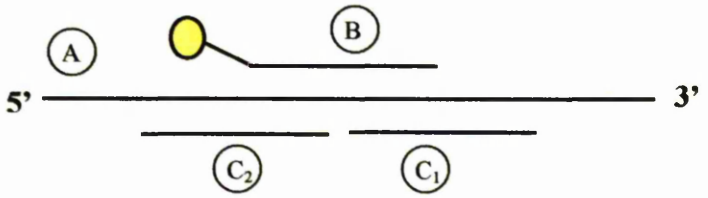

Figure 1.26: Schematic representation of the triplex formed by the Watson-Crick binding of probes C_1 and C_2 to the target so that they bind in adjacent positions, followed by Hoogsteen binding of probe B to the duplex ($A:C_1C_2$). Oligo B carries a reporter group.

1.12.3 Homogenous split-probe assays.

1.12.3.1 Split-probe systems for use with laser-based fluorescent detection.

A homogenous method using two oligo probes in conjunction with laser-based fluorescent detection has been proposed [89]. This method is very sensitive and can detect single DNA molecules. Two probes were used, each labelled with a different dye, these were allowed to bind to the target, which incorporated both binding sites. The sample was then analysed by ultra-sensitive laser-based fluorescent detection, which monitored two different emission wavelengths simultaneously over time in a flow cell. Since the probes were bound to the same DNA molecule their signals would appear at the same time. Therefore, fluorescent signals detected at the same time (coincident signal) indicated the presence of the target. If no target was present, or if only one probe bound to a DNA molecule, only one signal would be detected (non-coincident signal). This method was sensitive enough to detect a single copy of a gene in a complex genome without the need for amplification. However, specialised equipment is required for this type of detection.

1.12.3.2 FRET-Based Split-Probe systems.

Heller *et al.* [90] described an example of a homogeneous split-probe detector in 1983. In this case a chemiluminescent catalyst was attached to the 5'-terminus of one oligo probe and an absorber/ emitter moiety to the 3'-terminus of the other. On binding of the oligos to contiguous regions of the target, the catalyst and the absorber/ emitter moiety became juxtaposed (Figure 1.27). On correct binding of the probes light emission was induced for the chemiluminescent catalyst. This light was absorbed by the absorber/ emitter moiety, which then fluoresced at a longer wavelength. The chemiluminescent catalyst could also be replaced by an absorber/ emitter, which absorbs a shorter wavelength of light and transfers this by FRET to the other absorber/ emitter, which emits at a longer wavelength.

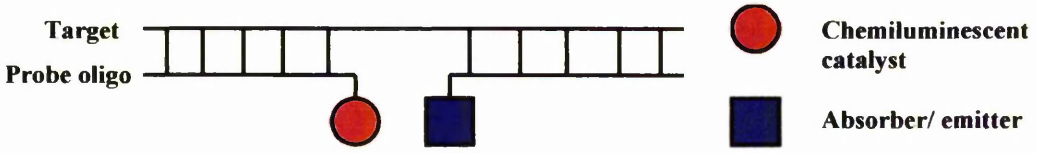

Figure 1.27: Diagram of the split-probe system proposed by Heller *et al.* [90].

This FRET-based method was illustrated by Cardullo *et al.* [90] using rhodamine and fluorescein. On correct binding and irradiation at the excitation wavelength of fluorescein, quenching of the fluorescein emission and increased rhodamine emission was observed.

Oser and Valet [91] used a similar split-probe system where the energy donor was a salicylate group attached to the 5'-terminus of one oligo. A diethylaminepentacetate ligand bearing an energy acceptor/ fluorescence emitter Tb^{3+} complexed to the ligand was attached to the 3'-terminus of the other (Figure 1.28). On hybridisation of both probes to the target and irradiation, long-lived fluorescence was observed from Tb^{3+}. This increased with increasing target concentration and was inhibited by addition of unlabelled probe oligo, showing that the signals seen were due to energy transfer between the salicylate group and the Tb^{3+} complex. A background signal of short-lived fluorescence from energy transfer from the bases could be removed by monitoring only the delayed fluorescence from the Tb^{3+} (time-gating).

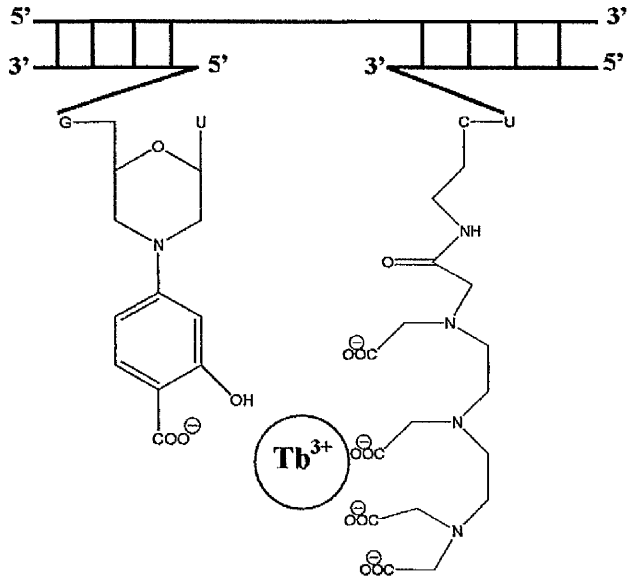

Figure 1.28: Schematic representation of the split-probe system of Oser & Valet [91]. The energy donor salicylate group was attached to the 5'-terminus of one oligo, and the diethylaminepentacetate ligand bearing the Tb^{3+} energy acceptor/ fluorescence emitter to the 3'-terminus of the other.

1.12.3.3 Excimer-based split-probe systems.

Split-probe systems based on excimer fluorescence have been described. Ebata *et al.* [92-94]attached pyrene to the 5'-terminus of one oligo probe and to the 3'-terminus of the other. The probes bound to contiguous regions of the target, bringing the pyrene molecules into close proximity (Figure 1.29).

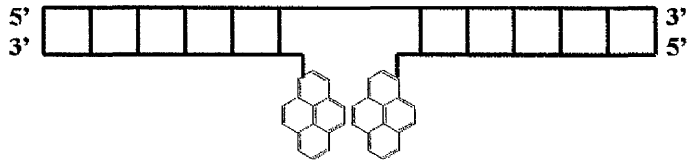

Figure 1.29: Diagram of the excimer-based split-probe system of Ebata *et al.*[92-94].

Hybridisation was carried out in phosphate buffer containing 20 % v/v DMF. As target concentration increased excimer fluorescence increased and monomer fluorescence decreased. The opposite effect was seen on heating. If one probe lacking a pyrene group was used no excimer fluorescence was seen. From this evidence it was concluded that the effect on the fluorescence spectrum was due to excimer formation between the two pyrene groups, and not due to intercalation or base stacking interactions between pyrene and the nucleobases. Melting curve experiments and CD spectral evidence also supported the fact that pyrene did not interact with the duplex. Intercalation would stabilise the duplex, raising the T_m. However, the T_m value was not appreciably affected and the CD spectrum

showed that pyrene was not in a chiral environment, suggesting no interaction with the helix. For targets containing one or two extra nucleotides in the centre of the target, which separated the two probes, excimer emission decreased suggesting that the pyrene molecules need to be close. In fact, the distances between bases in a B-DNA helix is ~3.4 Å, which corresponds to the interplanar distance of pyrene dimers in crystals. Excimer emission was affected by the percentage DMF, showing a maximum emission at 30-40 % v/v DMF. It was thought that the organic solvent could increase quantum efficiency due to pyrene-solvent dipole-dipole interactions or by preventing intercalation into the helix. Sodium ion concentration was also seen to affect excimer intensity, which peaked at 0.1 M NaCl. Sodium ions exert their effect indirectly by affecting duplex formation. The length of the linkers also affected excimer intensity, which was greatest when a shorter linker was used.

A similar excimer split-probe system using two contiguously binding probe oligos was employed by Paris *et al.* [95], who attached pyrene directly to the ribose sugar, replacing the natural DNA bases. Five different probe pairs were studied, each having different spacing between the pyrene groups. This was achieved by inserting or removing nucleotide residues in the probe sequences, as shown in Figure 1.30. For all the probe systems tested, addition of the target caused quenching of monomer emission, and the appearance of an excimer band around 490 nm. The N-2 spacing was found to give the best excimer: monomer ratio (intensity of excimer fluorescence at 490 nm: intensity of monomer emission at 398 nm). In this study excimer emission was detected in PIPES buffer without organic solvent. The system was also able to distinguish between a perfectly matched target and one possessing a mismatch along the binding site of one probe, with mismatched targets giving no excimer emission.

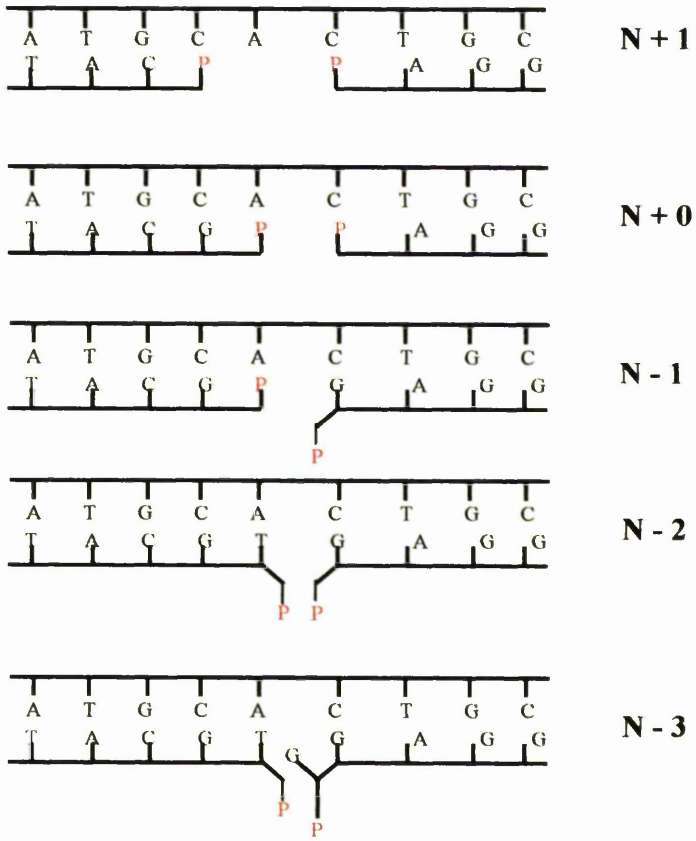

Figure 1.30: Diagramatic representations of the spacings between the pyrene groups (P) in the excimer split-probe systems of Paris *et al.* [95]

1.13 Split-probe exciplexes as detector systems.

In this thesis a split-probe system will be developed, similar in principal to the excimer systems described above, to detect the presence of particular DNA or RNA sequences in a sample. The 5'-and 3'-termini of the respective probe oligos used in the split-probe systems developed in this thesis will bear partners, which will form exciplexes with each other (Figure 1.31). Exciplexes, as described above, have the advantage over excimers that the range of structures possible for A and D is broad for exciplexes, but rather limited for excimers. Also there is a direct linear relationship between the emission frequency of an exciplex and the difference in redox potential of the partners [96;97]. Therefore the emitted fluorescence is tunable in principle for exciplexes, but not for excimers.

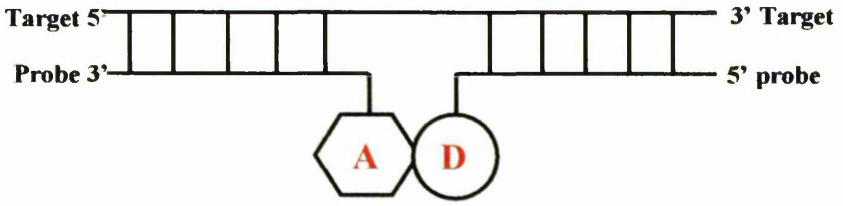

Figure 1.31: Diagramatic representation of the split-probe exciplex system to be studied in this thesis, where A and D represent the exci-partners capable of forming exciplexes if A≠D and excimers if A=D.

The split-probe system developed should be specific, an excimer/ exciplex emission should be detected only on correct hybridisation of the probes with the target sequence. In the absence of the target molecule the probes will display no excimer/ exciplex fluorescence. The signal will only develop if the probes are adjacently hybridised, as in order for excimer/ exciplex formation to occur the fluorophores must be within approximately 4 Å, although as mentioned earlier the relative geometry of the two fluorophores does not have to be strictly a sandwich structure. The exciplex/ excimer approach differs from other techniques such as fluorescence resonance energy transfer (FRET), as FRET can occur over 10-60 Å, Therefore, background signals for FRET systems arises from non-specific binding in the general region of the intended site. Also exciplex detection will be potentially highly sensitive as the excimer/ exciplex signal is red-shifted, with Stokes shifts typically more than 100 nm, relative to the monomer. Therefore, little or no background signal from the excitation light will be present. This overlap of excitation and emission peaks can be a source of reduced sensitivity as a portion of the excitation light can reach the detector by scattering and reflection if excitation and emission spectra overlap. Another advantage of this system over current methods is that the probes should be easy to prepare, have a long shelf-life and be safe to handle, unlike radio-labelled probes. Once the probes have been prepared no further reactions are necessary. Assays will be performed in solution without the need for probe immobilisation, with no washing steps required to remove unbound probe, and no cascade of reactions required for signal development, as for biotinylated probes. The split-probe system will be tested against targets containing various mismatches and insertions to determine whether this system could be of use in detecting SNPs in genetic sequences.

The system will be studied under various conditions using different linkers, RNA and DNA targets, LNA-based probes and a variety of solvents and additives. All these various conditions could affect the performance of the excimer/ exciplex split-probe

system by affecting how the exci-partners interact with each other and the duplex, or by affecting the structure of the duplex. These may affect how the exci-partners co-locate.

1.14 Three-dimensional Structure of Split-Probe Systems

At the concept stage of the split-probe exciplex approach it was necessary to have some structural basis on which to design potential probes. So, some discussion now follows on relevant DNA structures. From early studies of the structure of DNA using fibre diffraction, circular dichroism and infrared spectroscopy, it became apparent that the double helical structure could be categorised into two main families, A and B. A new structural family has since been found displaying a left-handed Z helix. Structures belonging to the A and B families show right-handed double helical structures which differ in the way the base pairs stack and how the sugar-phosphate backbones are arranged relative to one-another.

B-like DNA helices (Figure 1.33) typically have 10 base pairs per helical turn [98], with the bases perpendicular to the axis. The helix has a narrow but distinct minor groove and a wide major groove. The ribofuranyl sugars are generally found in a C3' exo or C2' endo conformation (N-type) (Figure 1.32). This notation describes the sugar pucker: XN' describes which atom is out of the plane of the 5-membered ring; exo or endo denotes whether the atom is out of plane on the opposite side, or the same side of the ring as the C5 atom, respectively.

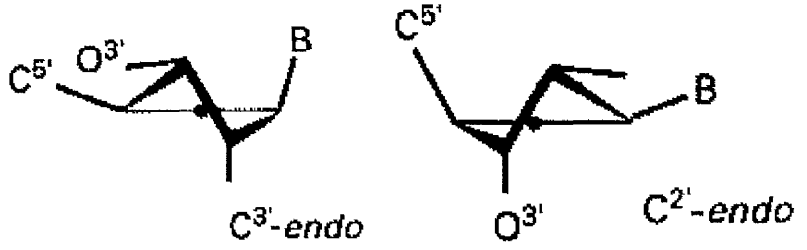

Figure 1.32: Schematic representation of the C3'-endo and the C2'-endo conformations adopted by the sugar rings of nucleotides [17].

A-like helices [99] (Figure 1.33) are wider than the respective B-like helices, they have 11 base pairs per turn, and the bases are sharply canted to the axis. The A-helix has a wide cavernous major groove, but the minor groove is virtually absent. The sugars are found in the C3' endo (S-type conformation) (Figure 1.32).

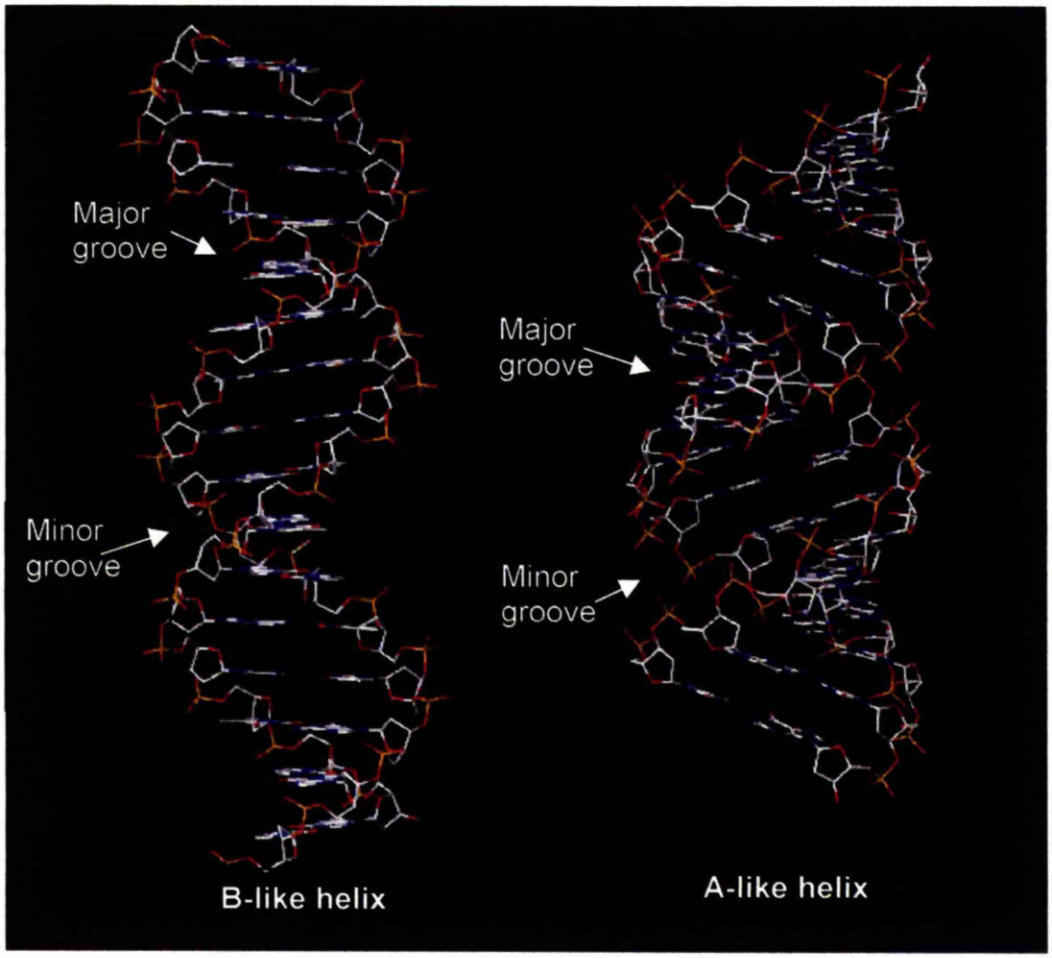

Figure 1.33: A and B forms of the DNA duplex (5'-dGCCAAACACAGAATCG-3'):(5'-dCGATTCTGTGTTTGGC-3') showing the major and minor grooves.

High-resolution NMR structural studies have been carried out on a split-probe system consisting of a 12-mer target and two 6-mer oligos, which bind contiguously to the target, one labelled with a pyrenyl group on its 5'-phosphate and the other labelled with a perfluoroazide group on its 3'-phosphate (see Figure 1.20). This tandem split-oligo system formed a tight specific duplex at temperatures less that 10 °C. The structure of this complex had characteristics of a B-type duplex, but there were strong conformational distortions throughout, especially at the site of the "nick" and modifying groups. The duplex half on the side of the azido group showed greater distortion. The tandem system behaved dynamically as the equivalent of two short B-DNA-like duplexes, hinged in the middle. In all the final structures the location of the pyrene group was very restricted, lying mainly in the minor groove. The azide group, on the other hand, showed a higher degree of flexibility, being located outside the duplex on the side of the minor groove [100;101].

FRET and photomodification data were used to determine the distance between the fluorophores in this system [70]. As described earlier the energy transfer rate depends on the inverse sixth power of the distance between the donor and the acceptor. If this distance is considered as fixed then the rate constant of sensitised photoreactions should also depend on the inverse sixth power of the distance between the donor and the acceptor. The distance between the pyrene and the azide group was found to be 11.2 Å as determined by FRET and 12.6 Å determined from photomodification data. From NMR studies this distance was found to be 8 Å.

Other studies on unmodified helices possessing backbone nicks have also shown the helices to adopt classical B-like structures comparable to the unnicked related structures [102-105]. These structures also showed a distortion near the nicked site, but this was only very slight. The bases on either side of the nick are well stacked, as in the corresponding intact duplexes. Melting experiments showed that melting of the nicked tandem duplexes was cooperative. Melting curves showed only one transition [105]. This is consistent with the modified tandem duplex of Dobrikov *et al.*, which also shows cooperative melting of the two modified oligos [100].

As the DNA split-probe systems to be developed in this thesis will be similar to the system described by Bichenkova *et al.* [100;101] they may also adopt similar distorted B-like structures in aqueous solution. However, no structural studies will performed in this thesis and this structure may be affected by various additives and co-solvent to be used. The split-probe oligo systems and the various studies to be performed on them are discussed in the "Aims of the Thesis" Section which follows.

1.15 Aims of the Thesis.

The aim of this thesis is to develop a split-probe exciplex/ excimer system that can be used to detect specific target oligonucleotide sequences. The model split-probe system to be studied will comprise a target sequence plus two probe oligos (two 8-mers), one bearing an exci-partner on its 5'-phosphate and the other bearing an exci-partner on its 3'-phosphate. The probes will be Watson-Crick complementary to the target sequence. The split-probes will assemble at the target oligo (16-mer), thereby bringing the exci-partners into close proximity (Figure 1.34). On irradiation an exciplex/ excimer signal will be detected if assembly has correctly taken place.

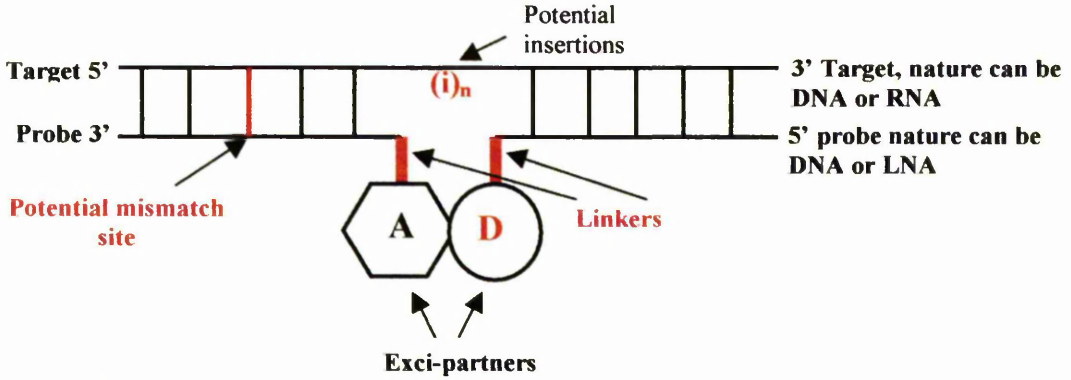

Figure 1.34: Schematic diagram of how the exci-partners, A and D, are brought together when the two split-probe oligos bind to the target.

The effects of various modifications to the system (Figure 1.34) and hybridisation conditions on exciplex/ excimer emission to be investigated include:

1. effect of linker
2. nature of the target
3. nature of the partners
4. effect of additives and co-solvents
5. effect of mismatches and insertions in the DNA target
6. nature of the oligo probe: LNA in comparison with DNA

1.15.1 Effect of linker.

Various methods of attaching potential exci-partners to probe oligos have been used in the literature, and thus there is a wide scope for variation. In this thesis two methods of linkage will be compared to determine their effect on excimer/ exciplex emission. The first linkers to be tested will be short linkers, such as NH_2-CH_2 groups or ethane-1,2-diamine ($NH_2(CH_2)_2NH_2$) groups. In addition, a short polypeptide chain (4 amino acids) will also be used as a linker. Parallel β-sheet-like formation (Figure 1.35 and 1.36) is possible in principle between the two peptide strands due to hydrogen bonding between the carbonyl oxygens and amide NHs of the backbone. This β-sheet formation could increase exciplex/ excimer emission in two ways. Firstly, formation of the β-structure could bring the exci-partners on the ends of the peptide strands into close proximity, as required for excimer/ exciplex emission. Secondly, the β-structure would rigidly hold the exci-partners away from the nucleobases, preventing any undesirable competing interaction between these and the exci-partners.

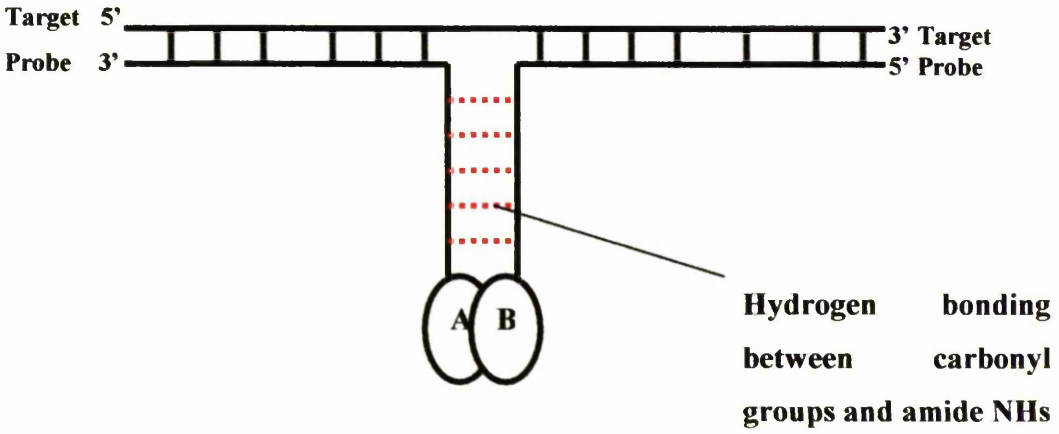

Figure 1.35: Diagramatic representation of how β-sheet formation between peptide linkers could bring exci-partners, A and B, into close proximity and minimise interaction with the nucleobases.

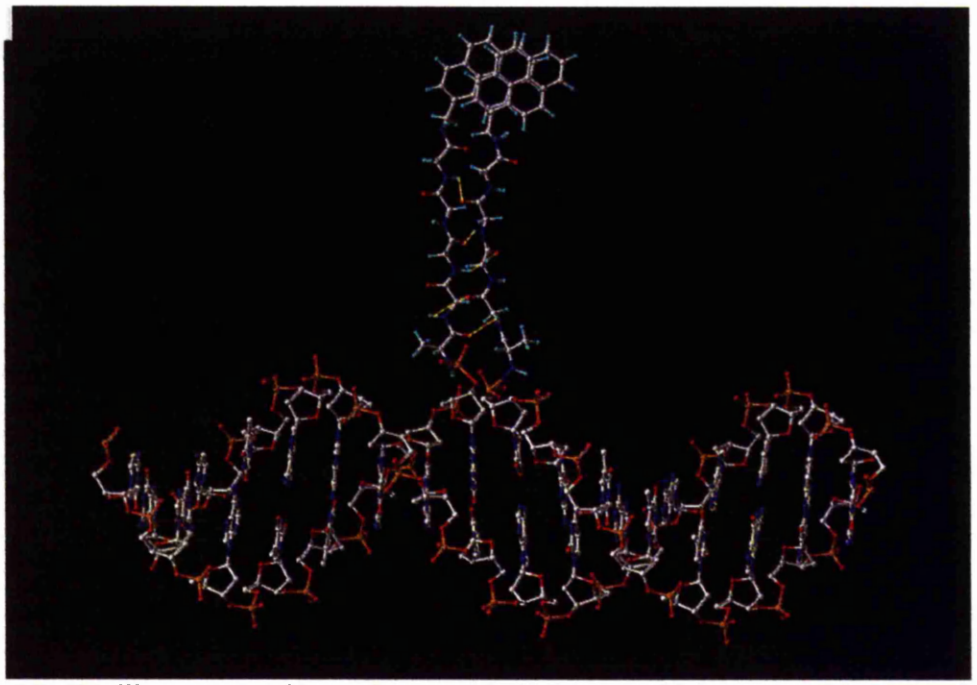

Figure 1.36: 3D illustration of how the peptide linkers could interact with each other to bring the exci-partners into close proximity to allow exciplex formation on irradition.

1.15.2 Nature of the target.

DNA-DNA homoduplexes are able to form A, B or Z-like structures. NMR structural analysis of a similar DNA-DNA split-probe system modified with pyrene and a perfluoroarlyazide group showed the structure to adopt a highly distorted B-DNA-like structure in aqueous solution [100;101]. Thus exciplex/ excimer formation will be studied using normal DNA base/ sugar structures in both target and probes. The standard DNA target

sequence chosen is dGCCAAACACAGAATCG, as this non self-complementory sequence is free from potential secondary structure complications.

However, the structure of the DNA-RNA heteroduplex is intermediate between the A and the B-type structure [106]. Exciplex/ excimer emission will therefore also be studied using a RNA:DNA heteroduplex. An analogous system will be tested using an RNA sequence as the target with the DNA-based probe oligos to determine whether these probes can also be used to detect RNA target sequences. The standard RNA sequence (using ribonucleotides) was GCCAAACACAGAAUCG (the RNA equivalent of the DNA target).

1.15.3 Nature of the Partners.

The effect on exciplex emission will be studied of *bis*-substituted probes, where the terminal phosphate group carries two substituents, with one substituent always an exci-partner. If one substituent is a hydrophobic (non-exci-partner) group this could preferentially interact with the nucleotide bases or DNA surface, leaving the other substituent, the exci-partner, free for excimer/ exciplex formation. Alternatively, it will be investigated if having more than one exci-partner substituent on the terminal phosphate increases excimer/ exciplex emission due to an increased probability of exci-partner interaction, or the possible formation of sandwich structures.

1.15.4 Effect of additives and co-solvents.

Various additives such as betaine, sulfolane, methylsulfone and dimethyl sulphoxide are used in PCR as denaturants to increase yield and specificity. They act by destabilising the double helix of DNA by hydrogen bonding to the major and minor grooves, thereby decreasing the T_m of DNA and RNA [107;108]. The binding of these PCR additives to the major and minor grooves could prevent possible interactions of the exci-partners with the nucleobases in the present split-probe structure, leaving the exci-partners free to interact with one-another. The effect of these PCR additives and various co-solvents will also be studied in terms of their differential effect on excimer and exciplex emission. Exciplex emission is more sensitive than excimer emission to solvent polarity as it contains an element of charge transfer [21].

1.15.5 Effect of Mismatches and Insertions in the DNA target.

The effect of various single and double mismatches and insertions in the DNA-target strand on excimer/ exciplex emission of split-probes will be evaluated. Signals

observed for such mismatches will be compared to a perfectly matched target as they could be exploited in the future to develop a split-probe system to detect the presence or absence of specific mutations in genetic sequences (SNPs).

1.15.6 Nature of the probe: LNA

An LNA residue contains a 2'-O, 4'-C methylene-linked ribofuranosyl nucleoside locking it into the N-type conformation. As LNA obeys Watson-Crick base pairing and displays unprecedented affinity to DNA, increasing the T_M by 3 to 8 °C per modified base in an LNA/DNA duplex [19;109] its inclusion into an exci-probe could be very desirable. Probes containing LNA residues will be compared to DNA-based probes with respect to the ability of the exci-partners to form excimer/ exciplexes. These probes will be designed as perfect matches to the part of the prothrombin gene that carries the G-A mutation at position 20210 in the 3-'untranslated section. This mutation causes an increase in plasma concentration of prothrombin, which in turn increases the risk of thrombosis [2;110]. Therefore this study will also investigate whether the system can be applied to actual genetic sequences.

2. Materials and Methods

2 Materials and methods.

2.1 Split-probe constructs studied.

2.1.1 Experimental split-probe systems.

Sequences used for systems SP-1 to SP-12 and control systems C-1 to C-3 are shown below along with the constructs of these systems:

Target $^{5'}$pdGCCAAACACAGAATCG

Oligo1 $^{5'}$pdTGTTTGGC **Oligo2 dCGATTCTG$^{3'}$p**

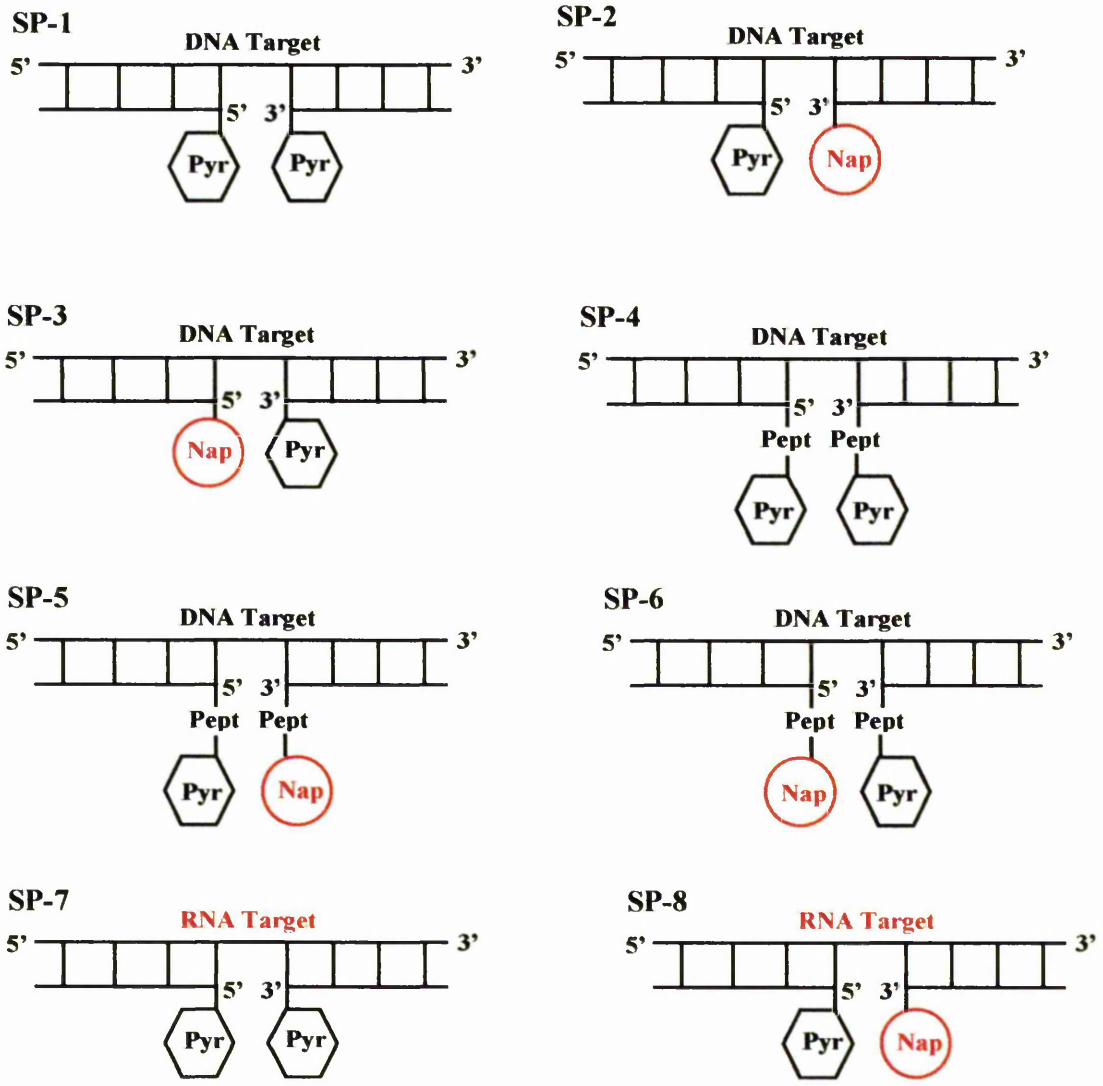

SP-9

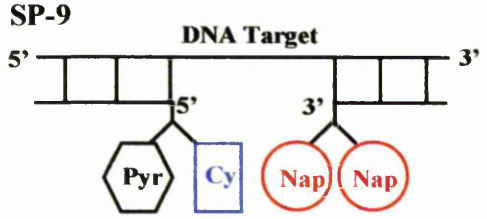

SP-10

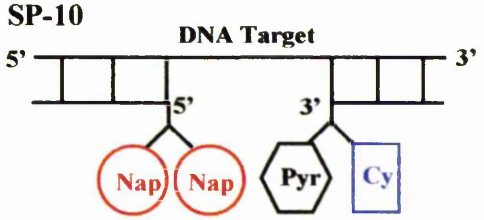

SP-11

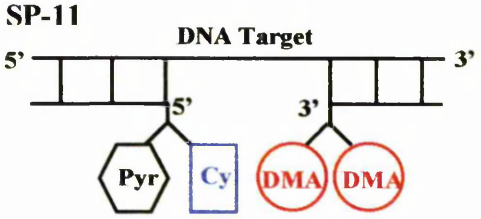

SP-12

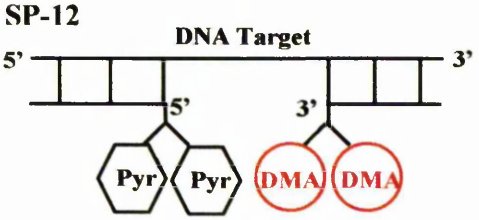

2.1.2 Control Systems

C-1

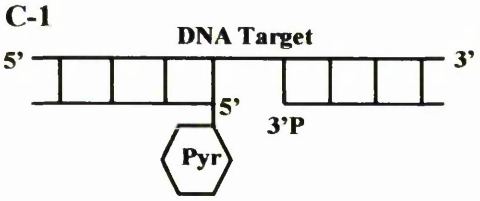

C-2

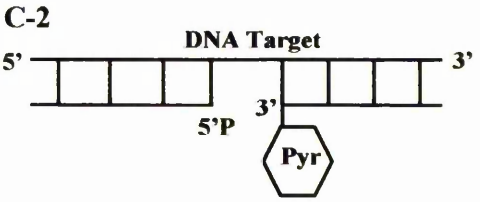

C-3

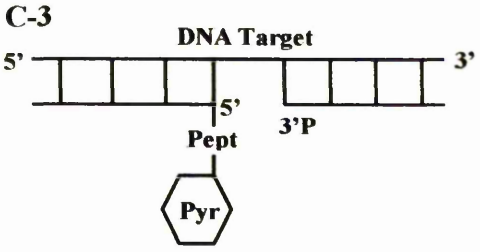

C-4

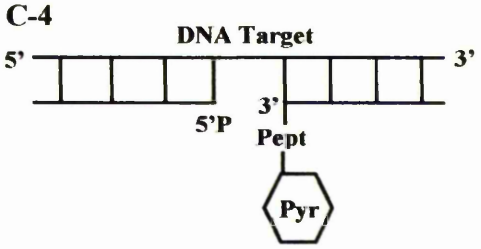

C-5

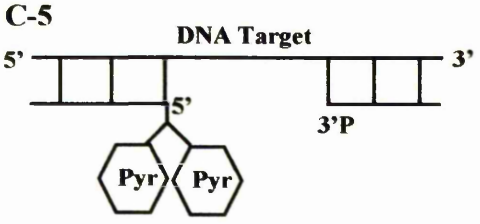

2.1.3 Prothrombin Systems

Sequences used for the prothrombin systems, SP-13 to SP-15, are shown below along with the nomenclature used for these sequences and the various constructs of these systems, red capital letters denote LNA nucleotides.

Proexc 1 $^{5'}$a a a g t g a c t c t c a g c g a g c c t c a a t g c t c c$^{3'}$

Proexc 10 $^{3'}$c t g a g a g t c g$_p$ $_p$c t c g g a g t t a$^{5'}$ Proexc 3

Proexc 11 $^{3'}$c t g a G a G t c g$_p$ $_p$c t c G g A g T t a$^{5'}$ Proexc 4

Proexc 9 $^{3'}$c t g a g a g t c g$_p$

SP-13 (LNA System)

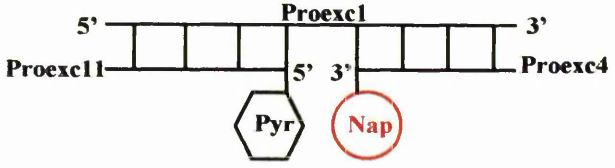

SP-14 (DNA System)

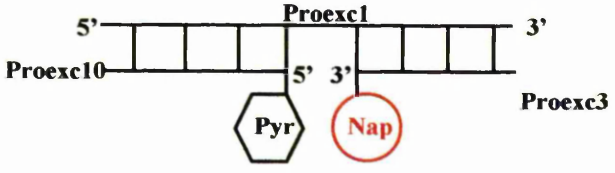

SP-15 (DNA Diene System)

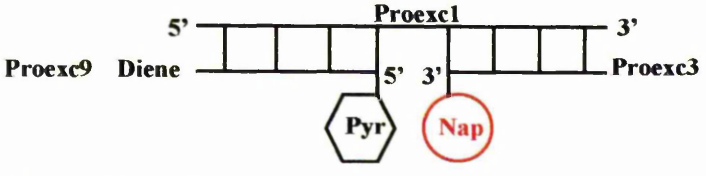

2.1.4 Prothrombin control systems

C-4 (LNA System)

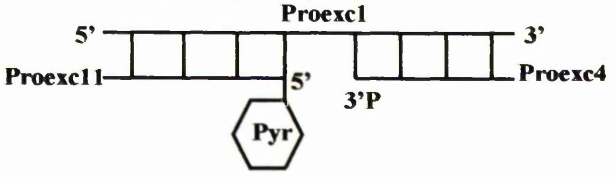

2.1.5 Structures of the exci-partners and the methods of attachment to the oligos.

The structures of the exci-partners used for the split-probe systems given above are now shown in Figures 2.1, 2.2 and 2.3, along with the method of attachment to the terminal phosphate groups of the olios

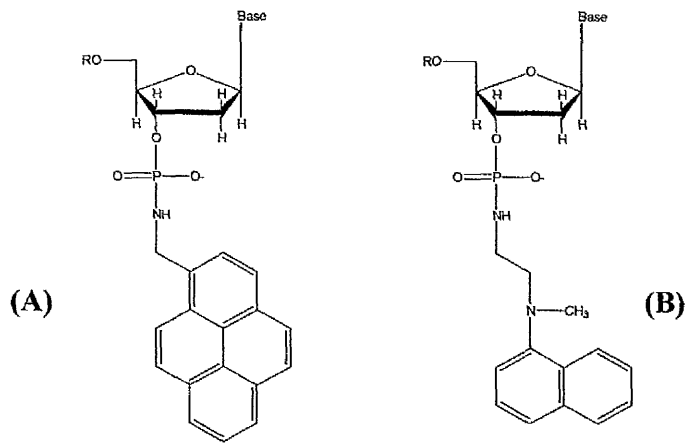

Figure 2.1A: Attachment at the 3'-site of the terminal phosphate group of the probe oligos. (R= oligonucleotide) of the exci-partners (A) 1-pyrenemethylamine and (B) N'-methyl-N'-naphthalen-1-yl-ethane diamine.

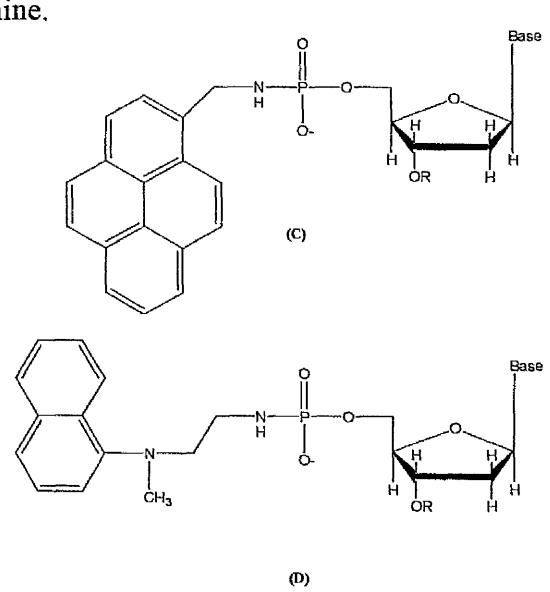

Figure 2.1B: Attachment at the 5'-site of the terminal phosphate group of the probe oligos of the exci-partners, (C) 1-pyrenemethylamine and (D) N'-methyl-N'-naphthalen-1-yl-ethane diamine.

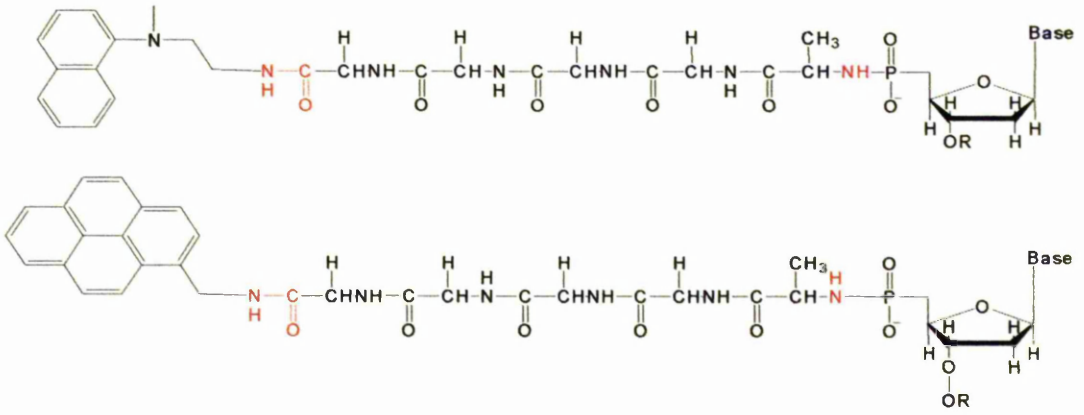

Figure 2.2: Structures of the peptide linker groups bearing the exci-partners, pyrene and naphthalene, attached to the 3'-positions. The substituents were similarly attached to 5'-phosphate. R = oligonucleotide.

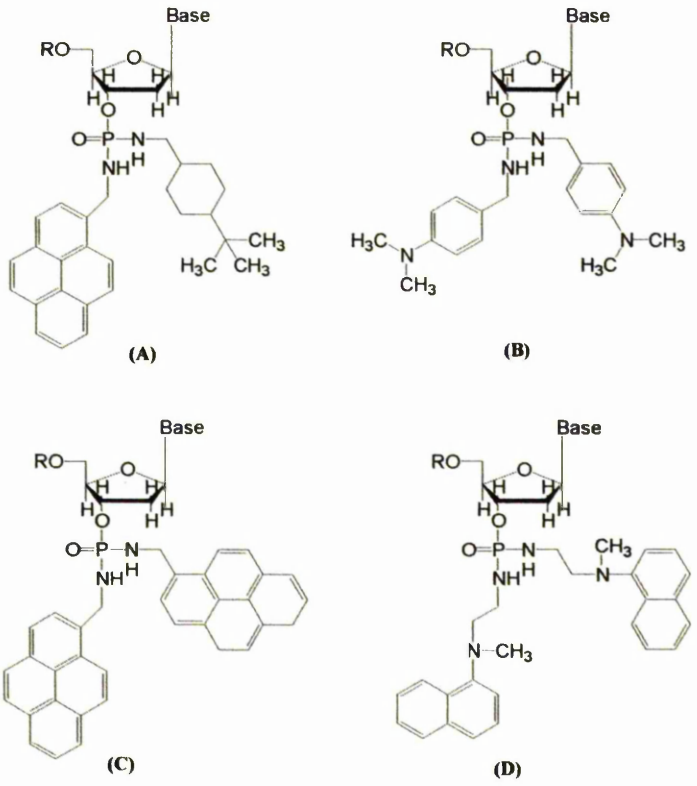

Figure 2.3: Bis-substituted terminal phosphates with: (A) 1-pyrenemethylamine and 4-tert-butylcyclohexylmethylamine (designated cyclohexylpyrene), (B) two molecules of dimethylaminobenzylamine (designated bis-DMA);(C) two molecules of 1-pyrene methylamine (designated bis-pyrene); (D) two molecules of N'-Methyl-N'-naphthalen-1-yl-ethane-1,2- diamine (designated bis-naphthalene). The diagrams show 3'-attachment but substituents were also similarly attached to 5'-phosphate. R = oligonucleotide.

2.2 Materials.

Reagents were obtained from the following suppliers.

Aldrich: 1-Pyrenemethylamine; cetyltrimethylammonium bromide; triphenylphosphine; dipyridyldiphosphate; dimethylaminopyridine; triethylamine; lithium perchlorate; dimethylformamide; hydroxybenzotriazole; N-methylmorpholine; dicyclohexylcarbodiimide; trifluoroacetic acid; tetramethylene sulfone (sulfolane); betaine monohydrate; methylsulfone; 2,2,3,3-tetrafluoro-1-propanol; N-methylformamide; 1,1,1,3,3,3-hexafluoro-2-propanol; ethylene glycol; ethylene glycol dimethyl ether; 3-chloro-1,2-propandiol; 2,2,3,3,3-pentafluoro-1-propanol; 2,2,3,3,4,4,4-heptafluoro-1-butanol; 2-(pentafluorophenoxy)ethanol; perfluoro-tert-butyl alcohol; 2,2,3,4,4,4,-hexafluoro-1-butanol; 2,2,2-trichloroethanol; 2,2,2-trifluoroethanol; 1-chloro-2-propanol.

Bachem: BocAla$(Gly)_4$OH

BDH: Acetone; ethyl acetate; methanol; ethanol; tris(hydroxymethyl)methylamine; sodium chloride; sodium hydrogen carbonate; citric acid.

Fisher Chemicals: Dimethyl sulfoxide.

Goss Scientific: d_1-chloroform, deuterium oxide.

Oswel: DNA oligo probes, DNA target (parent and mismatches), RNA target.

Proligo: DNA and LNA oligo probes, and DNA target for prothrombin study.

Riedel-de Haën: Hexane, acetonitrile

Cambridge Isotopes: d_4-methanol.

2.3 Instruments.

2.3.1 Reversed-phase HPLC

HPLC purification was performed on a Gilson system using a Kontron 332 UV detector, and a Vydac 218TP C18 column (length 100mm, inner diameter 10mm particle size 7μm).

2.3.2 Nuclear magnetic resonance spectroscopy.

NMR spectra were recorded on a Bruker spectrometer operating at 300 MHz for ^{1}H spectra. Chemical shifts (δ) are reported in parts per million (ppm) relative to tertramethylsilane (Me_4Si, δ_H 0.00).

2.3.3 UV-visible spectroscopy.

UV and visible spectra were recorded in 1 cm path length quartz cuvettes using a Peltier-thermostatted cuvette holder in a Cary 1E UV-visible spectrophotometer.

2.3.4 Melting curves.

Melting curve experiments were performed in a purpose-built, 6-position Peltier thermostatted cuvette holder in quartz cuvettes using a Cary 1E UV-visible spectrophotometer. The heating rate could be ramped at programmed values to record the change in absorbance on an increasing or decreasing temperature gradient. The usual heating rate was 2 °C/ minutes.

2.3.5 Spectrophotofluorimetry.

Fluorescence emission and excitation spectra were recorded in 4-sided quartz thermostatted cuvettes using a Shimadzu RF-5301PC spectrofluorophotometer with the temperature controlled by circulating water from a Haake GH water cooler.

2.4 Methods: Synthesis.

2.4.1 Attachment of 1-pyrenemethylamine to oligonucleotide probes.

1-Pyrenemethylamine was attached *via* a phosphoramide link to the terminal 5'-phosphate of Oligo1 (5'pdTGTTTGGC) or the 3'-phosphate of Oligo2 (dCGATTCTG3'p). To do this the cetyltrimethylammonium salt of the oligonucleotides (2 mg, 1 μmol) was prepared by addition of 4% aqueous cetyltrimethylammonium bromide (50 μl, 10 μl x 5) to a solution of the lithium salt of the oligonucleotide (2 mg, 1 μmol) in 200 μl of water, with centrifugation on each addition, until no more precipitation was observed. The supernatant was removed and the precipitate dried *in vacuo* overnight. The cetyltrimethylammonium salt of the oligonucleotide (~1 μmol) was dissolved in DMF (200 μl), triphenylphosphine (12 mg, 50 μmol) and 2,2'-dipyridyl disulfide (11 mg, 50 μmol) added, and the reaction mixtures incubated at 37 °C for 10 min. 4-*N'*, *N'*-Dimethylaminopyridine (6 mg, 50 μmol) was added and the reaction mixture incubated for a further 10 minutes at 37 °C. To the oligonucleotide reaction mixture 1-pyrenemethylamine hydrochloride (4 mg dissolved in 100 μl of DMF and 3 μl triethylamine) was added and the reaction mixtures were incubated at 37 °C for 6 hours. After this time the reaction mixture was split into two tubes and the oligonucleotide precipitated by 2 % $LiClO_4$ in acetone (2 ml). After centrifugation the supernatant was carefully removed and the precipitate redissolved in water (180 μl) and centrifuged to remove any activating agents still present. The supernatant was removed and the modified oligo reprecipitated in 2 % $LiClO_4$ by acetone. The oligonucleotide conjugate was then separated from unreacted precursors by reverse-phase HPLC (eluted by 0.05 M $LiClO_4$ with a gradient from 0 to 40 % acetonitrile). Products were characterised initially by UV/ visible spectroscopy. Yields were typically around 80%. The absorbance spectra of unmodified Oligo1 and Oligo1_5'pyrene are shown in Figure 2.4. The absorbance around 345 nm is due to the presence of pyrene, which also alters the band at 260 nm. The ratio between the absorbances at 260 and 345 nm was around 3.0, typical of mono-pyrene-substituted 8mer-oligos (Oligo1_5'pyrene A_{260} : A_{345} 3.2, Oligo2_3'pyrene A_{260} : A_{345} 2.9). If *bis*-pyrenylation had occured the A_{260} : A_{345} ratio would be typically 2.

Figure 2.4: UV/visible absorption spectra of unmodified Oligo1 and Oligo1_5'pyrene in 50% v/v acetonitrile at 20 °C. The ratio A_{260}:A_{345} = 3.2 refers to Oligo1_5'pyrene

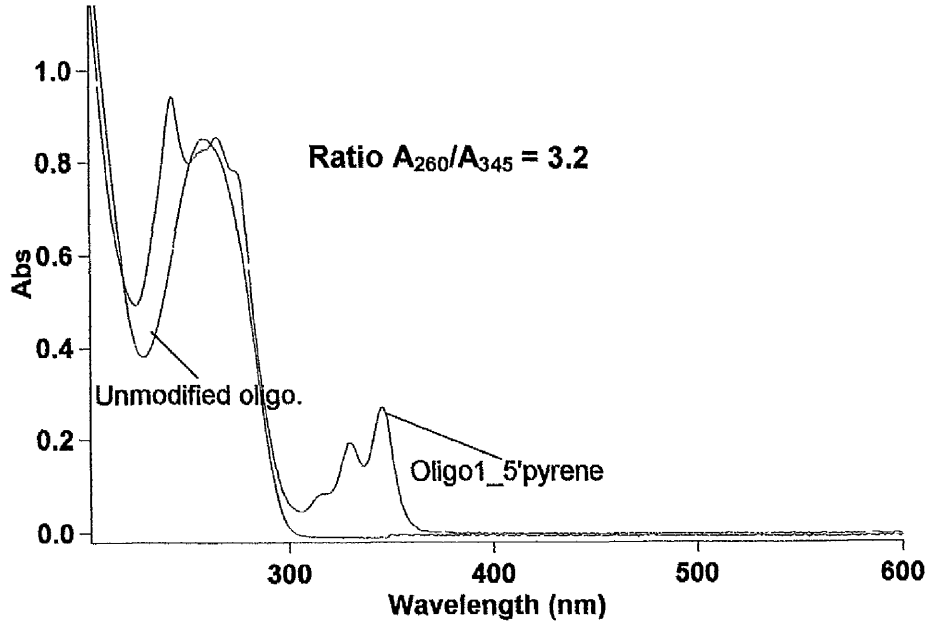

Appropriate fractions were combined, lyophilised and the oligos were characterised by ^1H NMR spectroscopy in D_2O.

Oligo1_5'pyrene: ^1H NMR (300 MHz, D_2O): δ_H 1.77-1.86 (m, 4 x CH_3 of 4 x dTs), 7.16-8.14 (m, 17H, 9 x Ar-H from pyrene and 8 x Ar-H from DNA bases; 1 from each dG (x3), dT(x4), 1 from dC).

2.4.2 Attachment of N'-methyl-N'-naphthalen-1-yl-ethane-1, 2-diamine to oligonucleotide probes.

N'-Methyl-N'-naphthalen-1-yl-ethane-1, 2-diamine was attached *via* a phosphoramide link to the terminal 5'-phosphate of Oligo1 (5'pdTGTTTGGC) or the 3'-phosphate of Oligo2 (dCGATTCTG3'p) by the procedure described, but using N'-methyl-N'-naphthalen-1-yl-ethane-1, 2-diamine dihydrochloride (2 mg, 7.3 μmol dissolved in 100 μl of DMF and 3μl triethylamine). The product was purified by reverse-phase HPLC (eluted by 0.05 M $LiClO_4$ with a gradient from 0 to 40 % acetonitrile). Products were identified by UV/ visible

spectroscopy and appropriate fractions were lyophilised and characterised by ^1H NMR spectroscopy in D_2O. Typical yields were around 80%. The UV/visible absorption spectra of unmodified Oligo1 and Oligo1_5'naphthalene are shown in Figure 2.5. The shoulder at 310 nm on the 260 nm absorption band indicates the presence of naphthalene.

Oligo2_3'naphthalene ^1H NMR (300 MHz, D_2O): δ_H 1.66-1.70 (m, 9H, 3 x CH_3 of 3 x dT), 2.79 (s, 5H, N'-methyl group), 5.4-6.37(10H 8 x H1' of sugar and 2 x H5' of 2 x dC), 6.91-8.34 (m, 18H, 7 Ar-H of naphthalene and 9 Ar-H from bases, 1 from each dG, dC and dT, 2 from each dA)

Oligo1_5'naphthalene ^1H NMR (300 MHz, D_2O): δ_H 1.54-1.65 (m, 15H, 4 x CH_3 of 4 x dT), 2.64 (s, 4H, CH_3 of N-methyl group), 5.65-6.09 (m, 9H, 8 x H1' of sugar and 1 x H5 of dC), 6.90-7.79 (m, 15H, 8 x Ar-H from bases, 7 x Ar-H of naphthalene)

Figure 2.5: UV/visible absorption spectra of unmodified oligo1 and oligo1_5'naphthalene in 50% v/v acetonitrile at 20°C.

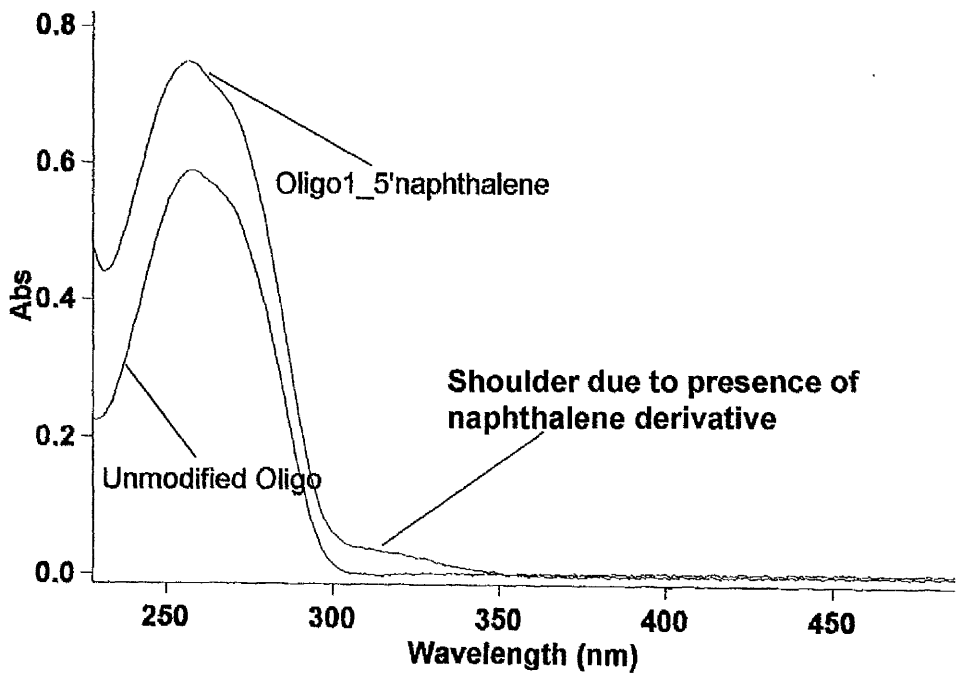

2.4.3 Synthesis of oligos modified with peptide linkers.

2.4.3.1 Synthesis of BocAla(Gly)$_4$NHCH$_2$Pyr.

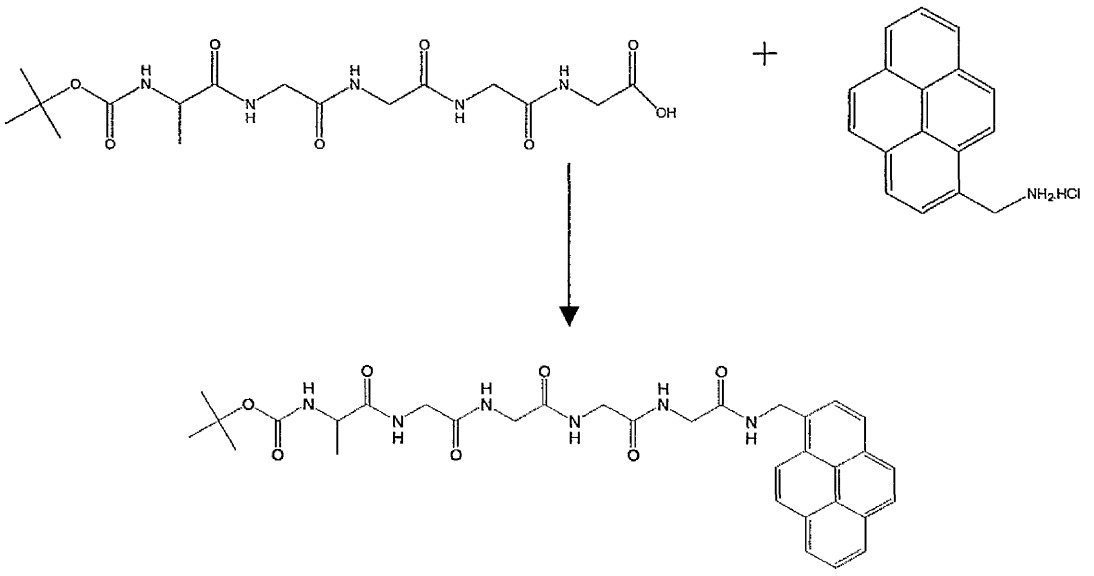

1-Pyrenemethylamine hydrochloride (0.25 g, 0.82 mmol) and triethylamine (0.11 ml, 0.82 mmol) were dissolved in DMF (15 ml) and stirred at room temperature for 30 minutes. BocAla(Gly)$_4$OH (0.25 g, 0.82 mmol), 1-hydroxybenzotriazole (0.11 g, 0.82 mmol) and N-methylmorpholine (0.091 ml, 0.82 mmol) were then added, the reaction cooled in an ice bath and dicyclohexylcarbodiimide (0.18 g, 0.8 6mmol) added. The reaction mixture was stirred in an ice bath for one hour, then refluxed for several hours, and stirred at room temperature overnight. The mixture was filtered to remove the urea formed and DMF was removed *in vacuo*. The residue was dissolved in ethyl acetate (50 ml) and extracted with 25 ml portions of saturated sodium hydrogen carbonate, 10 % citric acid, sodium hydrogen carbonate and finally water. The organic layer was dried over anhydrous sodium sulphate and the solvent removed *in vacuo* to give crude product as an orange solid. Attempts to recrystallise failed, so the peptide was deprotected before purification.

2.4.3.2 Removal of Boc from BocAla(Gly)$_4$NHCH$_2$Pyr.

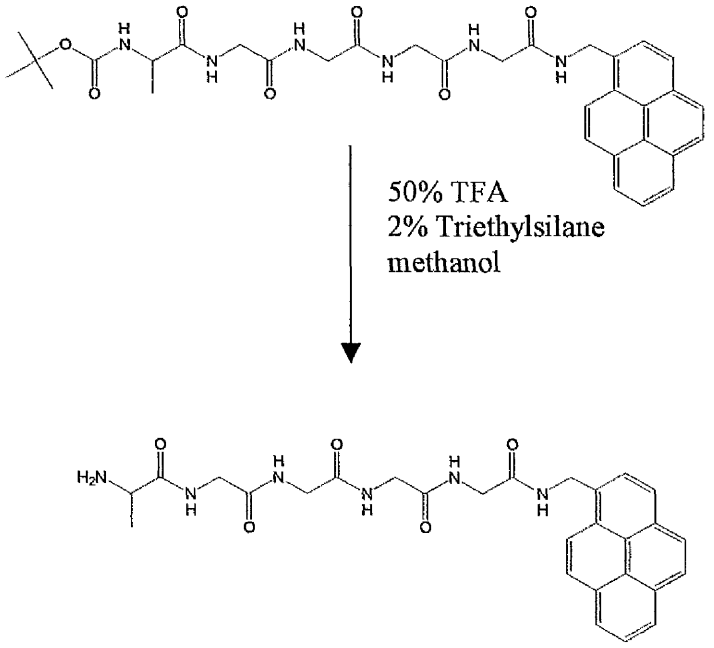

A solution of BocAla(Gly)$_4$NHCH$_2$Pyr in 50 % TFA and 2 % triethylsilane in methanol (total volume = 20 ml) was stirred for several hours at room temperature until TLC (ethyl acetate 60: methanol 40) showed complete reaction. Solvents and by-products were removed *in vacuo* and the product recrystallised from hexane and methanol as a slightly orange solid, which was characterised by ^{1}H NMR spectroscopy.

Ala(Gly)$_4$NHCH$_2$Pyr ^{1}H NMR (300 MHz, MeOD): δ_H 1.46 (d, 3H, CH_3 of alanine), 3.87-3.96 (m, 8H, 4 x CH_2 of glycine), 5.14 (s, 2H, methyl group of pyrenemethylamino group), 8.00-8.36 (m, 9H, 9 x Ar-H of pyrene)

2.4.3.3 Attachment of NH$_2$Ala(Gly)$_4$NHCH$_2$Pyr to oligonucleotide probes.

The modified peptide (NH$_2$Ala(Gly)$_4$NHCH$_2$Pyr) was attached *via* a phosphoramide link to the terminal 5'-phosphate of oligo 1 (5'pdTGTTTGGC) or the 3'-phosphate of Oligo 2 (dCGATTCTG3') as described above, but using NH$_2$Ala(Gly)$_4$CH$_2$Pyr (4.4 mg dissolved in 100 µl of DMF and 3 µl triethylamine). The product was purified by reverse-phase HPLC

(eluted by 0.05 M $LiClO_4$ with a gradient from 0 to 30 % acetonitrile). Products were identified by UV/ visible spectroscopy (Oligo1_5peptide-pyrene A_{260}: A_{345} 3.02, Oligo2_3'peptide_pyrene A_{260}: A_{345} 3.00) and appropriate fractions were lyophilised. Oligos were characterised by ^1H NMR spectroscopy in D_2O.

Oligo1_5'peptide-pyrene ^1H NMR (300 MHz, D_2O): δ_H 1.00-1.03 (d, 3H, CH_3 of alanine), 1.50-1.64 (m, 13H, 3 x CH_3 of 3 x dT), 5.40-6.06 (m, 9H, 8 x H1' of sugar and 1 x H5 of dC), 6.60-7.86 (m, 17H, 9 x ArH of pyrene, 8 x Ar-H of DNA bases, 1 from each dC, dG and dT, 2 from each dA)

Oligo2_3'peptide-pyrene: ^1H NMR (300 MHz, D_2O): δ_H 1.35-1.38 (d, 4H, CH_3 of alanine), 1.65-1.66 (d, 8H, 3 x CH_3 of 3 x dT), 5.69-6.06 (m, 8H, 8 x H1' of sugar), 7.15-8.06 (m, 17H, 9 x Ar-H of pyrene and 9 x Ar-H of bases (1 from dG and dT, 2 from dA)

2.4.3.4 Synthesis of BocAla(Gly)$_4$NHCH$_2$CH$_2$Nap.

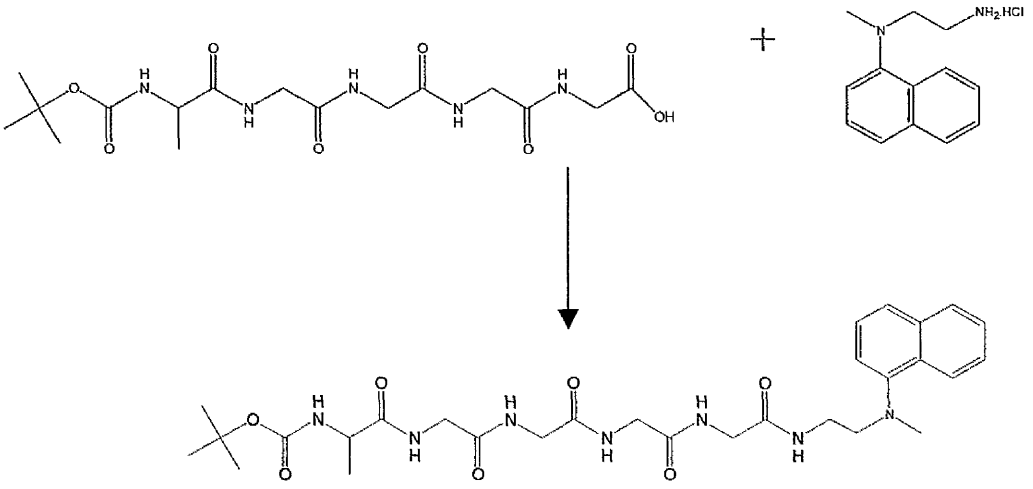

A solution of N'-methyl-N'-naphthalen-1-yl-ethane-1,2-diamine hydrochloride (0.08 g, 0.33 mmol) and triethylamine (0.07 ml, 0.33 mmol) in DMF (7 ml) was stirred at room temperature for 30 minutes. BocAla(Gly)$_4$OH (0.12 g, 0.33 mmol), 1-hydroxybenzotriazole

(0.04 g, 0.33 mmol) and N-methylmorpholine (0.036 ml, 0.33 mmol) were added, the mixture cooled in an ice bath and dicyclohexylcarbodiimide (0.07 g, 0.34 mmol) added. The reaction mixture was stirred in an ice bath for one hour, refluxed for three hours and then stirred at room temperature overnight. The reaction mixture was filtered to remove the urea formed and the DMF was removed *in vacuo*. The residue was dissolved in ethyl acetate (50 ml) and extracted with 25 ml portions of saturated sodium hydrogen carbonate, 10 % citric acid, sodium hydrogen carbonate and finally water. The organic layer was dried over anhydrous sodium sulphate and the solvent removed *in vacuo* to give an orange solid. This was found to be impure by TLC (DCM 80 : methanol 20) and, as attempts to recrystallise it failed, the peptide was deprotected before purification.

2.4.3.5 Removal of Boc from BocAla(Gly)$_4$NH(CH$_2$)N(CH$_3$)Nap

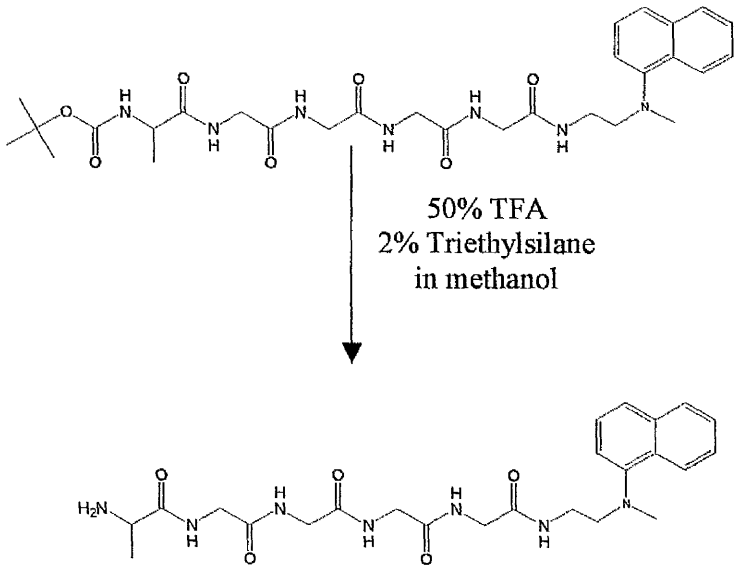

A solution of BocAla(Gly)$_4$NH(CH$_2$)N(CH$_3$)Nap in 50% TFA (10 ml) and 2 % triethylsilane in methanol (10 ml) was stirred for five hours at room temperature until TLC (ethyl acetate 60: methanol 40) showed reaction to be complete. Solvents and volatile side

products were then removed *in vacuo*, and the product recrystallised from hexane and methanol to give a slightly orange solid, which was characterized by ^{1}H-NMR spectroscopy.

Ala(Gly)$_2$NHCH$_2$Nap ^{1}H NMR (300 MHz, D_2O): δ_H 1.41 (d, 3H, CH_3 of alanine), 1.69-1.73 (m, 3H, CH_2 of N'-methyl-N'-naphthalen-1-yl-ethane-1,2-diamino group), 1.82-1.86 (m, 3H, CH_2 of N'-methyl-N'-naphthalen-1-yl-ethane-1,2-diamino group), 3.87-3.82 (m, 8H, 4 x CH_2 of glycine), 4.01-4.12 (m, 1H, CH of alanine), 7.22-8.32 (m, 6H, 7 x ArH of naphthalene)

2.4.3.6 Attachment of NH$_2$Ala(Gly)$_4$NH(CH$_2$)N(CH$_3$)Nap to oligonucleotide probes.

The modified peptide (NH_2Ala(Gly)$_4$NH(CH_2)N(CH_3)Nap) was attached *via* a phosphoramide link to the terminal 3'-phosphate of Oligo 2 (dCGATTCTG3'p) as described above, but using NH_2Ala(Gly)$_4$NH(CH_2)N(CH_3)Nap (8.7 mg dissolved in 100µl of DMF and 3 µl triethylamine). Product was purified by reverse-phase HPLC (eluted by 0.05 M $LiClO_4$ with a gradient from 0 to 50% acetonitrile). Products were identified by UV/ visible spectroscopy, which showed a shoulder on the absorption band at 260 nm similar to that seen in Figure 2.2. From this, appropriate fractions were lyophilised, and characterised by ^{1}H NMR spectroscopy in D_2O.

Oligo2_3'peptide-naphthalene: ^{1}H NMR (300 MHz, D_2O): δ_H 1.20-1.23 (d, 3H, CH_3 of alanine), 1.42-1.64 (m, 11H, 3 x CH_3 of 3 x dT, 1 x CH_2 group of N'-methyl-N'-naphthalen-1-yl-ethane-1, 2-diamino group), 2.67 (s, 3H, N'-methyl group of N'-methyl-N'-naphthalen-1-yl-ethane-1, 2-diamino group), 6.92-8.15 (m, 16H, 7 Ar-H of N'-methyl-N'-naphthalen-1-yl-ethane-1, 2-diamino group, 9 Ar-H from bases; 2 from each dA, 1 from each dG, dC and dT).

Oligo1_5'peptide-naphthalene: ^{1}H NMR (300 MHz, D_2O): δ_H 1.10 (m, 3H, CH_3 of alanine), 1.54-1.64 (m, 14H, 4 x CH_3 of 4 x dT, 1 x CH_2 N'-methyl-N'-naphthalen-1-yl-ethane-1, 2-diamino group), 2.6 (s, 3H, N'-methyl group of N'-methyl-N'-naphthalen-1-yl-ethane-1, 2-diamino group), 6.92-7,79 (m, 15H, 7 x Ar-H of N'-methyl-N'-naphthalen-1-yl-ethane-1, 2-diamino group, 8 Ar-H from bases)

2.4.4 *Bis*-attachment of 1-pyrenemethylamine to oligonucleotide probes.

Two equivalents of 1-pyrenemethylamine were attached *via* phosphoramide links to the terminal 5'-phosphate of oligo 1 (5'pdTGTTTGGC), or to the 3'-phosphate of Oligo 2 (dCGATTCTG3'p). To the cetyltrimethylammonium salts of the oligonucleotides (~1μmol) dissolved in DMF (200 μl) were added triphenylphosphine (80 mg, 300 μmol) and 2,2'-dipyridyl disulfide (70 mg, 318 μmol), and the reaction mixture was incubated at 37 °C for 10 min. 4-N',N'-Dimethylaminopyridine (40 mg, 329 μmol) was added, the reaction mixture incubated for a further 10 minutes at 37 °C and 1-pyrenemethylamine hydrochloride (4 mg, 14.9 μmol, dissolved in 100 μl of DMF and 3μl triethylamine) added. The reaction mixture was incubated at 37 °C for 24 hours, precipitated as described above and purified using reverse-phase HPLC (eluted by 0.05 M $LiClO_4$ with a gradient from 0 to 60 % acetonitrile). Products were identified by UV/ visible spectroscopy: Figure 2.6 shows the UV/visible spectrum for a *bis*-pyrene substituted oligo, showing a typical A_{260} : A_{345} ratio of ~2 (Oligo1_5'*bis*-pyrene 1.92), compared to ~ 3.0 for mono-pyrene substituted oligos. The appropriate fractions were lyophilised.

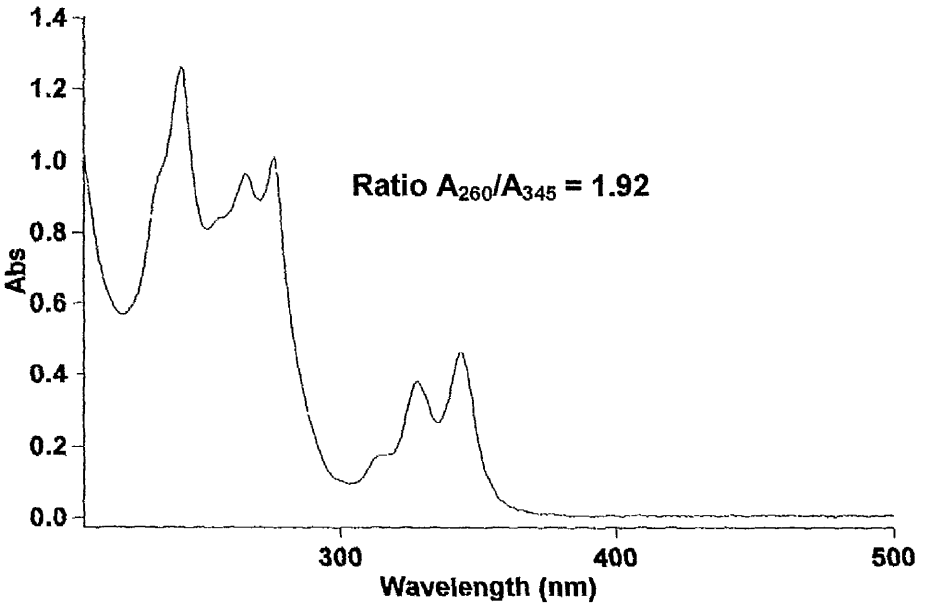

Figure 2.6: UV/visible absorption spectrum of Oligo1_5'*bis*-pyrene in ~ 50% acetonitrile at 20 °C

2.4.5 *Bis*-attachment of N'-methyl-N'-naphthalen-1-yl-ethane-1,2-diamine to oligonucleotide probes.

Two equivalents of N'-methyl-N'-naphthalen-1-yl-ethane-1,2-diamine were attached *via* phosphoramide links to the terminal 5'-phosphate of oligo 1 (5'pdTGTTTGGC), as described in Section 2.4.4, but using N'-methyl-N'-naphthalen-1-yl-ethane-1,2-diamine dihydrochloride (4 mg, 14.6 μmol, dissolved in 100 μl of DMF and 3μl triethylamine). Product was purified by reverse-phase HPLC (eluted by 0.05 M $LiClO_4$ with a gradient from 0 to 60 % acetonitrile). Products were identified by UV/ visible spectroscopy. The UV/visible spectra of *bis*-substituted oligos showed a shoulder to the 260 nm absorption band similar to mono-substituted derivatives, but this was more pronounced for the *bis*-derivatves (Figure 2.7). The appropriate fractions were lyophilised and characterised by ^1H NMR spectroscopy.

Oligo1_5'*bis*-naphthalene: ^1H NMR (300 MHz, D_2O): δ_H 1.224 (s, 3H, CH_3 of dT), 1.87-1.92 (t, 9H, 3 x CH_3 of 3 x dT), 2.78-2.82 (d, 9H, 2 x CH_2 of N'-methyl group), 5.88-6.31 (m, 9H, 8 x H1' of sugar ring and 1 x H5 of dC), 6.86-8.039 (m, 22H, 14 Ar-H of 2 naphthalene groups and 8 Ar-H of bases)

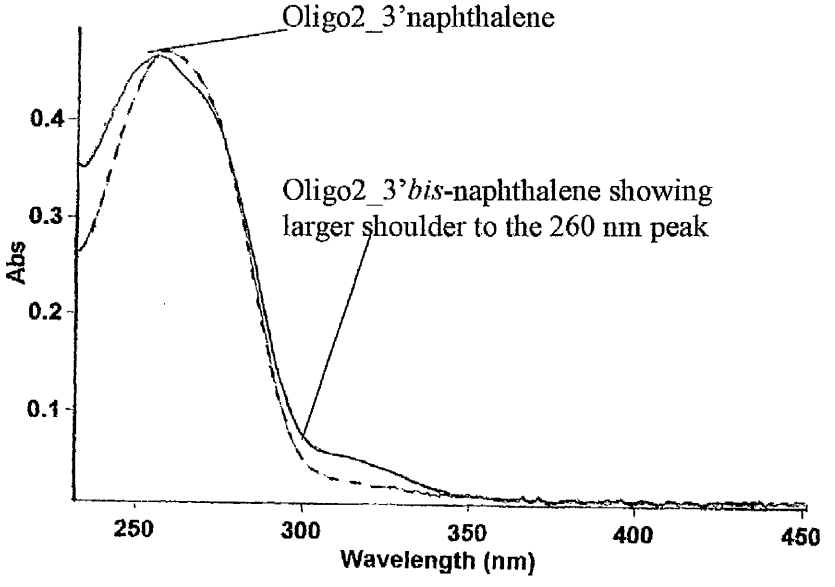

Figure 2.7: UV/visible spectra of Oligo2_3'naphthalene compared to Oligo2_3'*bis*-naphthalene showing the shoulder to the 260 nm absorption band. Spectra were taken in water at 20 °C.

The yield of Oligo2_3'*bis*-naphthalene was too low to allow NMR analysis, so appropriate fractions, determined by UV/visible spectroscopy, were lyophilised and used directly for fluorescence studies.

2.4.6 Attachment of 1-tert-butylcyclohexylamine and 1-pyrenemethylamine to the oligo probe.

First, a single equivalent of 1-tert-butylcyclohexylamine was attached via a phosphoramide link to the terminal 5'-phosphate of Oligo 1 (5'pdTGTTTGGC) or the 3'-phosphate of Oligo 2 (dCGATTCTG3'p) as described in Section 2.3.1, but using 4-tert-butylcyclohexylamine (2 mg, 13 μmol dissolved in 100 μl DMF). The reaction mixtures were incubated at 37 °C for 6 hours, precipitated, purified by reverse-phase HPLC (eluted by 0.05 M $LiClO_4$ with a gradient from 0 to 40 % acetonitrile). Fractions were collected and the largest, analysed by ^1H NMR spectroscopy in D_2O, was found to contain oligo with the ^{t}Bu-cyclohexyl group attached.

Oligo1_5'^{t}Bu-cyclohexane ^1H NMR (300 MHz, D_2O): δ_H 0.7 (s, 12H, 3 x CH_3, t-butyl group), 1.78-1.92 (m, 16H, 12 x CH_3 of 4 x dT, 4 x CH_2 of cyclohexyl), 6.19 (m, 9H, 8 x H1' of sugar and 1 x H6 of dC) 7.625 (m, 8H, 8 x Ar-H of bases)

One molecule of 1-pyrenemethylamine was then attached *via* a phosphoramide link to the terminal 5'-phosphate of Oligo1-tert-butyloxycyclohexane (5'pdTGTTTGGC) or to the 3'-phosphate of Oligo2_^{t}Bu-cyclohexane (dCGATTCTG3'p) as described in Section 2.3.4, but using 1-pyrenemethylamine hydrochloride (4 mg, 15 μmol, dissolved in 100 μl of DMF and 3μl triethylamine). The reaction mixtures were incubated at 37 °C for 24 hours, precipitated and product purified by reverse-phase HPLC (eluted by 0.05 M $LiClO_4$ with a gradient from 0 to 80 % acetonitrile). Product was identified by UV/ visible spectroscopy (Oligo1_5'cyclohexylpyrene A_{260}: A_{345} 2.8, Oligo2_3'cyclohexylpyrene A_{260}: A_{345} 4.3) and appropriate fractions were lyophilised.

2.4.7 *Bis-* attachment of 4-(dimethylamino)-benzylamine dihydrochloride (DMA) to the probe oligos.

Two molecules of 4-(dimethylamino)benzylamine dihydrochloride were attached *via* a phosphoramide link to the terminal 3'-phosphate of Oligo2 (dCGATTCTG3'p) as described in Section 2.3.4, but using 4-dimethylaminobenzylamine dihydrochloride (6 mg, 27 μmol), dissolved in 100 μl of DMF and 10 μl triethylamine. The reaction mixtures were incubated at 37 °C for 5 hours, precipitated, and product purified by reverse-phase HPLC (eluted by 0.05 M $LiClO_4$ with a gradient from 0 to 60 % acetonitrile). Products were identified by UV/ visible spectroscopy and appropriate fractions lyophilised and characterised by ^1H NMR spectroscopy.

Oligo2_3'*bis*-DMA ^1H NMR (300 MHz, D_2O): δ_H 1.54 (s, 3H, CH_3 of T), 1.67-1.72 (d, 6H, 2 x CH_3 of dT), 2.60-2.63 (d, 13H, 4 x N-methyl groups of 4-(dimethylamino)benzylamine), 5.76-6.20 (m, 10H, 8 x H1' of sugar, 2 x H5 of 2 x dC), 6.62-7.02 (m, 8H, 8 Ar-H of 2 x 4-(dimethylamino)benzylamine), 7.25-8.23 (m, 12 H, 9 Ar-H of bases)

2.4.8 Attachment of 1-Pyrenemethylamine to the 5'-phosphate of Proexc 9 (DNA-diene), Proexc 10 (DNA) and Proexc11 (LNA)

The oligonucleotides Proexc9 (0.1 μmol), Proexc 10 (0.17 μmol) and Proexc11 (0.16μmol) (5'pdGCTGAGAGTC) were dissolved in water (100 μl) and the cetyltrimethylammonium salts obtained by stepwise addition of 4% lithium perchlorate (50 μl, 5 x 10 μl) until no further precipitation was seen. The salts were then dried *in vacuo* overnight, and then dissolved in DMF (200 μl), but as solubility of the oligos was poor a further aliquot (100 μl) of DMF was added. To each oligo solution were added triphenylphosphine (8 mg, 50 μmol) and 2,2'-dipyridyl disulfide (7 mg, 50 μmol) and the reaction mixtures incubated at room temperature for 10 min. 4-*N'*,*N'*-Dimethylaminopyridine (4 mg, 50 μmol) was added and the reaction mixtures incubated for a further 10 minutes at room temperature. To each oligonucleotide reaction mixture 1-pyrenemethylamine hydrochloride (2 mg, 15 μmol, dissolved in 100 μl of DMF and 3 μl triethylamine) was added. The reaction mixtures were incubated at 37 °C overnight and for a further 5 hours at 55 °C. After this time the reaction products were precipitated as described above and purified by reverse-phase HPLC (eluted by

0.05 M $LiClO_4$ with a gradient from 0 to 80 % acetonitrile). UV/ visible spectroscopy indicated that fractions containing unreacted starting oligo, mono-pyrene and *bis*-pyrene-substituted oligos were obtained. Mono-pyrene substituted 10mer-oligos showed A_{260}: A_{345} ~5 (Proexc9 5.17, Proexc10 5.82, Proexc11 4.60) (Figure 2.8). The yields of mono-pyrene-substituted oligos were low in all cases, being 17% for Proexc9, 29% for Proexc10 and 21% for Proexc11. The appropriate fractions containing the mono-substituted oligos were lyophilised. Due to the low yields ^1H NMR spectroscopy was not possible and the purified mono-substituted products were used directly for fluorescence studies.

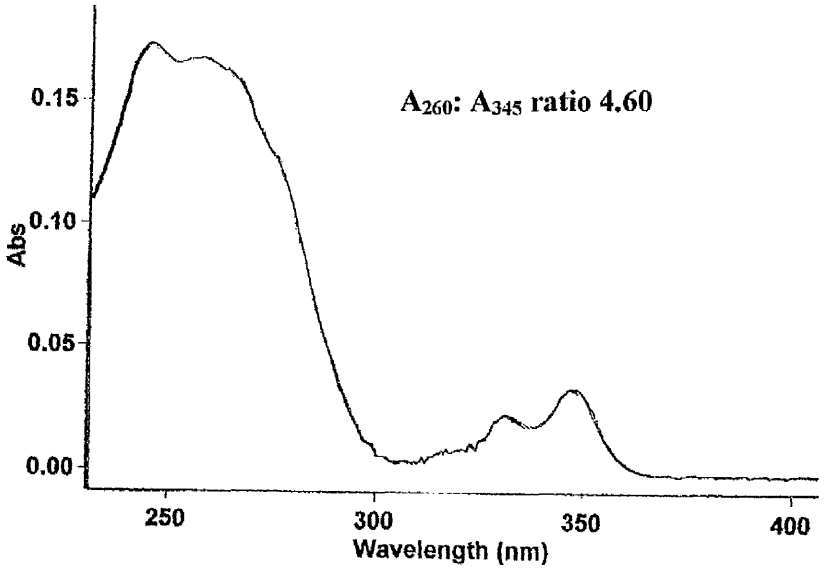

Figure 2.8: UV/visible spectrum of Proexcll_5'pyrene in 50% acetonitrile at 20 °C.

2.4.9 Attachment of N'-methyl-N'-naphthalen-1-yl-ethane-1,2-diamine to the 3'-phosphate of the Proexc3 and Proexc 4 oligonucleotide probes.

Oligonucleotides Proexc3 (DNA, 0.25 μmol) and Proexc4 (LNA, 0.16 μmol) (dATTGAGGCTCp3') were dissolved in 100 μl water, the cetyltrimethylammonium salts obtained and after being stored *in vacuo* overnight were dissolved in DMF (200 μl). The solubility of these oligos was much greater than of Proexc9, 10 and 11. To each oligo solution were added triphenylphosphine (8 mg, 50 μmol) and 2, 2'-dipyridyl disulfide (7 mg, 50 μmol)

and the reaction mixtures incubated at 37 °C for 10 min. 4-*N'*, *N'*-Dimethylaminopyridine (4 mg, 50 μmol) was then added and the reaction mixtures incubated for a further 10 minutes at 37 °C. To each oligonucleotide reaction mixtures was added N'-methyl-N'-naphthalen-1-yl-ethane-1, 2-diamine dihydrochloride (2 mg, 7.3 μmol, dissolved in 100 μl of DMF and 3μl triethylamine). The reaction mixtures were incubated at 37 °C overnight, precipitated as described above, and purified by reverse-phase HPLC (eluted by 0.05 M $LiClO_4$ with a gradient from 0 to 60 % acetonitrile). UV/ visible spectroscopy of the fractions showed that unreacted starting oligos were present, as were *bis*-substituted oligos, indicated by a larger shoulder to the absorption band at 260 nm. A typical absorption spectra for a mono-substitued oligo is shown in Figure 2.9. Fractions containing mono-substituted oligos were lyophilised; yields were low (8% for Proexc3, and 22% for Proexc4). Due to the low yield ^1H NMR spectroscopy was not possible and the purified products were used directly for fluorescence studies.

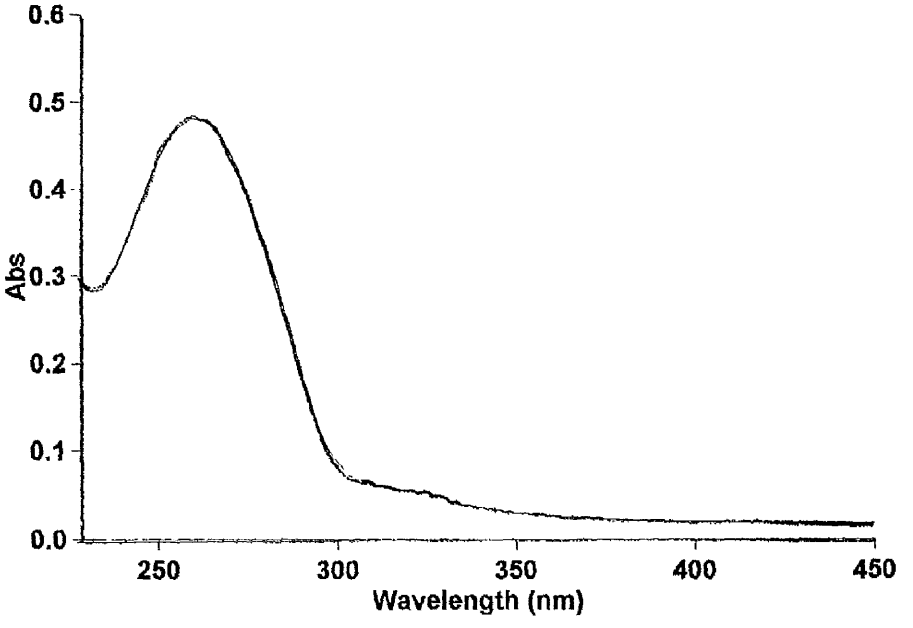

Figure 2.9: UV/visible spectrum of Proexc3_3'napthalene in 50% acetonitrile at 20 °C.

2.5 Methods: Testing.

2.5.1 Fluorescence experiments.

Emission and excitation spectra were recorded using a Shimadzu RF-5301PC spectrophotofluorimeter either in Tris buffer (10mM Tris, 0.1M NaCl, at pH 8.5) or Tris buffer containing various percentages of TFE or other co-solvents (see below). Emission spectra were recorded using a 2 ml thermostatted 4-sided quartz cuvette; excitation wavelengths used were 340 and 350 nm and slit-widths were set from 5 to 10 nm, depending on the intensity of emission. The automatic shutter-on function was used to minimise photo-bleaching of the sample. In some cases excitation spectra were taken as indicated below, using emission wavelengths of 375 nm for the probe components and 379 nm for the full systems. All spectra were buffer-corrected at the specific temperature and wavelength.

2.5.2 Inner filter effects.

Inner filter effects occur if the absorption band of a component in the sample overlaps the wavelength of the excitation beam. This component will attenuate the excitation beam, therefore acting as a filter. This causes the observed fluorescence intensity to be lower than the actual fluorescence intensity [111]. The following equation (1) can be used to correct for inner filter effects:

$$F_c = F \times 10^{0.5A_{ex}} \qquad (1)$$

where F_c is the fluorescence intensity at a particular wavelength corrected for inner filter effects, F is the observed fluorescence intensity at that wavelength and A_{ex} is the absorbance of the component at the excitation wavelength used [112]. There was no inner filter correction required for the oligonucleotide components as their absorbance band at 260 nm does not overlap with the excitation wavelength of 350 nm used. Inner filter correction was also not performed for the naphthalene component as the absorption band for naphthalene conjugated to the oligos only begins around 340 nm, therefore its absorption band does not overlap the with the excitation wavelengths used for this study (340 and 350 nm).

2.5.3 Buffers.

For most experiments 10 mM Tris buffer containing 0.1M NaCl at pH 8.5 or Tris buffer (10mM Tris, 0.1M NaCl at pH 8.5) containing 80% v/v TFE was used. Buffer containing 80% TFE was made by diluting 1 part of a 10-fold stock buffer (0.1M Tris, 1M NaCl, pH 8.5) with 8 parts TFE and 1 part water. In some cases other concentrations of TFE were used. These were either pre-made similarly, or (for samples in short supply) by adding TFE aliquots sequentially to the solution of the ready-formed system in the cuvette. The specific method used is indicated at appropriate points in the text. Buffers were stored below 4 °C until required.

2.5.4 Preparation of stock solutions.

After HPLC purification, samples containing product were lyophilised. To prepare stock solutions the residues were dissolved in an aliquot (50 µl) of Milli-Q water. An aliquot (2 µl) was taken and added to 1 ml water. The absorption spectrum of the sample was recorded and the concentration of the stock solution determined from the A_{260} value using the millimolar extinction coefficients (ε) of the oligonucleotides (the contribution of the exic-partners was ignored) (Oligo 1: ε 71.8 $mM^{-1}cm^{-1}$, Oligo2: ε 69.8 $mM^{-1}cm^{-1}$, Target: ε 162.6 $mM^{-1}cm^{-1}$, Proexc1 (target): ε 282.0 $mM^{-1}cm^{-1}$, Proexc 3 and 4: ε 96.6 $mM^{-1}cm^{-1}$, Proexc9, 10 and 11: ε 98.3 $mM^{-1}cm^{-1}$). The appropriate amount of water was then added to the stock solution to give a final concentration of 10^{-3} M. Preparation of target stock solution was performed similarly. All stock solutions were stored at –20 °C until required.

2.5.5 Standard method of complex formation and testing.

The complex was formed by sequential addition of aliquots (5 µl) of the components (see later for order of addition for each system) from the stock solutions (10^{-3} M) to Tris buffer (2 ml) containing the appropriate amount of TFE (0-80%) at 10 °C. The ratio of components used was 1:1:1, the concentration of each component being 2.5 µM. Emission spectra were recorded after each component was added, using the excitation wavelengths and slitwidths given above, to observe any changes in emission spectra resulting from complex formation. On formation of the full complex, the system was allowed to equilibrate for 10 minutes at 10 °C, and emission spectra then recorded at 3-minute intervals to monitor changes in excimer/ exciplex intensity. The cuvette was then

heated to 40 °C for 5 minutes and allowed to cool back to 10 °C over 15 minutes. Emission spectra were then recorded at 3-minute intervals until excimer emission did not further increase (this usually occurred after 9 minutes). All spectra were buffer-corrected. Where systems contained a naphthalene-bearing probe this was usually added first, and its contribution to subsequent spectra subtracted, as the emission signal from naphthalene (broad band with λ_{max} 430 nm) could obscure any excimer/ exciplex signal present.

2.5.6 DNA-based systems.

2.5.6.1 Emission and excitation spectra of SP-1 in 80% TFE/ Tris buffer.

Experiments were carried out in 80% TFE/ Tris buffer using the standard protocol described above. The order of addition was Oligo1_5'pyrene, Oligo2_3'naphthalene and finally target. Excitation spectra were taken after the addition of each component using emission wavelengths of 375 nm for the probe components and 370 nm for the full system; the recording range was 200-350 nm.

2.5.6.2 Emission and excitation spectra for the SP-2 system in 80% TFE/ Tris buffer.

Experiments were carried out in 80% TFE/ Tris using the standard method. The order of addition was Oligo2_3'naphthalene, Oligo1_5'pyrene, and finally target. Excitation spectra were taken after the addition of each component using emission wavelengths of 375 nm for the probe components and 370 nm, for the full system; the recording range used was 200-350 nm.

2.5.6.3 Emission spectra of the SP-3 system in 80% TFE/ Tris buffer.

Experiments were carried out in 80% TFE/ Tris buffer using the standard method. The order of addition was Oligo1_5'naphthalene, Oligo2_3'pyrene, and target. Control systems were also used in which the 3'- or 5'-naphthalene component of the probes was omitted (to give 5'-control and 3'-control, respectively)

2.5.6.4 Control systems, C-1 and C-2.

Each control experiment was performed in 80% TFE/ Tris buffer as for the experimental systems (SP-1, SP-2 and SP-3) using the standard method. The order of addition for the C-1 control system was: Oligo1_5'pyrene, Oligo2_3'phosphate, then target. For the C-2 control system it was: Oligo1_5'phosphate, Oligo2_3'pyrene, then target.

2.5.7 Peptide linker systems.

2.5.7.1 SP-4 System.

0, 50 and 60 % TFE/ Tris buffer.

The complex was pre-assembled in Tris buffer, and spectra taken using the standard method, the order of addition being: Oligo1_5'peptide-pyrene, Oligo2_3'peptide-pyrene, and finally target. This solution was retained and used to test the system in 50 and 60% TFE/ Tris buffer. An alioquot (1 ml) of buffer was removed from the cuvette and replaced by 1 ml of TFE (and 100 μl of 10-fold buffer to maintain ion concentration, and give a TFE concentration of 47.6% and component concentrations of 1.2 μM). The system was then allowed to re-equilibrate for 10 minutes at 10 °C before emission spectra were taken using parameters above. A further aliquot (500 μl) of solution was removed from the cuvette and replaced with 500 μl TFE (50 μl of 10-fold buffer) giving a TFE concentration of 58.1% and a component concentration 0.87 μM. The system was again allowed to equilibrate for 10 minutes and spectra taken. All spectra were buffer-corrected and the contribution from naphthalene subtracted.

80% TFE/ Tris buffer.

Experiments were carried out in 80% TFE/ Tris buffer using the standard method. The order of addition was: Oligo1_5'peptide-pyrene, Oligo2_3'peptide-pyrene, and finally target.

2.5.7.2 SP-5 system.

0, 50 and 60% TFE/ Tris buffer.

Experiments were performed as for SP-4 in 0, 50 and 60% TFE/ Tris buffer. The order of addition of the components was Oligo2_3'peptide-naphthalene, Oligo1_5'peptide-pyrene, and finally target. The spectrum of Oligo2_3'peptide-naphthalene was subtracted from each subsequent spectrum taken.

80% TFE/ Tris buffer.

Experiments were performed using the standard method in 80% TFE/ Tris buffer. The order of addition of the components was Oligo2_3'peptide-naphthalene, Oligo1_5'peptide-pyrene, and finally target. The spectrum of Oligo2_3'peptide-naphthalene was subtracted from each subsequent spectrum taken.

2.5.7.3 SP-6 System.

0, 50 and 60% TFE/ Tris buffer.

Experiments were performed as for SP-4 in 0, 50 and 60% TFE/ Tris buffer. The order of addition of the components was Oligo1_5'peptide-naphthalene, Oligo2_3'peptide-pyrene, and finally target. The spectrum of Oligo1_5'peptide-naphthalene was subtracted from each subsequent spectrum.

80% TFE/ Tris buffer.

Experiments were performed in 80% TFE/ Tris buffer using the standard method. The order of addition of the components was Oligo1_5'peptide-naphthalene, Oligo2_3'peptide-pyrene, and finally target.

2.5.7.4 Control experiments.

Each control experiment was performed in 80% TFE/ Tris buffer only using the standard method. The order of addition for the C-3 system was: Oligo1_5'peptide-pyrene, Oligo2_3'phosphate and finally target. The order was Oligo1_5'phosphate, Oligo2_3'peptide-pyrene and then target for the 3'-control system.

2.5.8 RNA systems.

All buffers used for testing the RNA target were made with DEPC-treated water (DEPC is added to inactivate any adventitious ribonucleases that may have been present). The RNA target sequence is shown in Section 1.15.2.

2.5.8.1 SP-7 system.

0 and 40% TFE/ Tris buffer.

First experiments were carried out in Tris buffer using the standard method. The order of component addition was: Oligo 1_5'pyrene, Oligo2_3'pyrene, then target. From this solution, retained after testing in Tris, an aliquot (1 ml) was removed from the cuvette, and replaced by 80% TFE/ Tris buffer (1 ml) to give a final TFE concentration of 40% (component concentrations 1.25 μM). Emission spectra were recorded. The sample was gradually heated to 40 °C over 20 minutes with emission spectra recorded every 10 °C, before being re-cooled to 10 °C (over 20 minutes).

80% TFE/ Tris buffer.

Experiments were carried out in 80% TFE/ Tris buffer using the standard method. The order of addition was: Oligo2_3'naphthalene, Oligo1_5'pyrene, then target.

2.5.8.2 SP-8 system.

0, 50, 60 and 70% TFE/ Tris buffer.

First experiments were carried out in Tris buffer using the standard method. After testing, the solution was retained, an aliquot (1 ml) removed from the cuvette, replaced by 1 ml TFE (plus 100 μl of 10-fold buffer to maintain ionic strength) to give a TFE concentration of 47.6% and component concentrations of 1.2 μM. Emission spectra were taken. A further aliquot (500 ul) was removed and replaced by 500 μl of TFE (plus 50 μl of 10-fold buffer) to give 58.1% TFE and a component concentration of 0.87 μM; emission spectra were recorded. Finally, a further aliquot (500 μl) of solution was removed from the cuvette and replaced by 500 μl of TFE (plus 50 μl of 10-fold buffer) to give a final TFE concentration of 68.2% and component concentration of 0.64 μM. After emission spectra had been recorded, the system was gradually heated to 35 °C over 20 minutes with emission spectra recorded at 5-minute intervals. The system was then cooled back to 10 °C over 20 minutes and the emission spectrum recorded.

2.5.9 *Bis*-substituted systems.

2.5.9.1 SP-9 system.

Experiments were carried out in 80% TFE/ Tris buffer using the standard method: the order of component addition was Oligo1_cyclohexylpyrene, Oligo2_3'*bis*-naphthalene, then target.

2.5.9.2 SP-12 system.

Experiments were performed in Tris buffer initially using the standard method. The order of addition was Oligo1_5'*bis*-naphthalene, Oligo2_3'cyclohexylpyrene, then target. This solution was retained for testing in 50% TFE/ Tris buffer. To achieve this concentration (47.6% TFE, component concentration 1.2 μM) an aliquot (1 ml) of solution was removed from the cuvette and replaced by 1 ml of TFE plus 100 μl of 10-fold buffer to maintain sodium ion concentration. The system was allowed to equilibrate at 10 °C for 10 minutes before emission spectra were recorded.

2.5.9.3 SP-13 system.

Experiments were performed in 80% TFE/ Tris buffer using the standard method, the order of addition of the components being Oligo1_5'cyclohexylpyrene, target and finally Oligo2_3'*Bis*-(*bis*DMA).

2.5.9.4 SP-14 system

Experiments were performed in 80% TFE/ Tris using the standard method, the order of addition of the components in this case being Oligo1_5'*bis*-pyrene, target and finally Oligo2_3'*bis*(*bis*DMA).

2.5.9.5 Control system (C-5)

Experiments were performed in 80% TFE/ Tris buffer using the standard method, the order of addition of the components in this case being Oligo1_5'*bis*-pyrene, target and finally Oligo2_3'phosphate.

2.5.10 Effect of PCR additives.

The effect of PCR additives (sulfolane, methylsulfone, betaine and DMSO, Figure 2.10) on exciplex emission was investigated using the SP-2 system in Tris and in 80% TFE/ Tris buffer (see above for details). For the experiments in Tris buffer, buffer containing the additives was prepared before the experiments by adding the appropriate amount of additive (Table 2.1) to 10 ml of Tris buffer. Concentrations were chosen based on the minimum and maximum concentrations of the range typically used in PCR reactions for that particular additive [107;108;113;114]. Experiments were performed in Tris buffer containing the appropriate additive using the standard method, components being added in the following order: Oligo2_3'napthalene, Oligo1_5'pyrene then target.

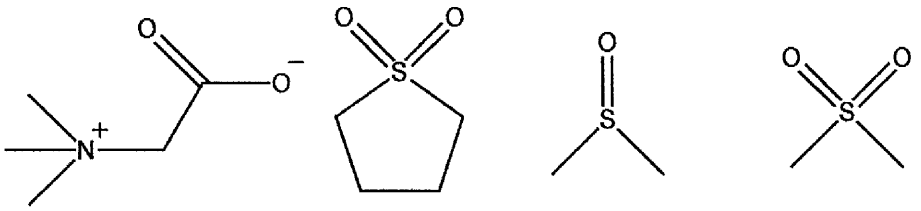

Betaine Sulfolane Dimethylsulfoxide Methylsulfone

Figure 2.10: Structures of compounds used to determine to determine the effect of PCR additives on exciplex formation.

Table 2.1: Amount of PCR additive added to Tris buffer (10 M) to give a solution of the concentration shown.

	Sulfolane $M_r = 120.17$ d = 1.261		**Methylsulfone $M_r = 94.13$**		**Betaine $M_r = 135.16$**		**DMSO $M_r = 78.13$**
Concentration	0.15 M	0.5 M	0.6 M	1.1 M	1 M	2 M	10% (1.16 M)
Amount added to 10 ml Tris buffer	143 µl	476 µl	0.57 g	1.04 g	1.35 g	2.70 g	1 ml

For experiments in 80% TFE/ Tris buffer the system was first prepared in 80% TFE/ Tris buffer (2 ml) containing no additive by sequential addition of the components from stock solutions (10^{-3} M) in the order: Oligo2_3'naphthalene, Oligo1_5'pyrene and then target. After each addition, emission spectra were recorded using the excitation wavelengths above. The additives were then added from stock solutions (betaine and sulfolane 10 M, methylsulfone 5 M) to give the required minimum concentration (see Table 2.2). The system was then allowed to equilibrate for 10 minutes at 10 °C, and emission spectra taken. Additive concentration was increased by further addition from stock solutions to give the maximum concentration (Table 2.2), and after 10 minutes re-equilibration emission spectra were again recorded. All spectra were buffer-corrected and had the Oligo2_3'naphthalene component subtracted.

Table 2.2: Amount of PCR additive stock solutions added to the fluorescence cuvette (2 ml) to give the appropriate concentrations.

	Sulfolane $M_r = 120.17$ d = 1.261		**Methylsulfone $M_r = 94.13$**		**Betaine $M_r = 135.16$**	**DMSO $M_r = 78.13$**
Concentration	0.15 M	0.5 M	0.6 M	1.1 M	1 M	10% (1.16 M)
Amount added to cuvette (µl)	30	Further 70 µl (100 µl stock in total)	240	Further 200 µl (440 µl stock in total)	200	200

2.5.11 Effect of co-solvents.

Organic co-solvents tested for their effect on excimer/ exciplex fluorescence in the SP-1, SP-2 and SP-3 DNA split-probe systems included: tetrafluoro-1-propanol, N-methylformamide, hexafluoro-2-propanol, ethylene glycol, acetone, methanol, ethanol, ethylene glycol dimethylether and 3-chloro-1, 2-propandiol.

2.5.11.1 SP-1 and SP-2 in 50% co-solvent/ Tris buffer.

Systems SP-1 and SP-2 were tested in the presence of 50 and 70% co-solvent/ Tris buffer (10 mM Tris, 0.1 M NaCl at pH 8.5) mixtures. To achieve a concentration of 50% co-solvent an aliquot (1 ml) of co-solvent, water (800 µl) and 10-fold buffer (200 µl of 0.1 M Tris, 1 M NaCl at pH 8.5) were added to the cuvette and cooled to 10 °C. The complex was then formed by sequential addition of aliquots (5µl) of the components from the stock solutions (10^{-3} M) in the order: Oligo1_5'pyrene, Oligo2_3'pyrene, target for SP-1; and Oligo2_3'naphthalene, Oligo1_5'pyrene and target for SP-2. The ratio of components used was 1:1:1, the concentration of each component being 2.5 µM. Excitation λ_{max} shifted slightly (several nm) depending on solvent. Emission spectra were recorded at each stage of addition, using excitation wavelengths and slitwidths above. On formation of the full complex the systems were allowed to equilibrate for 10 minutes at 10 °C, emission spectra were recorded at 3-minute intervals to monitor any change in excimer/ exciplex intensity. The systems were then heated to 40 °C for 5 minutes and allowed to cool back to 10 °C over a period of 10 minutes. Spectra were then taken at 3 minute intervals until excimer/ exciplex emission intensity was at a maximum, usually after 9 minutes. The solution was retained for experiments in 70% co-solvent.

2.5.11.2 SP-1 and SP-2 in 70% co-solvent/ Tris buffer.

From the cuvette solution retained from the previous experiment (full systems in 50% co-solvent) an aliquot (1 ml) was removed and replaced by co-solvent (1 ml), giving a co-solvent concentration of 71.4% and component concentrations of 1.2 μM (an aliquot (100 μl) of 10-fold buffer was also added to the cuvette to maintain ionic strength). The systems were allowed to equilibrate at 10 °C for 10 minutes before emission spectra were recorded. The systems were then heated to 40 °C for 5 minutes and allowed to cool back to 10 °C over a period of 10 minutes. Emission spectra were then taken at 3 minute intervals until excimer/ exciplex emission intensity was at a maximum, usually after 9 minutes

2.5.11.3 SP-3 in 80% TFE.

SP-3 was tested in 80% co-solvent/ Tris buffer (10 mM Tris, 0.1M NaCl at pH 8.5), prepared by diluting 1 part of a 10-fold buffer (0.1M Tris, 1M NaCl, pH8.5) with 8 parts co-solvent and 1 part water. The complex was formed by sequential addition of aliquots (5 μl) of the components in the order: Oligo1_5'naphthalene, Oligo2_3'pyrene then target from stock solutions (10^{-3} M) to 2 ml of ready-prepared 80% co-solvent/ Tris buffer at 10 °C. The ratio of components used was 1:1:1, the concentration of each component being 2.5 μM. Emission spectra were recorded at each stage of addition. On formation of the full complex, the system was allowed to equilibrate for 10 minutes at 10 °C, and emission spectra were recorded at 3-minute intervals to monitor any change in excimer intensity.

2.5.12 Mismatches.

The SP-1, SP-2 and SP-3 DNA split-probe systems were used to test the effect of various mismatches and insertions in the target sequence on exciplex/ excimer emission. All experiments were performed in 80% TFE/ Tris buffer at 10 °C unless otherwise stated. The variants of the 16-mer-target sequence are shown below in Figure 2.11 along with the nomenclature used.

Parent

G C C A A A C A -C A G A A T C G
C G G T T T G T -G T C T T A G C
P P

Insertion1

```
GCCAAACAGCAGAATCG
CGGTTTGT- GTCTTAGC
  P   P
```

Insertion2

```
GCCAAACAGTCAGAATCG
CGGTTTGT   -GTCTTAGC
  P     P
```

3'mismatch 1

```
GCCAAACA-CAGAATAG
CGGTTTGT-GTCTTAGC
  P P
```

3'mismatch 2

```
GCCAAACA–CAGGATCG
CGGTTTGT–GTCTTAGC
  P P
```

3'mismatch 3

```
GCCAAACA-AAGAATCG
CGGTTTGT-GTCTTAGC
  P P
```

3'Double mismatch

```
GCCAAACA-CAGGATGG
CGGTTTGT-GTCTTAGC
  P P
```

5'mismatch 1

```
GACAAACA-CAGAATCG
CGGTTTGT-GTCTTAGC
  P P
```

5'mismatch 2

G C C A G A C A -C A G A A T C G
C G G T T T G T -G T C T T A G C
P P

5'mismatch 3

G C C A A A C T -C A G A A T C G
C G G T T T G T -G T C T T A G C
P P

5'double mismatch

G A C A G A C A -C A G A A T C G
C G G T T T G T -G T C T T A G C
P P

Figure 2.11: Target strands and nomenclature used for excimer/ exciplex formation with mismatched targets. Mismatches are shown in red.

The standard method was used to test all the systems (SP-1, SP-2 and SP-3) with each mutant target in 80% TFE/ Tris buffer. The order of addition was: Oligo1_5'pyrene, Oligo2_3'pyrene, then mutant-target for SP-1; Oligo2_3'naphthalene, Oligo1_5'pyrene, then mutant-target for SP-2; Oligo1_5'naphthalene, Oligo2_3'pyrene and then mutant-target for SP-3. All spectra were buffer-corrected. For SP-2 and SP-3 systems the appropriate naphthalene spectrum (taken first) was subtracted from subsequent spectra. This method was used for all mutant targets.

2.5.13 LNA Systems

2.5.13.1 Proexc11_5'Pyrene + Proexc4_3'Napthalene + Proexc1 (target).

Tris Buffer

The complex was formed by sequential addition of aliquots (5 µl) of the components in the order: Proexc11_5'pyrene, Proexc4_3'napthalene and finally target (Proexc1) from stock solutions (1 mM). The ratio of components used was 1:1:1, the concentration of each component being 2.5 µM. Emission spectra were recorded at each

stage to observe any changes resulting from complex formation The system was allowed to equilibrate at 10°C for 10 minutes. To obtain evidence of exciplex emission within a fully assembled complex, melting temperature experiments were performed by slowly heating the system to 70 °C over 30 minutes. The system was then reannealed by cooling back to 10 °C over 30 minutes. During the heating and reannealing processes emission spectra were recorded at 5 °C increments.

Tris buffer/20% TFE.

Experiments were performed as above, but using ready-prepared Tris buffer containing 20% TFE v/v. To investigate melting, the system was heated to 60°C over 30 minutes with spectra taken at 10 °C increments and re-cooled to 10 °C over 30 minutes. A control experiment was performed under the above conditions (20% TFE/ Tris buffer) using the same method, but using unmodified Proexc4 (control system: Proexc11_5'Pyrene +Proexc4_3'phosphate + target (Proexc1)).

Tris buffer/40% TFE

Experiments were performed as above, but using ready-prepared Tris buffer containing 40% TFE. Melting of the system was performed by heating to 80°C (over 30 minutes, with spectra taken every 10 °C); the system was then re-annealed by cooling to 10 °C (over 30 minutes), and spectra taken.

Tris buffer/80%TFE

First the complex between Proexc11_5'pyrene and target was formed by addition of an aliquot (5 µl) of each component from stock solutions to 2 ml of Tris buffer, emission spectra being taken at each stage of addition. This was followed by a heating and cooling cycle (heated to 70 °C over 30 minutes, then cooled to 10 °C over a further 30 minutes) to allow hybridisation to occur and to remove background exciplex signal from Proexc10_5'pyrene. In the next stage an aliquot (5 µl) of the Proexc4_3'naphthalene component was added from the stock solution to form the complete system. The heating/ re-annealing procedure (heat to 70 °C over 30 minutes and cool back to 10 °C over 30 minutes) was applied and exciplex disappearance monitored for the complex.

2.5.13.2 DNA-diene system: Proexc9_5'Pyrene + Proexc3_3'BisNapthalene + Proexc1 (target).

Tris buffer/80% TFE

The complex was formed by sequential addition of the components in the order: Proexc9_5'pyrene, Proexc3_3'napthalene, then Target (Proexc1) from stock solutions (1mM) to Tris buffer containing 80% TFE. The ratio of components used was 1:1:1, the concentration of each component being 2.5 μM. Emission spectra were recorded at each stage to observe the changes in the emission spectra resulting from complex formation. The system was allowed to equilibrate at 10°C for 10 minutes. Melting temperature experiments were performed by heating the system to 40 °C over 15 minutes, and re-annealing by cooling to 10°C over 15 minutes. During the heating and re-annealing procedures emission spectra were recorded at 5 °C increments.

2.5.13.3 DNA system: Proexc10_5'Pyrene + Proexc3_3'BisNapthalene + Proexc1 (target).

Tris Buffer.

The complex between Proexc10_5'pyrene and target was formed first by addition of aliquots (5 μl) of each component from the stock solutions to 2 ml of Tris buffer, emission spectra being taken at each stage of addition. This was followed by a heating and cooling cycle (heating to 60 °C over 30 minutes, then cooling to 10 °C over a further 30 minutes) to allow hybridisation to occur and to remove background exciplex signal from Proexc10_5'pyrene. In the next stage an aliquot (5 μl) of the Proexc3_3'naphthalene component was added from its stock solution to form the complete system. The heating/ re-annealing procedure (heating to 60 °C over 30 minutes and cooling back to 10 °C over 30 minutes) was applied and exciplex disappearance/ formation monitored for the complex.

Tris Buffer/80% TFE

Experiments were performed as above, but in the presence of 80% TFE.

2.5.14 Treatment of data.

In many cases spectra were scaled to the pyrene–monomer emission at 380 nm of the pyrene-bearing probe to facilitate visualisation of and changes in the ratio between the

monomer and excimer/ exciplex band. Scaling was achieved by applying a calculated scaling factor to the spectrum using the Shimadzu RFPC-software. The ratio between the emission intensity of the excimer/ exciplex band at 480 nm and the monomer band at 380 nm (I_E/I_M) was also calculated for each spectrum. Peak areas (areas under curves) were also measured using the Shimadzu RFPC software.

2.5.15 Melting curve experiments.

Melting curve experiments (based on A_{260} profiles) were performed using a Cary 1E UV/visible spectrophotometer (Section 2.2.4) by measuring the change in absorbance at 260 nm with temperature. Melting temperatures (T_m) were determined either by taking the point at half the curve height as T_m, or using the first derivative method. The Cary software calculates and plots the first derivative of the melting curve; the point at which the plot peaks indicates the maximum (or minimum) gradient of the melting curve and is reported as T_m. For this method errors were estimated as shown in Figure 2.12, lines were drawn either side of the curve encompassing the noise and the width between these (number of °C) were taken as the error.

For excimer/ exciplex split-probe systems melting temperatures were also estimated from emission spectra by plotting the change in relative fluorescence of the excimer/ exciplex band at 480 nm against temperature, with T_m obtained by taking the point at half the curve height.

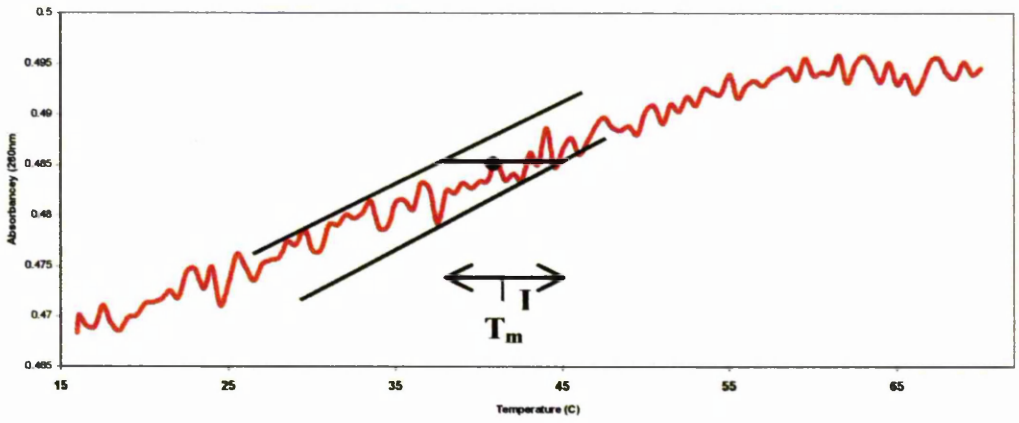

Figure 2.12: Diagram of procedure for error estimation for the first derivative method in A_{260} melting temperature profiles (data for unmodified Proexc11 in Tris buffer).

3. Results.

3.1 Results of DNA-based split-probe systems.

3.1.1 Introduction.

The model split-probe systems consisted of two 8-mer probes, one bearing the exci-partner on the 5'-phosphate and the other bearing an exci-partner on the 3'-phosphate. The exci-partners, in the studies of this thesis (pyrene-based or naphthalene-based) were linked to the oligo *via* a phosphoramide link to the terminal phosphate groups (see Section 2.1.5 Figure 2.1) The probes were designed so that when they bound to the 16-mer target strand as shown in Section 2.1 the exci-partners would be brought into close proximity. Under the right conditions excimer/ exciplex emission would be seen on irradiation at the appropriate wavelength.

Three DNA systems were studied, the first an excimer system (SP-1, Section 2.1) and the other two based on exciplex formation. The first exciplex construct (SP-2) had a pyrenyl group attached to the 5'-phosphate of one 8-mer (Oligo1_5'pyrene) and a N'-methyl-N'-naphthalenyl-ethane diamino group (referred to as a naphthalene group henceforth) attached through its nitrogen atom to the 3'-phosphate of the other 8-mer (Oligo2_3'naphthalene). SP-3 (the other exciplex system) had the N'-methyl-N'-naphthalenyl moiety attached to the 5'-phosphate site through its nitrogen atom (Oligo1_5'naphthalene) and a pyrenyl group attached to the 3'-phosphate (Oligo2_5'pyrene).

The systems were assembled for fluorescence or other studies by the sequential addition of the components (first probes, then target) to 80% TFE/ Tris (pH 8.5) buffer (10 mM Tris, 0.1 M NaCl, pH 8.5), to give a component concentration of 2.5 μM unless otherwise stated. TFE at 80% v/v was used as under these conditions it typically gave the strongest excimer/ exciplex signal. In pure Tris buffer no signal was seen, perhaps because the hydrophobic exci-partners interact with the nucleotide bases to avoid the polar aqueous hydrophilic environment. After each addition, emission spectra were recorded (excitation wavelengths 340 and 350 nm, slitwidth 5 nm) to follow the formation of the system and the appearance of the excimer or exciplex signal. After the formation of the tandem duplex, the system was generally heated and cooled to allow the duplex to melt and slowly reform more perfectly.

3.1.2 Excimer emission for SP-1

Emission spectra at different stages of formation of the SP-1 system in 80% TFE/ Tris (pH 8.5) are shown in Figure 3.1 (unscaled) and 3.2 (scaled to the LES emission at

380 nm). I_E/I_M values increased with increasing TFE concentration (Table 3.1). Of the TFE percentages tested 80% TFE gave the highest I_E/I_M value. The emission spectrum of Oligo1_5'pyrene showed λ_{max} 376 nm. The wavelength of this band did not alter on addition of Oligo2_3'pyrene, showing that no interaction takes place between these two probe oligos in the absence of the complementary target strand. However, the intensity of this band greatly increased (by 4-fold) due to the presence of a second pyrene group in the cuvette. On addition of the target strand the pyrene emission band was red-shifted slightly to 379 nm, consistent with duplex formation. This band was also slightly quenched (1.3-fold) and an additional broad band (λ_{max} 481 nm) appeared, due to excimer formation between the two exci-partners. The excimer band intensity reached a maximum after 10 minutes at 10 °C, the excimer/ LES intensity ratio (I_E/ I_M) being 2.3. After the system had been heated to 40 °C over 5 minutes and allowed to cool back to 10 °C (over approximately 15 minutes) the excimer band reappeared, this time more intense with an I_E/ I_M of 2.74; the LES band showed further quenching. Figure 3.2 shows emission spectra (scaled to LES emission at 380 nm) of Oligo1_5'pyrene at 376 nm to illustrate more clearly the change in I_E/I_M.

Table 3.1: I_E/I_M values for SP-1 in Tris buffer (10 mM Tris, 0.1 M NaCl, pH 8.5) at various TFE concentrations.

Percentage TFE concentration v/v	**I_E/I_M value**
20	0.24
40	0.46
60	0.62
80	2.24

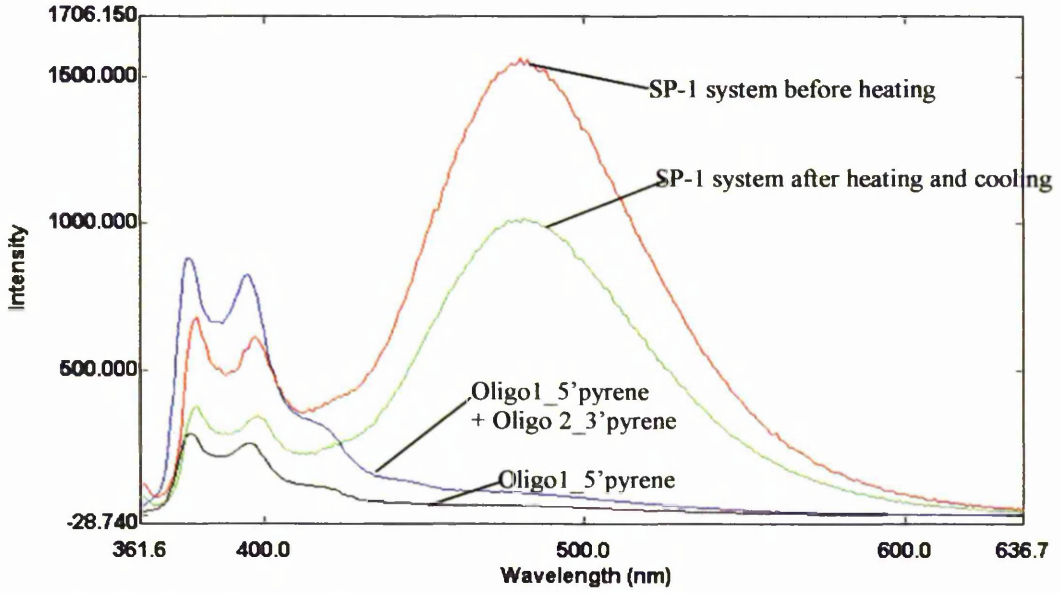

Figure 3.1: Fluorescence spectra at 10 °C for the SP-1 system in 80% TFE/ Tris (pH 8.5) before and after heating to 40 °C compared with the Oligo1_5'pyrene spectrum. Spectra are unscaled. Excitation at 350 nm, slitwidth 5 nm.

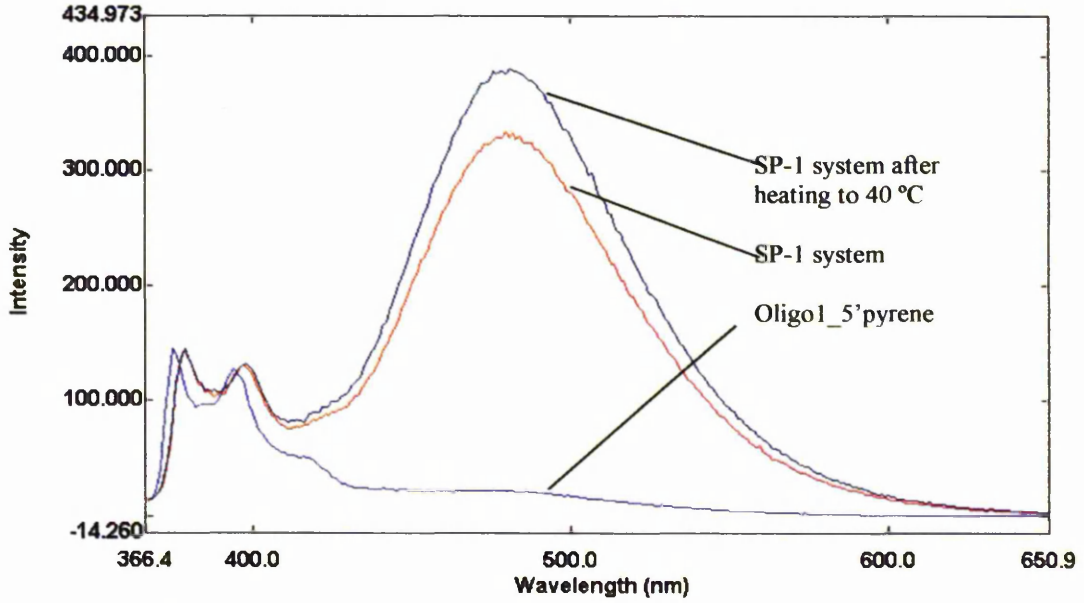

Figure 3.2: Fluorescence spectra at 10 °C for the SP-1 system in 80% TFE/ Tris (pH 8.5) before and after heating to 40 °C compared with the Oligo1_5'pyrene spectrum. Spectra are scaled to LES emission at 376 nm. Excitation at 350 nm, slitwidth 5 nm.

Figure 3.3 shows how the emission and excitation spectra of the probe oligos change on addition of the target strand. The excitation spectrum of Oligo1_5'pyrene showed the maximum excitation wavelength of this component to be 340 nm. The

emission spectrum of this component, for 340 nm excitation, shown alongside the excitation spectrum, has λ_{max} 375 nm. Addition of the second probe oligo (Oligo2_3'pyrene) did not cause any change in the maximum excitation or emission wavelength, but the intensity of both increased greatly, presumably due to the presence of a second pyrene moiety. Addition of the target strand caused a slight red shift in both excitation and emission spectra, consistent with duplex formation. The maximum excitation wavelength shifted from 340 nm to 347 nm. The emission maximum of the full SP-1 system (excitation at 347 nm) also shifted slightly with respect to the two unbound probes, from 375 nm to 379 nm.

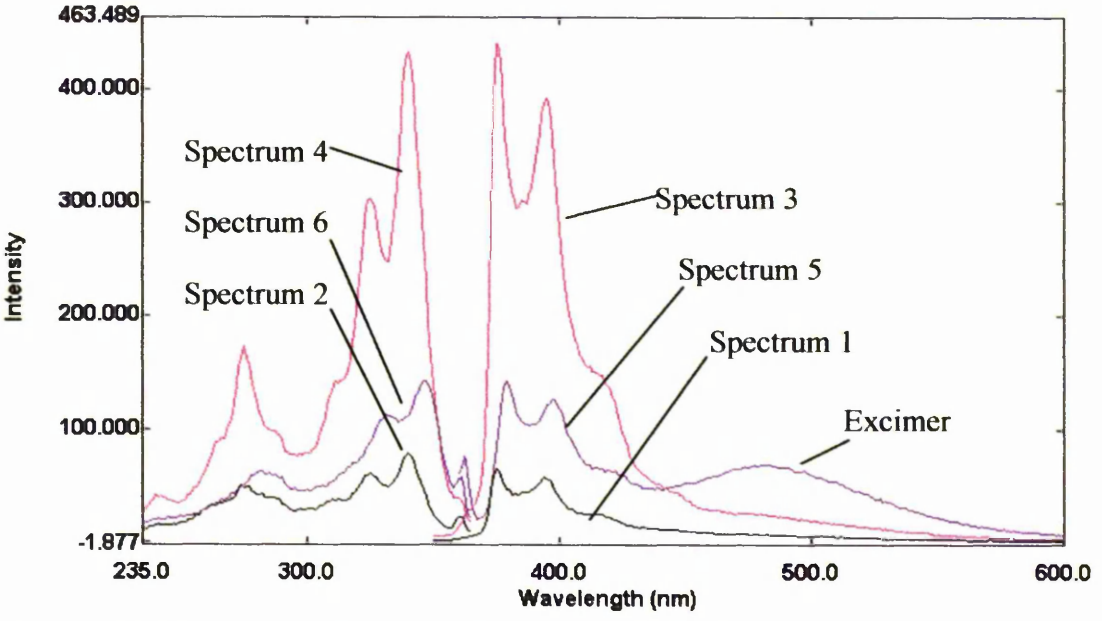

Figure 3.3: Excitation and emission spectra of the SP-1 system at various stages of formation of the full tandem duplex in 80% TFE/ Tris buffer at 10 °C. **Spectrum 1**: Emission spectrum of Oligo1_5'pyrene, excitation at 340 nm, emission λ_{max} 375 nm. **Spectrum 2:** Excitation spectrum of Oligo1_5'pyrene, emission λ_{max} 340 nm. **Spectrum 3:** Emission spectrum of Oligo1_5'pyrene + Oligo2_3'pyrene, excitation 340 nm, emission λ_{max} 375 nm. **Spectrum 4:** Excitation spectrum of Oligo1_5'pyrene + Oligo2_3'pyrene, emission λ_{max} 340 nm. **Spectrum 5**: Emission spectrum of full SP-1 system, excitation at 347 nm, emission λ_{max} 379 nm. **Spectrum 6:** Excitation spectrum of full SP-1 system, emission λ_{max} 347 nm.

The melting temperature (T_m) of the SP-1 system in 80% TFE/ Tris buffer (10 mM Tris, 0.1 M NaCl, pH 8.5), determined (Figure 3.4) from the change the in absorbance at 260 nm, taking the point at half the curve height as T_m, was 26 °C.

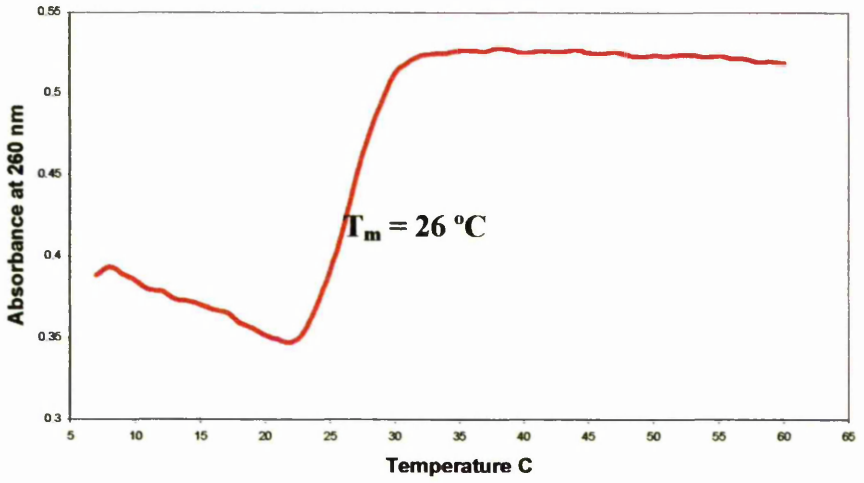

Figure 3.4: Melting curve of SP-1 in 80% TFE/ Tris buffer (10 mM Tris, 0.1 M NaCl, pH 8.5) showing change in absorbance at 260 nm as temperature was ramped at 0.5°C/min. Component concentration 2.5 μM. T_m was determined by the method of half heights.

3.1.3 Exciplex emission for the SP-2 system.

Figure 3.5 shows the unscaled emission spectra of the SP-2 system in 80% TFE/ Tris (pH 8.5) at different stages of tandem duplex formation. The spectra of the two components (Oligo1_5'pyrene + Oligo2_3'naphthalene) with the N'-methyl-N'-naphthalen-1-yl-ethane diamino signal subtracted showed a small background signal (λ_{max} 480 nm, Figure 3.6) possibly due to pyrene interacting to form exciplex(es) with the nucleotide bases of the probe. This phenomenon will be analysed in the Discussion chapter. Heating the sample containing the probes to 40 °C and re-cooling removed this background emission. The emission maximum of the LES was at 376 nm, characteristic of pyrene emission from the un-duplexed pyrene-bearing probe. On addition of the target strand, λ_{max} of LES emission shifted slightly (to 379 nm), accompanied by an increase of almost 5-fold in LES emission intensity. This increase in intensity occurred because all spectra shown here were recorded using an excitation wavelength of 350 nm. However, the excitation maximum of the unbound probe is 340 nm. When the probe binds to the target, the excitation spectrum shifts slightly and the maximum becomes 347 nm (see Figure 3.7). The addition of the target also caused the appearance of a signal with an emission

maximum at 482 nm, typical of an exciplex, accompanied by a 2.6-fold quenching of the LES band. The intensity of the exciplex band increased to a maximum after 9 minutes (I_E/ I_M 0.45). After heating (40 °C for 5 minutes) and cooling back to 10 °C the exciplex band (still λ_{max} 482 nm) became more intense (I_E/ I_M 0.47). Scaled data are shown in Figure 3.6.

For the SP-2 system in 80% TFE/ Tris buffer (10 mM Tris, 0.1 M NaCl, pH 8.5) the value of T_m was found to be 24 °C (Figure 3.8, derived from change in absorbance at 260 nm taking the point at half the curve height to be T_m).

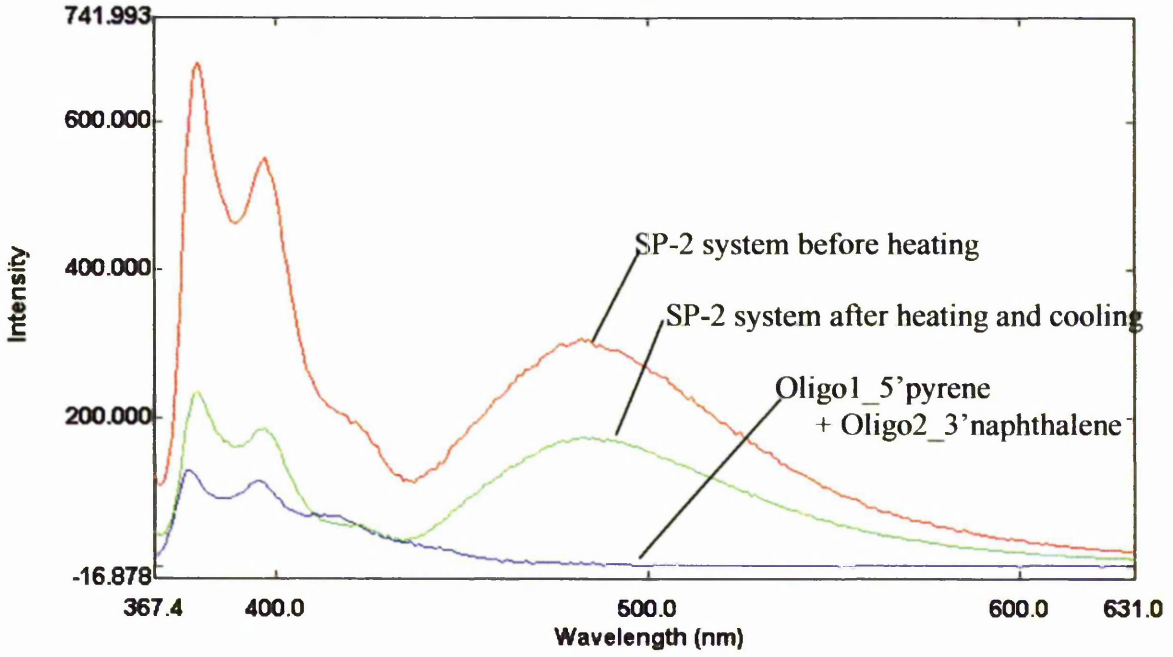

Figure 3.5: Unscaled emission spectra at 10 °C at different stages of formation of the SP-2 system (Oligo1_5'pyrene + Oligo2_3'naphthalene + DNA target) in 80% TFE/ Tris (pH 8.5) before and after heating to 40 °C (5 min) and cooling. Spectra were recorded using excitation at of 350 nm and slitwidth 5 nm.

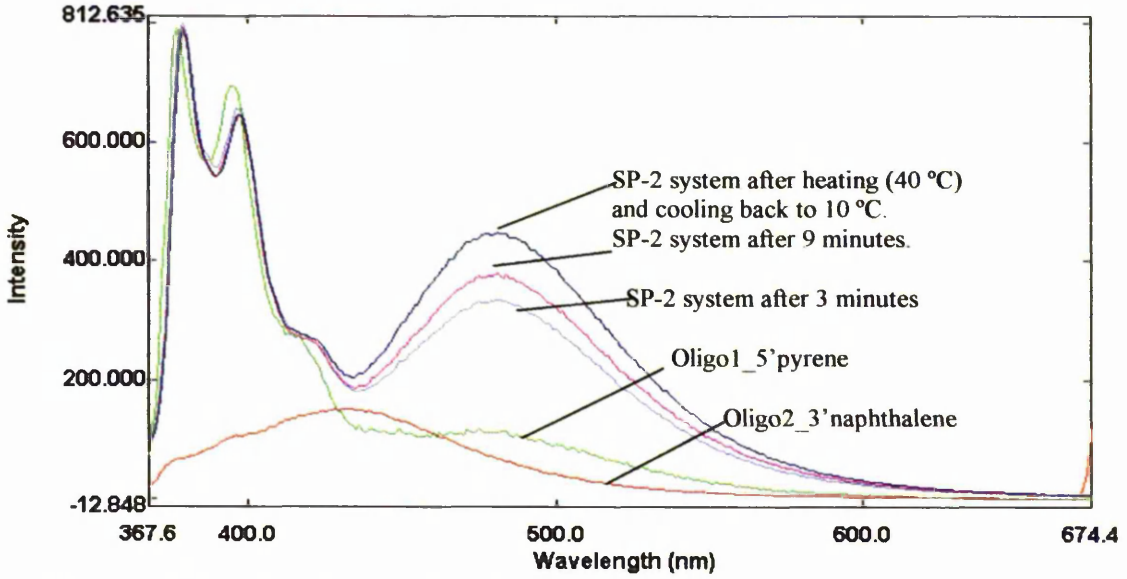

Figure 3.6: Emission spectra at 10 °C at different stages of formation of the SP-2 system (Oligo1_5'pyrene + Oligo2_3'naphthalene + DNA target) in 80% TFE/ Tris (pH 8.5). Spectra were recorded 3 and 9 minutes after formation of the full system (at 10 °C) and after heating to 40 °C (5 min) and cooling. All spectra were recorded using excitation at 350 nm and slitwidth 5 nm. Spectra are scaled to LES emission for comparison.

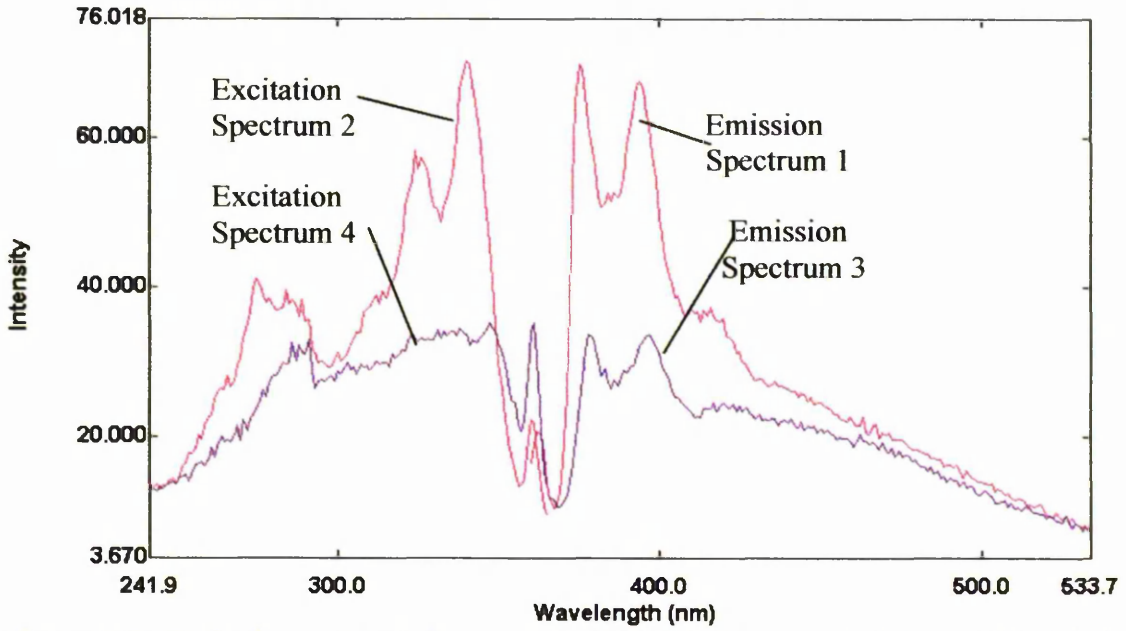

Figure 3.7: Excitation and emission spectra of Oligo1_5'pyrene + Oligo2_3'Naphthalene and the full SP-2 system in 80 % TFE/ Tris buffer at 10 °C. **Spectrum 1**: emission spectrum of Oligo1_5'pyrene + Oligo2_3'naphthalene, excitation wavelength 340 nm, emission λ_{max} 375 nm. **Spectrum 2**: Excitation spectrum of Oligo1_5'pyrene + Oligo2_3'naphthalene, excitation λ_{max} 340 nm, **Spectrum 3**: Emission spectrum of SP-2 system, excitation wavelength 347 nm, emission λ_{max} 379 nm. **Spectrum 4:** Excitation spectrum of SP-2 system, λ_{max} 347 nm.

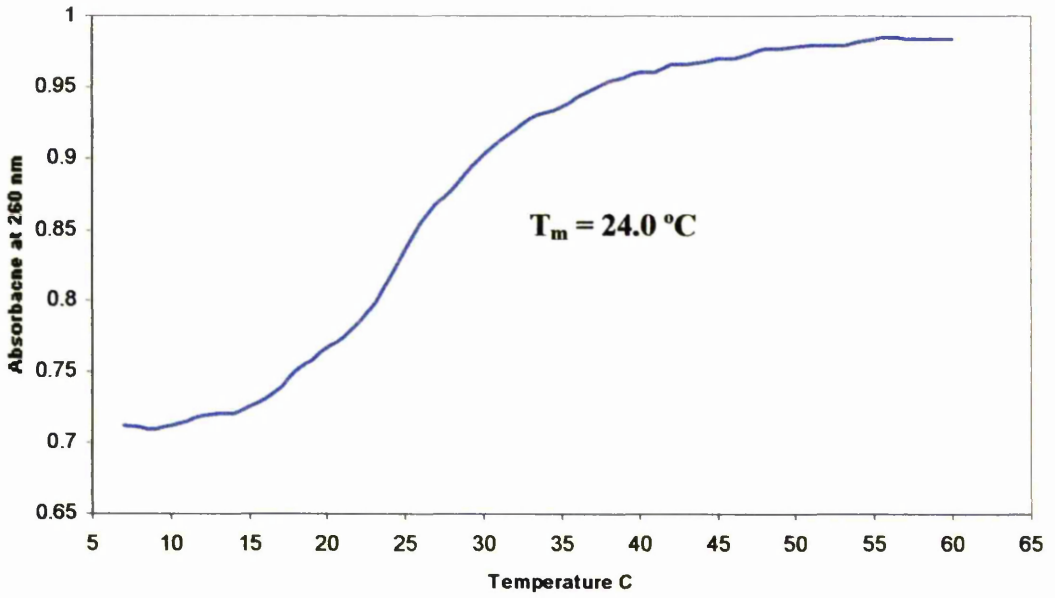

Figure 3.8: Melting curve of SP-2 in 80% TFE/ Tris buffer (10 mM Tris, 0.1 M NaCl, pH 8.5) showing the change in absorbance at 260 nm as the temperature was ramped at 0.5°C/min. Component concentration 2.5 μM. T_m was determined by the method of half heights.

3.1.4 Exciplex emission for the SP-3 system.

Figure 3.9 shows unscaled emission spectra for the full SP-3 system (Oligo1_5'naphthalene + Oligo2_3'pyrene + DNA target) together with the spectrum of Oligo2_3'pyrene. (The emission spectrum of the naphthalene-bearing probe, which was added to the buffer first, was subtracted in each case). The LES emission of pyrene in the presence of the naphthalene-bearing probe had λ_{max} 376 nm. On addition of the target this was slightly quenched and slightly red-shifted to 379 nm, a broad exciplex emission band also appearing at 482 nm. The exciplex band intensity increased over time, reaching a maximum after about 10 minutes (initially I_E/ I_M was 0.38, becoming 0.87 after 10 minutes, see Figure 3.10, scaled data). The spectrum taken after heating the system to 40 °C and cooling back to 10 °C showed a large increase in exciplex emission relative to before heating and also large quenching of the LES emission band (over a 3-fold drop in intensity of this band was observed). After heating the I_E/ I_M was 1.10, compared to 0.87 before heating.

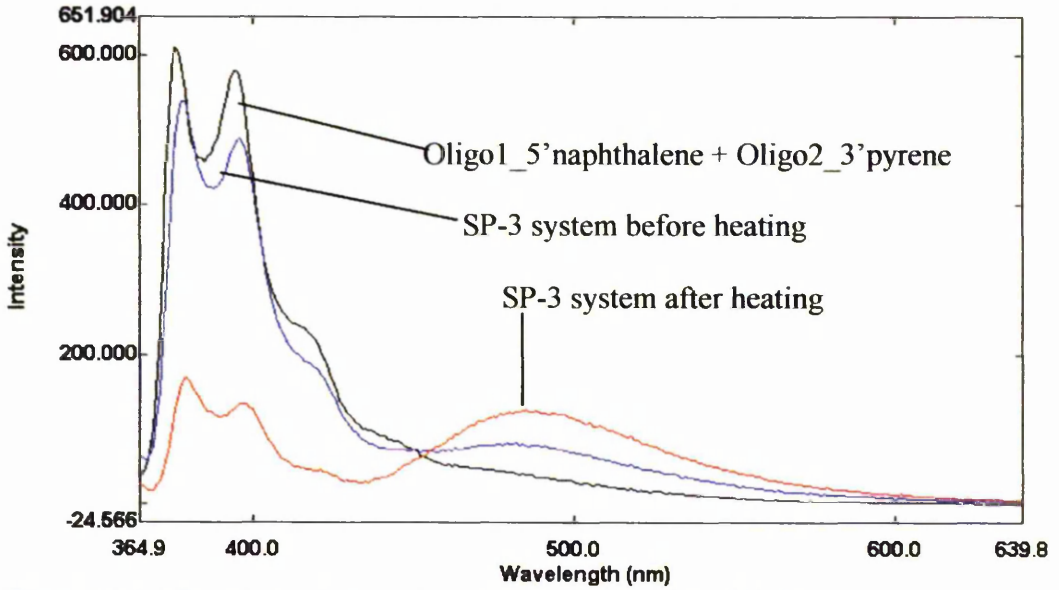

Figure 3.9: Unscaled emission spectra of (Oligo1_5'naphthalene + Oligo2_3'pyrene) and the full SP-3 system (Oligo1_5'naphthalene + Oligo2_3'pyrene + target) in 80% TFE/ Tris (pH 8.5) at 10 °C, showing the effect of heating to 40 °C for 5 minutes and cooling back to 10 °C. Excitation wavelength 350 nm, slitwidth 5 nm.

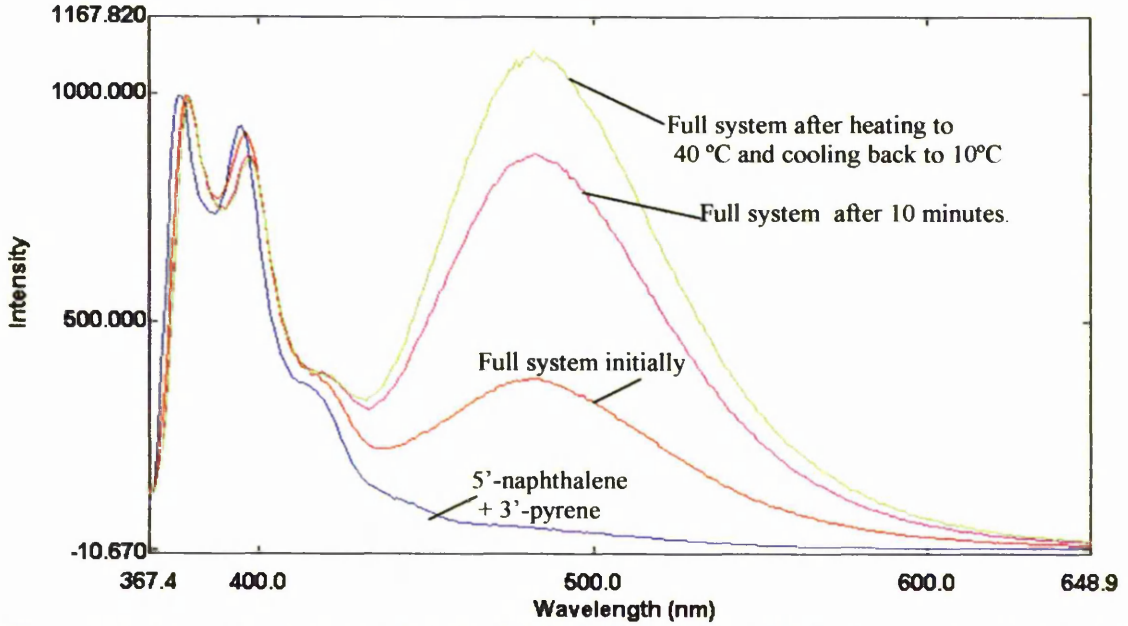

Figure 3.10: Emission spectra in 80% TFE/ Tris (pH 8.5) at 10 °C of SP-3, (Oligo1_5'naphthalene + Oligo2_3'pyrene + target) at various stages of formation of the tandem duplex, showing the effect of incubation time after target addition and of heating to 40 °C for 5 minutes and cooling back to 10 °C. Excitation wavelength 350 nm, spectra are scaled to LES signal.

3.1.5. Control experiments.

Control experiments were carried out in 80% TFE/ Tris (pH 8.5) to determine whether the exciplex/ excimer fluorescence arose from pyrene interacting with the planned

exci-partner or with the bases of the oligonucleotides. This was important to assess as sometimes weak exciplex emission was detected from pyrene attached to the 5'-terminus of Oligo1 in the absence of any added oligo. No such exciplex was seen for the naphthalene derivative attached to the probe oligos, the emission of naphthalene was seen only to shift a few nanometers (from 429 nm unconjugated to 434 nm on conjugation to the oligos) on conjugation to the oligonucleotide probe: no new band appeared. Two control systems were investigated. The first (C-1) had a pyrene group attached to the 5'-phosphate of Oligo1, but the 3'-phosphate of Oligo2 was left unmodified as free phosphate (no other exci-partner was attached). The second (C-2) had the pyrene moiety attached to the 3'-phosphate of Oligo2, and no exci-partner attached to the 5'-phosphate of Oligo1. Experiments were performed as for the experimental systems, but the stepwise addition of the components from stock solution was in the order: pyrene-bearing probe-oligo, probe-oligo bearing no exci-partner and finally target. Spectra were taken at each stage of component addition.

3.1.5.1 Emission spectra for the C-1 system.

Figure 3.11 shows the emission spectra at various stages of component addition of the control system C-1. The Oligo1_5'pyrene probe showed no resolved exciplex band in the absence of any other component. On addition of the second probe oligo, still no exciplex band was detected and there was no shift in λ_{max} (377 nm) of LES emission. Addition of the target strand caused a slight shift in λ_{max} of LES emission to 379 nm, consistent with binding. However, no resolved exciplex band was seen, even after heating the system to 50 °C and re-annealing by cooling back to 10 °C. The Oligo1_5'pyrene did show a large structureless shoulder from 430-500 nm approximately, and this was stronger for the full system (although it did not change markedly on the heating-cooling cycle).

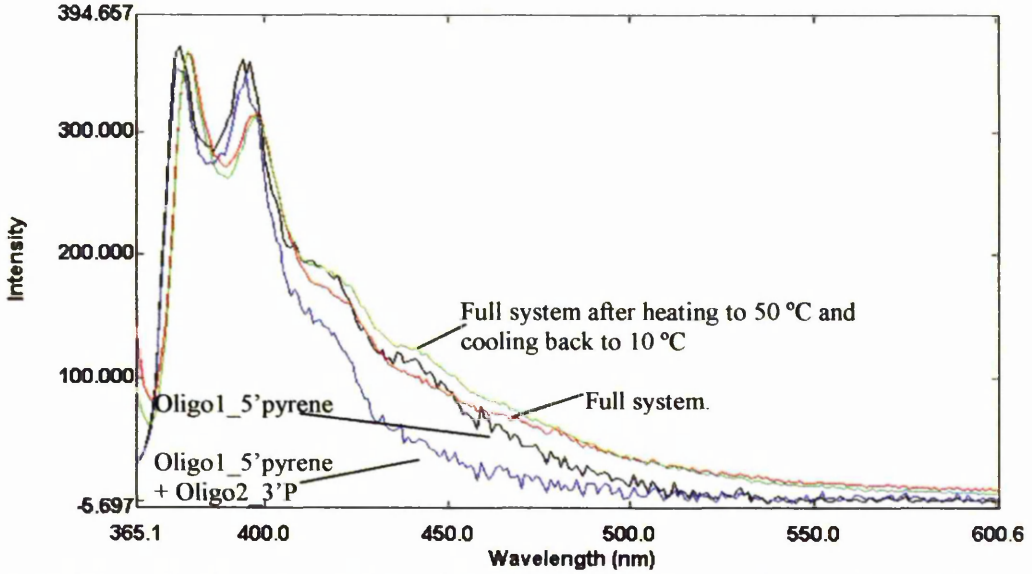

Figure 3.11: Emission spectra for control system C-1 (Oligo1_5'pyrene + Oligo2_3'phosphate + Target) in 80% TFE/ Tris (pH 8.5) at 10 °C. Excitation wavelength 350 nm, slitwidth 5 nm. Spectra are buffer-corrected and scaled to LES emission at 379 nm.

3.1.5.2 Emission spectra for the C-2 system.

No exciplex signal was seen at any stage of formation of the 3'-control system (Figure 3.12). Oligo2_3'pyrene had λ_{max} 377 nm for emission, which did not alter on addition of the second probe-oligo, Oligo1_5'-phosphate. Addition of the target caused a shift in LES band emission to 380 nm consistent with formation of the duplex, but no resolved exciplex band was detected. Heating the system to 50 °C (5 minutes) and re-annealing by cooling back to 10 °C did not alter the emission spectrum.

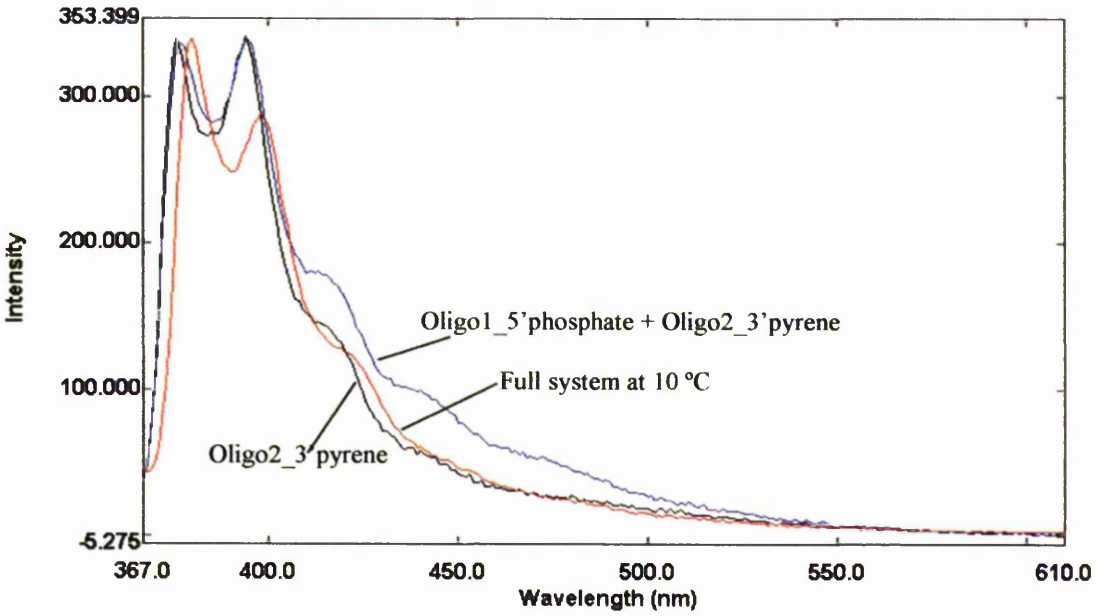

Figure 3.12: Emission spectra for the C-2 (Oligo1_5'phosphate + Oligo2_3'pyrene + target) at various stages of tandem duplex formation in 80% TFE/ Tris (pH 8.5) at 10 °C. Excitation wavelength 350 nm, slitwidth 5 nm. Spectra are buffer-corrected and scaled to LES emission at 377 nm

3.2 Effect of peptide-based linkers on excimer/exciplex emission.

3.2.1 Introduction.

In an attempt to improve excimer/ exciplex emission, an alternative linker system was studied using the same exci-partner systems as described for SP-1, SP-2 and SP-3. Peptide-based linkers ($Ala(Gly)_4$) were used to attach the exci-partners to the 5'or 3'-terminal phosphate groups of the probe oligos. The exci-partners were thus separated from the nucleotides by five amino acids (see Aims, Section 1.15.1). The structures and methods of attachment are shown in Section 2.1.5 Figure 2.2.

The systems tested (see Section 2.1) were modifications of the excimer and exciplex systems used above. SP-4 had peptide-pyrene attached to the 5'- and 3' -terminal phosphate groups of both probes. SP-5 had peptide-pyrene on the 5'-terminus of Oligo 1 and peptide-(N'-methyl-N'-naphth-1''-ylamino)-2-ethylamine (peptide-naphthalene) on the 3'-terminus of oligo 2. SP-6 had peptide-naphthalene on the 5'-phosphate and peptide-pyrene on the 3'-phosphate. The systems were tested as before in Tris buffer (10 mM Tris, 0.1 M NaCl, pH 8.5, component concentration 2.5 μM, unless otherwise stated), but with various TFE concentrations (0-80%) to determine the effect of linker on the optimal TFE requirement for exci-signal generation.

3.2.2 Excimer emission for the SP-4 system.

For the 5'-pyrene and 3'-pyrene oligos with the exci-partners attached *via* peptide linkers the fluorescence spectra of the individual oligos were similar to those with a direct phosphoramidate linkage. At all TFE concentrations tested Oligo1-5'peptide-pyrene had emission λ_{max} 376 nm. The spectrum was not affected by the addition of the Oligo2_3'peptide-pyrene, apart from an increase in intensity of the pyrene LES signal, indicating that no interaction of these oligos occurs. In 80% TFE/ Tris (pH 8.5) Oligo1_5'peptide-pyrene showed a background exciplex signal in the absence of any other components (see Figure 3.13). By heating the oligo to about 40 °C this intramolecular exciplex, presumably formed by pyrene and the nucleobases of the probe, disappeared and did not reappear on cooling back to 10 °C. On formation of the full tandem duplex system the pyrene LES signal was quenched and shifted slightly to 379 nm. In the absence of TFE no excimer formed. In the presence of 50, 60 and 80% TFE v/v an excimer signal was detected with λ_{max} values of 483 nm in 50% TFE (component concentration 1.2 μM), 485 nm in 60% TFE (component concentration 0.87 μM) and 480 nm in 80% TFE/ Tris (pH 8.5, component concentration 2.5 μM) (Figure 3.13). The intensity of the excimer also

varied with percentage of TFE (see Table 3.2) being most intense in 60% TFE. In 80% TFE/ Tris (pH 8.5) the band was fairly weak before heating, but on heating the intensity increased (Figure 3.14). However, the SP-1 system, with direct phosphoramidate linkage, gave a much higher signal than the corresponding peptide version SP-4 in the presence of 80% TFE/ Tris (pH 8.5), see Figure 3.15 below.

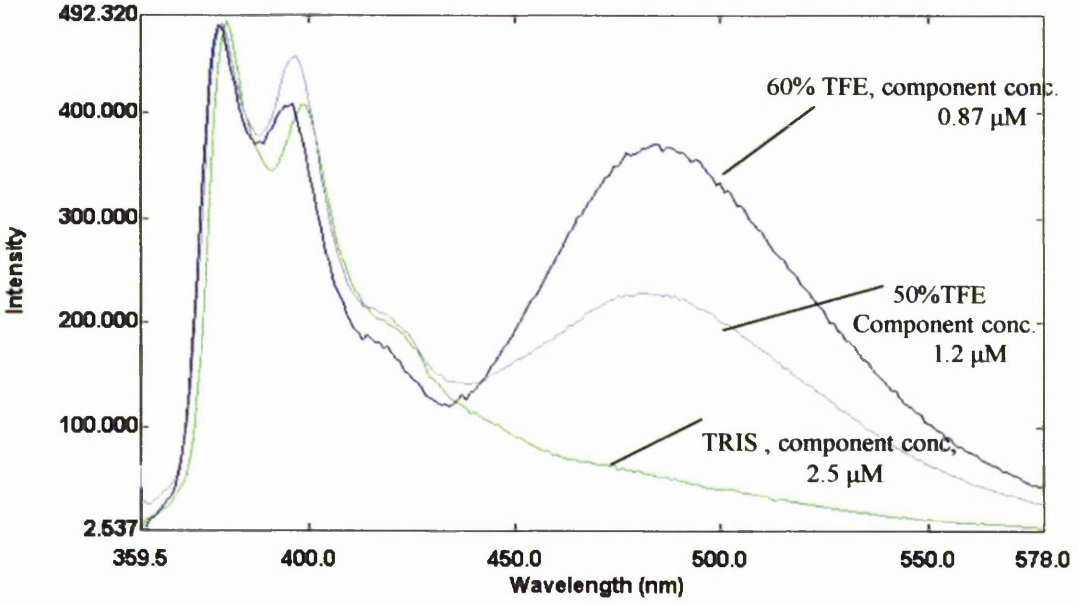

Figure 3.13: Comprison of fluorescence spectra of SP-4 (Oligo1_5'pyrene-peptide + Oligo2_3'pyrene-peptide + target) at various TFE concentrations in Tris buffer (pH 8.5) at 10 °C. Excitation at 350 nm, slitwidth 5 nm. Component concentrations: 2.5 µM in Tris, 1.2 µM in 50% TFE/ Tris and 0.87 µM in 60% TFE/ Tris. Spectra are scaled to LES emission for comparison.

Table 3.2: Values of I_E/ I_M and emission maxima for the SP-4 system at 10 °C in Tris buffer containing various percentages of TFE. The system in 80% TFE was also heated to 40 °C for 5 minutes and allowed to cool back to 10 °C (value in parentheses).

TFE %	Component conc. (µM)	λ_{max} for excimer (nm)	I_E/I_M
0	2.5	-	0.12
50	1.2	483	0.47
60	0.87	485	0.77
80	2.5	480	0.23 (0.68)

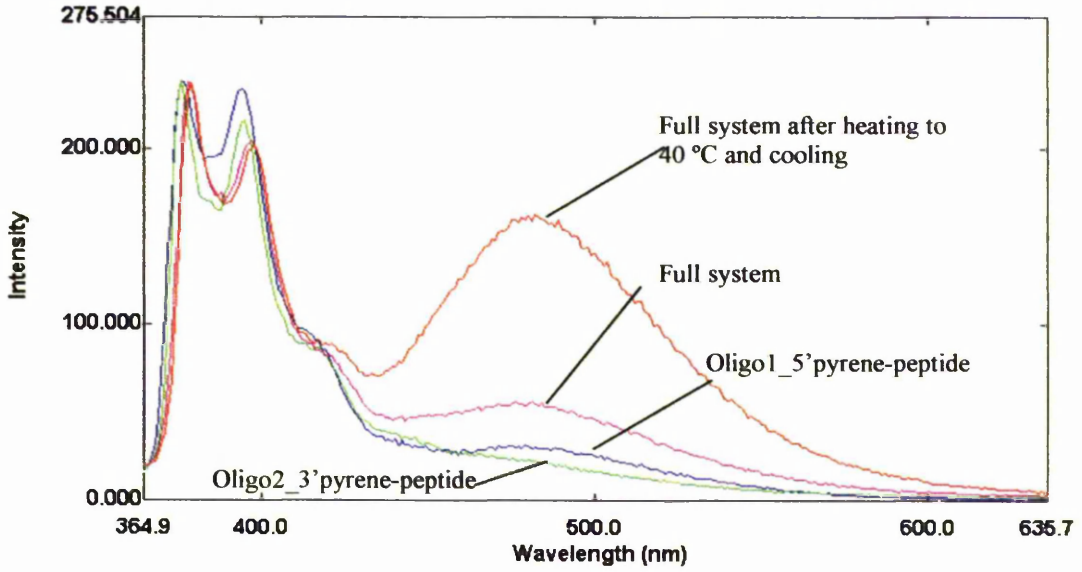

Figure 3.14: Fluorescence spectra at various stages of formation of the complete SP-4 tandem duplex system in 80% TFE/ Tris (pH 8.5) at 10 °C. The system was heated to 40 °C for 5 minutes and allowed to cool back to 10 °C. Excitation 350 nm, slitwidth 5 nm. Spectra are scaled to LES emission

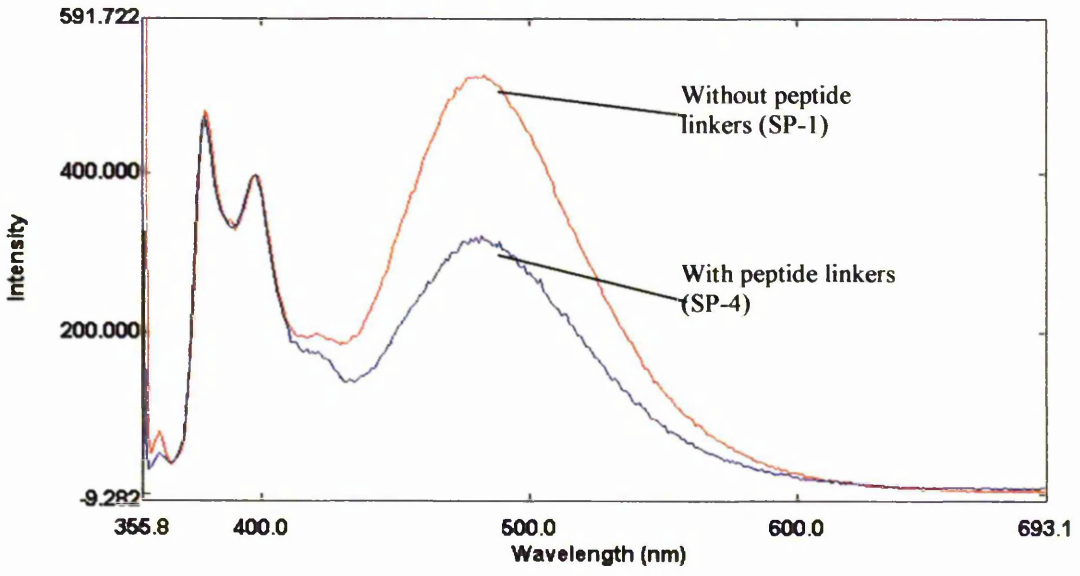

Figure 3.15: Comparision of fluorescence spectra of SP-1 and SP-4 systems (Oligo1_5'pyrene +Oligo2-3'Pyrene + target system with either peptide linkage (SP-4) or direct phosphoramidate linkage (SP-1) to exci-partners) in 80% TFE/ Tris (pH 8.5) at 10 °C. Excitation at 350 nm, slitwidth 5 nm. Spectra are scaled to LES emission at 379 nm.

3.2.3 Exciplex emission for the SP-5 system.

For the SP-5 system with the peptide linkers no exciplex signal was observed on addition of the target strand in Tris buffer (pH 8.5) containing 0, 50 or 60% TFE (component concentrations 1.2 μM in 50 % TFE and 0.87 μM in 60% TFE). The maximum wavelength of LES emission of Oligo1_5'peptide-pyrene (naphthalene emission subtracted) shifted slightly from 377 to 379 nm on addition of the target strand to the two probes, consistent with duplex formation.

On formation of the full system in 80% TFE/ Tris (pH 8.5) the LES emission band of pyrene was quenched and shifted from 377 nm to 379 nm. An exciplex band with λ_{max} 480nm was observed and its intensity increased to a maximum after 12 minutes (I_E/ I_M 0.45) (Figure 3.16). On heating the system to 40 °C and cooling back to 10 °C the exciplex signal observed was much weaker than that seen before heating, having an I_E/I_M value of 0.20 (see Figure 3.17).

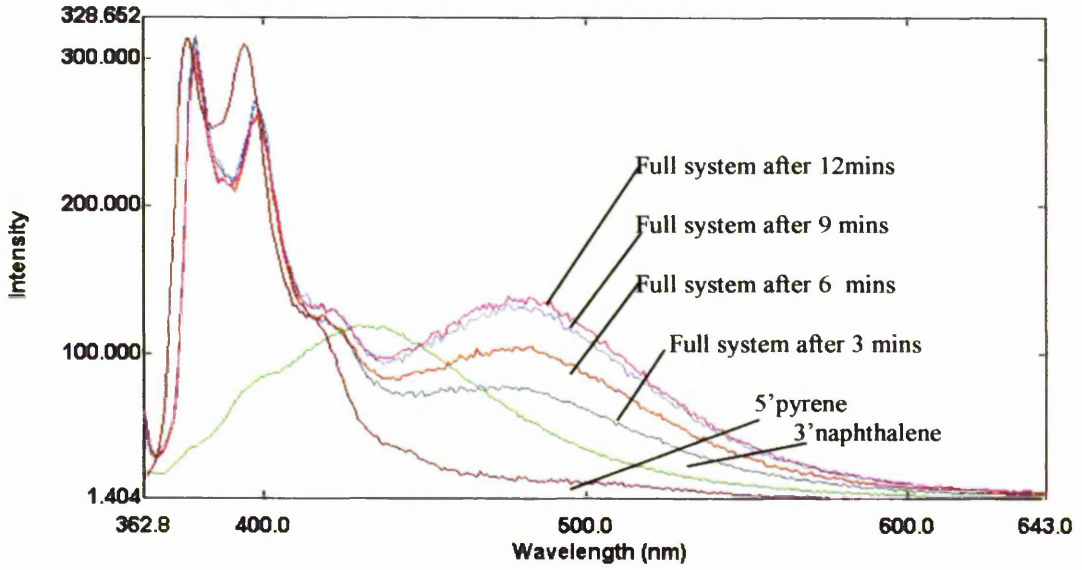

Figure 3.16: Emission spectra at various stages of formation of the SP-5 system in 80% TFE/ Tris buffer at 10 °C showing the effect of incubation time after formation of the full system. Excitation at 350 nm, slitwidth 5 nm. Spectra are scaled to LES emission.

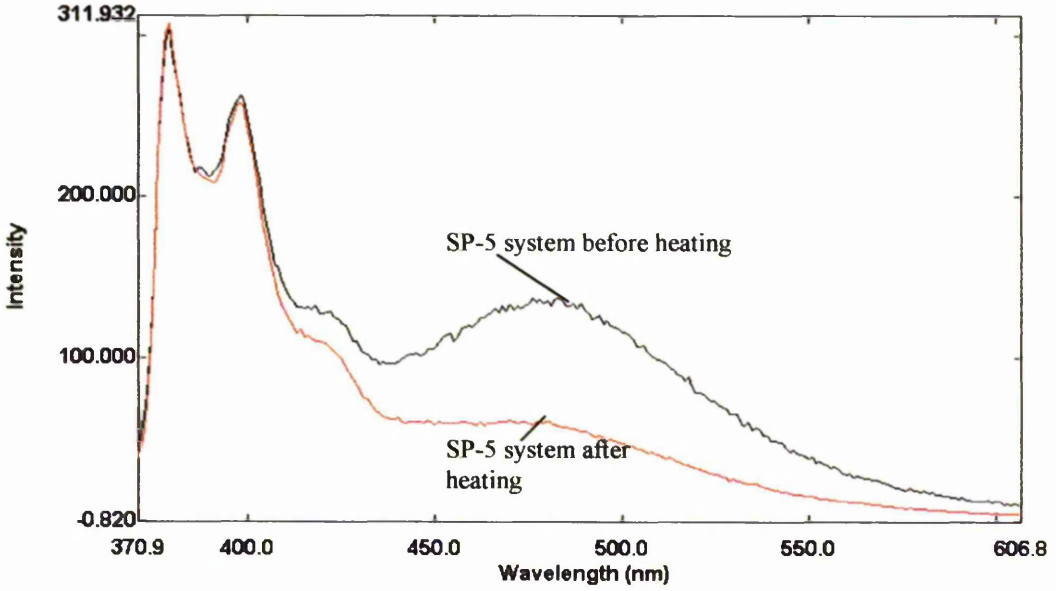

Figure 3.17: Comparison of emission spectra taken at 10 °C of SP-5 in 80% TFE/ Tris buffer before and after heating to 40 °C for 5 minutes and cooling back to 10 °C. Excitation wavelength 350 nm, spectra are scaled to LES emission.

3.2.4 Exciplex emission for the SP-6 system.

For the SP-6 system in Tris buffer at 10 °C no exciplex emission was detected for the full system at TFE concentrations of 0 and 50 (component concentrations: 2.5 μM in Tris, 1.2 μM in 50% TFE) (Figure 3.18). The emission maximum of Oligo2_3'peptide-pyrene (with the naphthalene signal subtracted) was 376 nm in the presence of the second probe. On addition of the target strand this shifted to 377 nm, consistent with binding. No exciplex emission appeared even after the system had been allowed to equilibrate at 10 °C for 15 minutes. A very small exciplex signal was seen in 60 % TFE (component concentration 0.87 μM) (Figure 3.18).

In 80% TFE/ Tris (pH 8.5) an exciplex emission band with λ_{max} 484 nm appeared when the target strand was added, the LES band shifting from 376 nm to 378 nm. Exciplex emission intensity increased to a maximum after 10 minutes at 10 °C (I_E/ I_M 0.43) (Figure 3.19). When the system was heated to 40 °C over 30 minutes, with spectra taken at 5 °C increments (only selective spectra are shown in Figure 3.19), the exciplex emission intensity decreased considerably. At 15 °C the I_E/ I_M value had dropped to 0.12 from 0.43, and by 20 °C the exciplex signal had completely disappeared (Figure 3.19). The LES band (λ_{max} 378 nm at 10 °C) shifted to 377 nm at 15 °C, and to 376 nm by 30 °C, corresponding to the unbound state. This shift indicated that melting of the duplex had occurred. Cooling

the system back to 10 °C caused the exciplex emission to return, and to a slightly greater intensity (I_E/ I_M 0.48) than before the heating-cooling cycle.

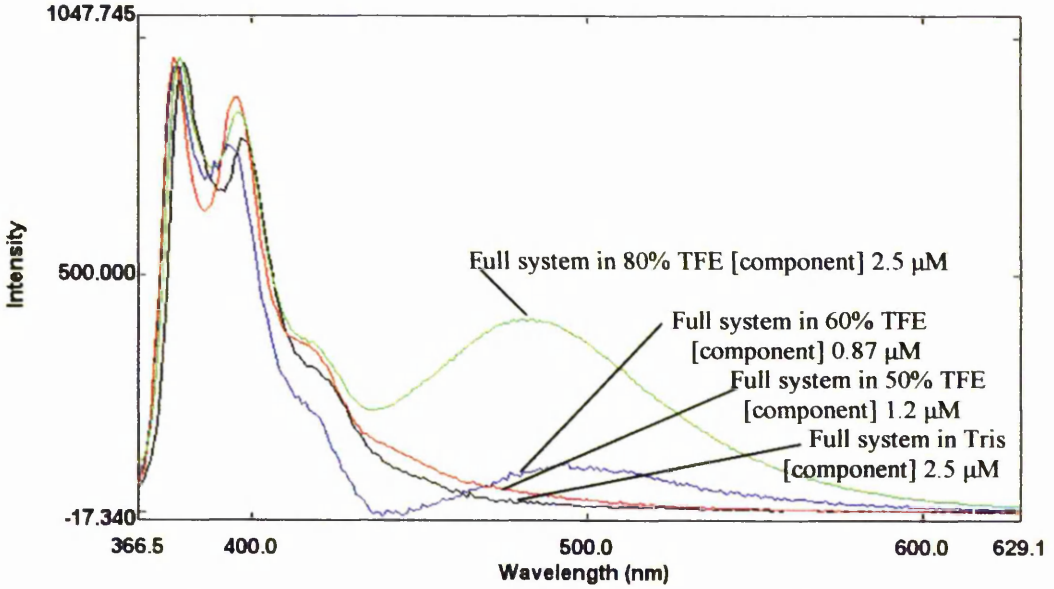

Figure 3.18: Emission spectra of the SP_6 system in Tris buffer (pH 8.5) at 10 °C (Oligo1_5'Naphthalene + Oligo2_3'pyrene + target) showing the effect of TFE concentration on exciplex emission. Excitation wavelength 350 nm, slitwidth 5 nm. Component concentrations: 2.5 µM in Tris and 80% TFE/Tris, 1.2 µM in 50% TFE and 0.87 in 60% TFE. Spectra are scaled to LES emission.

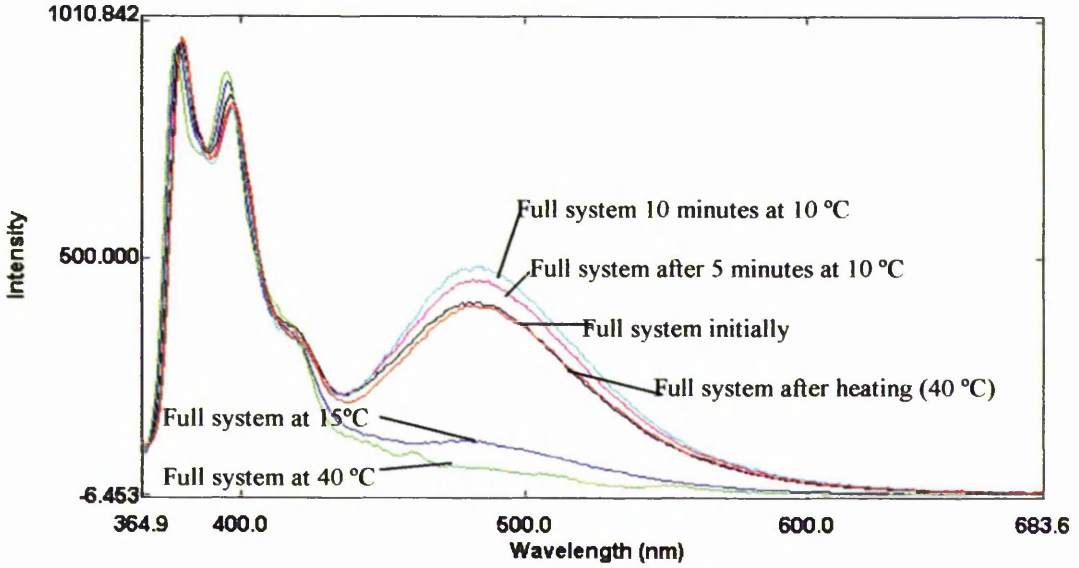

Figure 3.19: Emission spectra of SP-6 in 80% TFE/ Tris buffer at 10 °C, showing the effect of time after formation of the full system and the effect of heating to 40 °C and cooling back to 10 °C on exciplex emission. Excitation wavelength 350 nm, slitwidth 5 nm. Spectra are scaled to LES emission.

Peptide linkers did not enhance exciplex emission for the SP-6 system relative to the corresponding exciplex system with a direct phosphoramidate linkage to the exci-partners (SP-3) under the conditions tested. In fact, the linkers actually resulted in a lower intensity exciplex emission (Figure 3.20). For the SP-3 system in 80% TFE/ Tris buffer the I_E/ I_M value was 1.10 after the heating and cooling cycle (heating to 40 °C and cooling back to 10 °C). However, for the SP-6 system the I_E/ I_M value was only 0.48 under the same conditions. The I_E/ I_M values were also lower for the SP-6 system relative to the SP-3 system for spectra taken before heating the systems.

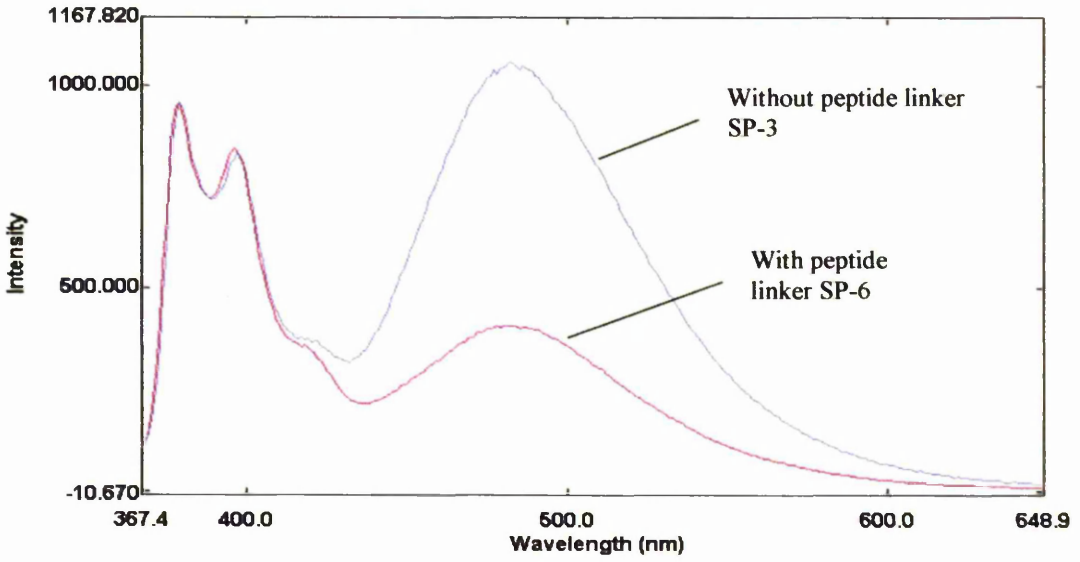

Figure 3.20: Comparision of the emission spectra of the SP-6 and SP-3 systems in 80% TFE/ Tris (pH 8.5) at 10 °C after heating to 40 °C and cooling back to 10 °C showing the difference in exciplex intensity. Excitation wavelength 350 nm, slitwidth 5 nm. Spectra are scaled to LES emission at 377 nm.

3.2.5 Control system for the peptide linkers.

Control experiments were carried out in 80% TFE/ Tris (pH 8.5) at 10 °C to elucidate if the excimer/ exciplex signal detected for the experimental systems was due to interaction of exci-partners, or had background components from pyrene exciplexes with the nucleotide bases. The two systems used to investigate this aspect were:

- C-3 system where Oligo1 had a pyrene moiety attached, *via* the peptide linker, to its 5'-phosphate group. Oligo_2 had an unmodified 3'-phosphate group (see Section 2.1.2).

- C-4 system with the pyrene group attached *via* the peptide linker to the 3'-terminal phosphate group of Oligo2, and Oligo1 had an unmodified terminal 5'-phosphate (see Section 2.1.2).

The control experiments were carried out as for the experimental systems. Each component was added stepwise from a stock solution in the order: pyrene-bearing oligo, unmodified-oligo and finally target. Emission spectra were taken at each stage.

3.2.5.1 Emission spectra for the C-3 system.

Emission spectra at various stages of component addition of the C-3 system are shown in Figure 3.21. No resolved exciplex fluorescence band was seen at any stage. The emission maximum of the LES band (377 nm) for the Oligo1_5'peptide-pyrene probe was not affected by addition of the second unmodified-probe (Oligo2_3'phosphate). However, on addition of the target this band shifted to 380 nm, indicating that duplex formation occurred. No exciplex signal appeared, even after the heating-cooling cycle (heating to 40 °C and cooling back to 10 °C) was applied.

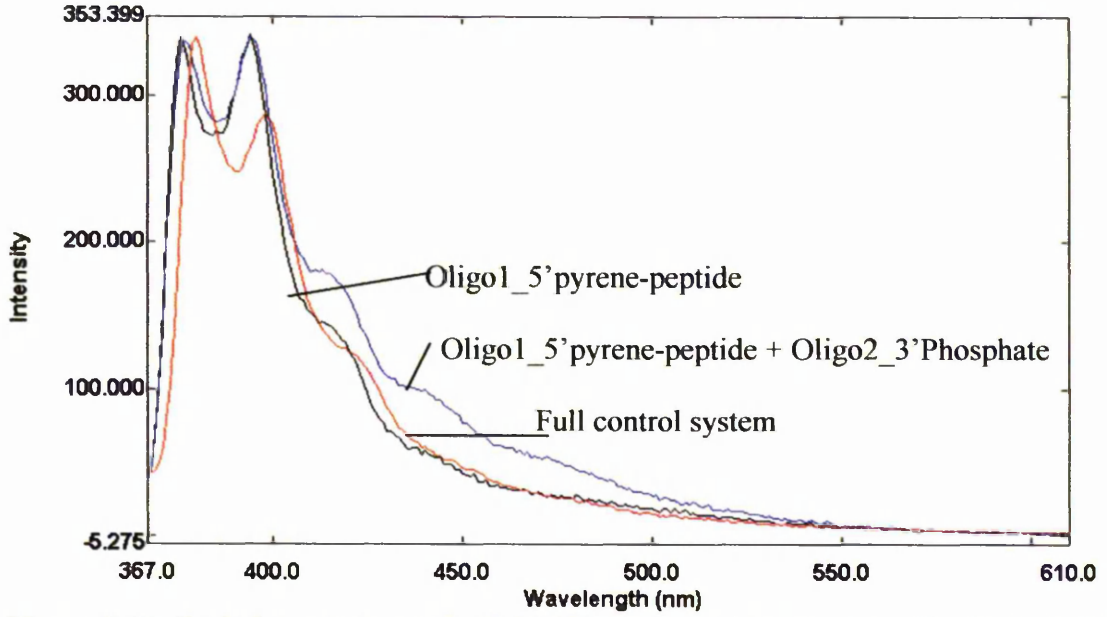

Figure 3.21: Emission spectra of the C-3 (Oligo1_5'peptide-pyrene + Oligo2_3'phosphate + target) in 80% TFE/ Tris (pH 8.5) at 10 °C during formation of the system: no exciplex emission was detected. Excitation wavelength 350 nm, slitwidth 5 nm. Spectra are buffer-corrected and scaled to LES emission at 377 nm.

3.2.5.2 Emission spectra for the C-4 system.

For the C-4 system no exciplex emission was seen for the pyrene-bearing probe (Oligo2_3'peptide-pyrene) in the presence or absence of the other components

(Oligo1_5'phosphate and the target) (Figure 3.22). The emission spectrum of Oligo2_3'peptide-pyrene showed LES emission with λ_{max} 377 nm. Addition of the second oligo probe shifted this maximum to 378 nm. Addition of the target to the two probes caused this band to shift further to 380 nm, which indicated that duplex formation occurred, but without the formation of an exciplex. Applying the heating-cooling cycle (heating to 40 °C and cooling back to 10 °C) did not greatly affect the emission spectra, and still no exciplex emission was observed.

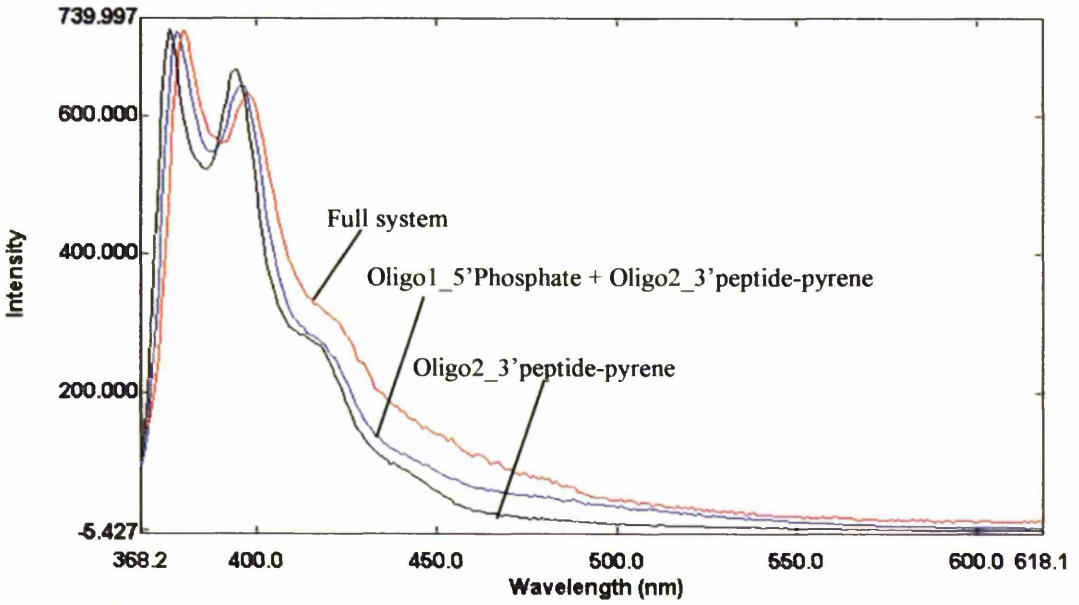

Figure 3.22: Emission spectra at each stage of development of the C-4 system (Oligo1_5'phosphate + Oligo2_3'peptide-Pyrene + target) in 80% TFE/ Tris (pH 8.5) at 10 °C. Excitation wavelength 350 nm, slitwidth 5 nm. Spectra are buffer-corrected and scaled to LES emission at 377 nm.

3.3 Effect of an RNA target on excimer/ exciplex emission.

3.3.1 Introduction.

RNA-DNA hybrid systems were studied to determine whether these gave exciplex signals on formation of the full split-probe system.The DNA 8-mer probes used for the SP-1 and SP-2 systems were employed, with the exci-partners linked directly to the oligos *via* a phosphoramidate link to the terminal phosphate groups. However, the 16-mer target strand was RNA instead of DNA and had the sequence: GCCAAACACAGAAUCG. Systems investigated were SP-7 and SP-8 (see Section 2.1). These are RNA-DNA hybrid analogues of the SP-1 and SP-2 systems, respectively. The systems were tested in 0, 40 and 80% TFE/ Tris (pH 8.5). Each system was formed by the sequential addition of the components (probes first and then target; component concentrations 2.5 μM unless otherwise stated) to the buffer and spectra were recorded on each addition using excitation wavelengths of 340 and 350 nm.

3.3.2 Emission spectra for the SP-7 system.

Excimer emission was observed for the SP-7 split-probe system with the RNA target in 80% TFE/ Tris (pH 8.5). The emission spectrum of the 5'-pyrene-bearing probe had λ_{max} 375 nm. On addition of the RNA target the LES band was quenched (not shown in Figure 3.23) and the emission maximum shifted slightly to 377 nm (Figure 3.23). This was accompanied by the appearance of an excimer band with λ_{max} 477 nm and I_E/ I_M of 0.48. The I_E/ I_M value for the equivalent DNA target (SP-1. I_E/ I_M 2.31) was almost 5 times that of the DNA-RNA hybrid.

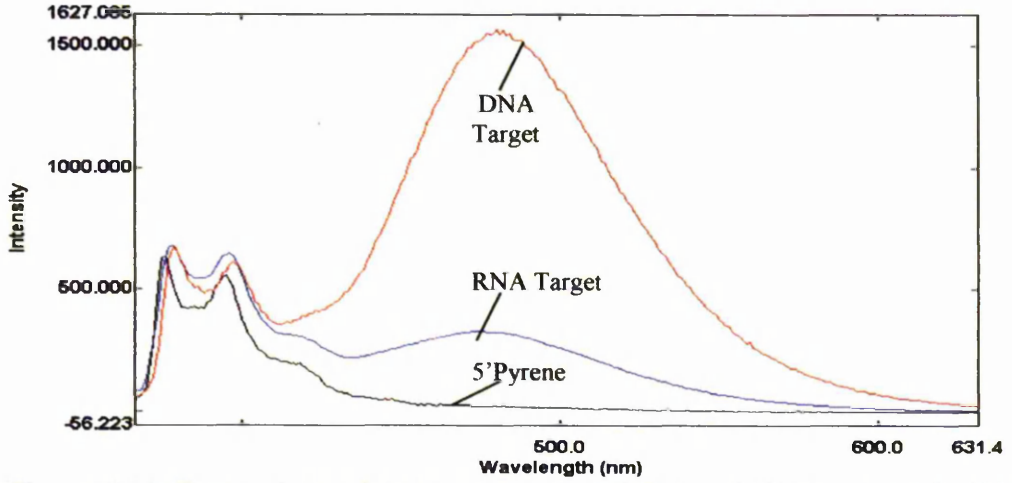

Figure 3.23: Comparison of emission spectra of SP-1 and SP-7 systems in 80% TFE/ Tris (pH 8.5) at 10 °C, component concentration 2.5μM. Excitation wavelength 350 nm; slitwidth 5 nm; spectra are scaled to LES emission.

On addition of the RNA target to the DNA probe components in the absence of TFE (Tris buffer) the LES band shifted from 377 nm to 380 nm and a small band for excimer emission was also detected (λ_{max} 482 nm, I_E/ I_M 0.15) (Figure 3.24). Addition of TFE, to a concentration of 40% (component concentration 1.25 μM), caused the intensity of this excimer band excimer to increase greatly to a higher I_E/ I_M (0.95) than in the presence of 80% TFE/ Tris (Figure 3.25). Gradually heating the system in 40% TFE/ Tris to 50 °C over 30 minutes caused a decrease in excimer emission, which fully disappeared above 40 °C (Figure 3.26).

Although in the presence of the RNA target excimer formation did occur between the two DNA-mounted exci-partner probes, the intensity of the excimer was almost 5 times weaker than the equivalent DNA-DNA system (SP-1). Also, although excimer emission appears to be more intense at lower TFE concentrations for the RNA system, a stronger excimer signal was still emitted by the DNA-DNA system. However, it is worth noting that excimer emission was detected in the absence of TFE for the RNA:DNA hybrid system, although the band was very weak.

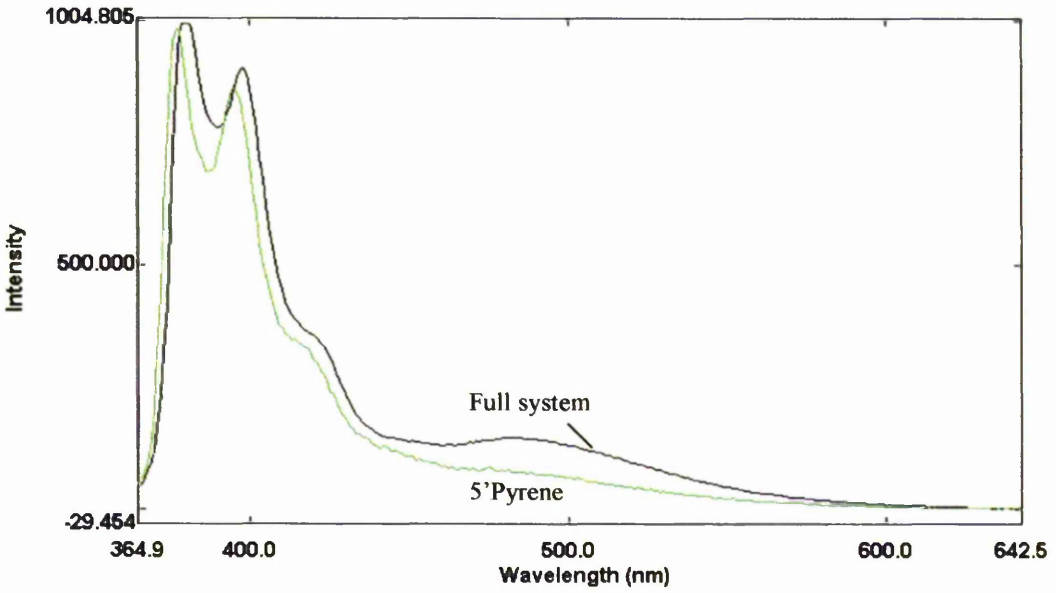

Figure 3.24: Emission spectra of Oligo1_5'pyrene and the full SP-7 system in Tris buffer (pH 8.5, component concentration 2.5 μM) at 10 °C, showing the weak excimer emission. Excitation wavelength 350 nm; slitwidth 5 nm; spectra are scaled to LES emission.

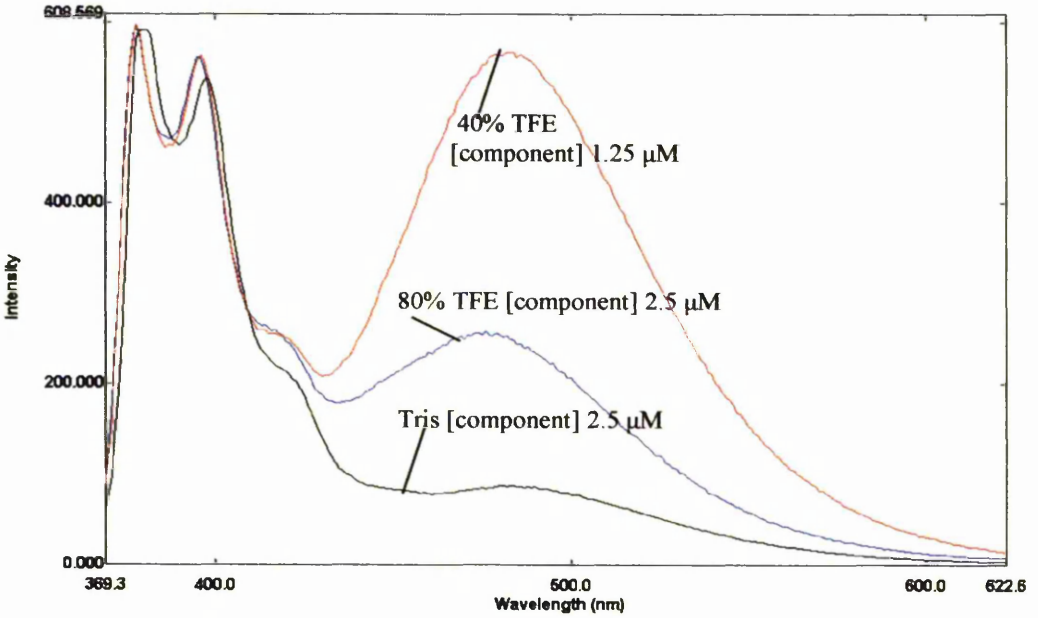

Figure 3.25: Comparison of emission spectra of the SP-7 system in Tris buffer (component concentration 2.5 μM), 40% TFE (component concentration 1.25 μM) and 80% TFE/ Tris buffer (component concentration 2.5 μM) at 10 °C. Excitation wavelength 350 nm; slitwidth 5 nm; spectra are scaled to LES emission.

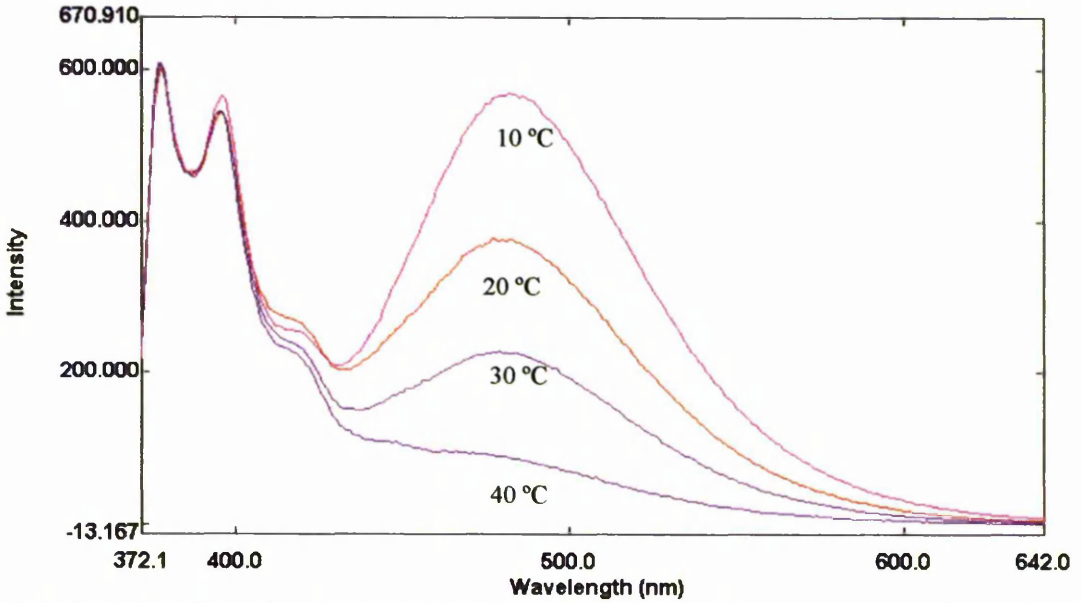

Figure 3.26: Emission spectra showing the decrease in excimer emission intensity on heating the SP-7 system to 40 °C in 40 % TFE/Tris buffer (component concentration 2.5 μM). Excitation wavelength 350 nm; slitwidth 5 nm; spectra are scaled to LES emission.

A melting curve was constructed from the fluorescence data by plotting fluorescence intensity at 480 nm against temperature for SP-7 in 40% TFE/ Tris buffer (10

mM Tris, 0.1 M NaCl, pH 8.5) (Figure 3.27), but the value of T_m could not be reliably determined this because of incomplete sigmoidicity.

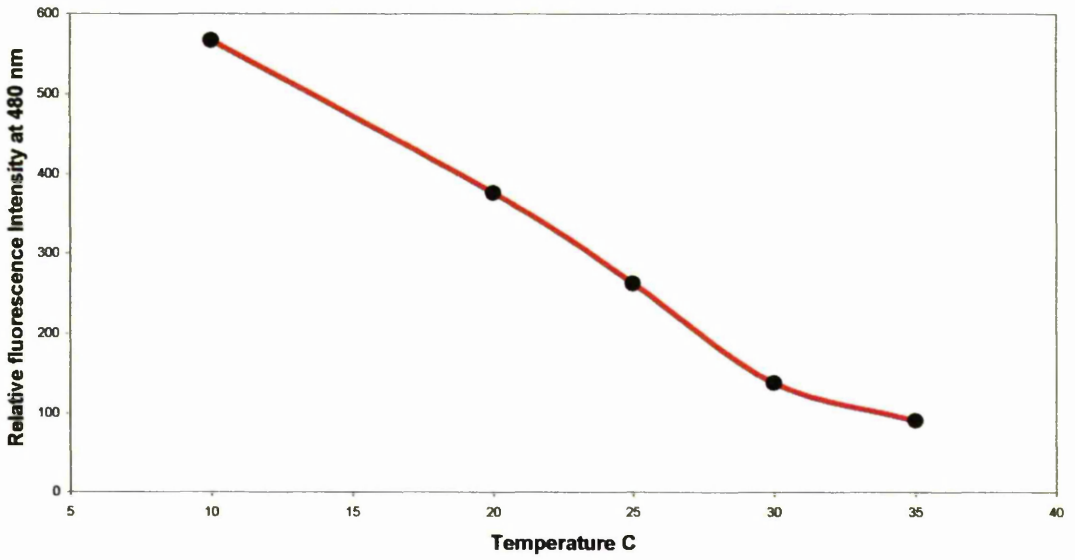

Figure 3.27: Melting curve for SP-7 in 40% TFE/ Tris buffer (10 mM Tris, 0.1 M NaCl, pH 8.5) derived from plotting fluorescence intensity at 480 nm against temperature (data taken from Figure 3.26).

3.3.3 Emission spectra for the SP-8 system.

Figure 3.28 shows the emission spectra for the SP-8 system comparing the RNA target to the equivalent DNA target system (SP-2). For the system with the RNA target (SP-8) in 80% TFE/ Tris (pH 8.5), exciplex emission was observed, but λ_{max} value was shifted to 469 nm (compare the DNA–DNA system with λ_{max} 480 nm). The value of I_E/I_M in the presence of either target (DNA or RNA) was similar, being 0.45 for DNA and 0.41 for RNA. However, for the SP-2 DNA-DNA hybrid the exciplex signal appeared to be better resolved from the LES band, advantageous for a detection system.

In the absence of TFE no exciplex emission was seen for the SP-8 system, the small emission observed being also present for 5'-pyrene-bearing probe (Figure 3.29). This was due to background emission caused by pyrene forming an exciplex with the aromatic rings of the nucleotide bases. Exciplex emission resulting from the exci-partners was not seen at TFE concentrations lower than 70%. However, at 70% TFE (component concentration 0.64 μM) a relatively large exciplex emission band was observed with λ_{max} 480 nm (Figure 3.30). The I_E/I_M value of the system with the RNA target was slightly greater at 70% TFE (0.57) than for SP-2 in 80% TFE/ Tris (0.45).

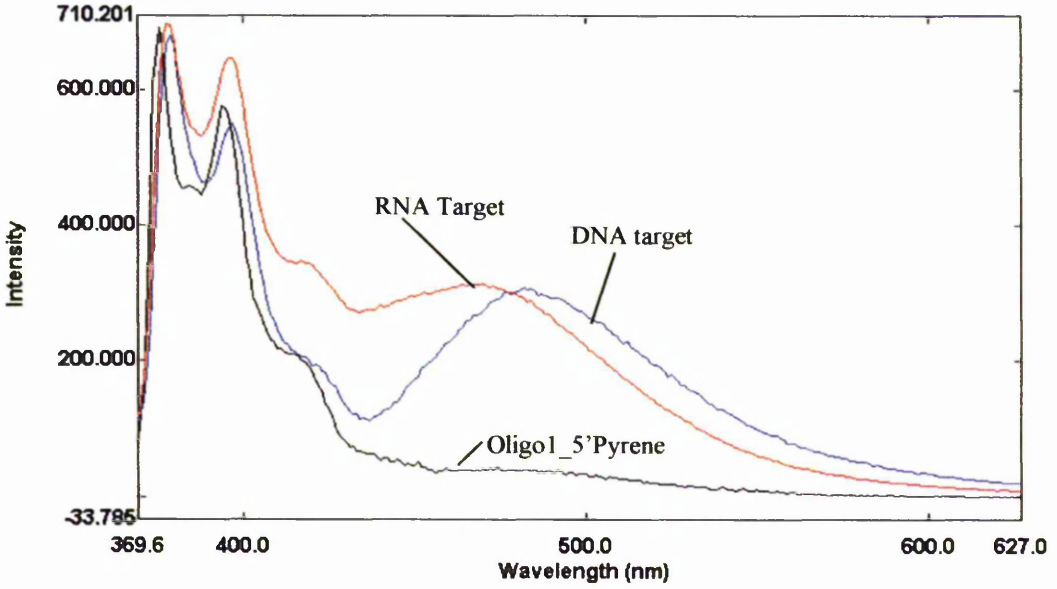

Figure 3.28: Comparison of emission spectra of the SP-8 system with the SP-2 system in 80% TFE/ Tris (pH 8.5) at 10 °C. Excitation wavelength 350 nm; slitwidth 5 nm; spectra are scaled to LES emission.

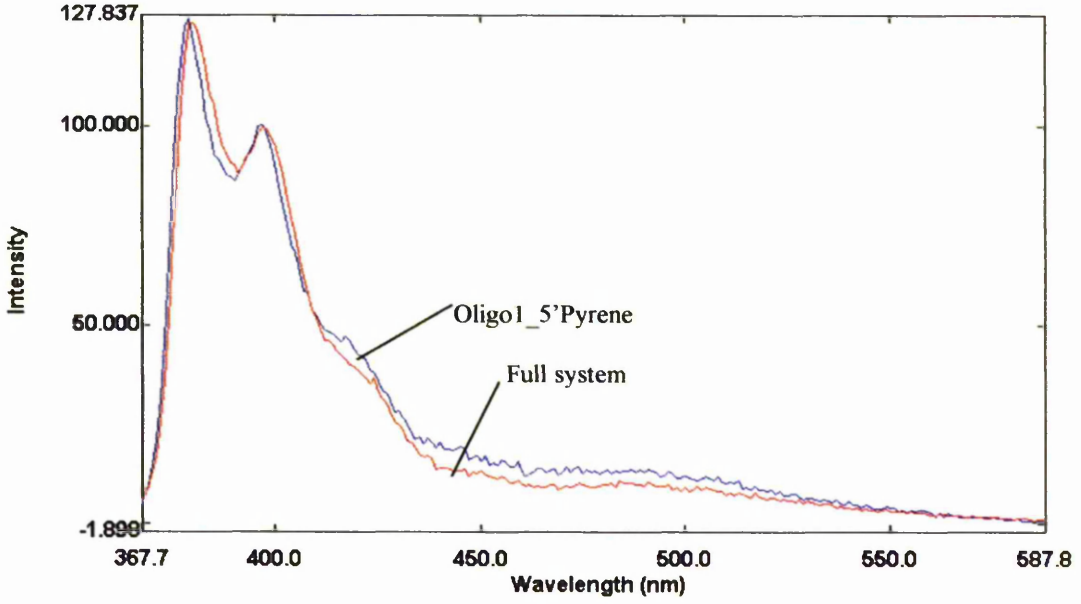

Figure 3.29: Emission spectra of 5-pyrene-bearing oligo and the full SP-8 system in Tris buffer at 10 °C showing the weak background exciplex fluorescence. Excitation wavelength 350 nm; slitwidth 5 nm; spectra are scaled to LES emission.

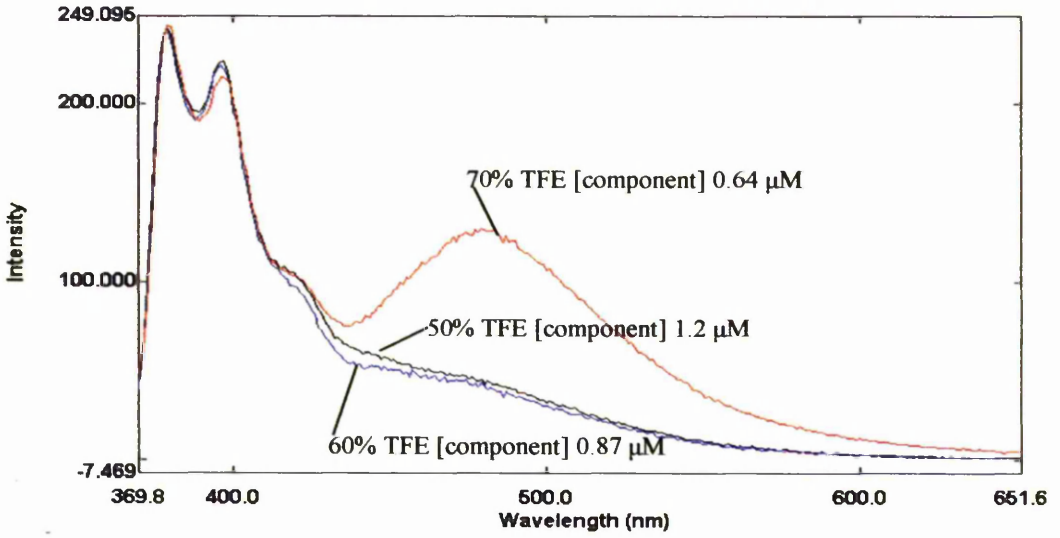

Figure 3.30: Emission spectra at 10 °C of SP-8 in Tris buffer at various TFE concentrations, recorded using an excitation at of 350 nm, slitwidth of 5 nm, and scaled to LES emission.

Heating the SP-8 system to 40 °C over 30 minutes caused a decrease of the exciplex emission intensity, which disappeared almost entirely on heating to 35 °C due to melting of the duplex. On cooling the system in 80% TFE/ Tris (pH 8.5 component concentration 2.5 μM) back to 10 °C, the exciplex emission did not reappear. This could be due to hydrolysis of the RNA strand during the heating-cycle. In 70% TFE/ Tris buffer (component concentration 0.64 μM) exciplex emission did recover, but was not as intense as before the heating-cooling cycle (Figure 3.31). For the equivalent DNA-DNA system (SP-1) after cooling back to 10 °C, exciplex emission appeared more intense than before.

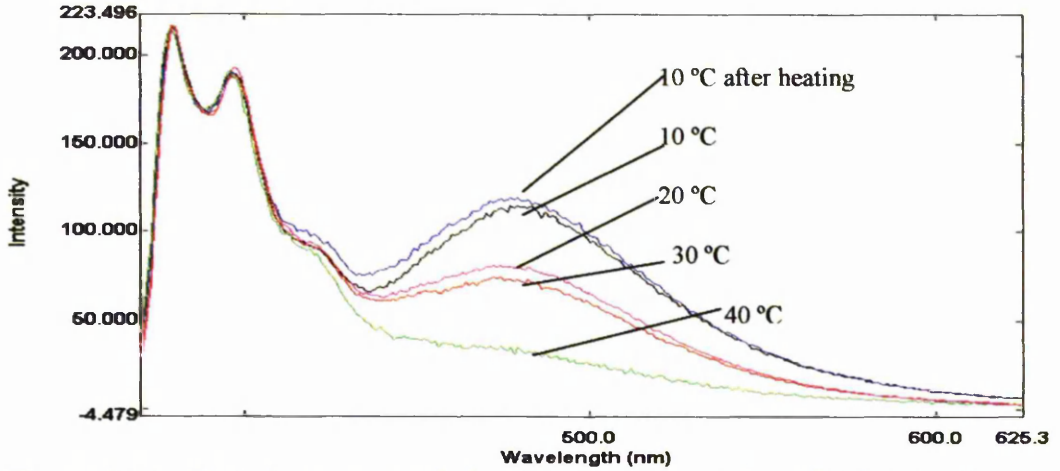

Figure 3.31: Emission spectra of the SP-8 system in 70% TFE/ Tris buffer (component concentration 0.64 μM) showing how exciplex emission decreases on heating to 40 °C and reappears after cooling back to 10 °C. Excitation wavelength 350 nm; slitwidth 5 nm; spectra are scaled to LES emission.

The value of T_m for the SP-8 system in 70% TFE was 23 °C taking the temperature at curve half-height from the temperature profile of fluorescence intensity at 380 nm against temperature (Figure 3.32) (*cf.* For SP-2 T_m was determined to be 24 °C in 80% TFE/ Tris from the A_{260} temperature profile).

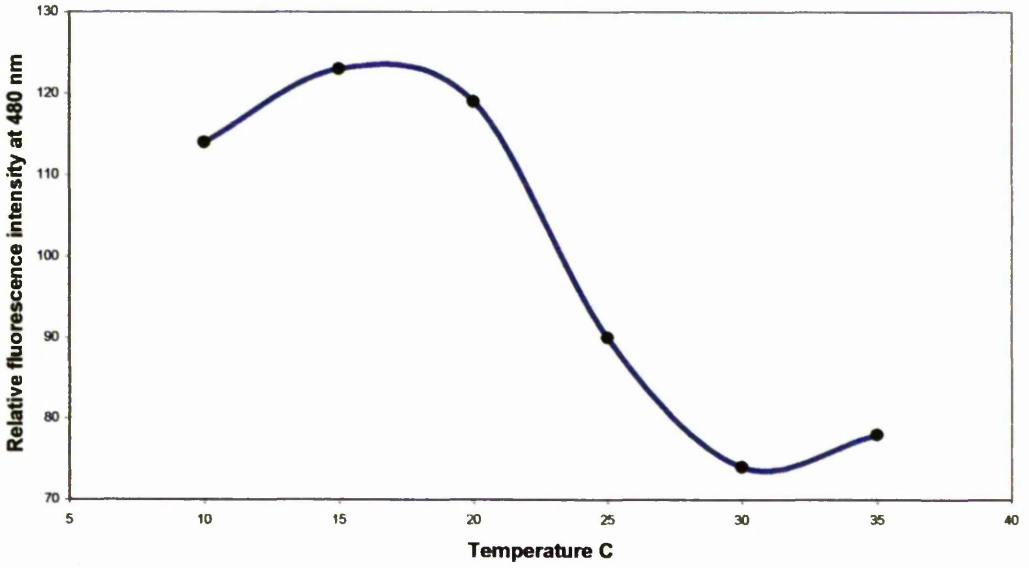

Figure 3.32: Melting curve of SP-8 in 70% TFE/ Tris buffer (10 mM Tris, 0.1 M NaCl, pH 8.5) obtained by plotting fluorescence intensity at 480 nm against temperature (data from Figure 3.31).

3.4 Results of optimisation of exciplex emission using *bis*-substituents.

3.4.1 Introduction.

Some systems were tested where the terminal phosphate group of the probes carried two substituents (*bis*–substituted), attached *via* a phosphoramidate link (Section 2.1). These systems were attempts to obtain improved exciplex signals. One substituent was always an exci-partner. In some cases the other was a hydrophobic 4-t-butylcyclohexyl group, chosen because it might preferentially (sterically) interact with the nucleotide residues of the probe leaving the exci-partner free to form an exciplex with the exci-partner of the other probe. In some systems the terminal phosphate carried two copies of the same exci-partner (e.g. two N-methylnaphthalene moieties) to increase the chances of the exci-partners on the two separate probes interacting on formation of the full system. In this case if one exci-partner bound non-productively to the nucleotide, the other would still be free to interact with the second exci-partner. The structures of the *bis*-derivatives used are shown Section 2.1 and the methods of attachment shown in Figure 2.3.

3.4.2 Emission spectra of the SP-9 system (5'Cyclohexylpyrene + 3'*Bi-s*naphthalene + Target strand).

Figure 3.33 shows emission spectra at various stages of development of the SP-9 system. Oligo1_5'cyclohexylpyrene showed a large background exciplex signal (λ_{max} 477 nm) with an I_E/I_M value of 0.55, presumably arising from the pyrene moeity interacting with the nucleotide bases. Addition of the target strand (before addition of the second probe oligo) caused the exciplex emission to drop slightly (I_E/I_M 0.29), but the background signal was still present. Addition of the 3'-probe, Oligo2_3'*bis*-naphthalene, caused the exciplex signal to overlap that from the LES signal (see Figure 3.33). A shoulder to the LES emission developed, which could have been due to exciplex formation, but this system would be unsuitable for use as a probe system due to the large background and unresolved signal. Due to pyrene's greater hydrophobicity than cyclohexane, the former may interact preferentially with the nucleotide residues forming an exciplex, therefore being unable to interact with the naphthalene exci-partner. It is possible that the two naphthalene partners may also interact with each other preventing exciplex formation. These could potentially form an excimer, however, no excimer signal was seen from the probe oligo components bearing *bis*-naphthalene groups.

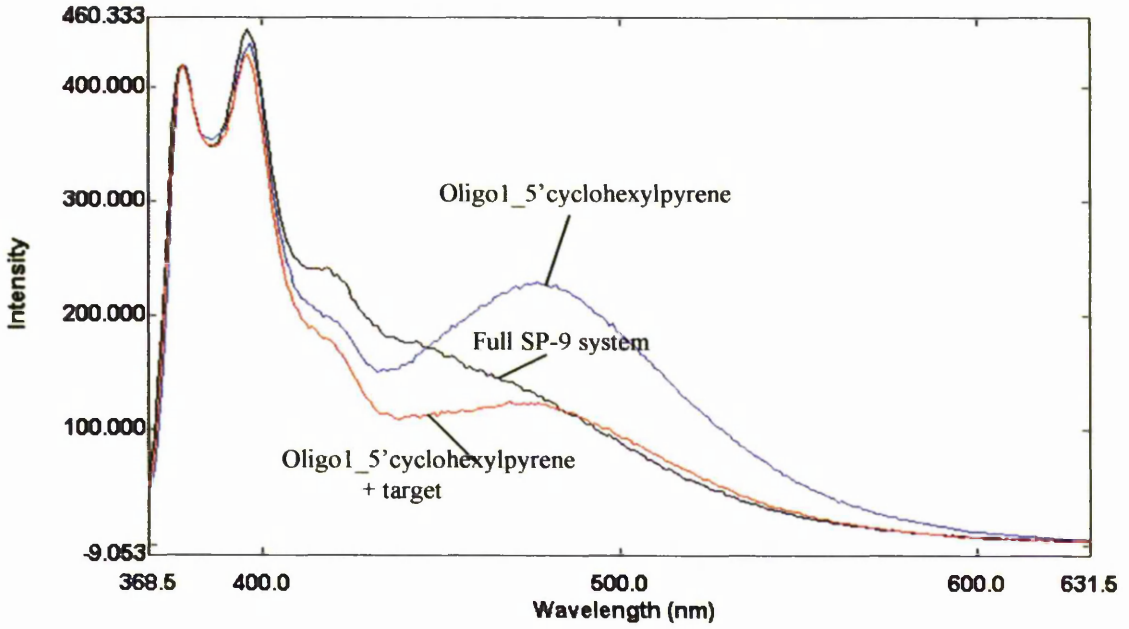

Figure 3.33: Emission spectra at various stages of development of the SP-9 system (Oligo1_5'cyclohexylpyrene + Oligo2_3'*bis*-naphthalene + target) in 80% TFE/ Tris buffer (10 mM Tris, 0.1 M NaCl, pH 8.5) at 10 °C. Excitation wavelength 350 nm, slitwidth 5 nm. Spectra are scaled to LES emission.

3.4.3 Emission spectra for the SP-10 system (5'*Bis*-naphthalene + 3'Cyclohexylpyrene + Target strand).

In Tris buffer at pH 8.5 in the absence of TFE the emission spectra of the exci-partner bearing probes showed no background exciplex fluorescence in the absence of the target (Figure 3.34). Even on addition of the target in Tris buffer no exciplex signal was observed. On addition of TFE to the system (to a concentration of 70% v/v) an exciplex signal was observed with λ_{max} 470 nm and I_E/I_M 0.38. However, it was not clear if this exciplex was formed between the exci-partners, or between pyrene and the nucleotide bases. The λ_{max} value of the LES emission band shifted slightly from 380 nm to 377 nm (Figure 3.34). For the SP-10 system the presence of the cyclohexyl group and the additional naphthalene group did not appear to enhance the exciplex signal relative to the SP-3 system (the analogous mono-substituted system), which had I_E/I_M 0.87 before heating.

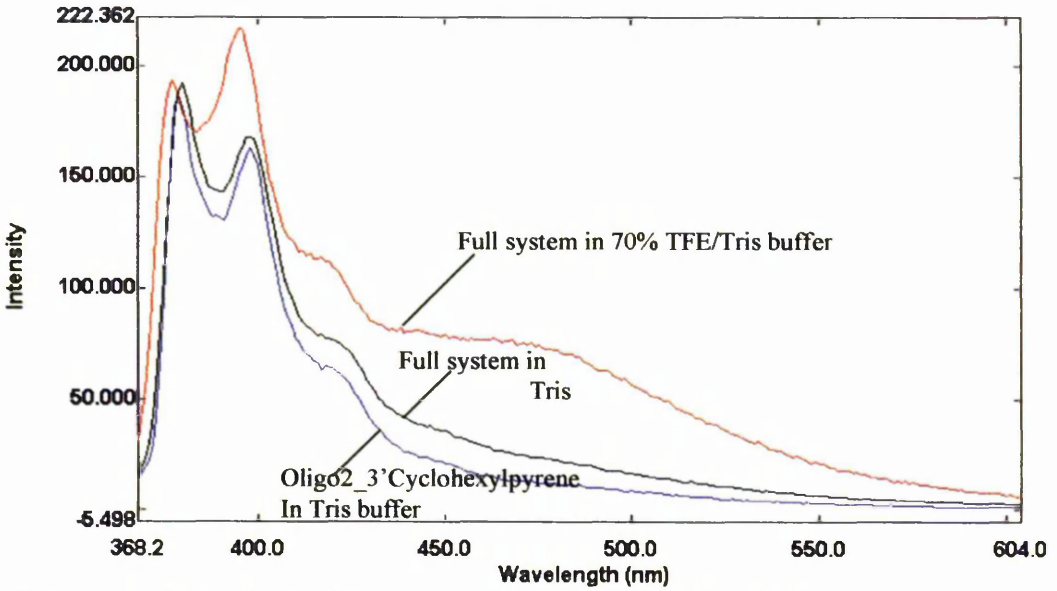

Figure 3.34: Emission spectra for SP-10 (Oligo1_5'*bis*-naphthalene + Oligo2_3'cyclohexylpyrene + target strand) in Tris buffer (pH 8.5) and 70% TFE/ Tris buffer (pH 8.5) at 10 °C. Excitation wavelength 350 nm, slitwidth 5 nm. Spectra are scaled to LES emission at 380 nm.

3.4.4 Emission spectra of the SP-11 system (5'Cyclohexylpyrene + 3'*Bis*-DMA + target strand).

Figure 3.35 shows the SP-11 system at various stages of development in 80% TFE/ Tris buffer (pH 8.5). Oligo1_5'-cyclohexylpyrene showed a large background intramolecular exciplex emission in the absence of the other components. On addition of the target strand the intensity of this exciplex emission dropped almost 2-fold, but a background signal was still present. Addition of the final component, Oligo2_3'*bis*-DMA, caused the exciplex emission to diminish further, resulting in a weak exciplex signal. The emission maximum (λ_{max}) of the exciplex signal varied slightly at each stage, presumably because of different types of interaction of the pyrene group with bases and/ or exci-partners. This is shown along with the I_E/I_M values in Table 3.3. This system would again be undesirable for use as a detection system due to the large background signal of Oligo1_5'cyclohexylpyrene and weak exciplex signal on formation of the full system.

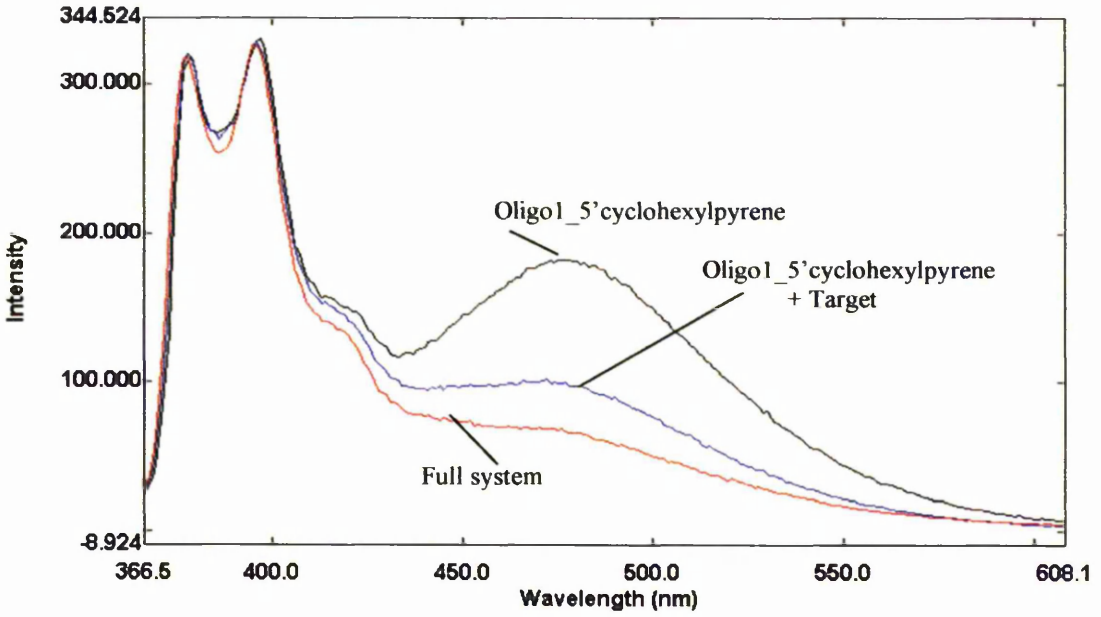

Figure 3.35: Emission spectra at various stages of assembly of the SP-11 system (Oligo1_5'cyclohexylpyrene + Oligo2_3'*bis*-DMA + target strand) in 80% TFE/ Tris buffer (10 mM Tris, 0.1 M NaCl, pH 8.5) at 10 °C. Excitation wavelength 350 nm, slitwidth 5 nm; spectra are buffer-corrected and scaled to LES emission at 379nm.

Table 3.3: Emission maxima of the exciplex and LES bands and I_E/I_M values for the SP-11 system at various stages of assembly in 80% TFE/ Tris buffer (10 mM Tris, 0.1 M NaCl, pH 8.5) at 10 °C.

Components	λ_{max} LES (nm)	λ_{max} exciplex (nm)	I_E/I_M
Oligo1_5'cyclohexylpyrene	378	474	0.32
Oligo1_5'cyclohexylpyrene + target strand	379	478	0.58
Full system	380	477	0.21

3.4.5 Emission spectra of the SP-12 (5'*Bis*-pyrene + 3'*Bis*-DMA + target) system.

In 80% TFE/ Tris buffer a very large background exciplex with λ_{max} 479 nm (I_E/I_M 2.24) was observed for Oligo1_5'*bis*-pyrene in the absence of any other component (Figure 3.36), and is possibly a pyrene:pyrene excimer. On addition of the target strand this emission dropped by 2.3–fold (I_E/I_M 0.97, λ_{max} 479 nm), but the strong background fluorescence was still present. Addition of the second probe oligo, Oligo2_3'*bis*-DMA, to complete the system caused the exciplex emission to increase further (I_E/I_M 1.98), to an intensity that was not quite as high as for the Oligo1_5'*bis*-pyrene probe alone (Figure 3.36). The emission maximum for each of the exciplex bands observed was 479 nm.

The control system, C-5 (Oligo1_5'*bis*-pyrene + Oligo2_3'phosphate + target), behaved similarly to the experimental system, having much larger background exciplex signals for Oligo1_5'*bis*-pyrene alone, or for Oligo1_5'*bis*-pyrene in the presence of the target. On addition of Oligo2_3'phosphate exci-emission increased, but only slightly, see Figure 3.37. λ_{max} for exci-emission was 479 nm in all cases. The very large background signal makes this system unsuitable for use as a molecular probe.

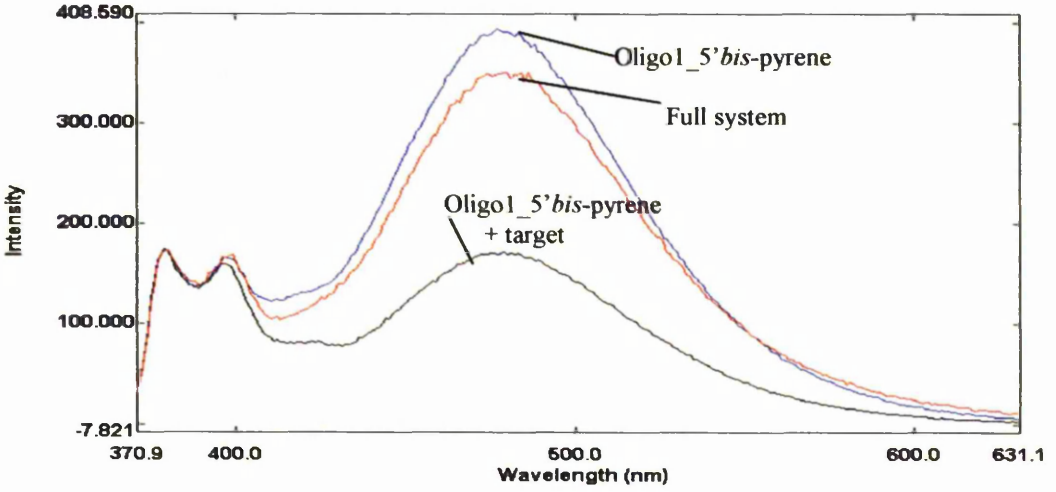

Figure 3.36: Emission spectra at various stages of assembly of the SP-12 (Oligo1_5'*bis*-pyrene + Oligo2_3'*bis*-DMA) + target) system in 80% TFE/ Tris buffer (10 mM Tris, 0.1 M NaCl, pH 8.5) at 10 °C showing the large background signals. Excitation at 350 nm, slitwidth 5 nm. Spectra are buffer-corrected and scaled to LES emission at 378 nm.

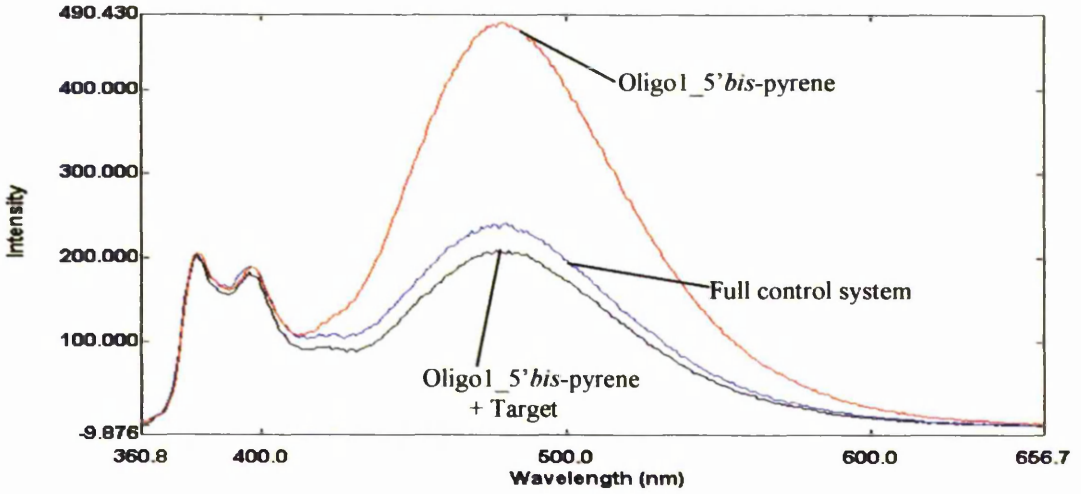

Figure 3.37: Emission spectra at various stages of assembly of the control system C-5 (Oligo1_5'*bis*-pyrene + Oligo2_3'phosphate + target) in 80% TFE/ Tris buffer (10 mM Tris, 0.1 M NaCl, pH 8.5) at 10 °C showing the large background signals. Excitation at 350 nm, slitwidths 5 nm. Spectra are buffer-corrected and scaled to LES emission.

3.5 Effects of some PCR additives on exciplex emission.

3.5.1 Introduction.

The effect was investigated of several PCR additives (sulfolane, methyl sulfone, betaine and DMSO, see Figure 2.10, Section 2.5.10) on SP-2 exciplex emission (Oligo1_5'pyrene + Oligo2_3'naphthalene + DNA target strand) in Tris buffer (10 mM Tris, 0.1 M NaCl, pH 8.5) in the absence of TFE and in 80% TFE/ Tris buffer at pH 8.5. For the experiments in TFE / Tris buffer the system was formed first in 80% TFE/ Tris buffer in the absence of additive, spectra were taken, and the PCR additive added from a stock solution and spectra taken. Having the additive present before the formation of the system gave similar results. All experiments were performed at 10 °C.

3.5.2 Tris Buffer in the absence of TFE.

Irrespective of the additive or its concentration, the emission spectra of Oligo1_5'pyrene + Oligo2_3'naphthalene (naphthalene signal subtracted) showed λ_{max} 375 nm. On addition of the DNA target strand to the two probe components the emission maximum red-shifted by a few nanometers, and emission intensity decreased indicating duplex formation. No exciplex emission was seen for this system in the presence of any of the additives tested in Tris buffer, see Figure 3.38. The magnitude of the shift in λ_{max} and the decrease in intensity on addition of target (Table 3.4) depended on the additive used and its concentration. On average a 45% drop in intensity was seen. Generally, the larger the drop in intensity, the larger the shift in λ_{max}. In addition, the higher the concentration of a particular additive the smaller the intensity drop and shift in λ_{max}.

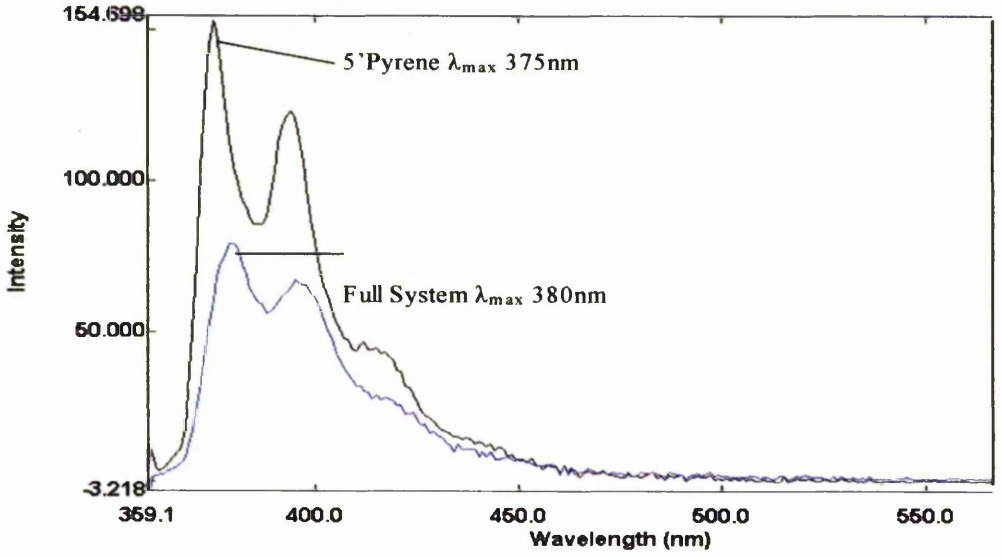

Figure 3.38: Emission spectra of Oligo1_5'pyrene and Oligo2_3'naphthalene in the presence and absence of the target strand in Tris buffer at 10 °C, both in the presence of 0.15 M sulfolane, showing the shift in λ_{max} and decrease in intensity on addition of target. Excitation 350 nm, slitwidth 5 nm.

Table 3.4: Values of λ_{max} and percentage decrease in intensity on addition of target strand to Oligo1_5'pyrene and Oligo2_3'naphthalene in Tris buffer (10 mM Tris, 0.1 M NaCl, pH 8.5 at 10 °C) in the presence of various PCR additives. Excitation wavelength 350 nm, slitwidth 5 nm.

Additive and concentration	λ_{max} (nm) Oligo1_5'pyrene + Oligo2_3'naphthalene	λ_{max} (nm) Oligo1_5'pyrene + Oligo2_3'naphthalene + Target	Percentage drop in intensity on binding
10% DMSO	375	376	40.9
1 M Betaine	375	377	52.2
2 M Betaine	375	376	34.0
0.6 M Methylsulfone	375	379	51.6
1.1 M Methylsulfone	375	377	44.9
0.15 M Sulfolane	375	380	48.4
0.5 M Sulfolane	375	378	42.4

3.5.3 80% TFE/ Tris buffer (10 mM Tris, 0.1 M NaCl, pH 8.5).

3.5.3.1 Betaine

Figure 3.39 shows emission spectra for SP-2 in 80% TFE/ Tris buffer (10 mM Tris, 0.1 M NaCl, pH 8.5) at 10 °C in the presence of 0.1 and 1.5 M betaine. In the absence of betaine in 80% TFE/ Tris buffer the exciplex signal observed on formation of the full split-probe system increased to a maximum over 10 minutes to give an I_E/ I_M value of 0.33.

Addition of betaine (200 µl stock solution to 2 ml 80% TFE/ Tris buffer containing SP-2 system) at this point to give 1 M betaine caused the exciplex signal to increase by a further 33% (I_E/ I_M 0.44). Further addition of betaine (100 µl to the cuvette, to give 1.5 M betaine) further increased the exciplex: LES ratio to I_E/ I_M 0.48 (46% increase.). In all cases the λ_{max} values of emissions for the LES and exciplex were unaffected by betaine: the LES band showed λ_{max} 379 nm and the exciplex λ_{max} 474 nm. Heating the system to 40 °C and re-cooling to 10 °C gave no detectable change in I_E/ I_M.

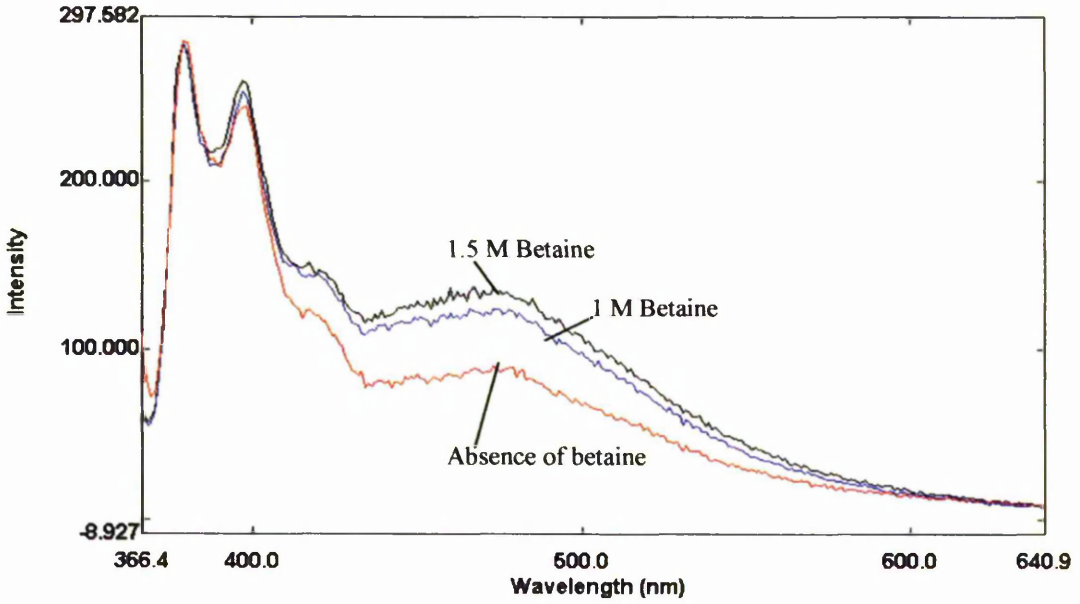

Figure 3.39: Emission spectra of SP-2 in 80% TFE/ Tris buffer (10 mM Tris, 0.1 M NaCl, pH 8.5) at 10 °C in the presence of 1 and 1.5 M betaine. Excitation wavelength 350 nm, slitwidth 5nm. Spectra are scaled to LES emission at 378 nm to correct for dilution effects.

3.5.3.2 Sulfolane

On formation of the SP-2 system in 80%TFE/ Tris buffer (10 mM Tris, 0.1 M NaCl, pH 8.5) the exciplex λ_{max} was 473 nm, the LES 376 nm, and I_E/ I_M was 0.34. On addition of sulfolane (30 µl added to the cuvette from a stock solution to give 0.15 M in the cuvette), the exciplex signal increased by approximately 20% (I_E/ I_M 0.40) (Figure 3.40). Further addition of sulfolane (a further 70 µl added from stock to give 0.5 M) resulted in a further increase in exciplex emission intensity (Figure 3.40) to give I_E/ I_M 0.46 (~35% increase relative to the signal in the absence of sulfolane). The emission maxima of LES and exciplex bands were not affected by the addition or concentration of sulfolane, remaining at 379 nm and 473 nm, respectively. Heating the system to 40 °C and cooling back to 10 °C did not greatly affect the value of I_E/ I_M.

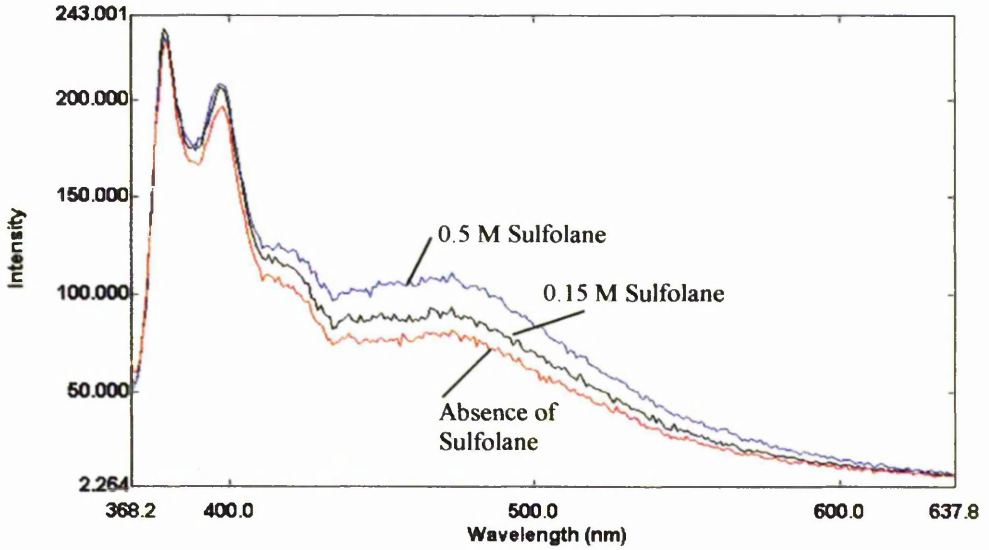

Figure 3.40: Emission spectra showing the effect of 0.15 M and 0.5 M sulfolane on the emission spectra of SP-2 in 80% TFE/ Tris buffer (10 mM Tris, 0.1 M NaCl, pH 8.5) at 10 °C. Excitation wavelength 350 nm; slitwidth 5 nm. Spectra are scaled to LES emission at 379 nm to correct for dilution effects.

3.5.3.3 Methylsulfone.

Addition of methylsulfone to the full SP-2 system reduced the value of I_E/ I_M. On formation of the full system in 80% TFE/ Tris buffer (10 mM Tris, 0.1 M NaCl, pH 8.5) at 10 °C, an exciplex band with I_E/ I_M 0.34 was observed on irradiation at 350 nm. The emission spectra (Figure 3.41) showed λ_{max} 379 nm for the LES and 472 nm for the exciplex. On addition of methylsulfone (240 µl from stock to give 0.6 M cuvette concentration) the spectrum appeared unchanged in intensity and emission maxima. Further addition of sulfolane to 1.1 M (200 µl stock solution added) caused the exciplex emission band intensity to decrease relative to the LES band (I_E/ I_M 0.28), and λ_{max} for the exciplex band to shift from 472 to 479 nm, with λ_{max} for the LES remaining unchanged (see Figure 3.41).

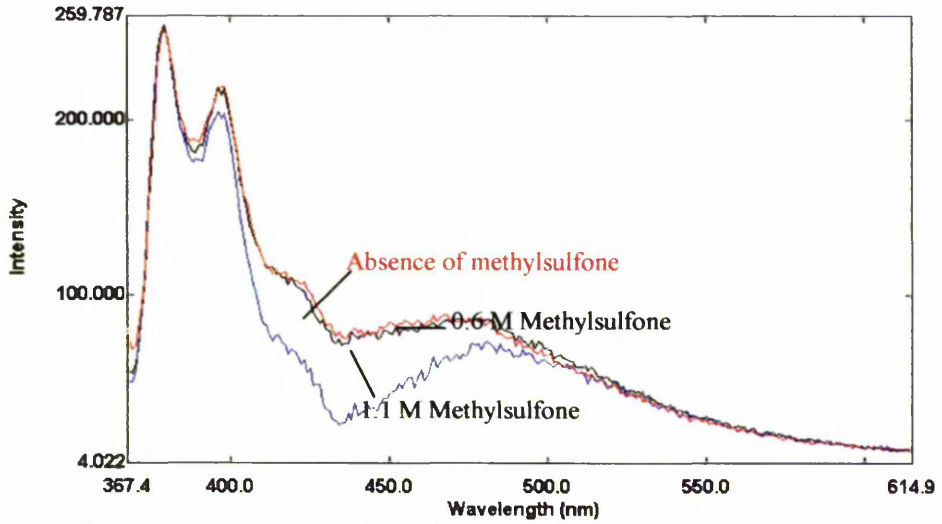

Figure 3.41: Emission spectra of the SP-2 system in 80% TFE/ Tris buffer (10 mM Tris, 0.1 M NaCl, pH 8.5) at 10 °C showing the effect of addition of methylsulfone to give 0.6 and 1.1 M solutions. Excitation wavelength 350 nm; slitwidth 5 nm. Spectra are buffer-corrected and scaled to LES emission at 379 nm to correct for dilution effects.

3.5.3.4 Dimethylsulfoxide.

Addition of DMSO to 10% (1.41 M), did not intensify the exciplex signal of SP-2 (Figure 3.42). For the system in 80% TFE/ Tris buffer (10 mM Tris, 0.1 M NaCl, pH 8.5) at 10 °C the exciplex band was clearly observed with λ_{max} 480 nm and I_E/ I_M 0.26. However, on addition of DMSO (10%) the exciplex band became a shoulder, poorly resolved from the LES band, the emission maximum of which remained unchanged (379 nm). Heating to 40 °C and subsequent cooling back to 10 °C failed to resolve the exciplex signal.

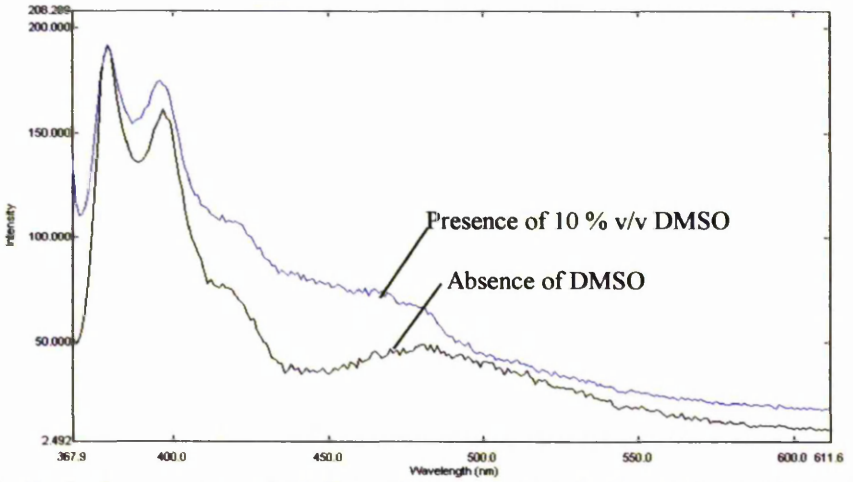

Figure 3.42: Emission spectra of SP-2 in 80% TFE/ Tris buffer (10 mM Tris, 0.1 M NaCl, pH 8.5) at 10 °C showing the effect of addition of DMSO (final level 10%, 1.41 M). Excitation wavelength 350 nm, slitwidth 5 nm. Spectra are buffer-corrected and scaled to LES emission at 379 nm to correct for dilution effects.

Of the additives tested, betaine and sulfolane increased exciplex emission relative to LES emission in 80% TFE/ Tris buffer. Methylsulfolane and DMSO did not give any improvement as methylsulfolane decreased emission intensity and DMSO decreased the resolution of the exciplex band. In all cases heating and re-annealing of the system had no marked effect on the emission spectra and therefore these data have not been shown.

3.6 Studies of the effects of Co-solvents on Excimer/Exciplex Emission.

3.6.1 Introduction.

To this point for the purely DNA systems tested exciplex/ excimer emission had only been observed in the presence of TFE, with the strongest excimer/ exciplex signal observed in 80% TFE/ Tris buffer. A range of other co-solvents was tested to determine whether other solvents could also affect excimer or exciplex fluorescence of the DNA-mounted exci-partners within the split-probe systems. These organic solvent additives were: tetrafluoro-1-propanol, N-methylformamide, hexafluoro-2-propanol, ethylene glycol, acetone, methanol, ethanol, ethylene glycol dimethylether and 3-chloro-1, 2-propanediol. As pentafluoro-1-propanol, heptafluoro-1-butanol, pentafluorophenoxyethanol, perfluoro-tertbutyl alcohol, hexafluoro-1-butanol, hexafluorobenzene, trichloroethanol and 1-chloropropanol proved immiscible with water, they could not be tested. The DNA systems SP-1, SP-2 and SP-3 were tested in the presence of 50 and 70% co-solvent. Table 3.5 summarises data.

Table 3.5: Summary of the influence of various organic co-solvents on excimer and exciplex emission of DNA-mounted exci-partners within DNA-split-probe systems. Dielectric constants (ε), refractive indices (n) at 293.15K, and viscosities at 293.15K are given.

Solvent additives tested	**Viscosity Pa.s(10^{-3}) 293.15K** (a)	**ε 293.15K** (a)	**n 293.15K** (a)	**Presence of excimer/exciplex formation for:**				
				SP-1		**SP-2**		**SP-3**
				50%	**70%**	**50%**	**70%**	**80%**
N-methylformamide	1.82	181.56	1.432	✗	✗	✗	✗	✗
Ethylene glycol	21.95	40.245	1.432	✓	✓	✗	✓	✗
Methanol	0.59	32.613	1.328	✓	✓	✗	✗	✗
Trifluoroethanol	2.04	26.726	1.291	✓	✓	✗	✓	✓
Ethanol	1.21	24.852	1.361	✓	✓	✗	✗	✗
Acetone	0.325	20.493	1.359	✓	✓	✗	✗	✗
Ethyleneglycol dimethylether	0.52	7.200	1.380	✓	✓	✗	✓	✓
Hexafluoro-2-propanol	1.62	16.75	1.275	✓	✓	–	–	✗
Tetrafluoro-1-propanol	4.577	-	1.321	✓	✓	✗	✗	✗
3-Chloro-1,2-propandiol	-	-	1.480	–	✗	✗	✗	✗

(a) Properties were obtained from the Detherm database (version 14).

3.6.2 SP-1 System.

All solvents tested, except N-methylformamide and 3-chloro-1, 2-propandiol, supported excimer formation between the exci-partners for SP-1. The solvents which resulted in the strongest excimer emission were hexafluoropropanol, tetrafluoropropanol, and, weakest, ethylene glycol. Emission spectra of SP-1 in Tris (10mM TRIS, pH 8.5, 0.1M NaCl) in the presence of hexafluoro-2-propanol (50% v/v) and tetrafluoro-1-propanol (50% and 70%, v/v) are in Figures 3.43 and 3.44, respectively.

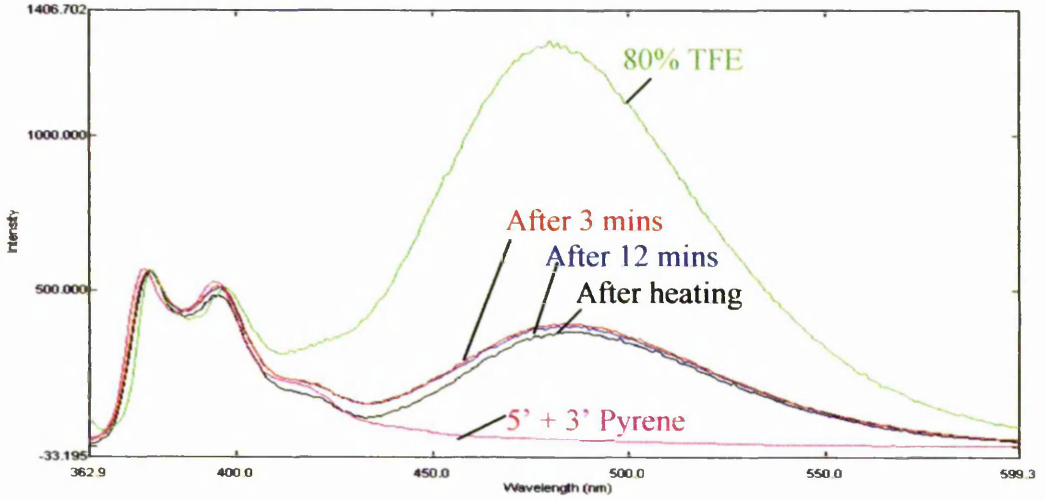

Figure 3.43: Emission spectra of **SP-1** in Tris buffer (10 mM Tris, 0.1 M NaCl, pH 8.5) at 10 °C in the presence of hexafluoro-2-propanol (50% v/v) compared with 80% TFE v/v. The effect of heating (to 40 °C) and cooling back to 10 °C on excimer emission is shown. Excitation at 350 nm. Baseline-corrected spectra are scaled against the LES emission band at 380 nm.

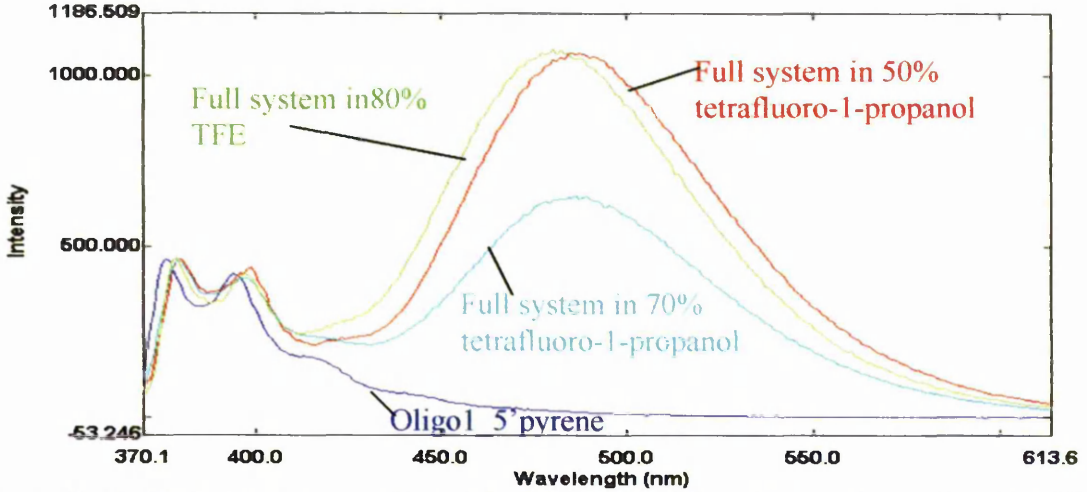

Figure 3.44: Emission spectra of **SP-1** in Tris buffer (10mM Tris, pH 8.5, 0.1M NaCl) at 10 °C in the presence of tetrafluoro-1-propanol (50% and 70%, v/v) compared with 80% TFE, v/v. Excitation was at 350 nm. Baseline-corrected spectra are scaled against the LES emission at 380 nm.

The spectrum of SP-1 in the presence of 80% TFE is also shown in Figure 3.44 for comparative purposes. Note that 50% tetrafluoro-1-propanol induced the same level of excimer emission as 80% TFE (Figure 3.44). The maximum of excimer emission was shifted to 488 nm in tetrafluoro-1-propanol, compared to 480 nm in TFE. Hexafluoro-2-propanol was found to be less effective than TFE or tetrafluoro-1-propanol in its ability to induce excimer formation (Figure 3.43). Excimer emission maximum in hexafluoro-2-propanol was at 485 nm.

Excimer formation within the SP-1 split-probe system was also observed in 50%, and, more strongly, in 70% ethylene glycol (Figure 3.45), although the maximum intensity of excimer emission was much less than in 80% TFE. The excimer fluorescence band required time to reach a maximum intensity, presumably due to the high viscosity of the solution. In ethylene glycol λ_{max} for excimer emission was 482 nm.

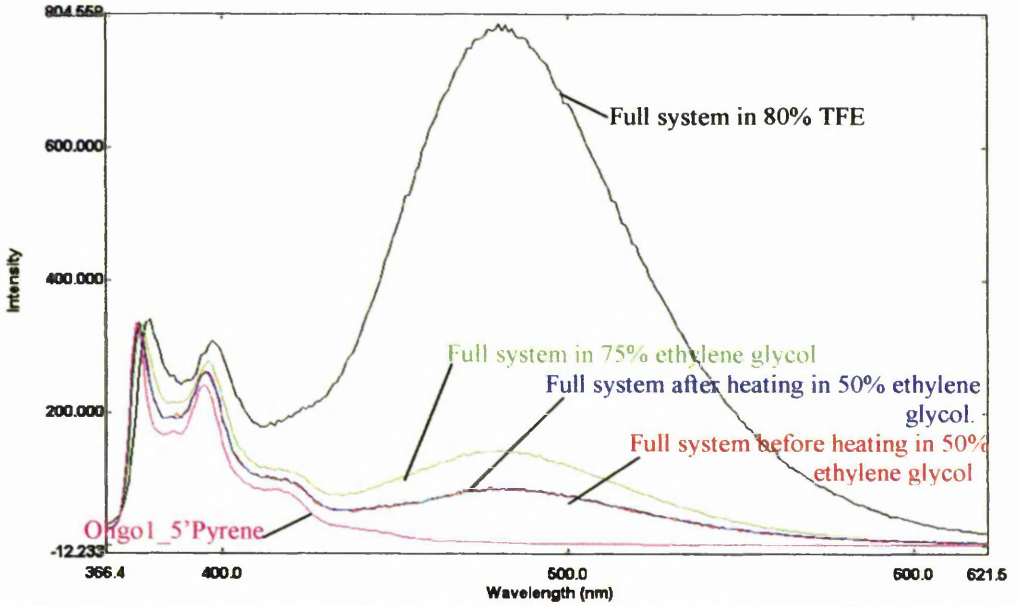

Figure 3.45: Emission spectra of **SP-1** in Tris buffer (10mM Tris, pH 8.5, 0.1M NaCl) at 10 °C in the presence of ethylene glycol (50% and 70%) compared with 80% TFE. The effect of heating to 40 °C and cooling back to 10 °C is also shown. Excitation was at 350 nm; slitwidth 5nm. Baseline-corrected spectra are scaled against LES emission band at 380 nm.

3.6.3 Effect of solvents on excimer emission of 1,3-*bis*(pyrenyl)propane.

Fluorescence emission spectra of 1,3-*bis*(pyrenyl)propane were recorded in Tris buffer (10 mM Tris, 0.1 M NaCl, pH 8.5) containing various percentages of the co-solvents, TFE, ethylene glycol, hexafluoropropanol, tetrafluopropanol. Data in Table 3.6 (a, b, c, d) show that λ_{max} for the excimer emission varied with solvent and solvent

concentration, as did the emission intensity, and I_E/I_M values. Generally at low solvent concentration no LES emission was seen, but it appeared at higher solvent concentrations. For example, below 60% TFE no LES emission was seen and λ_{max} for the excimer was 477 nm. At 80 and 100% TFE a LES emission appeared and λ_{max} for the excimer shifted to 484 nm. The I_E/I_M values also decreased with increasing solvent concentration; this is the opposite of what was observed for the oligo probes, where I_E/I_M increased with TFE concentration (see Section 3.1.2).

Table 3.6: Effect of solvent and solvent concentration on the emission maxima of the LES and excimer, plus I_E/I_M values of 1,3-*bis*-pyrenylpropane in Tris buffer (10 mM Tris, 0.1 M NaCl, pH 8.5) at 10 °C. $I_{excimer}$ and I_{LES} are the relative fluorescence intensity readings for excimer and LES, respectively, measured in terms of peak height at 380 nm and 480 nm, respectively.

(a)

Trifluoroethanol					
% cosolvent	**λ_{max} excimer**	**λ_{max} LES**	**$I_{excimer}$**	**I_{LES}**	**I_E/I_M**
0	477	-	893	-	-
20	477	-	530	-	-
60	477	-	783	-	-
80	484	374	49	22	2.33
100	484	374	33	25	1.32

(b)

Ethylene glycol					
% cosolvent	**λ_{max} excimer**	**λ_{max} LES**	**$I_{excimer}$**	**I_{LES}**	**I_E/I_M**
50	478	-	63	-	-
70	483	376	72	27	2.67
100	491	376	43	188	0.23

(c)

Tetrafluoropropanol					
% cosolvent	**λ_{max} excimer**	**λ_{max} LES**	**$I_{excimer}$**	**I_{LES}**	**I_E/I_M**
50	477	375	864	22	39.3
70	490	375	92	41	2.24
100	490	375	74	87	0.85

(d)

Hexafluoropropanol					
% cosolvent	**λ_{max} excimer**	**λ_{max} LES**	**$I_{excimer}$**	**I_{LES}**	**I_E/I_M**
50	478	376	659	6	109.8
70	490	374	47	15	3.13

3.6.4 SP-2 System.

In contrast to excimers, exciplex formation was found to be much more sensitive to the immediate solvent environment (see Table 3.5). For the SP-2 split-probe system, exciplex emission was only seen in the presence of TFE, ethylene glycol or ethylene glycol

dimethylether, and weak exciplex emission only at 70% co-solvent concentration for the last two (Figure 3.46 and Figure 3.47). These data are with exciplex emission for SP-2 in 80% TFE/Tris buffer.

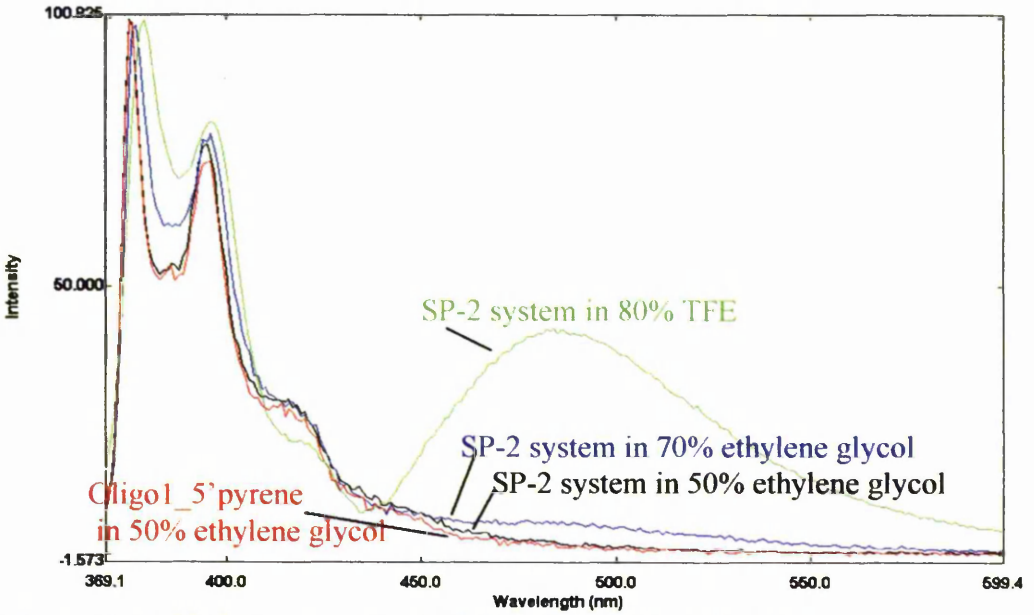

Figure 3.46: Emission spectra of **SP-2** in Tris buffer (10mM Tris, pH 8.5, 0.1M NaCl) at 10 °C in the presence of ethylene glycol (50% and 70%) compared with 80% TFE. The effect of heating to 40 °C and cooling back to 10 °C is also shown. Excitation was at 350 nm; slitwidth 3 nm, baseline-corrected spectra were scaled against LES emission at 380 nm.

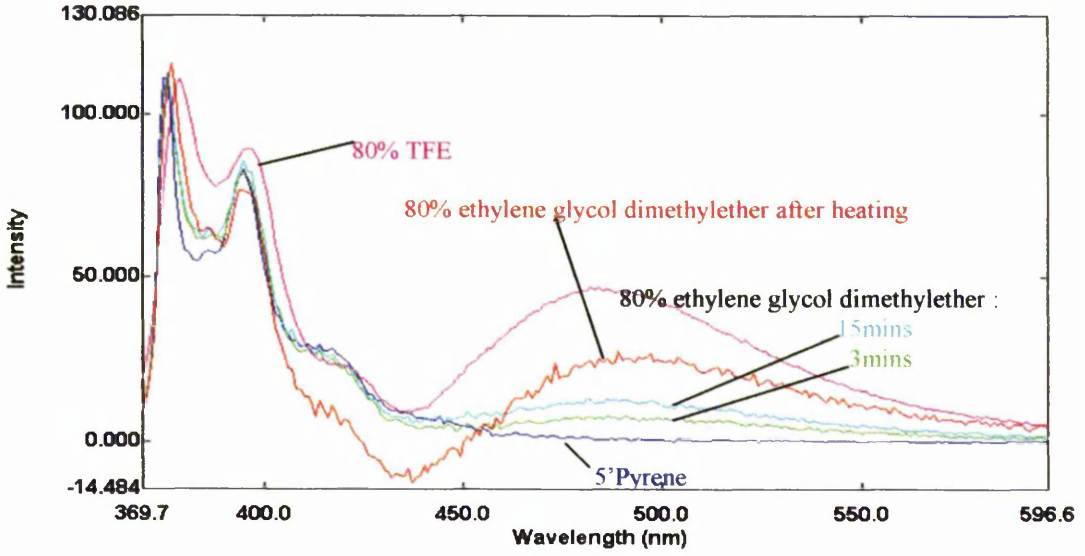

Figure 3.47: Emission spectra of **SP-2** in Tris buffer (10mM Tris, pH 8.5, 0.1M NaCl) at 10 °C in the presence of ethylene glycol (70%) compared with 80% TFE. The effect of incubation time after complete addition of the components in ethylene glycol, followed by heating to 40 °C then cooling back to 10 °C is also shown. Excitation was at 350 nm; slitwidth 3 nm, baseline-corrected spectra were scaled against LES emission at 380 nm.

3.6.5 SP-3 system.

For the SP-3 system, apart from TFE (see Section 3.1.4), only the presence of 80% ethylene glycol dimethylether gave rise to a (weak) exciplex emission band (Figure 3.48).

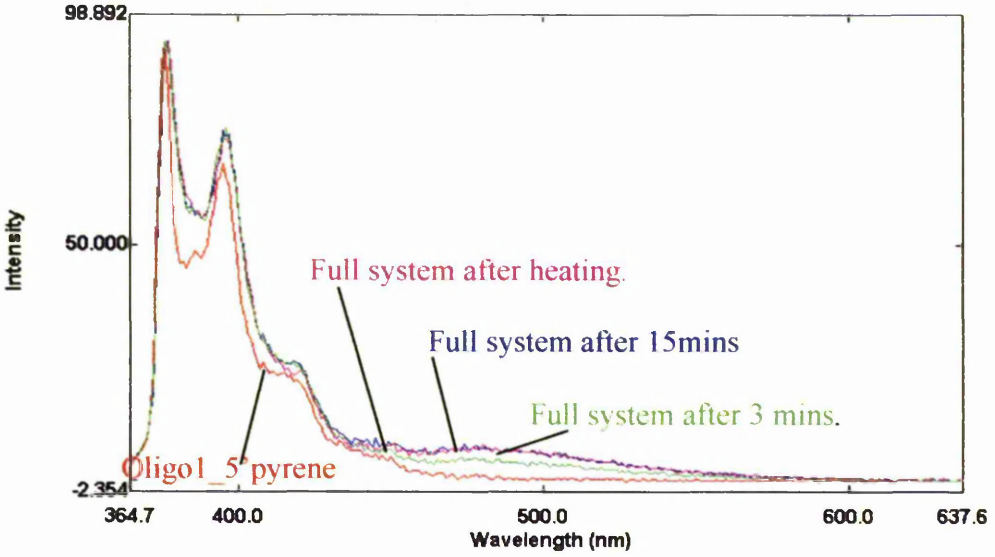

Figure 3.48: Emission spectra of **SP-3** in Tris buffer (10mM Tris, pH 8.5, 0.1M NaCl) at 10 °C in the presence of ethylene glycol dimethylether (80% v/v). The effects of incubation time after complete addition of the components, followed by heating to 40 °C and cooling back to 10 °C are also shown. Excitation was at 350 nm; slitwidth 3 nm, baseline-corrected spectra were scaled against the LES emission at 380 nm.

3.7 Detection of mismatched probes and targets by excimers and exciplexes

3.7.1 Introduction

The SP-1, SP-2 and SP-3 systems were used to determine the effects on excimer/ exciplex fluorescence when there was a mismatch or gap/mismatch between the target and the probe sequences. The variants of the 16-mer-parent target sequence used to test the effects of changes at various positions, using probes whose sequences were kept constant, are shown in Figure 2.11 in Section 2.5.12, along with the nomenclature used for the various constructs.

3.7.2 Emission spectra for the SP-1 system.

Excimer emission was seen (broad band around 480 nm) for both systems with insertions (*insertion 1* and *insertion 2*) in 80% TFE/ Tris buffer (10 mM Tris, 0.1 M NaCl, pH 8.5). The intensity of this emission increased to a maximum over 10 minutes while the sample was held at 10 °C (Figure 3.49). The intensity of the excimer band observed with the parent target increased by 4.6-fold after the sample was heated to 40 °C for 2 minutes and allowed to cool back to 10 °C. The same heating and cooling cycle caused 4.2 and 4.5-fold increases in the intensities of the excimer band for *insertion 1* and *insertion 2*, respectively (Figure 3.50). Emission for both *insertion* systems was less intense than for the *parent* system (*insertion 1* showed stronger excimer emission than *insertion 2*).

Table 3.7 collects I_E/I_M values and excimer emission intensities for the SP-1 system with *parent, insertion 1* and *insertion 2* targets before and after the heating: cooling cycle.

Table 3.7: I_E/I_M values and intensities of the excimer (480 nm) for the SP-1 *parent, insertion 1* and *insertion 2* target systems in 80% TFE/ Tris buffer (10 mM Tris, 0.1 M NaCl, pH 8.5) at 10 °C before and after heating to 40 °C. Ratios of the excimer intensity before and after heating are also given. Excitation was at 350 nm; slitwidth 3 nm. Spectra were buffer-corrected.

	Before heating		After heating		
System	**I_E/I_M**	**Intensity at 480 nm**	**I_E/I_M**	**Intensity at 480 nm**	**$I_{Before\ heating}/I_{after\ heating}$**
Parent	2.3	230	2.65	1016	4.6
Insertion 1	0.62	62	0.68	261	4.2
Insertion 2	0.54	50	0.58	223	4.5

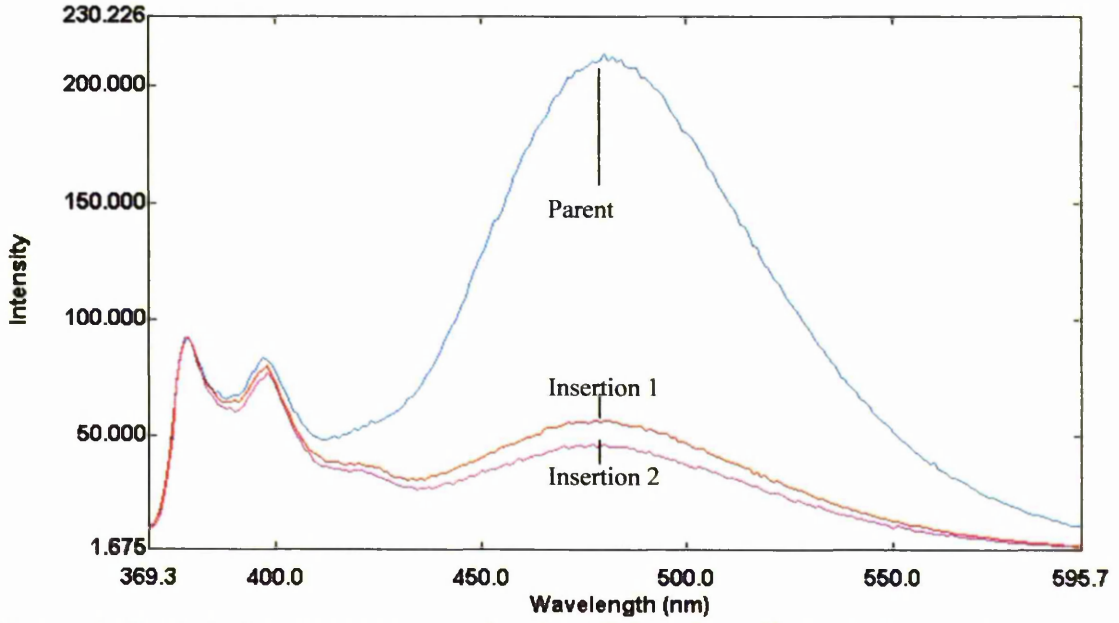

Figure 3.49: Emission spectra comparing the SP-1 probes oligos of the *parent target* and both *insertion 1* and *insertion 2 targets* in 80% TFE/ Tris buffer (10 mM Tris, 0.1 M NaCl, pH 8.5) at 10 °C. Spectra were recorded when the emission had reached a maximum value (after 10 minutes at 10 °C). Excitation was at 350 nm, slitwidth 5 nm. Spectra are buffer-corrected and scaled to LES emission.

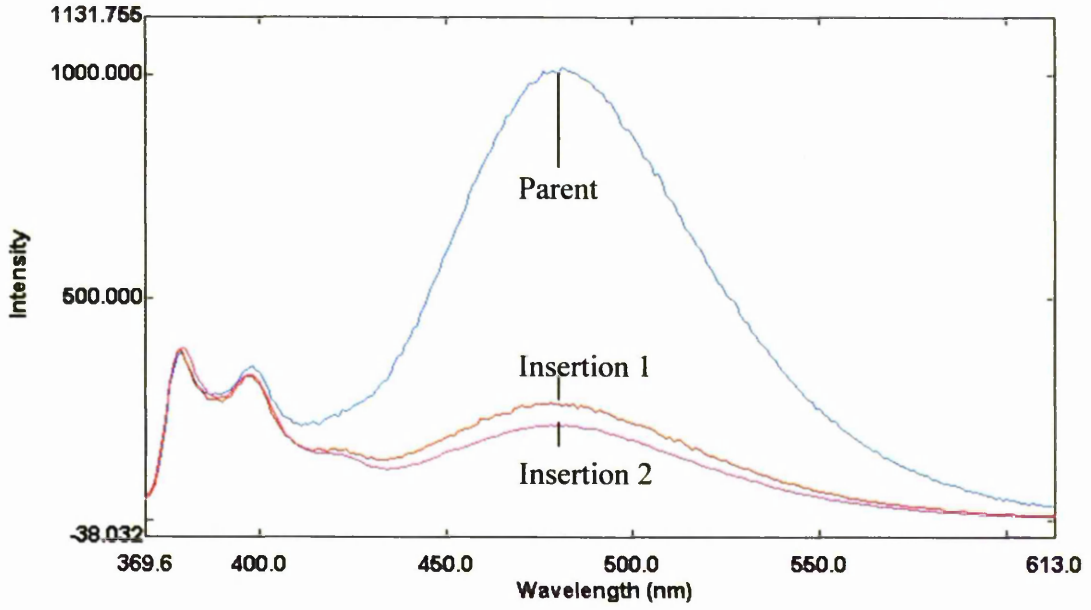

Figure 3.50: Comparison of SP-1 system with *parent, insertion 1 and insertion 2* target sequences in 80% TFE/ Tris buffer (10 mM Tris, 0.1 M NaCl, pH 8.5) at 10 °C after heating to 40 °C and cooling back to 10 °C. Excitation was at 350 nm, slitwidth 5 nm. Spectra, buffer-corrected, are scaled to LES emission.

Excimer emission was detected for most of the mismatched target sequences, except for both *double mismatches* and *5'mismatch 1* systems. In all cases where excimer

emission was seen, the intensity increased over time to a maximum (Figure 3.51) and further increased after the systems were heated to 40 °C and re-cooled to 10 °C (Figure 3.52). The excimer emission intensity was always less intense for mismatches/ insertions than for the parent system, and varied according to the position of the mismatch. A quantitative summary of intensity data is recorded as Table 3.9. I_E/I_M values show that stronger excimer signals are detected after the heating-cooling cycle (Table 3.8).

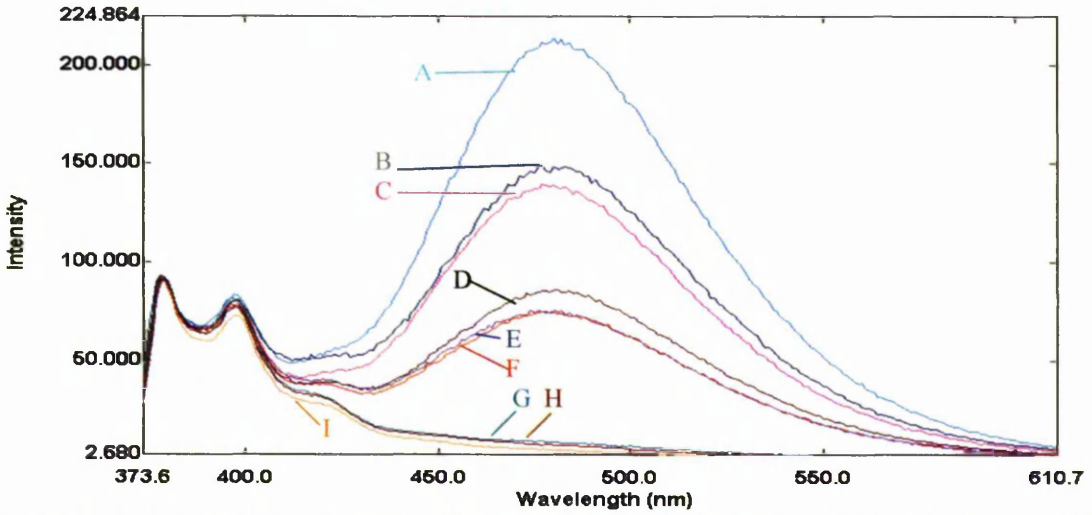

Figure 3.51: Comparison of mismatch systems for SP-1 in 80% TFE/ Tris buffer at pH 8.5 at 10 °C before heating. Spectra are scaled to parent LES emission at 480 nm. (A=*Parent*, B=*5'mismatch 3*, C=*3'mismatch 3*, D= *5'Mismatch 2*, E=*3'mismatch 2*, F= *3'Mismatch 1*, G=*5'mismatch 1*, H=*5'double mismatch*, I=*3'double mismatch*). Excitation was at 350 nm, slitwidth 5 nm.

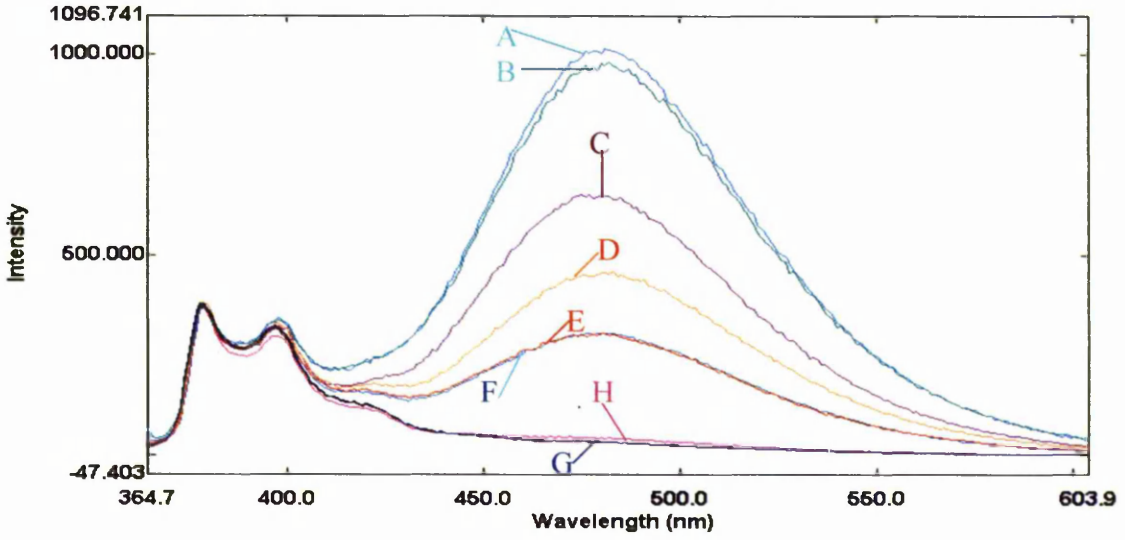

Figure 3.52: Comparison of mismatch systems for SP-1 in 80% TFE/ Tris buffer at 10 °C after heating to 40 °C and cooling back to 10 °C. Spectra are scaled to LES emission of parent spectrum.(A=*Parent*, B=*5'mismatch* 3, C=*3'mismatch 3*, D= *5'Mismatch 2*, E=*3'mismatch 2*, F= *3'Mismatch 1*, G=*5'double mismatch*, H=*3'double mismatch*). Excitation was at 350 nm, slitwidth 5 nm.

Table 3.8: I_E/I_M values and intensities of excimer emission at 480 nm for the SP-1 parent and mismatched target systems in 80% TFE/ Tris buffer (10 mM Tris, 0.1 M NaCl, pH 8.5) at 10 °C before and after heating to 40 °C. Ratios of the excimer intensity before and after heating are also shown. Excitation wavelength 350 nm; slitwidth 3 nm. Spectra were buffer-corrected.

	Before heating		After heating		
System	**I_E/I_M**	**Intensity at 480 nm**	**I_E/I_M**	**Intensity at 480 nm**	**$I_{after\ heating}/I_{before\ heating}$**
Parent	2.30	211	2.68	1019	4.8
5'mismatch 1	0.10	9			
5'mismatch 2	0.90	87	1.20	456	5.2
5'mismatch 3	1.62	149	2.57	979	6.5
5'double mismatch	0.09	8	0.13	49	6.1
3'mismatch 1	0.82	75	0.22	85	1.1
3'mismatch 2	0.83	76	0.23	86	1.0
3'mismatch 3	1.47	135	1.72	655	4.8
3'double mismatch	0.07	6	0.09	36	4.3

Table 3.9 shows the area under the excimer band from 480nm (the peak of excimer emission) to 600nm before heating and after heating to 40 °C and re-cooling to 10 °C. This wavelength range was chosen, rather than the whole excimer band, because for systems showing only weak excimer emission, the relative importance (background) of LES emission is greater, as there is a tail of emission extending from the 430 nm LES emission into the region of the excimer band, see Figure 3.53. These data were quantified using only the portion of the excimer emission above 480 nm.

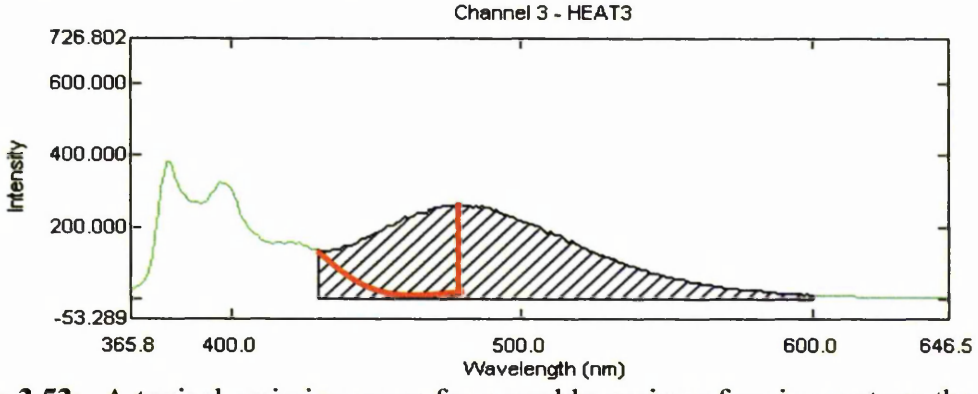

Figure 3.53: A typical emission curve for a weakly excimer-forming system: the shaded area shows signal from 430nm to 600nm. The excimer emission signal (centred around 480 nm) in this sample clearly has only a small component from the tail of the 430 nm peak from the locally excited state (monomer).

Table 3.9 also gives the ratio of the area under the mismatch curve to the area under the parent curve for each system, both before and after the heating to 40 °C/ cooling cycle. Again all spectra were scaled to corresponding parent spectrum.

Table 3.9: Area under the curve (AUC, 480-600nm) and ratio of area under mismatch curve : area under parent curve for the SP1 and variant target systems in 80% TFE/ Tris buffer (10 mM Tris, 0.1 M NaCl, pH 8.5) at 10 °C.

Target	AUC before heating.	AUC mismatch : AUC partent	AUC after heating	AUC mismatch: AUC parent
Parent	10934	1.00	52231	1.00
insertion 1	2975	0.27	13409	0.26
insertion 2	2353	0.22	10768	0.21
3'mismatch 1	3926	0.36	15613	0.30
3'mismatch 2	3857	0.35	15352	0.29
3'mismatch 3	7053	0.65	32377	0.62
3'double mismatch	235	0.02	2135	0.04
5'mismatch 1	440	0.04		
5'mismatch 2	4355	0.40	23743	0.45
5'mismatch 3	7857	0.72	50909	0.97
5'double mismatch	350	0.03	1645	0.03

3.7.3 Emission spectra for the SP-2 mismatch systems.

Exciplex emission was detected (broad band around 480 nm) for both systems with insertions (*insertion 1* and *insertion 2*). However, that for *insertion 2* was weak. The intensity of the exciplex emission for both variants was less than for the parent and increased to a maximum over 10 minutes while the sample was held at 10 °C (Figure 3.54). The increase in exciplex emission, seen for the SP-1 pyrene-pyrene excimer systems after the samples were heated to 40 °C for 2 minutes and allowed to cool back to 10 °C, was not observed for these systems. In fact, the signal for the SP-2 system was less intense after the heating-cooling cycle, even after the sample was allowed to equilibrate for a further 10 minutes on re-cooling 10 °C. This may be due to the temperature ramping profiles not being optimized, for example these systems may require an even longer re-annealing time.

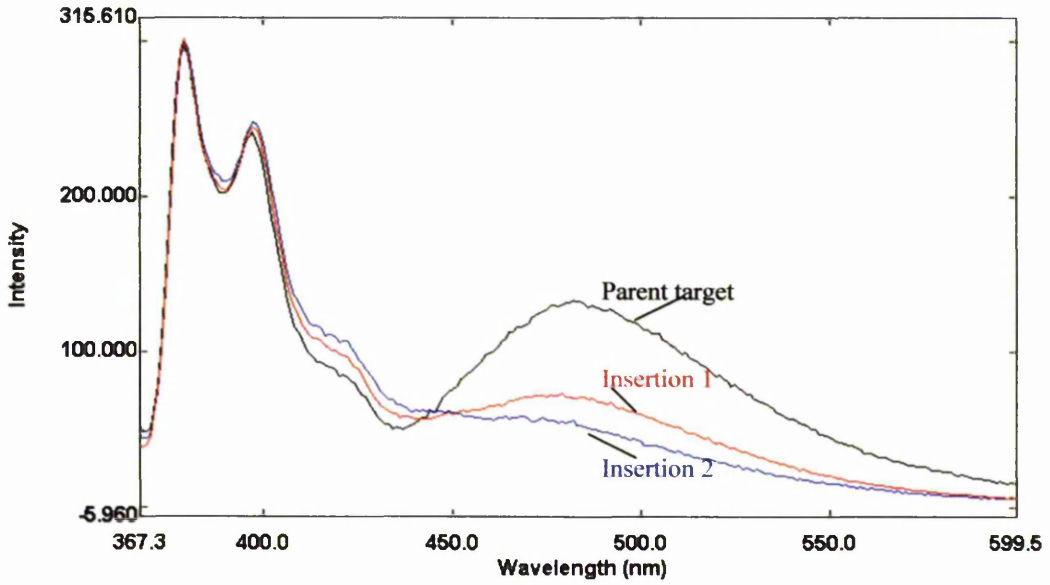

Figure 3.54: Emission spectra comparing the *parent target* (SP-2) with *insertion 1* and *insertion 2* targets in 80% TFE/ Tris buffer (10 mM Tris, 0.1 M NaCl, pH 8.5) at 10 °C before heating the samples. Spectra were recorded when emission intensity had reached a maximum after 10 minutes at 10 °C. Excitation was at 350 nm, slitwidth 5 nm. Spectra, buffer-corrected, are scaled to LES emission.

Exciplex emission to some level was observed for most of the mismatched target sequences, except for both *double mismatches* and *5'mismatch 1 and 2* systems. In all cases where exciplex emission was detected it increased over time to a maximum, usually after 10 minutes (Figure 3.55). However, the increase seen for SP-1 after the samples had been heated to 40 °C and re-cooled to 10 °C was again not observed for most systems, and signal intensity was actually reduced.

The exciplex emission intensity was always less intense for the mismatches/ insertions than for the *parent* system, and varied according to the position of the mismatch. In all cases (parent, insertions and mismatches) exciplex emission was weaker than excimer emission for SP-1 pyrene-pyrene systems.

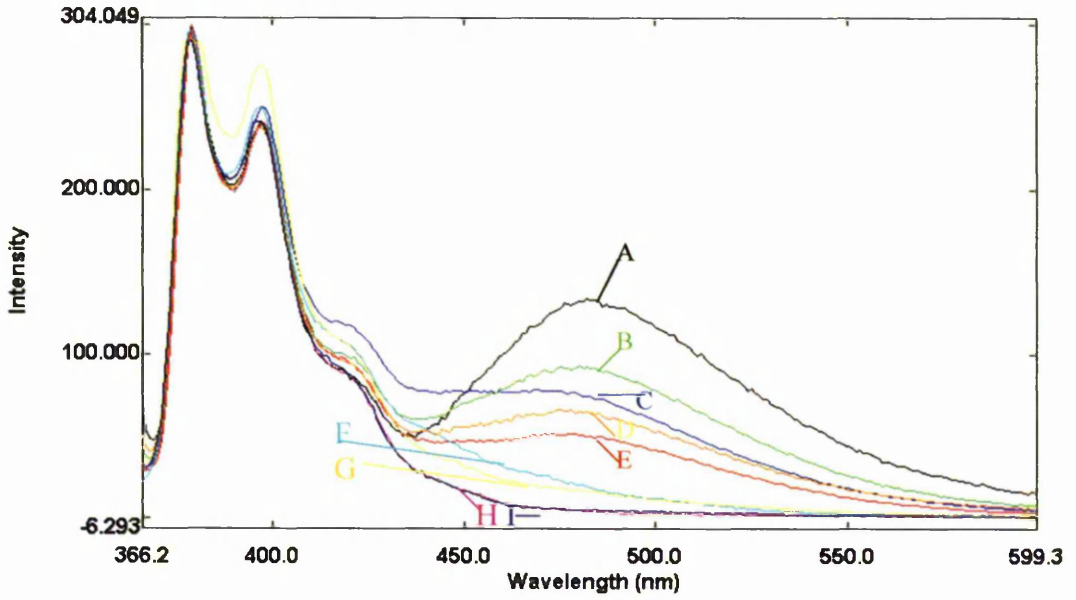

Figure 3.55: Spectra comparing mismatches to parent target for the SP-2 system in 80% TFE/ Tris buffer (10 mM Tris, 0.1 M NaCl, pH 8.5) at 10 °C. Spectra are scaled to the parent spectrum for LES emission at 380 nm. Excitation was at 350 nm, slit width 3 nm. A=*Parent*, B=3'mismatch 3, C= *3'mismatch 1*, D=*5'mismatch 3* E= *3'mismatch 2*, F= *5'mismatch 1*, G=*5'mismatch 2* H=*3'double mismatch*, I=*5'double mismatch.*

Table 3.10 shows areas under the exciplex emission bands between 480-600 nm, 490-600 nm and 500-600 nm, and also the ratio between the AUCs for the mismatch spectra and the parent spectrum between 480-600 nm for the SP-2 system at 10 °C before heating. Table 3.11 shows the data after heating to 40 °C and re-cooling to 10 °C.

Table 3.10: Areas under curve between 480-600 nm, 490-600 nm and 500-600 nm plus ratio of AUC of the mismatch/ insertion spectra : AUC of the parent spectra (from 480-600 nm) for SP-2 in 80% TFE/ Tris buffer (10 mM Tris, 0.1 M NaCl, pH 8.5) at 10 °C before heating.

Target	AUC 480-600 nm	AUC 490-600 nm	AUC 500-600 nm	AUC mismatch(480-600 nm): AUC parent (480-600 nm)	AUC mismatch(490-600 nm): AUC parent (480-600 nm)	AUC mismatch(500-600 nm): AUC parent (480-600 nm)
Parent	7879	6565	5326	1.00	0.83	0.68
Insertion 1	2752	2245	1800	0.35	0.28	0.23
Insertion 2	3775	3087	2459	0.48	0.39	0.31
3'mismatch 1	3762	3033	2386	0.48	0.38	0.30
3'mismatch 2	2500	2027	1599	0.32	0.26	0.20
3'mismatch 3	5035	4128	3298	0.64	0.52	0.42
3'double mismatch	247	204	174	0.03	0.03	0.02
5'mismatch 1	736	555	418	0.09	0.07	0.05
5'mismatch 2	686	549	437	0.09	0.07	0.06
5'mismatch 3	3471	2839	2266	0.44	0.36	0.29
5'double mismatch	330	277	233	0.04	0.04	0.03

Table 3.11: Areas under the curves between 480-600 nm, 490-600 nm and 500-600 nm plus ratio of AUC of the mismatch/ insertion spectra : AUC of the parent spectra (from 480-600 nm) for SP-2 in 80% TFE/ Tris buffer (10 mM Tris, 0.1 M NaCl, pH 8.5) at 10 °C after heating to 40 °C.

	AUC 480-600 nm	AUC 490-600 nm	AUC 500-600 nm	AUC mismatch(480-600 nm): AUC parent (480-600 nm)	AUC mismatch(490-600 nm): AUC parent (480-600 nm)	AUC mismatch(500-600 nm): AUC parent (480-600 nm)
Parent	10377	8650	6996	1.00	0.83	0.67
Insertion 1	2437	1993	1597	0.23	0.19	0.15
Insertion 2	3107	2549	2034	0.30	0.25	0.20
3'mismatch 1	2615	2121	1671	0.25	0.20	0.16
3'mismatch 2	2819	2260	1970	0.27	0.22	0.19
3'mismatch 3	4253	3484	2773	0.41	0.34	0.27
3'double mismatch	500	405	329	0.05	0.04	0.03
5'mismatch 1	533	401	305	0.05	0.04	0.03
5'mismatch 2	667	533	421	0.06	0.05	0.04
5'mismatch 3	4070	3305	2614	0.39	0.32	0.25
5'double mismatch	270	222	182	0.03	0.02	0.02

3.7.4 Emission spectra for the SP-3 mismatch systems.

For the SP-3 system, exciplex emission was seen for both *insertion 1* and *insertion 2* (Figure 3.56) and all mismatch systems except for *5'mismatch 1* and both *3'double mismatch* and *5'double mismatch* (Figure 3.57). Unlike SP-2, *5'mismatch 2* gave an exciplex signal. This was the same pattern as detected by the excimer system (SP-1). In all cases exciplex emission for the mismatch or insertion target systems was much weaker than for the parent target system.

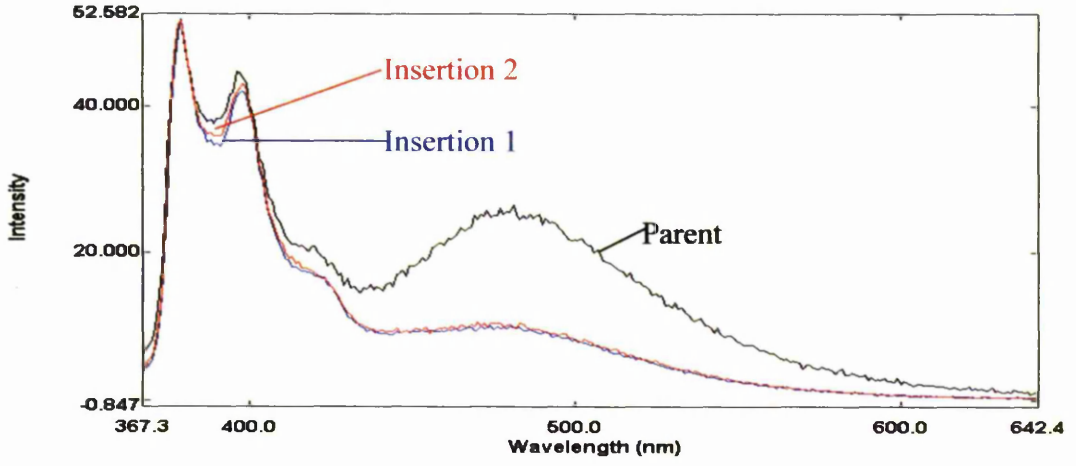

Figure 3.56: Comparison of emission spectra for insertion systems for the SP-3 system in 80% TFE/ Tris buffer (10 mM Tris, 0.1 M NaCl, pH 8.5) at 10 °C before heating. Excitation was at 350 nm; slitwidth 3 nm. Spectra are scaled to LES emission at 380 nm of the parent spectrum.

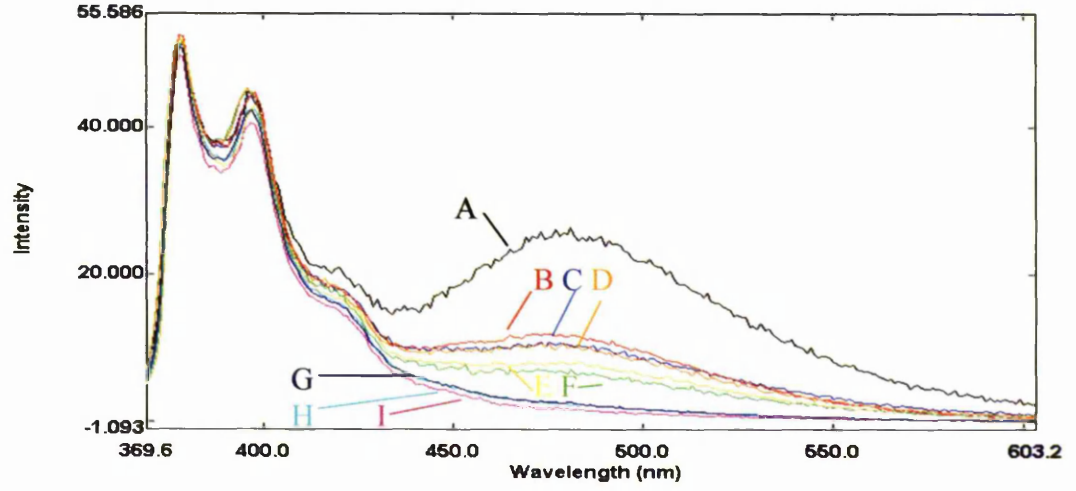

Figure 3.57: Comparison of emission spectra for the mismatch systems of SP-3 system in 80% TFE/ Tris buffer at 10 °C before heating. Excitation wavelength 350 nm, slitwidth 3 nm. Spectra are scaled to LES band of parent system. A=*Parent*, B=*3'mismatch 2*, C=*3'mismatch 3*, D=*5'mismatch 3*, E=*5'mismatch 2*, F=*3'mismatch 1*, G=*5'double mismatch* H=*3'double mismatch*, I=*5'mismatch 1*.

The areas under the exciplex bands along with the ratio between AUC for the mismatches and AUC for the parent from 480-600 nm, for the SP-3 systems before heating are given in Table 3.12 and for the systems after heating after heating to 40 ° C and cooling back to 10 °C in Table 3.13. These data show that both the *double mismatches* and *5'mismatch 1* gave no appreciable exciplex signal even after heating to 40 °C and re-cooling. However, unlike the SP-2 system the heating and cooling cycle did significantly increase exciplex emission, as for the excimer SP-1 system.

Table 3.12: Areas under emission curves (AUC) for parent and insertion/mismatch sequences (between 480-600 nm) and ratio of AUC mismatch : AUC parent (480-600 nm) for split-probe SP-3 system in 80% TFE/ Tris buffer (10 mM Tris, 0.1 M NaCl, pH 8.5) at 10 °C before heating.

Target	AUC 480-600 nm	AUC mismatch : AUC parent
Parent	1469	1.00
insertion 1	520	0.35
insertion 2	537	0.37
3'mismatch 1	580	0.40
3'mismatch 2	572	0.39
3'mismatch 3	359	0.24
3'double mismatch	71	0.05
5'mismatch 1	106	0.07
5'mismatch 2	405	0.28
5'mismatch 3	523	0.36
5'double mismatch	109	0.07

Table 3.13: Areas under exciplex emission curves for parent and insertion/mismatch sequences (480-600 nm) and AUC mismatch : AUC parent ratios for SP-3 system after heating to 40 °C and re-cooling to 10 °C in 80% TFE/ Tris. Excitation wavelength 350 nm; slitwidth 3 nm. Spectra were buffer corrected.

Target	AUC 480-600 nm	AUC mismatch : AUC parent
Parent	7631	1.00
insertion 1	1894	0.25
insertion 2	1590	0.21
3'mismatch 1	1972	0.26
3'mismatch 2	3507	0.46
3'mismatch 3	2056	0.27
3'double mismatch	226	0.03
5'mismatch 1	349	0.05
5'mismatch 2	1281	0.17
5'mismatch 3	4274	0.56
5'double mismatch	362	0.05

3.8 Use of Locked Nucleic Acid Residues in Split-Probes.

3.8.1 Applications of Split-Probe exciplex systems to the Prothrombin gene.

A genetic mutation of the prothrombin gene, resulting in a G-A transition at nucleotide position 20210 in the 3'-untranslated section, causes an increase in plasma concentration of prothrombin, which in turn increases the risk of thrombosis [2;110]. Prothrombin is the precursor of thrombin in the coagulation cascade, and while the exact mechanism how this increase in prothrombin leads to thrombosis is still unknown, it is thought to be a springboard upon which the clotting process can begin and may run out of control [115]. The split-probe detection system was applied to this mutation to determine whether a signal would be seen on duplex formation and irradiation. The system comprised two 10-mer probes, one with a pyrene group on its 5'-terminal phosphate site, and the other with a naphthalene-based group on its 3'-terminal phosphate. The probes, complementary to a 32-mer target, annealed to it in such a way that the two exci-partner components were positioned next to each other to permit exciplex formation as with SP-2. The 32-mer target was a region of the prothrombin gene containing the mutation and was perfectly matched to these probes. The sequences are shown in Section 2.1.3.

Three systems, composed of the same nucleotide sequences and exci-partners, were studied:

(1) A DNA-DNA system where both the probes and the target were composed only of DNA residues.

(2) As for (1), but with the pyrene-bearing probe having a diene group (structure not provided by collaborators) attached to its 3'-terminal phosphate group. Such a diene group can be used for conjugation of oligos to various carriers.

(3) A DNA-LNA (locked nucleic acid) hybrid system where the target was based on DNA, but the probes contained a number of LNA residues, the positions of which are shown in Figure 3.58.

Nomenclature of the various probe oligos used is shown in Section 2.1.3.

A-T-T-G-A-G-G-C-T-C$^{3'p}$ **$^{5'p}$G-C-T-G-A-G-A-G-T-C**

Figure 3.58: Sequences of probes used against the prothrombin target showing the position of LNA residues in red.

During conjugation of the probe oligos to the respective exci-partners evidence of secondary structures formed by the individual oligos (supplied as single-stranded) was found. 1D ^{1}H-NMR spectra, taken at 25 °C for all starting oligos (Proexc 3, 4, 9,10 and 11) and for the respective oligos conjugated with ligands, showed comprehensive line broadening at all positions, indicating the presence of secondary structure(s). Indirect evidence of this was obtained by recording NMR spectra at a higher temperature (50 °C), which resulted in signal sharpening, possibly through disruption of this secondary structure, due to an increased rate of exchange between conformations (Figure 3.59).

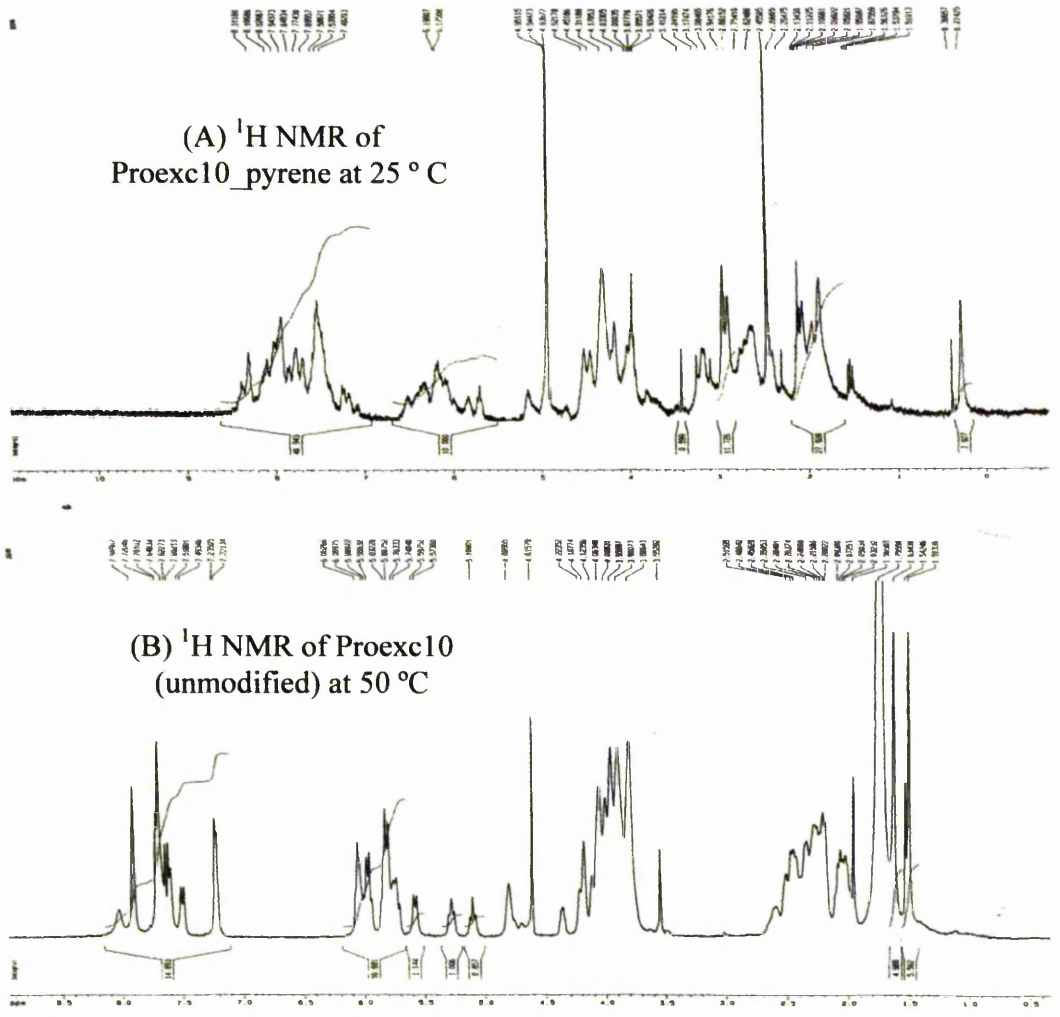

Figure 3.59: ^{1}H NMR spectra at 300 MHz of (A) Proexc10_5'pyrene recorded in D_2O at 25 °C showing line broadening due to internal structure formation and (B) Proexc10 (unmodified) recorded in D_2O at 50 °C showing sharpening of peaks

To confirm the presence of secondary structure(s), melting curve experiments were performed for unmodified 12-mers (Proexc 3, 4, 10 and 11, Figures 3.60, 3.61, 3.62 and 3.63, respectively) in Tris buffer (10mM Tris, 0.1M NaCl at pH 8.5). All probe oligos showed a broad range of transitions between 10 °C and 65 °C indicating that some form of secondary structure was present. For example, Proexc4 and Proexc 10 showed cooperative S-like transitions indicating the presence of stable double-stranded regions for these oligos. The estimated melting temperatures (T_m) for the unmodified oligos obtained from the melting curves are in Table 3.14.

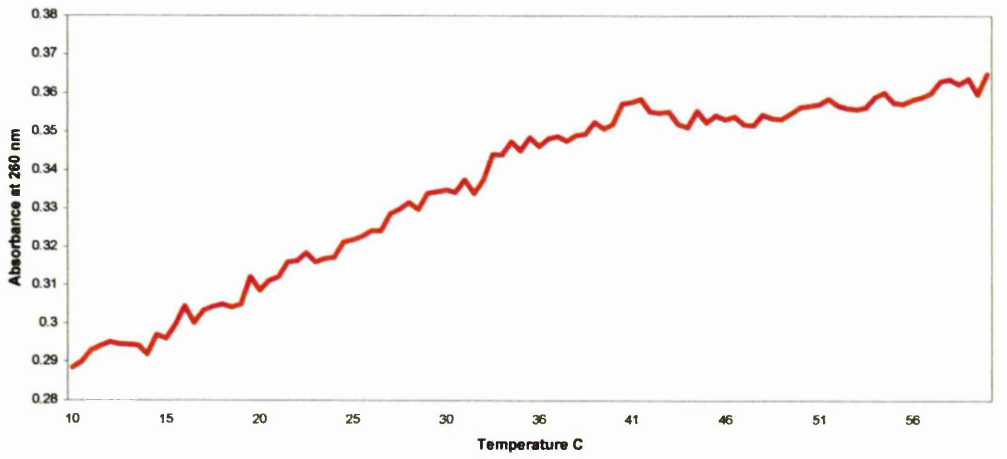

Figure 3.60: Melting curve of unmodified Proexc3 (1.25 µM) in Tris buffer (10 mM Tris, 0.1 M NaCl, pH 8.5) determined using the change in absorbance at 260 nm (temperature ramping: 0.5 °C/ min).

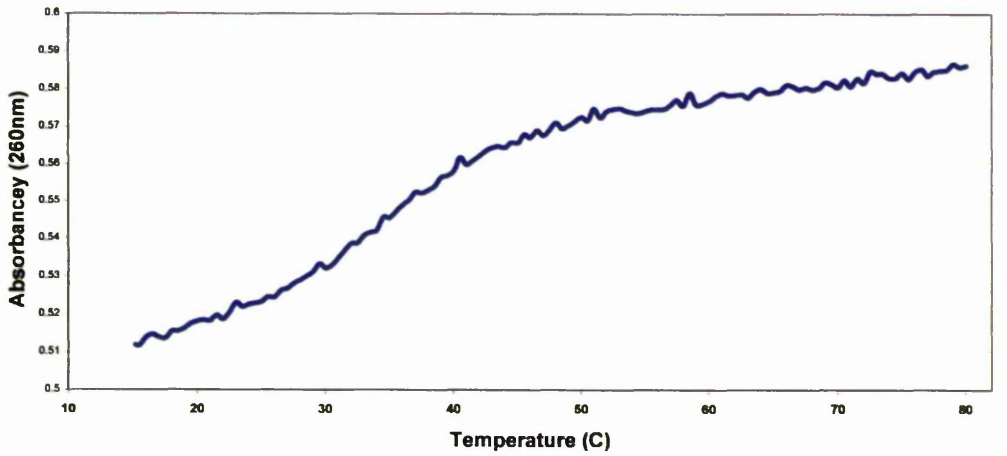

Figure 3.61: Melting curve of un-modified Proexc4 (1.25 µM) in Tris buffer buffer (10 mM Tris, 0.1 M NaCl, pH 8.5) determined using the change in absorbance at 260 nm (temperature ramping: 0.5 °C/ min).

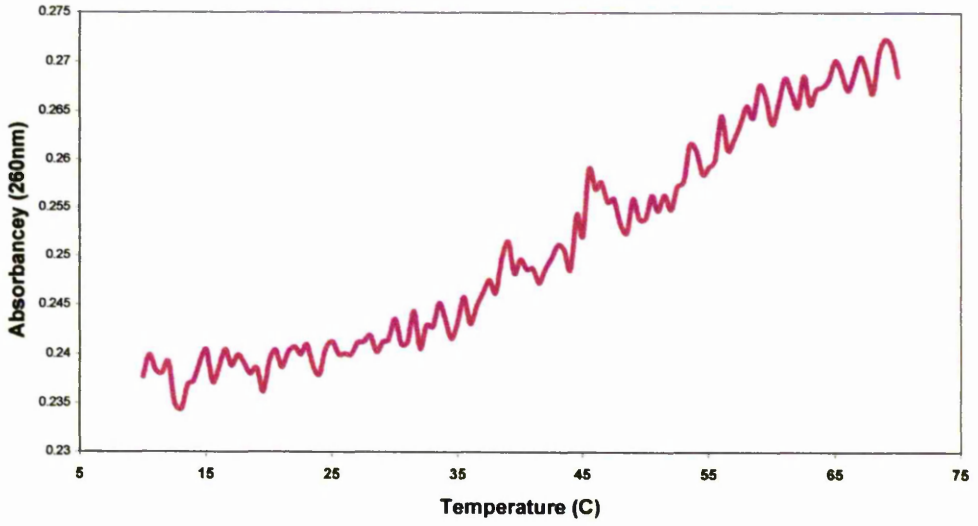

Figure 3.62: Melting curve of un-modified Proexc10 (1.25 μM) in Tris buffer buffer (10 mM Tris, 0.1 M NaCl, pH 8.5) determined using the change in absorbance at 260 nm (temperature ramping: 0.5 °C/ min).

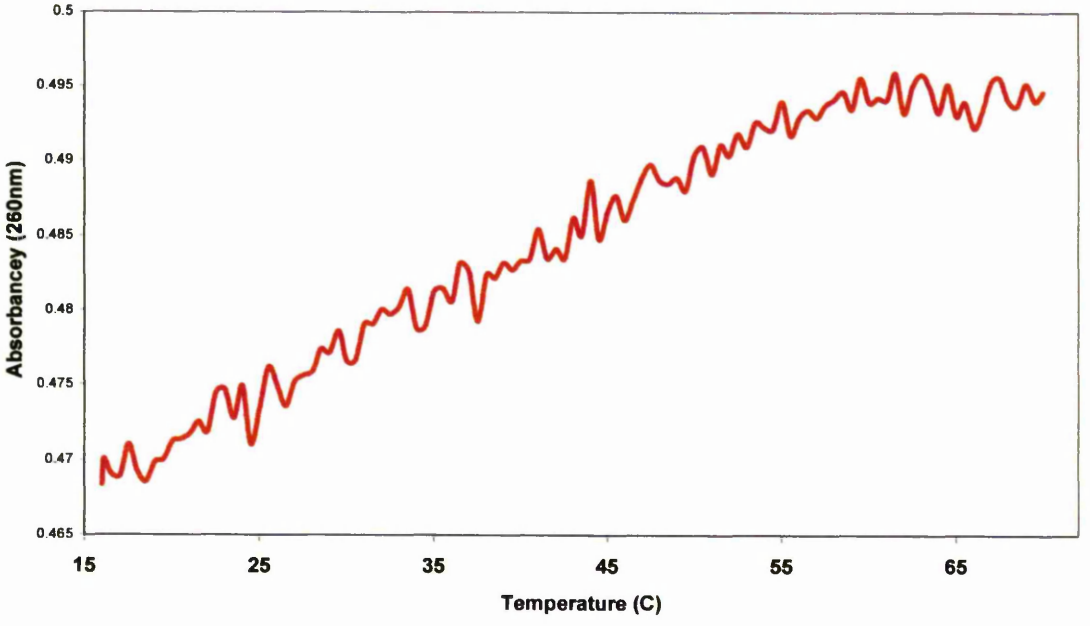

Figure 3.63: Melting curve of un-modified Proexc11 (1.25 μM) in Tris buffer buffer (10 mM Tris, 0.1 M NaCl, pH 8.5) determined using the change in absorbance at 260 nm (temperature ramping: 0.5 °C/ min).

Table 3.14: Melting temperatures estimated from melting curves obtained for unmodified probe oligos (Proexc 3, Proexc 4, Proexc 10 and Proexc11) in Tris buffer (10mM Tris, 0.1M NaCl at pH8.5) using first-derivative method and half-point at half curve height. (see Methods Section 2.4.15).

Unmodified Oligo ID	T_m (°C) from A_{260}	
	First derivative	Half curve height
Proexc3	15 ± 4	27
Proexc4	38 ± 2	36
Proexc10	45 ± 6	45
Proexc11	43 ± 3	37

Additional evidence of the presence of secondary structure was obtained by spectrophotofluorometric analysis of those oligos that were conjugated with pyrene. The 5'-pyrene-modified oligos exhibited exciplex emission in the presence of TFE (50 and 80 %) at 10 °C in the absence of any other component. This emission disappeared on heating (70 °C) and did not return on re-cooling to 10 °C. The λ_{max} value of this emission was found to be slightly different from that for the exciplex formed when all components of the tandem assembled split-probe duplex were present (see results below).

3.8.2 LNA System: SP-13 Proexc11_5'pyrene + Proexc4_3'*bis*-naphthalene + Proexc1 (target).

The emission spectra of this LNA system, SP-13, in Tris buffer (10 mM Tris, 0.1 M NaCl, pH 8.5 at 10 °C) at different stages of assembly are presented in Figure 3.64. The pyrene emission maximum at 380 nm, seen for Proexc_5'pyrene, was unaffected by the addition of the second component (Proexc4_3'naphthalene), indicating there was no interaction between the split-probe partners in the absence of the target strand. Addition of the target strand did not alter the spectrum: no exciplex emission was observed. After the system had been heated to 75 °C and cooled back to 10 °C weak exciplex emission became visible (shoulder around 480 nm). This band became visible on cooling to 50 °C, the intensity increased with further cooling to 10 °C (Figure 3.65). The exciplex signal seen is not clearly resolved from the LES signal. A melting curve was derived from fluorescence data, by plotting intensity at 470 nm against temperature (Figure 3.66), from this a T_m was found to be 43 °C. This was different from the T_m derived from the A_{260} temperature profile (Figure 3.67) (using first derivative method) of 63 °C.

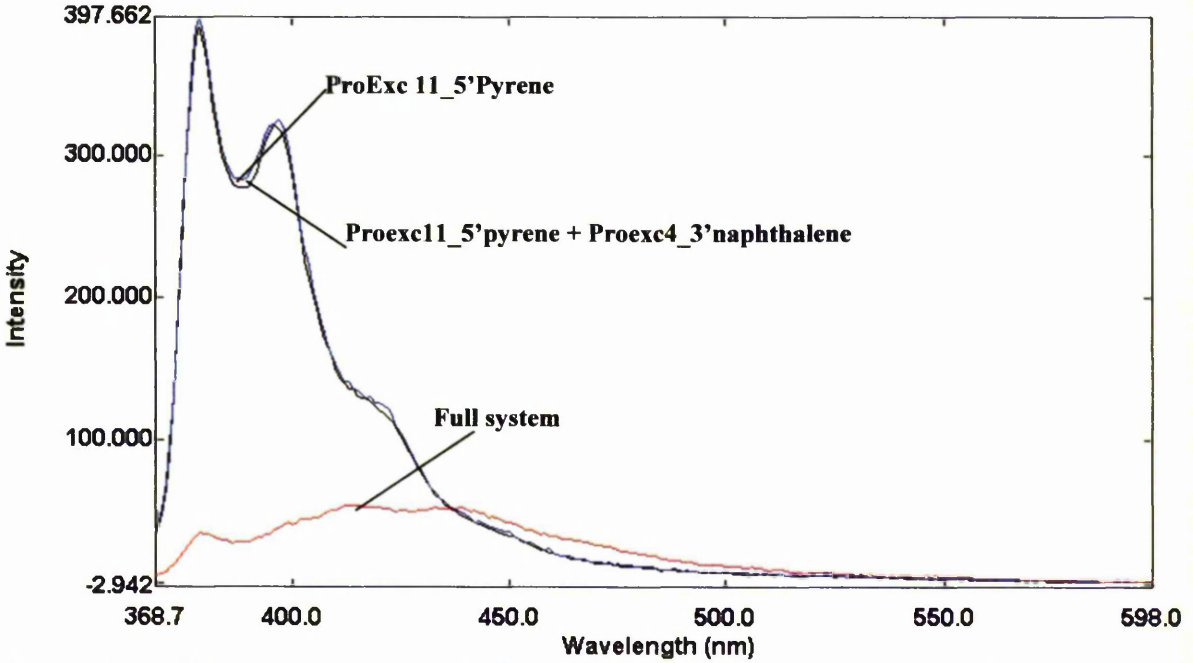

Figure 3.64: Fluorescence spectra of SP-13 (Proexc11_5'pyrene + Proexc4_3'naphthalene with target strand (ProExc1)) in Tris buffer at 10 °C. (10 mM Tris, 0.1 M NaCl, pH 8.5). Excitation wavelength 350 nm; slitwidth 10 nm. Spectra are buffer-corrected.

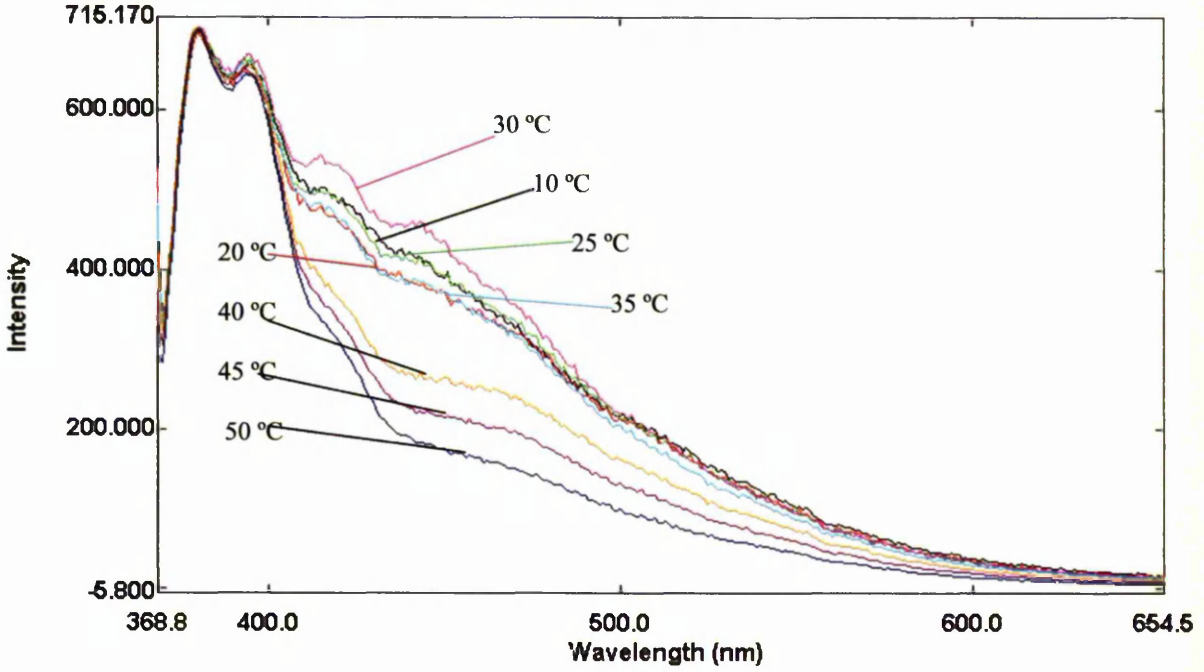

Figure 3.65: Fluorescence spectra showing re-annealing (cooling from 50 °C to 10 °C) of the SP-13 system (Proexc11_5'pyrene + Proexc4_3'naphthalene with target (ProExc1)) in Tris buffer (10 mM Tris, 0. 1M NaCl, pH 8.5). Excitation was at 350 nm, slit 10 nm. Spectra are buffer-corrected and scaled to LES emission at 380 nm to assist comparison.

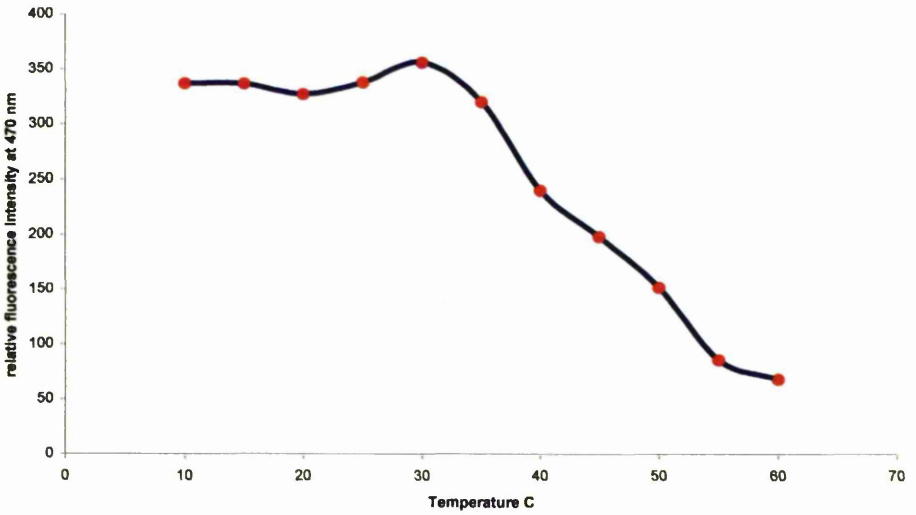

Figure 3.66: Melting curve of the SP-13 system (Proexc11 + Proexc4 + target) in Tris buffer (10 mM Tris, 0.1 M NaCl, pH 8.5) obtained by plotting relative fluorescence intensity at 470 nm against temperature. Excitation wavelength 350 nm; slitwidth 5 nm. Spectra were scaled to LES emission at 380 nm.

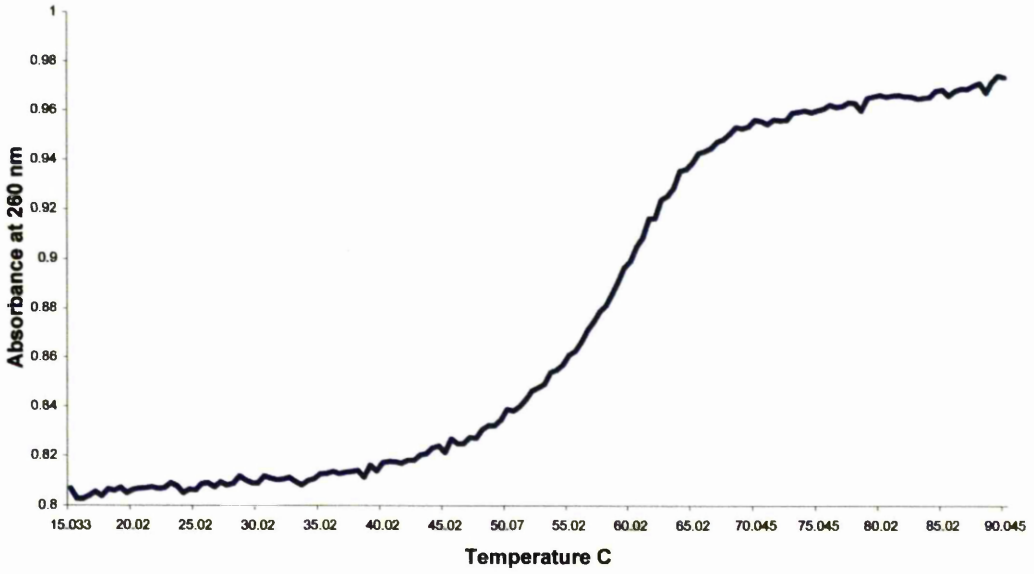

Figure 3.67: Melting curve for SP-13 (Proexc11 + Proexc4 + target) strand in Tris buffer (10 mM Tris, 0.1 M NaCl, pH 8.5) determined using the change in absorbance at 260 nm with temperature.

In the presence of 20% TFE the system behaved similarly to that in Tris buffer in the absence of TFE (Figure 3.68). Addition of the second component (Proexc4_3'naphthalene) did not change the emission spectrum of Proexc11_5'pyrene, again indicating the absence of interaction between the probe oligos in the absence of target strand. However, addition of the target strand caused the hybridisation of both oligo partners. This resulted in strong quenching of the pyrene LES emission, accompanied by the appearance of a strong exciplex band with λ_{max} 453 nm (quenching is not obvious from Figure 3.68 as spectra have been scaled to LES emission to monitor the change in I_E/ I_M). In addition, λ_{max} for the LES band was shifted by ~ 5 nm to the red, indicating duplex formation. On melting the duplex, the exciplex band disappeared completely at 60 °C and the LES band recovered its previous intensity and λ_{max} value. The exciplex reappeared on re-cooling to 10 °C. The melting temperature derived from the A_{260} *versus* temperature profile was 49 °C, lower than that in Tris buffer derived using the same method.

The system behaved similarly in 40% TFE, although λ_{max} for exciplex was 463 nm and the I_E/ I_M value was slightly higher. Figure 3.69 shows how the λ_{max} and I_E/ I_M values change with TFE concentration. Heating the system in 40% TFE did not cause the exciplex band to fully disappear, but the intensity decreased.

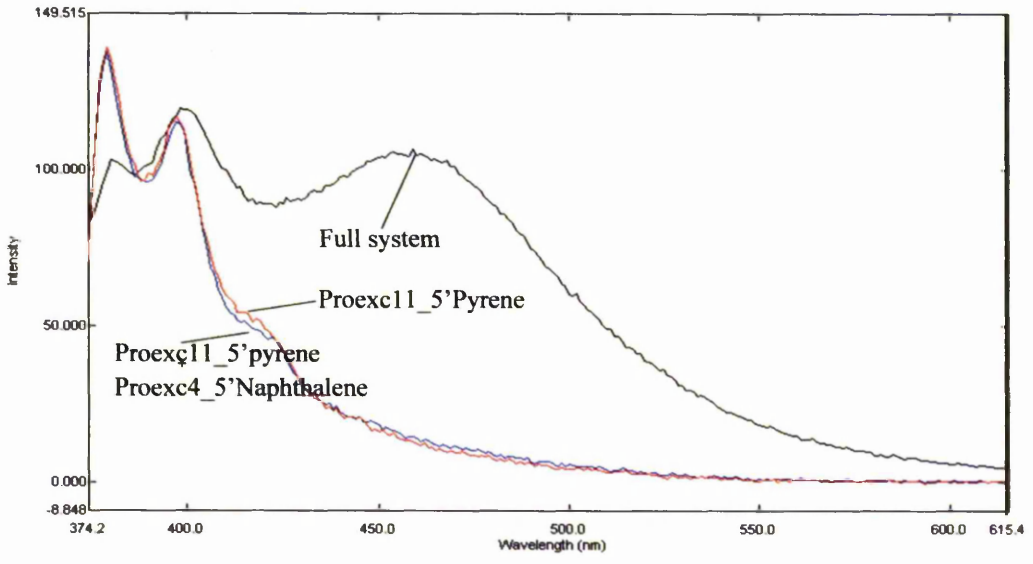

Figure 3.68: Fluorescence spectra showing SP-13 (Proexc11_5'pyrene + Proexc4_3'naphthalene with target (ProExc1)) in 20%TFE/ Tris buffer (10 mM Tris, 0.1 M NaCl, pH 8.5) at 10 °C. Excitation wavelength 355 nm; slitwidth 5 nm. Spectra are buffer-corrected and scaled to LES emission.

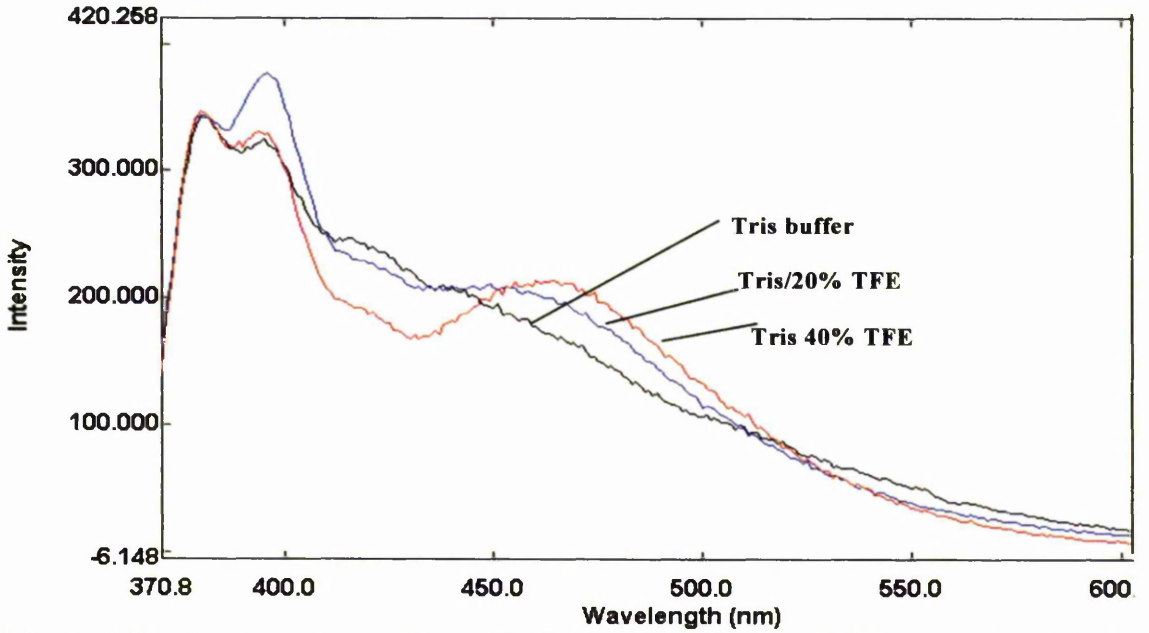

Figure 3.69: Fluorescence spectra of SP-13 (Proexc11_5'pyrene + Proexc4_3'naphthalene + target) system in Tris buffer (10 mM Tris, 0.1 M NaCl, pH 8.5) after heating to 60 °C and cooling back to 10 °C at various TFE concentrations Excitation at 350 nm; slitwidth 10 nm. Concentration of each component was 2.5 μM. Spectra are buffer-corrected and scaled to LES emission.

In 80% TFE/ Tris buffer (10 mM Tris, 0.1 M NaCl, pH 8.5) Proexc11_5'pyrene showed a very large background exciplex emission (λ_{max} 480 nm, Figure 3.70) in the absence of any other component. This provided strong evidence of the presence of internal structure for the single-strand sample of Proexc11_5'pyrene as provided by Proligo, presumably resulting from a pyrene exciplex with nucleotide bases. These data are consistent with NMR and melting curve data for this compound. It should be noticed that on addition of the target oligo at 10 °C no change in the spectrum was observed (Figure 3.70), indicating, that contrary to expectation, no interaction occurred between the target and its complementary probe. This could be explained if Proexc11_5'pyrene was already involved in stable secondary structure formation, preventing its hybridisation with the target. To destroy this secondary structure, a heating procedure (heating to 60 °C and cooling back to 10 °C) was applied. This resulted in complete disappearance of the exciplex signal (Figure 3.71), which indicated that the internal structure was destroyed. The T_m value of Proexc11, determined by plotting the fluorescence intensity at 480 nm against temperature (Figure 3.72) was 35 °C, compared to 42 °C using the A_{260} temperature profile. The exciplex signal did not reappear on re-annealing the sample at 10°C. This

indicated that on cooling the strand, Proexc11_5'pyrene re-annealed preferentially to the target oligo, driven by the more extensive base pairing possible between these two oligos than with a single strand, and resulting in a more stable structure. On addition of Proexc4_3'naphthalene at 10 °C no change in the emission spectrum was seen, possibly also due to the secondary structure formed by this oligo preventing interaction with the other components. However, after heating the system to 60 °C and re-annealing to 10 °C, exciplex emission appeared due to full tandem duplex formation. The λ_{max} value (474 nm) of this complex was slightly shifted with respect to the background exciplex emission arising from the internal structure of Proexc11_5'pyrene, again indicating interstrand hybridisation to the target after re-annealing (Figure 3.73).

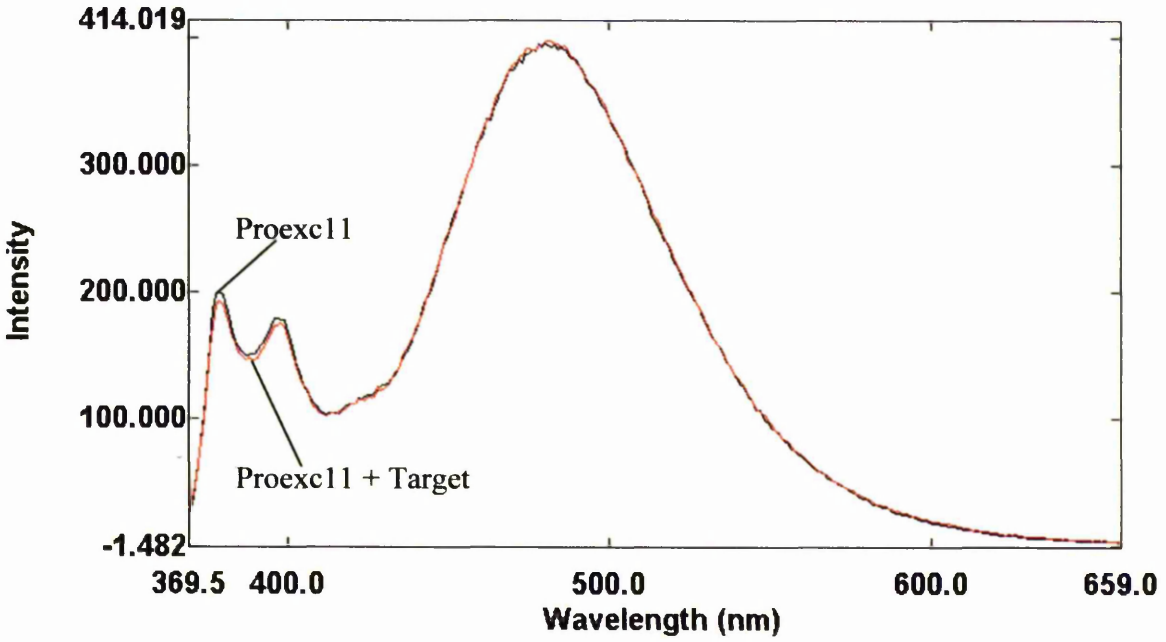

Figure 3.70: Fluorescence spectra of Proexc_5'Pyrene in the presence and absence of target strand in 80% TFE/ Tris buffer (10 mM Tris, 0.1 M NaCl, pH 8.5) at 10 °C. Excitation was at 350 nm; slitwidth 5 nm. Spectra are buffer-corrected, but not scaled.

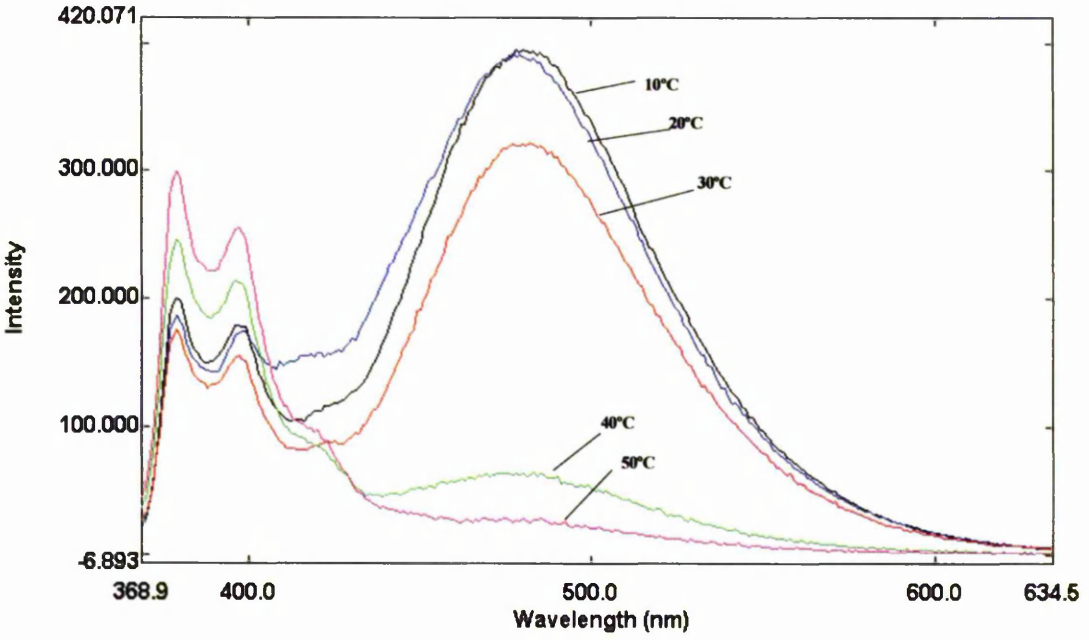

Figure 3.71: Fluorescence spectra showing melting of Proexc11_5'pyrene and target (ProExc1) in 80% TFE/ Tris buffer (10 mM Tris, 0.1 M NaCl, pH 8.5). Samples were heated to 60 °C over 30 minutes with spectra taken at 5 °C increments. Excitation wavelength 350 nm, slitwidth 5 nm. Spectra are buffer-corrected and unscaled.

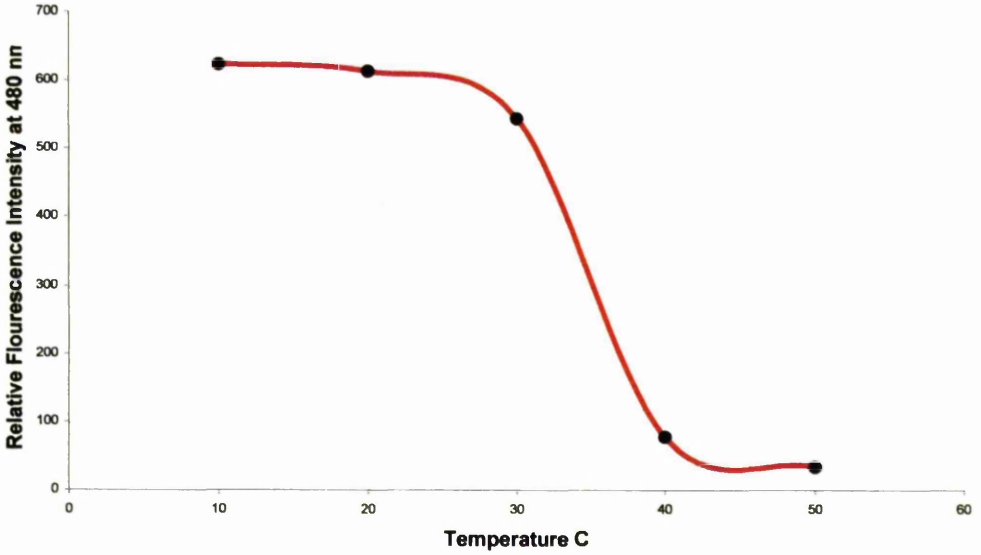

Figure 3.72: Melting curve of Proexc11 in 80% TFE/ Tris buffer (10 mM Tris, 0.1 M NaCl, pH 8.5) obtained by plotting relative fluorescence intensity at 480 nm against temperature. Excitation was at 350 nm; slitwidth 5 nm. Spectra were scaled to LES emission at 380 nm.

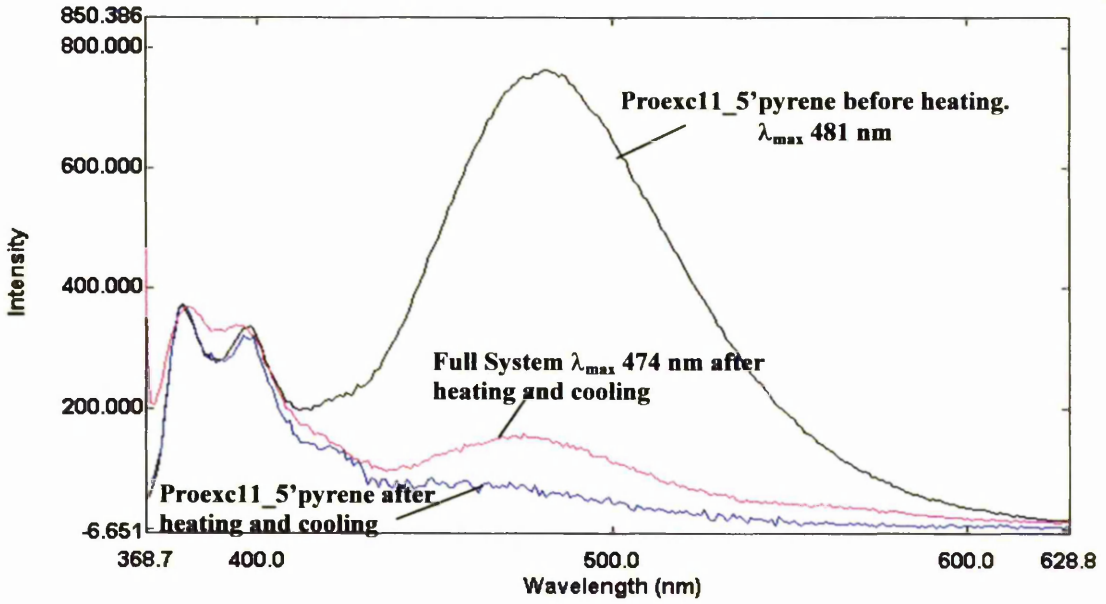

Figure 3.73: Comparison of the background exciplex from Proexc11_5'pyrene detected in 80% TFE/ Tris buffer (10 mM Tris, 0.1 M NaCl, pH 8.5) with the exciplex formed by the full SP-13 system (Proexc10_5'pyrene + Proexc11_3'naphthalene + target) after heating to 60 °C and cooling back to 10 °C in 80% TFE/ Tris buffer (10 mM Tris, 0.1 M NaCl, pH 8.5). The spectrum showing disappearance of background exciplex after heating to 60 °C and re-cooling to 10 °C is also shown. Excitation wavelength 350 nm, slitwidth 10 nm. Concentration of each component was 1.25 μM. Spectra are buffer-corrected, but unscaled

In a control experiment on the C-6 system (Proexc11_5'pyrene + Proexc4_3'Phosphate + Target) (Section 2.1.4) in 20% TFE/ Tris buffer (10 mM Tris, 0.1 M NaCl, pH 8.5) no exciplex emission was detected initially when all the components were added at 10 °C. However, heating (to 60 °C) and re-annealing resulted in exciplex emission. It is important to note that the λ_{max} value (450 nm) was at shorter wavelength than that of the experimental system (462 nm) (Figure 3.74).

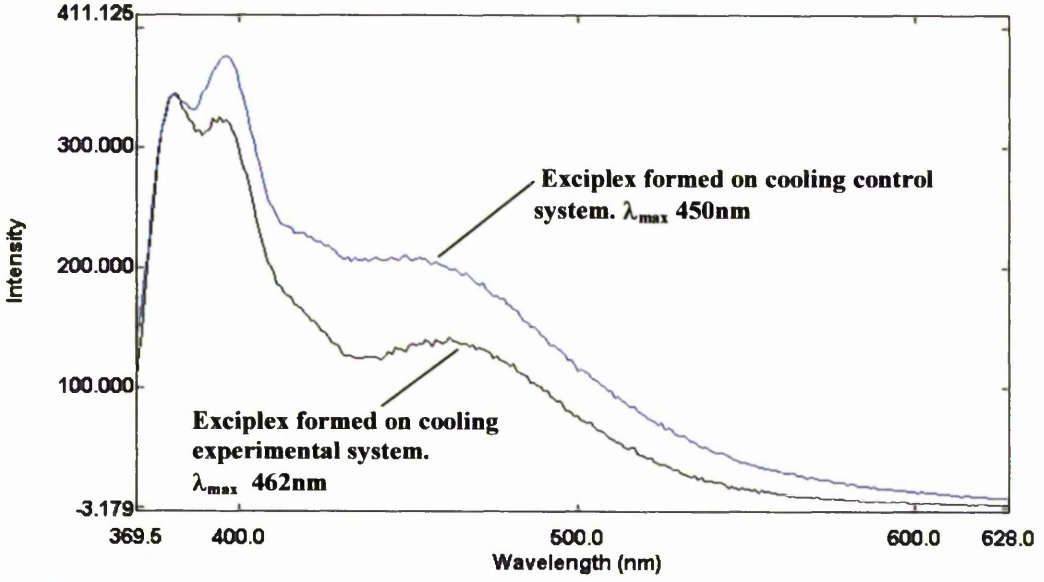

Figure 3.74: Fluorescence emission spectrum of exciplex formed on cooling the control system C-6 (Proexc11_5'pyrene + Proexc4_3'Phosphate + target) compared with that formed on cooling the experimental system (Proexc11_5'pyrene + Proexc4_3'naphthalene + target). Spectra were taken in 20% TFE/ Tris buffer. Excitation wavelength 350 nm; slitwidth 10 nm. Spectra are buffer-corrected and scaled to LES emission at 378 nm.

3.8.3 DNA-diene system: SP-14 (Proexc9_5'pyrene + Proexc3_3naphthalene + Proexc1 (target)).

The DNA-diene system, SP-14, was only investigated in 80% TFE/ Tris buffer (10 mM Tris, 0.1 M NaCl, pH 8.5). As for the simple DNA systems, Proexc9_5'Pyrene showed a large background exciplex emission (λ_{max} 479 nm), which did not change on addition of the naphthalene-bearing probe (Proexc3_3'naphthalene) or the target, at 10 °C. This indicated that no interaction with either of these oligos occurred, consistent with Proexc9_5'pyrene having an internal structure, not recognised by the target. This background disappeared completely when Proexc9_5'pyrene was heated to about 30 °C (T_m was 23 °C, determined by plotting fluorescence intensity at 480 nm against temperature), accompanied by an increase in LES emission intensity, indicating distortion of the internal structure on heating. As expected the stability of this internal structure is lower than that of the complex formed by both respective LNA analogues correctly and simultaneously annealing to target, the exciplex emission of which disappeared around 70 °C. On re-cooling to 10 °C, a new exciplex band emerged with λ_{max} (482 nm) at a slightly

longer wavelength (see Figure 3.75), again indicating a different type of exciplex or altered environment.

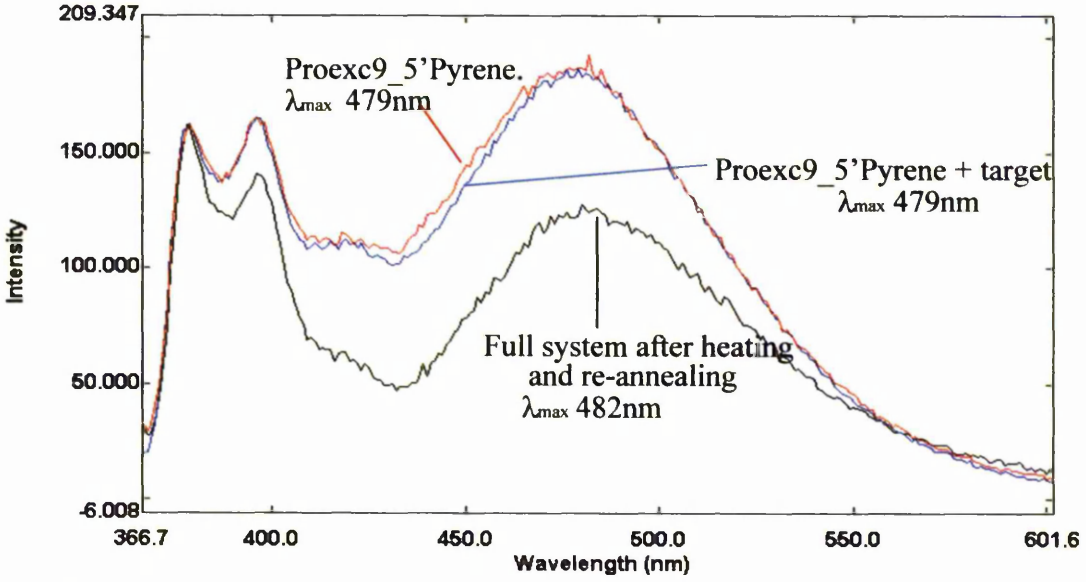

Figure 3.75: Comparison of background exciplex of Proexc9_5'Pyrene + target with that of the full SP-14 system (Proexc9_5'Pyrene + Proexc3_3'naphthalene + target) after heating to 40 °C and cooling back to 10 °C in 80% TFE/ Tris buffer (10 mM Tris, 0.1 M NaCl, pH 8.5). Excitation wavelength 350 nm, slitwidth 10 nm. Concentration of each component was 1.25 μM . Spectra are buffer-corrected and scaled to LES emission at 378 nm.

3.8.4 DNA system: SP-15 (Proexc10_5'pyrene + Proexc3_3naphthalene + Proexc1 (target)).

For the DNA system, SP-15, no exciplex signal was seen in Tris buffer (10 mM Tris, 0.1 M NaCl, pH 8.5) with no TFE present, even after heating and cooling. No exciplex signal has ever been reported for DNA-only systems under such conditions. In 80% TFE/ Tris buffer the probe with 5'-Pyrene group attached (Proexc10_5'pyrene) behaved similarly to its LNA and DNA-Diene analogues, namely showing a large background exciplex fluorescence (λ_{max} 479 nm) in the absence of any other component. This was not affected by addition of target. Heating (to 60 °C over 30 minutes) caused this exciplex signal to disappear (see Figure 3.76), and it did not reappear on cooling. An isoemissive point was present for the series of spectra shown in Figure 3.76 indicating the presence of two discrete states (bound and unbound). The T_m of Proexc 10_5'pyrene in 80% TFE/ Tris buffer was 37 °C (from a plot of relative fluorescence intensity at 480 nm

against temperature, Figure 3.77), and 45 °C in Tris buffer (from the A_{260}: temperature profile). On addition of Proexc3_3'naphthalene at 10 °C the LES band was quenched, and a new exciplex band appeared, slightly red-shifted to λ_{max} 482 nm, showing that the exciplex formed in the full system has different origins or environment from that formed by Proexc10_5'pyrene alone. The intensity of this band decreased on heating, accompanied by an increase in intensity of the LES band, shown in Figure 3.78. However, the exciplex did not fully disappear even on heating to 70 °C. On re-cooling its intensity increased to its previous magnitude.

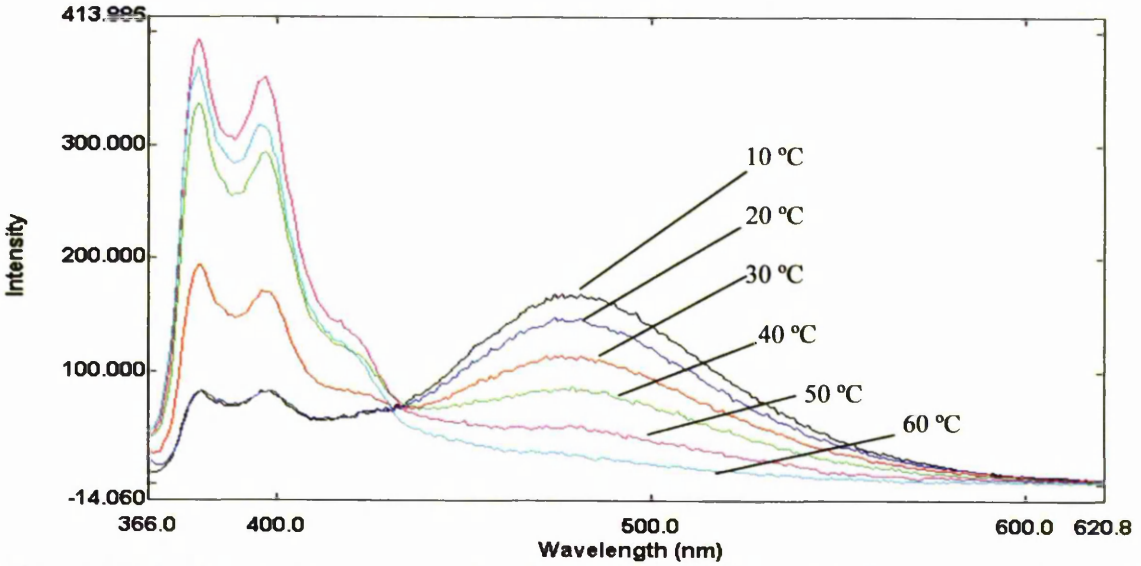

Figure 3.76: Fluorescence spectra showing melting of Proexc10_5'pyrene + with target (ProExc1) in 80%TFE / Tris buffer (10 mM Tris, 0.1 M NaCl, pH 8.5). The system was heated to 60 °C over 30 minutes with spectra recorded every 10 °C. Excitation wavelength 350 nm; slitwidth 5 nm. Spectra are buffer-corrected and unscaled.

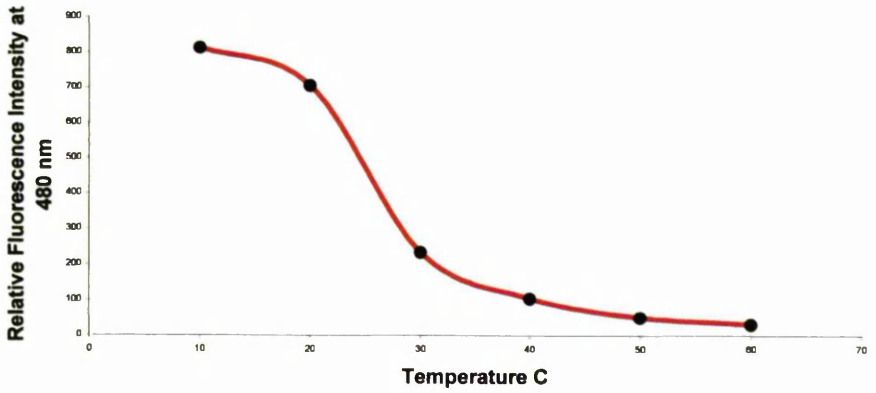

Figure 3.77: Melting curve of Proexc10_5'pyrene in 80% TFE/ Tris buffer (10 mM Tris, 0.1 M NaCl, pH 8.5) plotted using relative fluorescence intensity at 480 nm against temperature. Excitation wavelength 350 nm; slitwidth 5 nm, spectra scaled to LES emission at 380 nm.

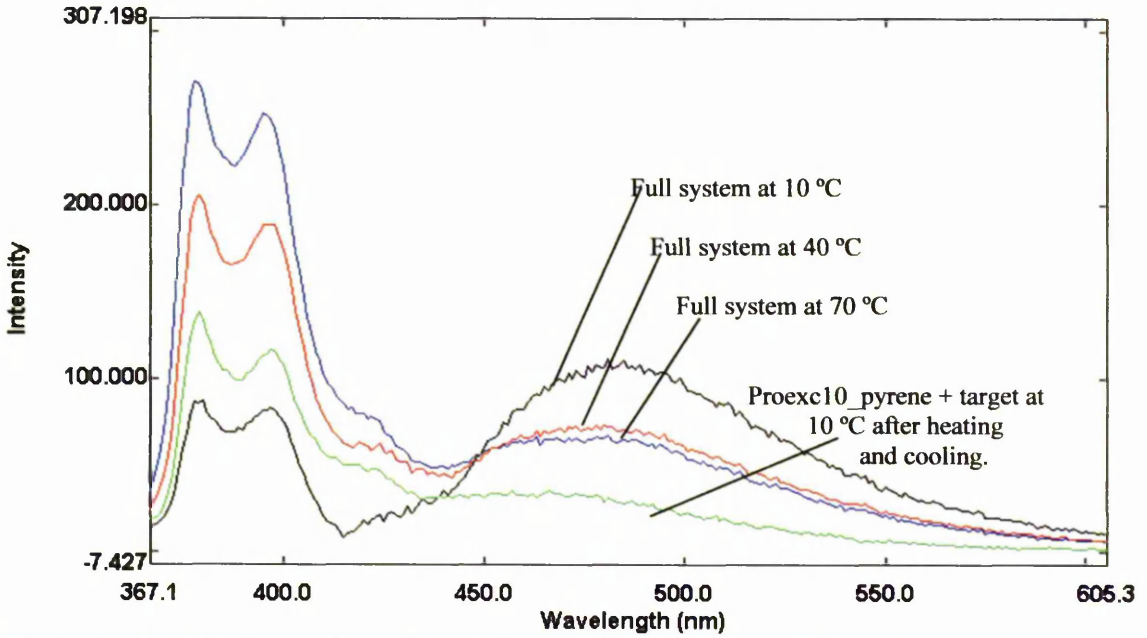

Figure 3.78: Fluorescence emission spectra showing re-annealing of the SP-15 system (Proexc10_5'pyrene + Proexc3_3'naphthalene with target (ProExc1)) in 80%TFE/ Tris buffer (10 mM Tris, 0.1 M NaCl, pH 8.5). The system was cooled from 70 °C to 10 °C over 30 minutes. Excitation wavelength 350 nm, slitwidth 5 nm. Spectra are buffer-corrected and scaled to LES emission at 380 nm.

4. Discussion.

4 Discussion.

4.1 Phenomenon of excimer/ exciplex fluorescence from the split-probe systems.

Most of the split-oligo systems tested in this thesis displayed excimer or exciplex emission under the correct conditions. This excimer/ exciplex emission was, in most cases, only seen after addition of all the components of the split-oligo system (both labelled probe oligos and the target oligo), and could therefore be used as the detectable signal in hybridisation analysis. For these systems, excimer and exciplex emission appeared as a broad emission band, which was greatly red-shifted from the monomer (LES) emission and was centred around 480 nm. However, the λ_{max} was solvent dependent for the exciplexes. In addition to the appearance of the 480 nm band the monomer band was quenched. Other conceptually similar split-oligo systems have been described in the literature (see those of Paris *et al.* [95] and Ebata *et al.* [92-94] in Section 1.12.3.3), which use an excimer emission as the detectable signal. The results presented in this thesis, however, detail the first case of an oligonucleotide split-probe system that is based on exciplex fluorescence emission.

These exciplex systems have a number of differences from excimer constructs. As discussed in Section 1.13 the possible range of structures for the two exci-partners is very broad but more restricted for excimers, being more or less limited to pyrene and perylene for excimer systems. Also there is a linear relationship between the exciplex emission frequency and the difference in redox potential of the two exci-partners [97], so that the emitted fluorescence is tuneable for exciplex systems. Therefore there is the potential to use several different split-probe systems simultaneously in a single genetic sample to detect the presence of different sequences.

This discussion, sets out initially to prove that the split-probe systems postulated are indeed able to form the tandem duplex required to bring the exci-partners together. Secondly, once this has been established, evidence that the changes in the emission spectra seen arise from excimer or exciplex formation between the two exci-partners will be examined. Finally, the different properties of the excimer and exciplex systems studied will be discussed and compared. These include the effects of the co-solvent, RNA target, linker between the oligo and the exci-partner, PCR additives, LNA-based probes and mismatches in the target strand. Finally the discoveries reported will be put into context in terms of their potential as the basis of novel fluorescence detector systems

4.2 Evidence that tandem duplex formation occurs.

In order for the split-probe exciplex systems to emit successfully, tandem duplex formation is required. Evidence from this study and from similar literature studies discussed below support the occurrence of duplex formation.

4.2.1 Literature evidence of tandem duplex formation.

Several nicked duplex structures have been studied in the literature [102-105]. These duplexes consist of an intact DNA strand (12-14-mer) and two shorter strands, which are complementary to the longer strand and hybridise to it in a contiguous manner. These oligos form duplex structures in which one strand essentially has a break or nick in the backbone. NMR [102;105] and X-ray crystal studies [104] of these structures showed that the duplexes formed are typically B-type with only slight deformations of the duplex in the region flanking the nicked site as compared to the parent un-nicked structures. The nicked duplexes were found to have similar flexibility as un-nicked duplexes and the base pairs on either side of the nick were well stacked. In fact, extra stability is associated with hybridisation reactions when two or more oligos hybridise contiguously to a target. This is due to base-stacking interaction at the nick. The free energy afforded by this hybridisation at contiguous sites was found to be between –1.4 and –2.4 Kcal/mol [65]. These studies show that nicked duplex structures of short oligos, similar in length to those used in this study, can form stable tandem duplexes. However, the split-probe systems used in this study have hydrophobic exci-partners attached to the phosphate groups of the probe oligos at the nick site. Nonetheless, evidence from this study suggests that it is possible that a duplex can form accommodating these two partners.

Successful split-probe systems consisting of two probe oligos, which bind contiguously to a target, and possess modifying groups at the nicked site have been described. One such system is the split-probe system of Dobrikov *et al* [71;72;74] for the specific photomodification of oligos. This system contains a photoreactive azide group attached to the 3'-phosphate of one probe oligo and a photosensitising group (anthracene, pyrene or perylene) attached to the 5'-phosphate of the other. The system causes photomodification of oligos to occur 300-3000 times faster than direct photomodification in the absence of the sensitiser group. This suggested that the oligos bound in the correct contiguous positions, bringing the photoreactive and the photosensitising groups together so that efficient resonance energy transfer could take place. NMR and molecular modelling

studies on these split-probe systems [100] showed that a tight specific duplex did form at temperatures less than 10 °C. The structure was a classical B-like duplex, but showed strong perturbations throughout, especially at the nick site. These perturbations were thought to be due to the nick and the modifying groups. The mobility of the 5'-sensitiser group, pyrene, was found to be restricted with pyrene lying mainly in the minor groove. The photoreactive azide group on the other hand showed a high degree of flexibility. The average distance between the two groups as determined by NMR data was 8 Å. From FRET and photomodification studies this distance was found to be 11.2 and 12.6 Å, respectively. This study showed that modifying groups similar to those used in this study can be accommodated at the nicked site of a tandem duplex structure.

The excimer split-probe systems described by Paris *et al.* and Ebata *et al.* [92-95] also provide evidence that such split-probe tandem duplexes are able to form. In the study by Ebata *et al.* the pyrene moieties were attached to the 5'- and 3'- termini of the probe oligos by linkers of similar length to those used in this thesis. Ebata *et al.* not only showed excimer emission on formation of the full split-probe system, and its disappearance on heating, but that the split-probe systems displayed typical melting curve profiles on heating. This suggested that the split-probe system was able to form a stable tandem duplex bringing the exci-partners into close proximity.

4.2.2 Evidence of tandem duplex formation from melting experiments.

Melting experiments performed on the tandem duplex systems of this thesis gave direct evidence of duplex formation. The split-probe systems all showed sigmoidal melting curves when absorption at 260 nm was plotted against temperature. Such melting curves are typical of the transition from double-stranded DNA to single-stranded DNA. DNA bases absorb strongly at 260 nm, but the absorption of double-stranded DNA is less than that of single-stranded. This is due to interactions between the electron systems of adjacent bases, which are stacked parallel in the double helix structure. The transition in absorption seen when double-stranded DNA is heated is termed hypochromicity and is due to a change from double-stranded to single-stranded DNA. The mid-point of the transition is taken to be the melting temperature, T_m. The melting curves seen for the split-probe tandem duplex showed only one transition state. This is consistent with literature findings that duplex structures containing a backbone nick in one strand, melt cooperatively, showing only one transition phase [100;105]. Melting starts simultaneously from both ends of the duplex and from the centre at the nick site and proceeds towards the centres of the two

half duplexes. This process has been monitored directly using the high resolution of NMR to record the melting fate of each base pair H-bond during the process [100;101]. The T_m obtained for the excimer (SP-1) and the exciplex (SP-2) systems were similar to those estimated by the OligoAnalyzer 3.0 program, showing that there is no stabilisation of the tandem duplex due to exci-partner intercalation into the duplex.

4.2.3 Evidence of tandem duplex formation from emission spectra.

Furthermore when excimer/ exciplex signals were seen for the split-probe systems they were generally only seen in the presence of all the components and at temperatures less than T_m. On heating excimer/ exciplex emission was seen to decrease and disappear, on cooling it was restored. This implies that excimer/ exciplex formation requires full duplex formation to bring the exci-partners into close proximity, and is further evidence that the split-probe components form a tandem duplex structure.

In all cases of tandem duplex formation using the standard method described in Section 2.5.5, addition of the second probe component to the first resulted in no appreciable change in the emission spectrum. For the exciplex systems subtraction of the naphthalene component resulted in a spectrum typical of pyrene monomer emission. This was of similar intensity and the same λ_{max} as that for the pyrene probe oligo alone. In the case of the excimer systems, where the second partner was pyrene, an increase in pyrene monomer emission was seen but this was accounted for by the presence of a second pyrene partner. No change in λ_{max} was observed. No exciplex or excimer signal was seen in the absence of the target. This evidence suggests that the two probe oligos did not interact with each other in the absence of the target strand.

Addition of the target strand to the two probe oligo components caused a slight red shift (3-5 nm) of the pyrene LES emission band, accompanied by its quenching and, under the right conditions, the emergence of a new structureless band at around 480 nm, as shown in Figure 4.1. This band was typical of a pyrene excimer [97;116]. A similar red shift in the excitation spectrum was also observed (see Figure 4.2). These spectral changes seen suggested that tandem duplex formation occurred. Indeed the fluorescence spectrum of pyrene is known to be sensitive to its microenvironment. It is well known that interaction with the bases of nucleic acids cause a red shift in the absorbance spectrum and a strong quenching of fluorescence [117-120]. The most potent quenchers of pyrene fluorescence are dC, dT and dG, with reactivity falling from dC to dG. Only very weak quenching is observed by dA nucleotides. This order of reactivity suggests that quenching occurs *via*

photoinduced electron transfer between pyrene and the nucleic acids. The ionisation potentials of polyaromatic hydrocarbons such as pyrene are usually smaller than those of the four nucleotides [119]. Thus pyrene probably acts as an electron donor and the nucleic acid base as an electron acceptor. On duplex formation the fluorescence of pyrene is perhaps more strongly quenched due to additional across-strand quenching in addition to same-strand quenching.

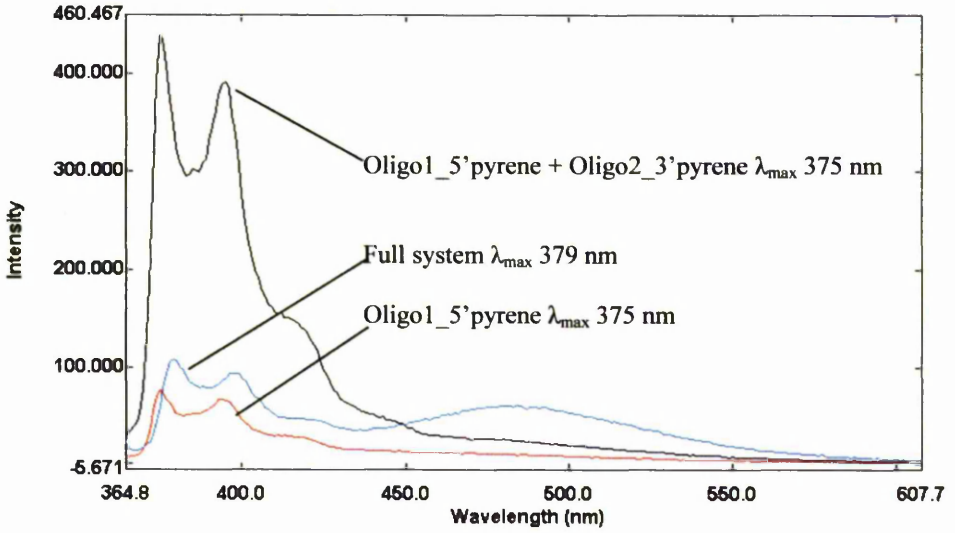

Figure 4.1: Emission spectra of SP-1 at various stages of development in 80% TFE/ Tris buffer at 10 °C showing the red shift from 375 nm to 379 nm, quenching of the LES band and emergence of an excimer band at 480 nm on full system formation.

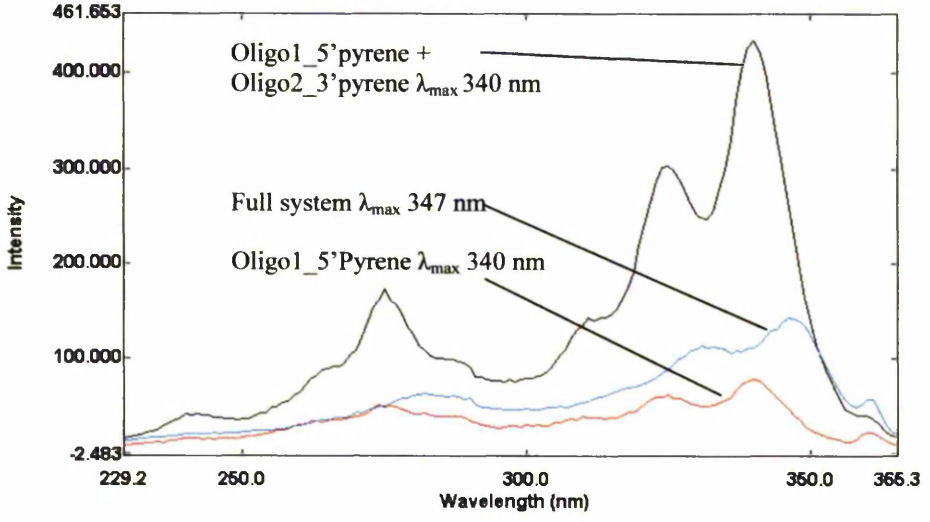

Figure 4.2: Excitation spectra of the SP1 system at various stages of development in 80% TFE/ Tris buffer at 10 °C showing the red shift from 340 nm to 347 nm on full system formation.

A similar quenching of pyrene LES emission and emergence of excimer emission was seen on formation of the tandem split-probe excimer systems of Paris *et al.* [95] and Ebata *et*

al. [92-94]. Both authors reported quenching of the LES emission band and the emergence of a pyrene excimer band on addition of the target strand to the probe components.

Further evidence of tandem duplex formation came from experiments involving a heating and cooling cycle. Heating of the systems to above 40 °C caused the LES band intensity to increase and a shift back to the emission wavelength seen in the absence of the target strand. The excimer/ exciplex band, if present, decreased and eventually disappeared. This spectral evidence suggested that the tandem duplex was intact at 10 °C, but that on heating the probe oligos dissociate from the target sequence, resulting in the spectra initially observed for the separate uninteracting probe oligos. The melting temperatures of these duplexes was estimated to be 27.8 °C for Oligo1 with target and 22.6 °C for Oligo2 with target, using OligoAnalyzer 3.0 program[121]. Hence, heating the duplex system to 40 °C or so would dissociate any duplex formed.

Re-cooling the system to 10 °C provided further evidence of tandem duplex formation. On cooling, the pyrene monomer emission was again red-shifted by several nanometers, back to the value of λ_{max} seen on initial target addition to the probe components. This was accompanied by quenching of this band and under suitable conditions, the reappearance of the excimer/ exciplex band. These spectral changes indicated that cooling the system causes re-annealing of the probe oligos to the target, thereby reforming tandem duplex. This brings the exci-partners into close proximity, enabling excimer/ exciplex formation. In fact, in many cases excimer/ exciplex emission seen after re-cooling was actually more intense than that seen before heating (see Figure 3.2). This could be due to more perfect duplex formation as a result of the slow cooling of the system. As the initial duplex was formed at 10 °C, much lower than the estimated T_m, it may have been possible for imperfect duplex structures to form. A more perfect duplex structure presumably enables the exci-partners to be better positioned for excimer/ exciplex formation. Also the heating cycle may disrupt hydrophobic interaction of pyrene with the nucleobases or grooves freeing it for excimer/ exciplex formation. The reversion of the spectra on cooling back to that seen initially when the full system was formed also indicates that no destruction of the components occurs on heating the system.

4.3 Evidence that excimer/ exciplex is formed due to interaction of intended partners.

4.3.1 Possible origins of the emission band at ~480 nm.

Although no high-resolution structural studies have yet been performed on the split-probe systems of the present thesis, the evidence discussed above strongly suggests

that some form of tandem duplex is able to assemble accommodating the exci-partners. Spectral changes seen on formation of the full system included, under the appropriate conditions, the emergence of a red-shifted structureless band characteristic of excimer or exciplex emission. The origin of this emission, however, must be elucidated. Excimer and exciplex emission is, of course, possible due to interaction of the exci-partners on duplex formation if they are correctly positioned within 4 Å of one another. However, it has been shown that pyrene is able to form an exciplex with certain nucleotide bases, especially guanine and to a lesser extent thymidine [118;119]. For pyrene attached to a uridine residue having two guanine or thymidine residues each side, flanking the uridine residue, exciplex emission was seen as a broad band centred around 495 nm. No such emission was seen in the case of adenine or cytosine flanking residues. However, this broad emission band was only seen for the single-stranded sequences studied and not from their respective duplexes.

Evidence discussed below suggests that exci-partner interaction accounts for excimer/ exciplex emission seen in most cases in the studies of this thesis. Nevertheless background exciplex signals were observed in certain cases, prior to manipulation of conditions to remove them, and these will also be discussed below.

4.3.2 Evidence from this study suggesting exci-partner interaction is responsible for the emission band at ~480 nm.

Generally, only emission typical of pyrene LES was seen in the absence of the target strand, suggesting that little or no background exciplex emission due to pyrene interacting with the probe oligo was present. On addition of the second probe oligo, and subtraction of the naphthalene signal if necessary, still no exciplex was seen. This absence of exciplex/ excimer emission also dismisses the possibility that the exci-partners form an exciplex with buffer components, namely the co-solvents used or an intermolecular exciplex with each other (unlikely at the low concentrations used). Excimer/ exciplex emission was only detected on addition of the target at 10 °C, and was accompanied by the red shift and quenching of LES emission. Heating the system caused the excimer/ exciplex emission intensity to decrease. This is due to dissociation of the duplex structure. On re-cooling the system excimer/ exciplex emission reappeared. Therefore, some form of duplex structure is required for excimer/ exciplex emission to be observed. But does this emission arise from excimer/ exciplex formation between the desired exci-partners, or is it due to exciplex formation between the exci-partners and the nucleobases?

Control experiments performed with a pyrene-labelled probe and one unlabelled probe bearing only a phosphate group at its "nick terminus", showed no exciplex emission on addition of the target strand. This indicates that the second exci-partner is required for excimer/ exciplex emission. Also observations by Manoharan *et al.* [119], where exciplex emission was seen between pyrene and guanine or thymidine nucleotides, showed that exciplex emission was not detected on duplex formation. This supports the view that the emission detected arises from interaction between the exci-partners, and thus the interpretation that the excimer/ exciplex signals detected in the assembled split-probe systems of this thesis arise from correct hybridisation of the probe oligos on the target strand and interaction of the exci-partners.

4.3.3 Evidence from other studies suggesting that the emission band at ~480 nm is due to exci-partner interaction.

There are many other studies in which pyrene has been attached in various ways to oligonucleotides, but showed no exciplex formation between pyrene and the nucleobases, even on duplex formation. Indeed the similar excimer split-probe systems of Paris *et al.* and Ebata *et al.* showed no exciplex emission band in the absence of the target. Other studies whereby pyrene was attached at an internal position to cytosine or thymidine residues of an oligonucleotide [35 31] showed that pyrene monomer emission was quenched on duplex formation, but no new emission band was seen to appear. A change in intensity of the monomer band of pyrene was also seen on duplex formation when pyrene was attached to the 2' sugar position of DNA and RNA strands, but again no exciplex band was seen. Attachment of pyrene to the 5'-terminal position of short oligos in a similar manner to this study, also resulted in no exciplex emission, with only a red shift and quenching of the monomer band on hybridisation to complementary sequences [39;122]. Such studies, in addition to the results of this thesis, support the interpretation that excimer/ exciplex emission seen from the full split-probe system is due to interaction of the exci-partners, and not to background emission from interaction with the nucleobases. In certain cases, however, a small background exciplex emission was seen for 5'-pyrene-labelled oligonucleotide, and this is now discussed.

4.3.4 Background exciplex signals from 5'-pyrenylated oligos.

This was only seen for systems SP-2 and SP-4 in 80% TFE/ Tris buffer and for SP-8 in Tris buffer. When present, this background was very weak, much weaker than that

seen on full system formation. It was removed before addition of the other components by heating to 40 °C and cooling back to 10 °C. No such background was seen for the 3'-labelled oligos. As background was seen in the absence of the other components this indicates that this emission does not arise from interaction of the exci-partners. Rather, the exci-partner pyrene formed an exciplex with the nucleic acid bases of the probe oligo. The fact that the 3'-linkage did not result in any background exciplex signal suggests that this phenomenon is either sequence-specific, or due to the different position of attachment of the exci-partner. The sequences of the probe oligos are shown in Figure 4.3 with the nucleotide to which the exci-partners are attached marked.

Figure 4.3: Sequences of probe oligos; the nucleotide to which the exci-partners are attached to is marked with an asterisk.

When attached to the 5'-terminal phosphate group the exci-partner is covalently attached to a thymidine nucleotide, adjacent to a guanosine residue. As discussed above, when benzopyrene is attached to a uridine nucleotide flanked by guanosine exciplex emission can be observed due to charge transfer between pyrene and the guanosine base. Therefore, in the systems of this thesis it is possible that the pyrene group attached *via* the 5'-phosphate group can interact with the adjacent guanosine base and under certain conditions form an exciplex. In future probe design this aspect should be borne in mind.

The exci-partner attached to the 3'-terminal phosphate group is attached directly to a guanosine nucleotide. This is adjacent to a thymidine, which has also been shown to give weak exciplex emission when pyrene is attached to flanking nucleotides. However, no background exciplex signal has ever been detected for this oligo. This suggests that the linkage at the 3'-phosphate may prevent back interaction of pyrene with the nucleobases. Indeed, NMR studies on the split-probe system of Dobrikov *et al.*, [100;101] where pyrene was attached *via* the 5'-phosphate of one oligo and an azide group was attached to the 3'-phosphate group of another oligo, showed that the flexibility of pyrene in the tandem duplex was restricted. This moiety lay mainly in the minor groove, and in this position it may be able to interact with the nucleobases. The azide group, on the other hand, was generally found to be more flexible, being free of the nucleobases, thereby avoiding interaction. However, these studies were performed on a duplex structure and in single-

stranded nucleotides the exci-partner moieties cannot adopt a completely similar orientation, as there are no grooves. However, direct interaction of pyrene with strand (base) components is possible.

The SP-4 system also showed weak background exciplex emission for the 5'-probe oligo. In this case the exci-partner was attached to the oligo *via* a long peptide linkage of four amino acids. The background exciplex emission detected was of a similar intensity to that seen for the SP-2 and SP-8 systems (Figure 4.4) and behaved in a similar manner, disappearing on heating and not reappearing on cooling. Therefore, it is probable that this exciplex had a similar origin and arose due to the increased flexibility of the linker. This would allow pyrene to interact with the nucleobases, particularly the (flanking) guanosine residue. On heating the Oligo1_5'pyrene component in each case (SP-2, SP-4 and SP-8) the small background was removed, possibly due to disruption of the interaction between the pyrene and the oligo. On cooling this interaction may not re-form (allowing the pyrene moiety to be free in the solution) as there will be direct competition from other structural interactions, presumably thermodynamically more favourable.

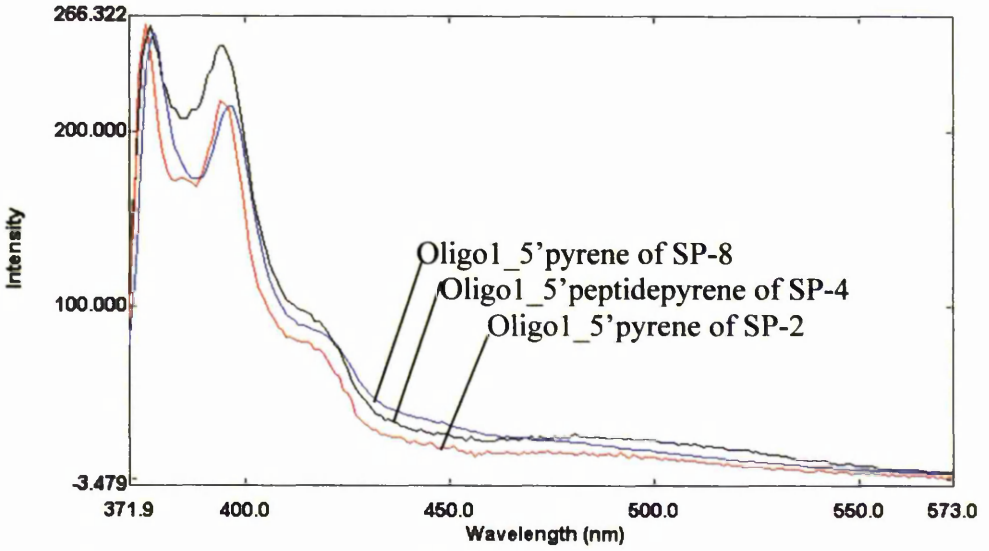

Figure 4.4: Emission spectra of the Oligo1_5'pyrene component of the SP-2 and SP-8 systems and the Oligo1_5'peptide-pyrene of the SP-4 system showing the weak background exciplex signal, which can be removed by heating and cooling. Spectra were recorded in 80% TFE/ Tris buffer at 10 °C.

The probe oligos and the target were specifically chosen so that they were not self-complementary to minimise secondary structure formation. Structural analysis using OligoAnalyzer 3.0 [121] also predicted no likely secondary structures. Thus, it is unlikely that the probe oligos and the target strand used for the split-probe systems (SP1 to SP-12)

formed any secondary structure, this could account for exciplex emission due to increased interaction of the exci-partners with the bases. It is also unlikely that duplex formation would occur between two Oligo1_5'pyrene probes, especially in a way that would bring the two exci-partners close enough to enable pyrene excimer or pyrene-naphthalene exciplex formation.

Larger background signals were seen for the *bis*-substituted systems and for the prothrombin systems. Although the origin of these signals may be similar to the systems described above these are discussed separately below in view of their magnitude.

4.3.5 Background emission from the Prothrombin systems.

A large background exciplex was seen in 80% TFE for pyrene attached to the 5'-phosphate position of Proexc9, Proexc10 and Proexc11 for all the prothrombin systems tested (SP-13, SP-14 and SP-15). This background was very intense, e.g. having a maximum I_E/I_M value 2.06 for the Proexc10 component (Figure 4.5).

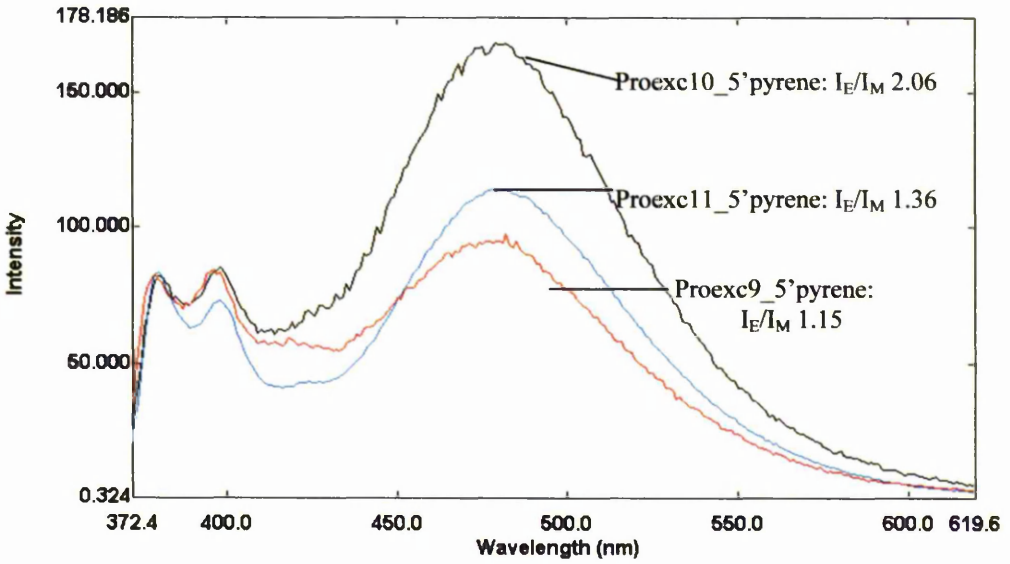

Figure 4.5: Emission spectra of the Proexc10_5'pyrene, Proexc11_5'pyrene and Proexc9_5'pyrene components before heating showing the large background exciplex signal. Spectra were recorded in 80% TFE/ Tris buffer (10mM Tris, 0.1M NaCl, pH 8.5) at 10 °C.

Tris buffer at pH 8.5 gave no background exciplex signal. Addition of the target caused no change in the initial spectrum. Nor was any change in the spectrum seen for the 5'pyrene oligos on addition of target in 80% TFE/ Tris. These results suggest that no interaction takes place between the target and probe oligos. This supports other evidence that suggested the probe oligos and the target participate in intramolecular secondary

structure formation. The NMR spectra of the unmodified probe oligos, Proexc10, Proexc 11, Proexc 3 and Proexc 4, showed line broadening at 25 °C, which was removed when spectra were recorded at 50 °C presumably due to increased exchange between conformations (see Figure 3.59). The presence of secondary structure was confirmed by running melting curve experiments. All probe oligos showed hypochromicity of the 260 nm absorbance band on heating, typical of the transition from double-stranded to single-stranded DNA. Detailed sequence analysis for each of the oligos provided showed the possibility of formation of intermolecular duplex structures or intramolecular hairpin structures, some of which are shown in Figure 4.6.

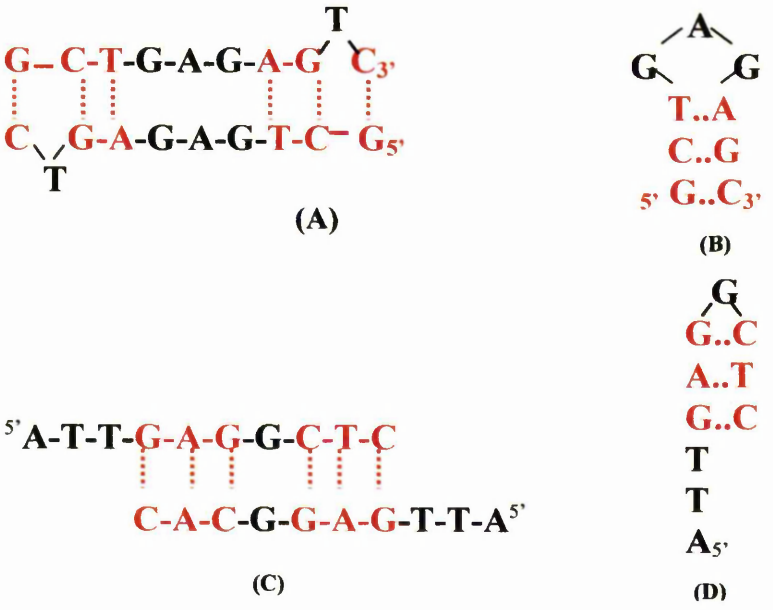

Figure 4.6: Some possible secondary structures formed by unmodified Proexc 10 and 11 (A and B), and Proexc 3 and 4 (C and D).

The stability of these secondary structures must be fairly high as addition of the target, which itself will have secondary structure, did not cause preferential hybridisation between the probe and the target, which would have been indicated by changes in the emission spectrum as described above in Section 4.2.3.

In 80% TFE/ Tris this secondary structure may be responsible for the intense background exciplex emission. This could arise from interaction of the exci-partners with

guanine bases, as described above. This interaction could be greatly increased by the presence of secondary structure, which may allow closer mutual approach of pyrene and guanine residues. Alternatively, two 5'-pyrenylated probe components may form a duplex structure in such a way that the two pyrene exci-partners are brought close together and are able to form a pyrene excimer. Background excimer/ exciplex signals were not seen in Tris buffer alone. If this background was due to exciplex formation between pyrene and the nucleobases exciplex emission may not occur in aqueous Tris buffer due to the exciplex being very sensitive to solvent polarity. Intermolecular exciplexes are not usually seen to emit in solvents as polar as acetonitrile (ε 35.9). However, several intramolecular exciplexes have been seen to emit in solvents as polar as acetonitrile [46;47] and in some cases in solvents more polar than acetonitrile (see Section 1.8.2) [48]. However, in Tris buffer the hydrophobic exci-partners may preferentially interact with the hydrophobic nucleic acids to avoid the hydrophilic environment. Thus they will be unavailable for excimer formation with the other pyrene moiety. Exciplexes have been reported in aqueous media from components in the clearly special environment of a nucleic acid [118].

For the LNA control system, C-6 (Proexc11_5'pyrene + Proexc4_3'phosphate + Proexc1) a background exciplex signal was not only still present after heating and cooling the system in 20% TFE/ Tris buffer, but actually was much higher than the initial background. These data show that background signals are an inherent problem for the prothrombin system. It is an inherent property of the particular sequence chosen by our collaborators for this test system. More careful probe design is required. Further discussion on the prothrombin systems is given in Section 4.7

4.3.6 Background emission from the alternative systems.

The 5'-*bis*-labelled probe components of the alternative systems all showed very large background emission in the 480 nm region in 80% TFE. The 5'-*bis*-pyrenylated probe oligo used for the SP-12 system showed a very large background signal at 480 nm in 80% TFE in the absence of any other component. This large emission band could originate from excimer formation between two pyrene moieties bound to the same phosphate group, or from exciplex formation between pyrene and the nucleobases, especially guanine, as described above. On addition of the target to this component the I_E/I_M ratio decreased. Further addition of the second probe component caused the emission at 480 nm to increase to almost the intensity seen for Oligo1_5'*bis*-pyrene alone. This increase could be due to interaction between the exci-partners, pyrene and DMA, but the control system behaved in

a similar way. A smaller increase in the 480 nm emission band was seen for the control system on addition of unlabelled Oligo2. Therefore it is likely that this emission band arises from background sources.

Similar *bis*-pyrenylated oligonucleotide probes to this study have been reported also using 1-pyrenemethylamine and the same mode of attachment *via* a phosphoramidate link to the 5'-terminal phosphate group [60]. The authors observed emission bands at 382 nm and 476 nm for the labelled probe oligos in the absence of any other component. The band at 382 nm was characteristic of pyrene monomer (LES) emission. Control mono-pyrenylated sequences showed no band at 476 nm, consequently this band was assigned to pyrene excimer formation between the two pyrene moieties, and not due to interaction of pyrene with the bases. The excimer: monomer ratio varied depending on the probe oligonucleotide sequence used. It was concluded that this was not a nearest neighbour effect, but rather a complex effect of oligonucleotide structures and sequences. Hybridisation of this probe to mRNA targets resulted in changes in the relative excimer and monomer emission intensities similar to the changes seen on duplex formation for the SP-12 system. Therefore, the large background signal seen for the *bis*-pyrenylated oligo is possibly also due to excimer formation between the two pyrene groups.

Other studies by Lewis *et al.* [59] and Balakin *et al.* [58] involved a 5'-terminal phosphate labelled with *bis*-pyrene groups, different to those used in this thesis. These labelled oligos also showed two emission bands, one around 380 nm and the other a broad band between 440 and 460 nm. Again both authors assigned the band at 380 nm to pyrene monomer emission and the broad band to pyrene excimer formation between the two closely linked pyrene groups. In both studies the excimer emission was seen to increase on duplex formation, which possibly prevented any interaction between pyrene and the nucleobases, leading to more efficient excimer formation between the pyrene groups. All these studies support the view that the broad 480 nm emission band detected for the SP-12 system arises from excimer formation between the two pyrene groups on the probe.

For the SP-9 and SP-11 systems the Oligo1_5'cyclohexylpyrene component showed a relatively large background emission at around 480 nm in the absence of any other probe component. This background was more intense than any band in this region after full system formation. It is unlikely that this band originates from exciplex formation between pyrene and the non-aromatic tBu-cyclohexane group. Indeed, a dilute solution of pyrene in cyclohexane shows no band in the 480 nm region [97;116] indicating no exciplex formation between pyrene and cyclohexane. It is more likely that the band arises due to

exciplex formation between pyrene and the nucleobases. This may occur due to preferential interaction of pyrene with the DNA strand due to its greater hydrophobicity (and/ or shape) over cyclohexane. The greater interaction of pyrene with the nucleobases in the *bis*-substituted oligos, over the mono-substituted oligos, resulting in exciplex formation may be due to steric hindrance forcing pyrene to interact with the DNA strand.

As all of the alternative systems tested showed the presence of background signals, *bis*-labelling is very unsuitable for use in a split-probe detection systems. One of the advantages of the split-probe system developed in this thesis is the very low background seen in the absence of the target. Therefore, for this purpose the singly labelled probe oligos are preferable. Properties of these, and the effects of various conditions on excimer/ exciplex emission, are now described.

4.3 Properties of the excimer and exciplex split-probe systems: Co-solvent effects.

4.3.1 Solvent effects on the excimer system, SP-1.

The excimer split-probe system, SP-1, was seen to behave in a similar manner in most of the solvents tested (Section 3.6.1), showing a small red shift and quenching of the monomer (LES) emission on full system formation. Excimer emission occurred in the presence all the solvents tested, except N-methylformamide and 2-chloropropanol. It is possible that in the case of N-methylformamide the duplex is disrupted, as this solvent is a denaturant [123]. This would affect the relative positioning of the exci-partners. The presence of TFE resulted in the most intense excimer bands, with I_E/I_M values increasing with increasing TFE concentration. Intense excimer bands were also observed in the presence of hexafluoropropanol and tetrafluoropropanol, which at 50% v/v induced the same level of excimer emission as 80% TFE (Figure 3.44). Weaker excimer emission was seen in the presence of ethylene glycol and ethylene glycol dimethylether. However, these bands took longer to develop, perhaps due to the high viscosity of these solvents as excimer formation is initiated by the collision of an excited molecule with an unexcited one and is therefore diffusion controlled in solution [116].

The λ_{max} value of the excimer band shifted in the presence of different solvents and solvent concentrations (Table 4.1). Similar shifts in λ_{max} of the excimer band was also observed for 1,3-*bis*(pyrenyl)propane in the presence of different solvents and solvent concentrations in Tris buffer (see Table 3.6 a, b, c, d). Therefore, is likely that this shift arises from solvent effects and not various interactions of the pyrene groups and the tandem duplex.

Table 4.1: Values of λ_{max} of the SP-1 split-probe system in different solvent systems.

Solvent system	*λ_{max} of excimer band (nm)*
80% TFE	480
50% Tetrafluoropropanol	488
70% tetrafluoropropanol	
50% hexafluoropropanol	485
Ethylene glycol	482

This effect, the solvatochromatic effect [124-126], is due to the difference in polarisability of a molecule between the ground state and the excited state. This leads to differences in the solvation energies of these states, which causes a shift in the emission spectrum. The shift in the emission spectra between two solvents is a result of three main factors: the solvent Stark effect, dispersion factors and the solute transition dipole moment [124;125]. The Stark effect is due to random motions of a polar solvent's permanent dipole around a polarisable solute, which induces dipole moments in the solute. Dispersion factors arise from the interaction of two non-polar polarisable molecules (solute and solvent), which causes fluctuations in their instantaneous dipoles. The transition dipole moment results from an electron transition: non-polar molecules may have large transition dipoles when an electron is promoted to another orbital [126]. The relative importance and contribution of each of these terms differs with the solvent and thus leads to different shifts in λ_{max}. Generally, increasing red shifts are seen on going to more polar solvents [124;125].

4.3.2 Solvent effects on the exciplex systems, SP-2 and SP-3.

The exciplex split-probes systems were found to be much more sensitive to solvent. Again the characteristic red shift of the LES emission was seen on full system formation, indicating that binding had occurred. However, exciplex emission was only seen in the presence of 70% TFE or 70% ethylene glycol for the SP-2 system and in 70% TFE, 70% ethylene glycol or 70% ethylene glycol dimethylether for the SP-3 system. Exciplexes are known to be sensitive to solvent polarity (discussed in Section 1.8.2) due to the dipolar nature of the exciplex. On increasing solvent polarity the exciplex becomes more dipolar until eventually complete electron transfer occurs to form solvated radical ions. However, the presence of the exciplex band for the split-probe systems does not seem to depend solely on solvent polarity. Exciplex emission was seen for the exciplex systems in ethylene glycol, which has a dielectric constant of 40.25, and for TFE, which has a dielectric constant of 26.73. No exciplex signals were observed, however, for other solvents with

dielectric constants lying in this range. Therefore, it is possible that exciplex emission from the split probe systems did not entirely depend on solvent polarity, but on some other intrinsic property of the solvent or the DNA duplex in that solvent.

For TFE, the solvent that induced the most intense excimer and exciplex signals, this could be related to reports in the literature of to its ability to induce a B to A transition in duplex DNA [127-129]. These effects are now discussed.

4.3.3 Effects of TFE on the double helical structure of DNA.

The degree of duplex hydration is important in determining which structure DNA duplexes adopt. At about 95% relative humidity duplexes adopt a B-like structure. When dried to around 75% relative humidity, the duplexes assume an A-like structure and below 55% relative humidity the helical structure starts to become very disordered. In B-like DNA at high relative humidity the hydration of the minor groove is regular and cooperative, with a geometric spine of water molecules running down it. Hydration of the major groove and the phosphate backbone appears more disordered. It is thought that this spine of hydration in the minor groove is a stabilising factor in B-DNA duplexes [99]. Duplexes containing more than two modified dA:dT base pairs, where the functional groups responsible for the hydration of the minor groove (N (3) of dA and O (2) carbonyl of dT) are absent, adopt A-like helices even at high relative humidity as no hydration spine can form [130]. No spine of hydration is seen in the A-like helix due to the minor groove being so shallow.

In the presence of 70-75% ethanol or trifluoroethanol the CD spectrum of DNA in solution shows a shift from that of the B-like helix to that resembling the A-form [130]. X-ray diffraction studies also show evidence of a B-A transition at high ethanol concentrations, showing that the change in the CD spectrum is caused by a structural transition and not aggregation caused by the ethanol [128]. In these studies the transition point occurred at about 70% v/v ethanol and the A-form persisted up to 85% v/v ethanol. At higher concentrations the structure became more disordered. Studies on DNA using various solvent systems showed that the water activity of a solution (water activity is equal to relative humidity if the non-ideality of water vapour is not taken into consideration) determines in which of the two forms DNA exists [129]. The more polar a solvent component, the lower its ability to bring about the B-A transition.

The transition between the B and the A form of DNA in the presence of alcohol is thought to be due to the hydrophobic alcohol molecules disrupting the ordered spine of

hydration in the minor groove. This is thought to be the first step necessary in the B-A transition. The cooperativity of the transition may occur because the break in the spine propagates in both directions [99]. The greater stacking of the bases, increasing the hydrophobic interactions, would stabilise the B-form in a medium with high water activity. In a medium with low water activity this hydrophobic effect is less important and the A-form is favoured [129].

At the high TFE concentrations used to study the split-probe systems it is therefore possible that the tandem duplex exists in the A-form. The difference in duplex structure between the A and the B forms may affect the interaction of the exci-partners. The A-type duplex structure, wider and more compact than the B-type helix, has a base-pair repeat distance of less than 3 Å (2.3 Å) [99;131], compared to 3.4 Å for the B-type helix [132]. Therefore, the relative positions of the exci-partners may differ if the duplex assumes an A-like geometry, altering their interaction and therefore the efficiency of excimer/ exciplex emission. Indeed, FRET and photomodification studies on the split-oligo system of Dobrikov *et al.* (Section 1.11 and Figure 1.20), showed that the modifying groups, attached at the same 5'- and 3'-phosphate positions as the exci-partners used in this study were in fact between 11.2 and 12.6 Å apart in a B-like DNA duplex. This distance is much greater than the optimum distance for the components of an excimer or exciplex. The distance between the planar pyrene ring systems in an excimer is about 3.5 Å [21]. The sugar pucker or conformation of the 5-membered ribofuranosyl ring is also different in A and B-type DNA conformations. In the A-type conformation the sugar ring assumes a C3'-endo conformation: in B-type duplexes the conformation is C2' endo (Figure 4.7). As the phosphate group to which the exci-partners are bound is attached directly to the sugar rings these different conformations may alter the positions of the attached exci-partners relative to one another.

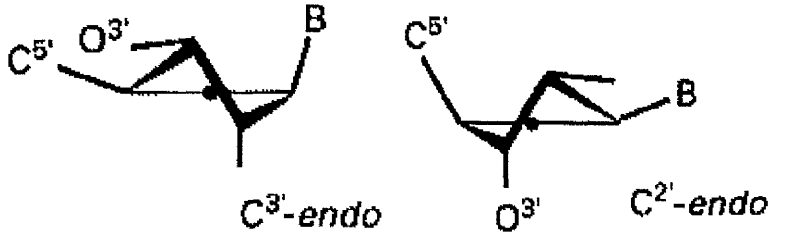

Figure 4.7: Schematic representation of the C3'-endo and the C2'-endo conformations adopted by the sugar rings of nucleotides [17].

This evidence suggests that the role of TFE in enhancing excimer and exciplex signals may be due to structural effects on the duplex. If this is the case, different

behaviour of the systems would be predicted if the target or probe oligos were composed of RNA or LNA, which would effect the duplex structure. The results of the split-probe system using an RNA target and DNA probes are discussed below. In addition, this analysis of the possible solvent effects points the way to additional experiments.

4.4 RNA target effects.

The excimer and exciplex split-probe systems were tested using an RNA target. This was of the same sequence as the DNA target so that the DNA exci-partner probes would bind in the same contiguous manner. Both of the RNA: DNA hybrid systems tested, SP-7 and SP-8, behaved in a similar manner to the corresponding DNA systems, SP-1 and SP-2, showing changes in emission spectra typical of tandem duplex formation. Excimer/ exciplex emission, when detected, also behaved similarly, increasing to its maximum after ten minutes. On heating this emission disappeared and in most cases reappeared on cooling, generally to a greater extent. Such evidence suggests that tandem duplex formation took place between the two DNA probes and the RNA target.

For the excimer system, SP-7, weak excimer emission was detected on full system formation in pure Tris buffer (see Figure 3.24). For the corresponding DNA system no excimer or background signal was ever seen in TFE concentrations less than 20%. Addition of TFE to the SP-7 system to give a concentration of 40% caused the excimer band to greatly increase (I_E/I_M 0.95) to a higher intensity than that seen for the analogous DNA system in 40% TFE (I_E/I_M 0.46), and even for the SP-7 system in 80% TFE (I_E/I_M 0.48).

No exciplex emission was seen below 70% TFE for the exciplex-RNA system SP-8. At 70% TFE the I_E/I_M value was higher than for the analogous DNA system in 80% TFE (SP-8 in 70% TFE: I_E/I_M 0.57, SP-2 in 80% TFE: I_E/I_M 0.48). At 80% TFE the exciplex emission intensities were comparable for both systems.

These results showed that observable excimer and exciplex emission was possible from a RNA: DNA hybrid split-probe system, and also showed that lower TFE concentrations gave more intense signals than for the corresponding DNA systems. Excimer emission was even seen in the absence of a co-solvent for the SP-7 system. These differences in behaviour between the DNA: DNA system and the RNA: DNA hybrid system could be a result of the different duplex structure types adopted on duplex formation. This could affect the distance between the exci-partners and their ability to

interact with one another as discussed above. The structure of DNA: RNA hybrids is discussed below.

4.4.1 DNA: RNA hybrid structure.

As described in Section 4.3.3, DNA homoduplexes adopt a B-like duplex in aqueous solution. However, in the presence of 70-75% ethanol or 70-75 % TFE, the duplexes undergo a structural transition to the A-form. These structural differences could account for the higher I_E/I_M values seen for the DNA excimer (SP-1) and the DNA exciplex (SP-2 and SP-3) systems at high TFE concentrations, with maximum emission always seen at 80% TFE. Under these conditions it would be expected that the DNA duplex would be in the A-type conformation. DNA: RNA hybrid duplexes, on the other hand, have been found to adopt a structure intermediate between the A and the B form in aqueous media [106;133].

The single crystal structures of DNA: RNA helices first studied initially suggested that these duplexes adopted a pure A-like geometry. However, subsequent NMR and circular dichroism studies on DNA: RNA hybrid duplexes in solution showed differences between these and DNA or RNA homoduplexes. These studies suggested that there may be structural differences between the DNA and the RNA strand in these hybrids. However, other early NMR studies suggested there was little conformational difference between DNA: DNA and DNA: RNA duplexes, with both of these displaying B-like helices [134]. Fibre diffraction studies also showed diffraction patterns similar to B-DNA [135]. However, molecular modelling studies showed that a C3' exo or C2' endo sugar pucker, typically seen for B-type duplexes, could not be accommodated for the RNA strand. Therefore, a structure fitting the diffraction pattern, and having a DNA strand in the B-like conformation and the RNA strand in the A-conformation was proposed. A similar structure, having a B-like DNA strand and a A-like RNA strand was proposed by Arnott *et al.* [133]. This structure had base stacking which was B-like, a major groove that was not as deep, and the minor groove not as exposed as in typical A-like structures. Other studies showed that RNA sugars adopted a N-type conformation, and that the DNA sugars had neither an N-nor a S-type conformation, but showed an unusual East-type (E-type) conformation, with pseudorotational angles between 100 and 130° [106]. The conformation of the DNA strand was intermediate between the classical A- and B-like geometries, whereas the RNA strand was clearly A-like. The width of the minor groove in these duplexes was

also intermediate between the A and B values and the base rise was small (around 2.5 Å), similar to that of a typical A-type duplex.

If DNA/ RNA hybrids do indeed form a structure intermediate between the A and B form then the exci-partner-partners could be held closer together resulting in more efficient excimer/ exciplex formation. This difference in aqueous structure between the DNA homoduplexes and DNA: RNA hybrid also may explain why lower TFE concentrations resulted in more intense excimer and exciplex bands for the DNA: RNA system relative to the analogous DNA systems. This could also explain why an excimer band was seen for SP-7 in Tris buffer.

It is possible that at higher TFE concentrations both strands may adopt an A-like geometry. In the RNA: DNA hybrid split-probe system the DNA probe strands may, according to Fedoroff's studies [106], adopt a conformation intermediate between the A and the B type in aqueous Tris buffer and at low TFE concentrations. This would reduce the base-pair repeat distance possibly bringing the exci-partners closer together.

No detailed structural studies have yet been performed on either the DNA or the RNA: DNA systems and these would be required to test these hypotheses. However, the studies performed in this thesis show that both excimer and exciplex split-probe systems can be used to detect RNA targets. This is the first example of a split-probe excimer or exciplex system being used for such a purpose.

4.5 Linker effects.

The effect of two different linker types on excimer/ exciplex formation/ emission was studied for the split-probe detection systems. Systems SP-1, SP-2 and SP-3 had the exci-partners attached to the oligos *via* a short linker and SP-4, SP-5 and SP-6 had them attached *via* a peptide linker of four amino acids. It was possible that hydrogen bonding could occur between the main chain carbonyl oxygen and amide groups of the peptide linkers, similar to that seen in β-sheet structures in proteins. This should bring the exci-partners into close proximity, thereby allowing efficient excimer/ exciplex emission.

4.5.1 Excimer Systems.

For the excimer systems, SP-1 and SP-4, changes in the LES band, characteristic of duplex formation were seen under all the conditions tested. No excimer signals were seen in pure Tris buffer. For SP-4 excimer emission was seen at TFE concentrations above 50%. This emission behaved in the same way as that for the SP-1 system, namely it increased to

a maximum ten minutes after full system formation and disappeared on heating. On cooling back to 10 °C the excimer band recovered to a greater intensity than before. These data, along with results from the control systems C-1 and C-2, showing no unresolved exciplex band for the 5' and 3'-pyrene labelled probe suggest that the band at 480 nm arises from exci-partner interaction. For the SP-4 system lower TFE concentrations resulted in somewhat more intense excimer intensities than for the corresponding short linker systems. However, overall SP-1 still gave a much more intense excimer emission than did SP-4, with maximum emission occurring in 80% TFE/Tris buffer. The I_E/I_M ratios for the SP-1 and the SP-4 systems in various TFE concentrations are shown in Table 4.2 for comparison.

Table 4.2: The I_E/I_M values of the SP-1 and SP-4 excimer systems in Tris buffer (10 mM Tris, 0.1 M NaCl, pH 8.5) at 10 °C containing different TFE concentrations.

Percentage TFE concentration	**I_E/I_M ratio. SP-1 system**	**I_E/I_M ratio. SP-4 system**
40	0.46	Not determined
50	Not determined	0.47
60	0.62	0.77
80	2.24	0.68

Only slightly larger I_E/I_M values were seen at lower TFE concentrations for the SP-4 system. These data suggest that it is unlikely that any rigid structure forms between the peptide linkers as this would be expected to be further stabilised at higher TFE concentrations, as discussed below. This would lead to greater exciplex emission if such a structure brought the exci-partners into close proximity. At 80% TFE excimer intensity for the SP-4 system was much lower than for the SP-1 system, and lower than for the other TFE concentrations.

In addition to affecting DNA duplex structure, TFE is rather better known to induce structure formation in small protein fragments and in peptides that are otherwise unstructured in solution [136]. TFE strengthens helix propensities in solution, the stability of these induced helical structures increases with increasing TFE concentration [137-140]. The exact mechanism by which TFE promotes and stabilises solution structures is unknown, but its effects are likely to be the result of several different mechanisms. TFE may enhance internal hydrogen bonding within the helical structures due to weakening of hydrogen

bonding to water. Indeed, TFE is a better hydrogen bond donor than water, but a poorer hydrogen bond acceptor. TFE, therefore, would preferentially bind to the carbonyl oxygens, leading to enhanced intra-polypeptide hydrogen bonding by the amide groups whose solvent exposure is thus minimised. The size of the TFE molecule, which is nine times that of water, may also contribute to stabilising intra-polypeptide hydrogen bonding. As the dielectric constant of TFE is much lower than that of water electrostatic interactions within the protein may also be stabilised by the presence of TFE. TFE molecules are also known to form clusters in water [141], and these may associate with hydrophobic surfaces, such as helices or sheets, thereby mimicking hydrophobic surfaces [138].

Although TFE preferentially stabilises peptides in α-helix conformations, it also induces β-sheet formation in solution [136;142;143]. However, β-sheet formation in TFE is usually only seen for protein fragments which form a β-sheet structure in the native protein. For example, the B_1 domain of protein G forms a β-sheet structure in the native protein resistant to denaturation and also forms a similar β-structure in TFE [142]. β-Sheet formation has also been reported for peptides that have been designed specifically to form a β-hairpin structure [143]. Thus, the effect of TFE on peptides depends not only on the properties of TFE but also on the secondary-structure propensities of the amino acid sequences.

For the peptide linkers used in the split-probe systems it was postulated that main chain interactions would occur between the two linkers, thereby bringing the exci-partners into close proximity. This should have resulted in an increase in excimer/ exciplex emission relative to the short linker systems. In view of the effects of TFE on peptide solution structure it should follow that the presence of TFE should stabilise any potential structure formed, thus resulting in a enhanced emission. However, emission was only slightly higher at lower TFE concentrations, but it was actually lower than compared to the analogous short-linker system at 80% TFE. It is therefore possible that no defined structure formed between the two peptide linker systems. Indeed, β-sheet formation in proteins and peptides occurs intramolecularly and nucleation of β-sheet building is thought to be the formation of the β-hairpin [144]. However, the peptide linkers in this study are separate molecules, therefore, no β-hairpin could form to initiate β-sheet formation. Another potential problem of the peptide linkers is that they consist of glycine residues, which are the most conformationally unrestrained amino acids and are known to actually break secondary structure [143]. Therefore, it is unlikely that β-sheet-like structure formation occurred between the peptides. However, interaction of the exci-partners did occur, hence

the excimer emission, but the interaction was not stabilised by TFE as excimer emission seen was lower at higher TFE concentration. The exciplex systems are now discussed.

4.5.2 Exciplex systems.

The exciplex-based split-probe systems also show a broad emission band in the 480 nm region. This was less intense than for both the excimer systems. Of the two short-linker exciplex systems, SP-3 gave a higher I_E/I_M value than SP-2 in 80% TFE both before and after heating. For these systems the exci-partners were the same, being pyrene and naphthalene, but these were bound to different oligos. For the SP-2 system pyrene was attached to the 5'-terminus of Oligo1 and naphthalene attached to the 3'-terminus of Oligo2: for the SP-3 system attachment was reversed. Therefore, exciplex emission could be sequence-dependent, depending on which of the nucleotide bases the partners are able to interact with. Different local nucleotides will alter the quenching rate of pyrene monomer (LES) emission by the nucleic acid bases. Highest quenching rates are seen for dT and dG, with dC being less reactive and dA only weakly able to quench pyrene [59;145-148]. Greater quenching rates could mean that pyrene excitation is quenched before it can efficiently form an exciplex with naphthalene.

For the SP-5 peptide-linker system exciplex emission was only seen at 80% TFE. This was of comparable intensity to the corresponding SP-2 short linker exciplex system. However, after the heating and cooling cycle the exciplex signal that reappeared for SP-5 was much less intense than before (I_E/I_M before heating 0.45, I_E/I_M after heating 0.2). Heating may have disrupted any potential interaction between the peptide linkers, and on cooling this structure may not be restored.

For exciplex system SP-6 appreciable exciplex emission was only seen in 80% TFE, although a very weak band was present at 60% TFE. The emission intensity at 80% TFE increased after the heating and cooling cycle, but was still not as intense as the corresponding short-linker system SP-3 (see Figure 3.20).

So, in this study excimer and exciplex emission occurred from split-probe systems where the exci-partners were joined to the probe oligo *via* a short linker or a longer peptide linker. The longer peptide linkers, however, did not improve the intensity of the excimer/ exciplex signal seen on full system formation relative to the corresponding short-linker systems. This could be due to the longer linkers enabling the exci-partners to fold back and interact in some way with the DNA duplex structure, or the linkers themselves. Alternatively, the increase in flexibility of the long peptide linkers in the solvent media

may ablate interaction between the two exci-partners. Excimer/ exciplex formation is initiated by collision of an excited molecule with an unexcited one, and is therefore diffusion controlled [116]. Longer linkers may reduce the probability of these collisions (the number of degree of rotational freedom in the linker does not favour mutual collision of the exci-partners).

4.5.3 Effects of other linkers on pyrene fluorescence.

Studies on the conceptually similar excimer-based split-probe system of Ebata *et al.* [94] also showed that linker length affected the ratio between the monomer and excimer intensities (I_E/I_M). The I_E/I_M values decreased as linker length increased from 1 to 3 spacer atoms between the sugar and the pyrene moieties. However, when pyrene was attached directly to the sugar (linker length 0) the I_E/I_M value was the lowest. In this case, however, pyrene was rigidly held and therefore unable to adopt the correct geometry for excimer formation, or possibly even to contact the other partner. Pyrene was not thought to intercalate into the tandem duplex as the melting temperature of the duplex was not appreciably different in the presence or absence of pyrene, and the CD spectrum suggested that pyrene was not in a chiral environment and therefore did not strongly interact with the duplex. In the split-oligo system of Dobrikov *et al.*, the presence of pyrene raised T_m by 7-5 °C due to hydrophobic interactions with the nearest nucleotide residue [101].

Other studies by Keizek *et al.* [39] and Yamana *et al.* [149] on single probe hybridisations also reported no intercalation of pyrene into the duplex structure. Keirzek *et al.* attached pyrene to the 5'-terminal position at the 5'-sugar position *via* an amide and a 3-atom spacer group. Attachment was not found to affect duplex stability, but molecular dynamics simulations showed pyrene to be docked into the minor groove of the duplex. Yamana *et al.* [149] also observed no appreciable change in T_m of duplex structures when pyrene was attached *via* a methylene spacer group to the 5'-OH or the 3'-OH of the terminal sugars.

In contrast to these studies, Koenig *et al.* [150] suggested from fluorescence and absorption data that pyrenebutyric acid attached to the 3'-terminus of RNA intercalated into the duplex structure on hybridisation to target RNA. Mann *et al.* [122] also suggested that pyrene attached to the 5'-phosphate *via* a four-atom linker either stacked to the exterior of the end base or intercalated into the duplex. A 6 nm red shift in the absorption spectrum of pyrene was observed on duplex formation; this accompanied quenching of pyrene fluorescence. An increase in duplex stability was also observed. Pyrene moieties attached

at internal positions of oligonucleotides, such as the N4 position of cytidine bases *via* long linkers of 8 atoms have also been shown to intercalate into the duplex structure [35].

The results from this thesis and the literature (described in this section and in Section 1.7) suggest that for the split-probe systems there is scope for varying the linkage method of the exci-partners to the oligonucleotide probes. However, care must be taken when designing new systems as long linkers have the potential to allow intercalation of pyrene into the duplex structure or allow groove binding. Both these interactions would decrease interaction between exci-partners and therefore reduce excimer/ exciplex emission intensity.

4.6 Effect of PCR Additives.

4.6.1 The use of additives in PCR.

The polymerase chain reaction (PCR) is a widely used *in vitro* method of amplifying DNA sequences. In order to perform PCR some prior sequence information is required so that primers, sequences that initiate the reaction, can be designed. These primers are short oligonuleotides of 15-30 bp, which bind to the opposite denatured strands of the DNA to be amplified. They are complementary to regions flanking the desired sequence. In the presence of a DNA polymerase and dideoxynucleotides, the primers are extended in a template-dependent manner to form new DNA strands. The new duplexes are then thermally denatured, new primers are allowed to bind, and another cycle of replication takes place. The newly synthesised DNA strands also act as templates for replication so that in this way DNA product increases exponentially. After 30 cycles about 10^5 copies of the target DNA, in addition to the starting material, will be present [14]. In some cases PCR additives such as betaine, methylsulfone, sulfolane and DMSO are added to the reaction mixture. These additives act as denaturants, and destabilise the double helix of DNA by hydrogen bonding to the major and minor grooves. They are used in PCR to increase yield and specificity by decreasing the T_m of DNA and RNA. This decreases secondary structure formation, such as loops and hairpins in self-complementary regions, which can lead to the sudden termination of DNA synthesis [107;108].

The detection of PCR products was originally carried out by heterogeneous assays once amplification had been completed. However, the development of new probes such as Molecular Beacons, Scorpions and Taqman (see Sections 1.6.2, 1.6.3 and 1.6.4 respectively), which are added to the PCR reaction mixture, has allowed the real-time monitoring of PCR-product accumulation. For the split-probe system to be a useful probe it

should potentially be applicable for use in PCR. Therefore, initial experiments were carried out in the presence of some PCR additives to determine their effects on exciplex fluorescence for the SP-2 system.

4.6.2 Effect of PCR additives on the emission spectra of the SP-2 system.

On addition of all the components of the SP-2 system to Tris buffer containing the PCR additives, the quenching and red shift of pyrene monomer emission, characteristic of duplex formation, was observed. Therefore, these additives do not greatly affect tandem duplex formation of the split-probe system.

In 80% TFE/ Tris buffer, addition of betaine and sulfolane to the pre-formed tandem duplex actually caused an increase in exciplex emission. Betaine increased the I_E/I_M value by 33% at 1 M betaine and 46% at 1.5 M. Sulfolane caused a 20% increase in the I_E/I_M value at 0.15 M and 35% at 0.5 M. These additives may increase exciplex emission by binding to the minor groove of the tandem duplex, thereby preventing its interaction with pyrene and/ or naphthalene. This would increase the availability of the exci-partners for exciplex formation. In principle, the additives may also disrupt any secondary structures formed by self-complementary regions of the probe components or the target, thereby allowing a more perfect duplex formation. However, the prototype sequence used for SP-2 was designed to be free of such complications.

On the other hand, addition of methylsulfone to the SP-2 system caused a reduction in exciplex emission intensity. Addition of DMSO changed the exciplex band from a resolved red-shifted band to an unresolved shoulder to the monomer emission band. These additives may be stronger denaturants than methylsulfone or sulfolane, or may be present at a concentration high enough to disrupt the duplex structure. This would in turn interfere with exciplex formation and account for the decrease in exciplex fluorescence.

These preliminary experiments on the SP-2 system show that in the presence of certain PCR additives, at the concentrations used in PCR, exciplex emission is observed and in some cases enhanced. However, other additives have a detrimental effect on exciplex emission. Thus, the use of the split-probe system in PCR reaction mixtures may be viable with careful selection of PCR additives. One problem that may arise is the presence of co-solvent, as excimer and exciplex emission is only seen in the presence of a co-solvent, the best being TFE. TFE, however, is known to denature proteins and therefore may disrupt the activity of the Taq polymerase, especially at the high concentrations used. However, the Taq polymerase is used because of its high thermal stability and hence its

stable 3D structure. It may thus resist TFE effects successfully. This has not yet been tested.

4.7 Prothrombin systems/ LNA probes.

The split-probe exciplex system, SP-2, was applied to detect the G-A mutation at position 20210 of the prothrombin gene. Three systems were tested; a DNA system (SP-15), a DNA-diene system (SP-14) and a LNA system (SP-13) (see Sections 3.8.4, 3.8.3 and 3.8.2 respectively). In each case the probes were a perfect match to the part of the prothrombin gene sequence containing the mutation. As previously described LNA capture probes have successfully been used for genotyping the $ApoB_{R3500Q}$ mutation [19] and the coagulation factor V gene [20] (see Section 1.4.1). Therefore, their application to the split-probe systems was investigated.

As previously described (Section 4.3.5) background signals are a major problem for all the prothrombin systems in 80% TFE/ Tris buffer. This is due to stable secondary structure formation by the probe components and the target. For the LNA system, SP-13, in Tris buffer no spectral changes were seen initially on full system formation at 10 °C. After heating the system to 75 °C, cooling back to 10 °C resulted in a red shift and quenching of the pyrene LES emission, typical of duplex formation. This was accompanied by a weak exciplex emission band, which appeared as an unresolved shoulder to the monomer band at around 480 nm. This increased in intensity on further cooling. As no background emission was seen for the individual probe components in Tris buffer, the appearance of this new band could have arisen from exciplex formation between two partners. If this is the case, it gives LNA probes a distinct advantage over DNA, as an exciplex has never been seen for the split-probe systems in Tris buffer alone without co-solvent. Indeed, exciplex emission is very sensitive to solvent polarity as described previously, and exciplexes have only very rarely been seen in very polar solvents such as water [151;152]. No exciplex emission was seen for the prothrombin DNA systems, SP-14 and SP-15, in Tris buffer alone even after heating and cooling. Therefore, this seems to be unique to the LNA-containing probes. This could be due to a difference in the structure of the tandem duplex as compared to DNA duplexes. LNA monomers are locked into an N-type conformation. 2D-NMR solution studies [18;153] on DNA duplexes, where one strand contains one or more LNA modifications, show that nucleotides flanking the modifications show N-type character. The duplexes show mainly B-type character, with A-like character near the modifications. The average base pair rise is also less than that seen for normal B-

type DNA, being 3.0 Å. Other crystal studies [154] on a 10-mer DNA duplex containing one LNA modification per strand showed that the duplex crystallised in the A-form with all the LNA and deoxynucleotides having a C3'-endo sugar pucker. The base pair rise was found to be 2.95 Å. These studies suggest that the LNA split-probe systems may form tandem duplexes, which have a smaller base pair rise than classical B-type DNA duplexes. This may bring the exci-partners closer together, especially at lower TFE concentrations, leading to more efficient exciplex formation.

In 20% TFE/ Tris buffer addition of the target to the LNA probes resulted in quenching of the LES bands and the appearance of a strong exciplex emission band with λ_{max} 453 nm. Addition of TFE to 40 % caused the exciplex band to shift to 463 nm and slightly increase in intensity. In both cases exciplex emission decreased on heating and recovered on cooling. In 40% TFE, however, heating did not cause the exciplex band to fully disappear suggesting that the exciplex emission may not arise solely from interaction between the exci-partners. Heating to 60 °C would be expected to disrupt the duplex separating the exci-partners. Further to these experiments, control experiments carried out on the C-6 system in 20% TFE/ Tris buffer, showed the appearance of a relatively intense exciplex band after heating to 60 °C and re-cooling to 10 °C (see Figure 3.74) even though the control system (Proexc11_5'pyrene + Proexc4_3'Phosphate + target) only contained one exci-partner, 5'-pyrene. The λ_{max} value of this band was at the slightly shorter wavelength of 450 nm compared to 453 nm for the experimental system. This could mean that the origin of these bands in the control and experimental systems are different, i.e. the control exciplex may arise from exci-partner-nucleotide interactions and that of the experimental system may be due to exci-partner-exci-partner interaction. The results show that background emission is a problem for the LNA systems and, although a shift in λ_{max} of emission bands is observed, the origin of the exciplex signal is presently not determined.

In 80% TFE/ Tris all of the systems behaved similarly, *viz.* showing a strong emission band at ~480 nm for the 5'-pyrene-bearing probe in the absence of any other component. The possible origin of this, discussed in Section 4.3.5, is probably stable secondary structure formation. Heating and cooling of this component in the presence of the target caused the exciplex band to disappear. Addition of the naphthalene-bearing probe caused the appearance of a new exciplex band, with λ_{max} slightly shifted compared to that of the background (Table 4.3). This shift suggests that the exciplexes have a different origin, and it is possible that the exciplex emission seen from the full system is due to exci-partner interaction. However, the very large background signal seen is very undesirable for

detector applications and greatly reduces the systems sensitivity. The results show the importance of probe design and choice of target sequence to minimise secondary structure formation.

Table 4.3: Comparison of λ_{max} and I_E/I_M values of the broad emission band at ~480 nm seen for the 5'-pyrenylated probes (Proexc9, Proexc10 and Proexc11) in the absence of any other component, and for the full split-probe systems in 80% TFE/Tris (10 mM Tris, 0.1 M NaCl, pH 8.5) buffer at 10 °C.

System	Background emission from 5'-Pyrenylated Oligo alone.		Emission from Full system	
	λ_{max} (nm)	I_E/I_M	λ_{max} (nm)	I_E/I_M
LNA	481	1.36	474	0.38
DNA-diene	479	2.06	482	1.33
DNA	479	1.15	482	

The effect of the presence of LNA nucleotide in the probe oligos on the stability of the secondary structures formed is shown in Table 3.14, Section 3.8.1. for the 3'-phosphorylated oligos (Proexc3 and Proexc4). The presence of LNA monomers increases the T_m relative to the DNA probe oligo. However, for the 5'-phosphorylated probes (Proexc9, Proexc10 and Proexc11) a lower value of T_m was actually seen for the LNA-containing probe component as compared to the analogous DNA probe. It is thus possible that the populations of secondary structures differ for LNA and the DNA oligos.

4.8 Mismatches.

The ability of oligo probes to distinguish between a perfectly matched target and one containing a mismatched base pair is very desirable. Many genetic diseases are the result of a single base mutation (SNP), and probes that can detect these mutations are required in the genetic screening of these diseases. The DNA split-probe systems were tested against a variety of DNA targets containing various mismatches and insertions to determine whether they could discriminate between perfectly matched and mismatched targets.

Several other split-oligo systems, reviewed in the Introduction, have been reported to discriminate between SNPs. These include the ligation method of Landegen *et al.* [75] (Section 1.12.1), nanoparticle probes [85;86](Section 1.12.2.1) and the template-directed

ligagtion method [83;84] (Section 1.12.1). The split-probe excimer system of Paris *et al.* [95] (Section 1.12.3.3) was found to be sensitive to a single-base mutation in the target, positioned four base pairs from the 3'-junction (the same position as 3' mismatch 2), and gave no excimer signal and an I_E/I_M value of 0.04, whereas that of the fully matched system was 2.7. This was the only mismatch tested for this system.

4.8.1 Mismatched excimer systems.

The mismatched split-probe excimer systems studied in this thesis (see Methods 2.5.12) all showed the characteristic red shift in LES emission indicating that duplex formation occurred on target addition. As for the parent system, SP-1, excimer emission when seen, was only observed in the presence of the target. This band further increased to a maximum 10 minutes after target addition. A further increase in intensity was seen after heating to 40 °C and cooling back to 10 °C. Excimer emission was seen for both *insertion* 1 and *insertion* 2, although this was not as intense as that from the parent system. These results are similar to those observed from the excimer split-probe system of Ebata *et al.* [92;93]. Here excimer emission was observed when using a target with either one or two thymine nucleotides inserted into the centre of the target. The authors reported that the excimer band at 495 nm was significantly diminished in both cases. These results, and those seen in this thesis, suggest that the optimum geometry for efficient excimer emission is when the probe oligos are adjacently bound.

Excimer emission was seen for all of the mismatches, except *5'mismatch 1* and both the double mismatches (Figure 3.51). For each system the excimer band became more intense the closer the mismatch occurred to the "backbone nick" and exci-partners. This is illustrated in Figure 4.8, which shows the area under the excimer band (AUC) between 480 and 600 nm for all the mismatch systems and the parent system.

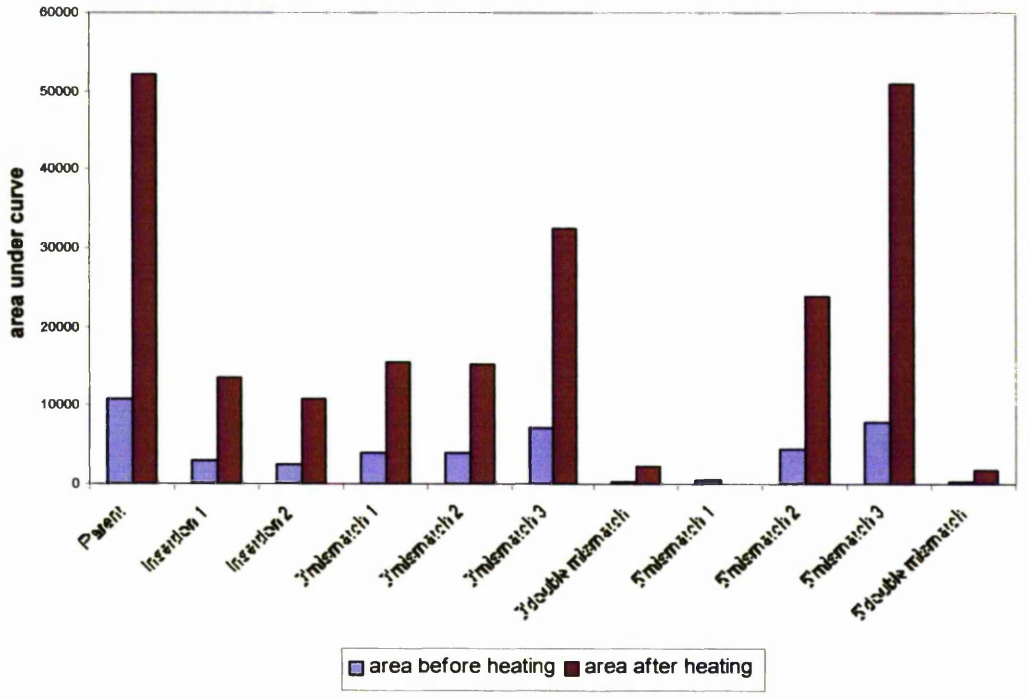

Figure 4.8: Area under the curves (from 480-600 nm) for the SP-1 system in 80% TFE/ Tris buffer (10 mM Tris, 0.1 M NaCl, pH 8.5) before and after the heating cycle was applied. Excitation wavelength 350 nm; slitwidth 5 nm. Spectra are buffer-corrected.

The area under the excimer band was used instead of intensity as potentially it could increase sensitivity in terms of signal to noise ratio. A ratio of AUC mismatch: AUC parent was calculated (see Table 3.10), as this value makes it easier to compare the excimer bands of the mismatches to each other and to the parent. Using I_E/I_M values it is more difficult to compare results of a mismatch series in this manner.

4.8.2 Mismatched exciplex systems.

Both exciplex systems yielded results grossly similar to the excimer system. On formation of the full systems a red shift in monomer emission was observed indicating tandem duplex formation. Exciplex emission when seen increased to a maximum 10 minutes after full system formation. For the SP-2 system exciplex emission did not always increase on heating and cooling. However, that from the SP-3 systems did. These differences could be due to the temperature ramping cycle, which had not been optimised.

For both the exciplex systems both *insertion 1* and *insertion 2* gave exciplex signals which were weaker that that from the parent system (Figure 3.54 and Figure 3.56). The *5'mismatch 1, 5'mismatch 2* and both double mismatches gave no exciplex band for the

SP-2 systems. For the SP-3 system the *5'mismatch 1* and both double mismatches gave no exciplex signals. These results are again illustrated in Figure 4.9 and 4.10 as area-under-the-exciplex-band from 480-600 nm.

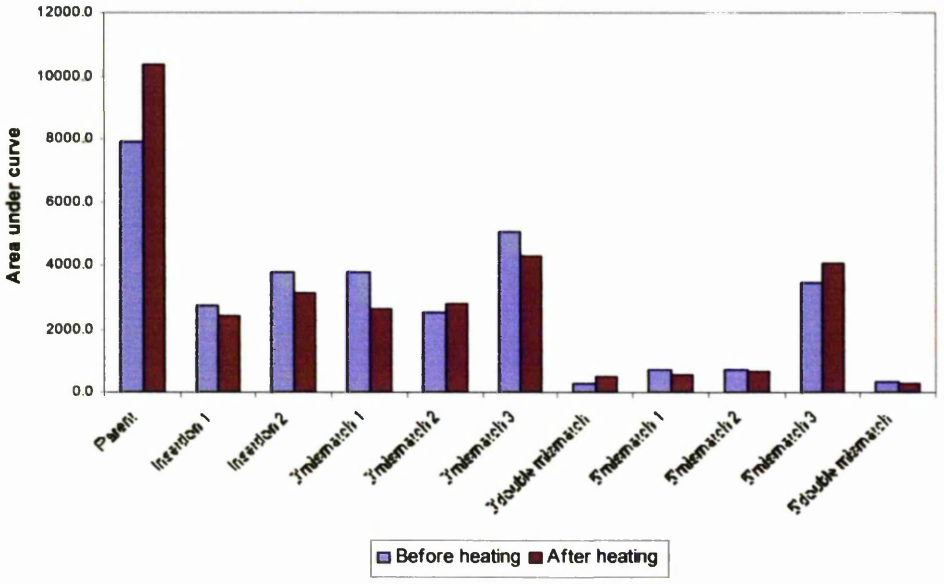

Figure 4.9: Area under the curve for the SP-2 system from 480-600 nm before and after heating to 40 °C. Spectra were recorded in 80% TFE/ Tris buffer (10 mM Tris, 0.1 M NaCl, pH 8.5) at 10 °C. Excitation wavelength 350 nm; slitwidth 3 nm. Spectra are buffer-corrected.

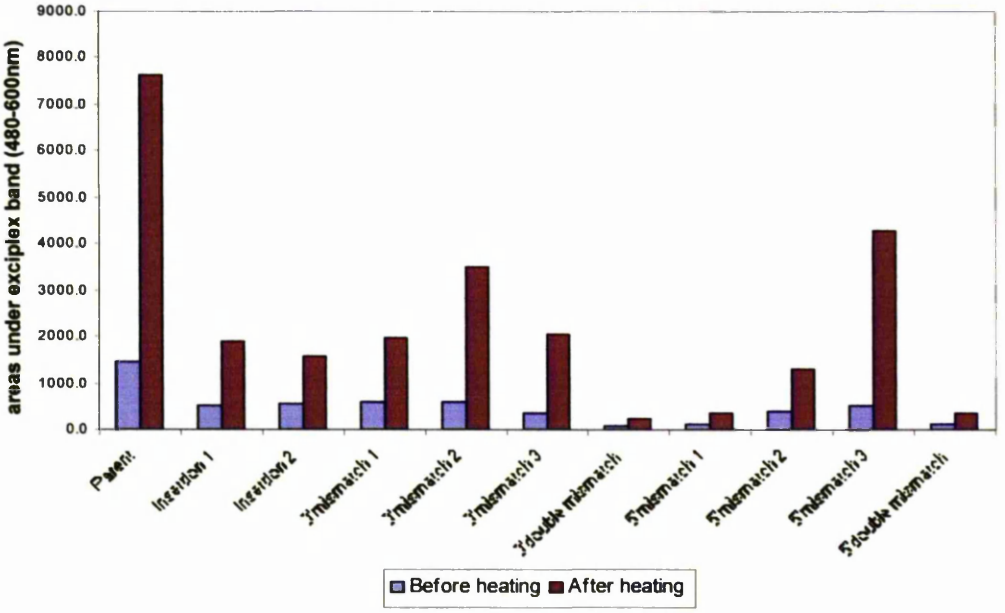

Figure 4.10: Area under the exciplex band (480-600 nm) for the SP-3 mismatch and insertion systems in 80% TFE/ Tris buffer (10 mM Tris, 0.1 M NaCl, pH 8.5) at 10 °C before and after heating to 40 °C. Excitation wavelength 350 nm; slitwidth 3 nm. Spectra were buffer-corrected.

For all the systems that did not give excimer or exciplex emission a red shift in monomer emission was seen on full system formation indicating that duplex formation had occurred. However, the duplex may be very distorted, thereby affecting excimer or exciplex emission. From the NMR data of a similar tandem split-oligo system [100;101] it is thought that the tandem duplex may already be distorted at the centre due to the backbone nick and the modifying groups. Koval *et al.* [63], however, suggested that discrimination of mismatches at the junction of tandem duplexes was much higher in comparison to normal duplexes. Mismatches at this area, however, seem to be tolerated by the split-probe systems. This is perhaps because they may cause little further distortion to the duplex. Mismatches towards the ends of the duplex may cause further distortion of the tandem duplex, away from the centre, thus affecting the ability of the exci-partners to form an excimer or exciplex.

4.8.3 Excimer and exciplex split-probe systems as SNP detectors.

Only mismatches that occurred in the binding site of the 5'-labelled oligo could be detected. This is in contrast to the results of Paris *et al.* [112], as that system detected a mismatch in the 3'-labelled binding site. The mismatch discrimination of the exciplex split-probe systems did not seem dependent on whether pyrene or naphthalene was attached to the 5'-position. Both resulted in mismatch discrimination in the 5'-labelled oligo-binding site only. The SP-2 system with 5'-pyrene and 3'-naphthalene was, however, more sensitive to mismatches. However, even so, mismatch discrimination seemed to be either sequence-dependent, or dependent on the position of attachment. Further studies are required on different sequences to determine sequence effects and to construct rules for SNP detection by the split-probe exciplex systems. These preliminary results show that it is possible for both the excimer and the exciplex systems to act as SNP detectors. Therefore, in the future with careful probe design such systems could be made sensitive to single-base mismatches, and thus be used in the genotyping of genetic samples.

4.9 Conclusion.

Both the excimer and exciplex-based split-probe systems described in this thesis are able to signal the presence of a target DNA or RNA sequence *via* excimer or exciplex emission. Evidence derived from this study and supported by literature data suggests that the tandem split-probe system, consisting of the target sequence and the two probe oligos bearing the exci-partners, are to assemble correctly at the specified target so that both the

exci-partners are juxtaposed. On correct assembly, and under suitable conditions a red-shifted excimer or exciplex emission is observed on irradiation at a suitable wavelength. The results of these studies suggest that for suitably designed protocols this emission at ~ 480 nm is due to exci-partner interaction, and not background sources. This excimer/ exciplex emission shows a very large Stokes shift (typically 130 nm) and in most cases a very small background.

Exciplex emission was also seen from split-probe systems where the probe oligos contained several LNA nucleotides and were targeted at the prothrombin SNP. However, prior to the final detection mixture conditions being reached these systems showed very large background exciplex emission due to the high degree of intramolecular secondary structure that was inherently present for these oligo sequences. So, from studies on these sequences it was difficult to determine whether LNA probes are suitable for application to these excimer/ exciplex split-probe systems. Further studies are required on sequences known to have no secondary structure to determine whether the split-probe systems can make use of LNA technologies.

The excimer and the exciplex split-probe systems behaved differently in different solvents, with the exciplex system being more sensitive to co-solvent. However, surprisingly both systems showed intense excimer/ exciplex signals at high TFE concentrations (80%). Both the excimer and the exciplex systems also showed lower requirements for TFE when an RNA target was used. As TFE affects the structure of duplexes, these results suggest that the helical structure of the tandem duplex may affect excimer/ exciplex emission, possibly *via* exci-partner interaction. This hypothesis, however, needs further testing by additional higher resolution biophysical techniques compatable with very high organic solvent levels (e.g. NMR with perdeuterated 2,2,2-trifluoroethanol).

Two different linker systems were also tested in this thesis, a short linker of several methylene groups and a long linker of five amino acids. Both linker types resulted in excimer or exciplex emission. However, the shorter linkers were found to give more intense signals. No improvement of signal was seen at high TFE concentrations for the peptide linker systems suggesting little secondary structure formation stabilised in TFE. These studies, along with other literature data, suggest that there is scope for use of a variety of linkers, but the use of shorter linkers decreased interaction with the DNA duplex and possibly increased collision of the exci-partners. Short linkers also prevent intercalation of fluorophores, such as pyrene, in to the duplex.

The preliminary studies on these split-probe systems show promise for future applications in genetic testing. Exciplex emission is still observed on full system formation in the presence of the PCR additives betaine and sulfolane at the concentration ranges used in PCR. No loss of signal intensity was seen, and in fact exciplex emission was actually slightly more intense in the presence of these additives. Therefore, there is future possibility for the use of exciplex split-probe systems as real-time monitors of PCR reactions. In addition, both the excimer system and the exciplex split-probe systems were able to detect the presence of a mismatch in the binding site of the 5'-labelled oligo. The rules of this SNP detection approach have not been elucidated as yet. For example it is unclear whether this is dependent on the position of exci-partner attachment or if the phenomenon is sequence dependent. However, in the future with careful probe design such a split-probe system could potentially be made sensitive to specific SNPs and therefore lend itself to routine genetic analysis.

The studies in this thesis have demonstrated the first examples of split-probe exciplexes for nucleic acids. Moreover, they have shown that exciplex and excimer based split-probe systems have the ability to detect RNA and DNA target sequences, giving a signal which has a large Stokes shift and a very low background. However, further work is required to further develop and improve these systems in comparison with commercially available fluorescent probes. Some such possible work is described in the section below.

4.10 Future work.

Studies are required on the full split-probe tandem duplexes, under conditions where intense excimer or exciplex emission is seen (*i.e.* at high TFE concentrations) to determine the structure of the duplex. Such studies would test the hypothesis that excimer/ exciplex emission may depend on duplex structure, with A-like duplexes giving rise to more intense excimer/ exciplex emission. These studies could include circular dichroism and X-ray diffraction. NMR approaches may be more difficult given the solvent medium but may be applicable.

To test the suitability of using LNA technology, the LNA systems must be tested using sequences known to possess little or no intramolecular secondary structure. LNA probes would be advantageous as they show a greater affinity towards the target sequence and form more stable tandem duplexes.

The mismatch systems should also be tested using different sequences to determine if mismatch detection is position and/ or sequence dependent. Once rules of mismatch

detection have been elucidated, split-probe systems can be designed to detect known SNPs. The split-probes should also be tested along with other PCR reaction constituents and buffers to determine their effect on excimer/ exciplex emission, and the effect of the exciplex systems with DNA replication in PCR cycles.

Experiments should also be carried out to compare the split-probe excimer/ exciplex systems with current fluorescent probes. Such studies could involve testing the sensitivity of the split-probes, that is the lowest concentration the split-probe systems are able to detect. The brightness of these systems should also be compared to commercially available probes. This would include quantum yield determination, as brightness is sometimes quoted as the product of quantum yield and extinction coefficient. Such studies would give an indication of how competitive the excimer/ exciplex split-probe systems will be in the field of genetic analysis.

5. References.

5 References.

(1) Human Gemone Information. www.ornl.gov/hgmis/project/about.html 2002.
(2) Poort, S. R.; Rosendaal, F. R.; Reitsma, P. H.; Bertina, R. M. *Blood* 1996, *88*, 3698-3703.
(3) Rosendaal, F. R.; Siscovick, D. S.; Schwartz, S. H.; Psaty, B. M.; Raghunathan, T. E.; Vos, H. I. *Blood* 1997, *90*, 1747-1750.
(4) Gehring, N. H.; Frede, U.; Neu-Yilik, G.; Hundsdoefer, P.; Vetter, B.; Hentze, M. W.; Kulozik, A. E. *Nature Genetics* 2001, *28*, 389-392.
(5) Strachan, T.; Read, A. P. DNA Hybridisation Assays; In *Human Molecular Genetics*; BIOS Scientific Publishing: Oxford. 1996.
(6) Wilchek, M.; Bayer, E. A. *Methods Enzymol.* 1990, *184*, 5-11.
(7) Garman, A. Use of tags in the labelling and detection of biomolecules.; In *Non-radioactive Labelling: A Practical Approach*; Academic Press: London, 1997; pp 65-71.
(8) Garman, A. Labelling of oligonucleotides.; In *Non-radioactiveLabelling: A Practical Approach.*; Academic Press: London, 1997; pp 73-87.
(9) Wilchek, M.; Bayer, E. A. *Anal. Biochem.*1988, *171*, 1-32.
(10) www.pasteur.fr/recherche/unites/biophyadn/e-Ffish.html#references 2002.
(11) Kricka, L. J. Nucleic Acid Hybridisation Test Formats: Strategies and Applications.; In *Nonisotopic DNA Probe Techniques.*; Kricka, L. J., ed. 1992; pp 3-19.
(12) Verlander, P. C. Detection of Horseradish Peroxidase by Colorimetry.; In *Nonisotopic DNA Probe Techniques.*; Kricka, L. J., ed. Academic Press: London, 1992; pp 185-199.
(13) Durrant, I. Detection of Horseradish Peroxidase by Enhanced Chemiluminescence.; In *Nonisotopic DNA Probe Techniques.*; Kricka, L. J., ed. Academic Press: London, 1992; pp 167-182.
(14) Strachan, T.; Read, A. P. PCR-based DNA Cloning and DNA Analysis; In *Human Molecular Genetics*; BIOS Scientific Publishing: Oxford, 1996.
(15) Kvaerno, L.; Wengel, J. *Chem. Commun.* 1999, 657-658.
(16) Wahlestedt; Salmi, P.; Good, L.; Keld, J.; Johnsson, T.; Hokfelt, T. *Proc. Natl. Acad. Sci. USA.* 2000, *97*, 5633-5638.
(17) DNA and RNA structure; In *Nucleic Acids in Chemistry and Biology*; Blackburn, G. M., Gait, M. J., eds. Oxford University Press: New York, 1996; pp 15-75.
(18) Peterson, M.; Nielsen, C. B.; Nielsen, K. E.; Jensen, G. A.; Bondensgaard, K.; Singh, S. K.; Rajwanshi, V. K.; Koshkin, A. A.; Dahl, B. M.; Wengel, J.; Jacobsen, J. P. *J. Mol. Recognit.* 2000, *13*, 44-53.
(19) Jacobsen, N.; Fenger, M.; Bentzen, J.; Rasmussen, S. L.; Jakobsen, M. H.; Fenstholt, J.; Skouv, J. *Clin. Chem.* 2002, *48*, 657-660.
(20) Orum, H.; Jakobsen, M. H.; Koch, T.; Vuust, J.; Borre, M. B. *Clin. Chem.* 1999, *45*, 1898-1905.
(21) Gilbert, A.; Baggot, J. Photochemical Reactions; In *Essentials of Molecular Photochemistry*; Blackwell Scientific: Oxford 1991; p 145.
(22) Young, M.; Millar, D. P. *Methods Enzymol.* 1977, *46*, 3-4.
(23) Stryer, L. *Annu. Rev. Biochem.* 1978, *47*, 846.
(24) Tyagi, S.; Krammer, F. R. *Nat. Biotechnol.* 1996, *14*, 303-308.
(25) Tyagi, S.; Marras, S. A. E.; Krammer, F. R. *Nat. Biotechnol.* 2000, *18*, 1191-1196.
(26) Knemeyer, J. P.; Marme, N.; Sauer, M. *Anal. Chem.* 2000, *72*, 3717-3724.

(27) Whitcombe, D.; Theaker, J.; Guy, S. P.; Brown, T.; Little, S. *Nat. Biotechnol.* 1999, *17*, 804-807.
(28) Holland, P. M.; Abramson, R. D.; Watson, R.; Gelfand, D. H. *Proc. Natl. Acad. Sci. USA.* 1991, *88*, 7276-7280.
(29) Heid, C. A.; Stevens, J.; Livak, K. J.; Williams, P. M. *Genome Research* 1996, *6*, 986-994.
(30) Kong, D.; Gu, L.; Shen, H. X.; Mi, H. F. *Chem. Commun.* 2002, 854-855.
(31) Ygerabide, J.; Talavera, E.; Alvarez, J. M.; Afkir, M. *Anal. Biochem.* 1996, *241*, 238-247.
(32) Talavera, E.; Afkir, M.; Salto, R.; Vargas, A. M.; Alvarez, J. M. *J Photochem Photobiol., B.* 2000, *59*, 9-14.
(33) Martin, M. M.; Lindqvist, L. J. *Luminescence* 1975, *10*, 381.
(34) Talavera, E.; Alvarez, J. M.; Sanz-Aparicio, J.; Romero-Garrido, A. *Appl. Spectrosc.* 1997, *51*, 401-406.
(35) Telser, J.; Cruickshank, K. A.; Morrison, L. E.; Netzel, T. L. *J. Am. Chem. Soc.* 1989, *111*, 6966-6976.
(36) Wolfe, A.; Shimer, G. H.; Meehan, T. *Biochemistry* 1987, *26*, 6392-6396.
(37) Bassani, D. M.; Wirz, J.; Hochstrasser, R.; Leupin, W. *J Photochem Photobiol., A* 1996, *100*, 65-76.
(38) Yamana, K.; Zako, H.; Asazuma, K.; Iwase, R.; Nakano, H.; Murakami, A. *Angew. Chem. Int. Ed.* 2001, *40*, 1104-1106.
(39) Kierzek, R.; Turner, D. H.; Bevilacqua, P. C. *J. Am. Chem. Soc.* 1993, *115*, 4985-4992.
(40) Gordon, M.; Ware, W. A. *The Exciplex*; Academic Press: London, 1975.
(41) Nakajima, A. *Bull. Chem. Soc. Jpn.*1971, *44*, 3272-3277.
(42) Stevens, B. *Spectrochim. Acta* 1962, *18*, 439-448.
(43) Orbach, N.; Ottolenghi, M. *Chem. Phys. Lett.* 1975, *35*, 175-179.
(44) Knibbe, H.; Rollig, K.; Schafer, F. P.; Weller, A. *J. Chem. Phys.* 1967, *47*, 1184-1185.
(45) Van Haver, P.; Helsen, N.; Depaemelaere, S.; Van der Auweraer, M.; De Schryver, F. C. *J. Am. Chem. Soc.* 1991, *113*, 6849-6857.
(46) Okada, T.; Saito, T.; Mataga, N.; Sakata, Y.; Misumi, S. *Bull. Chem. Soc. Jpn.* 1977, *50*, 331-336.
(47) Verhoeven, J. W.; Scherer, T.; Willemse, R. J. *Pure Appl. Chem.* 1993, *65*, 1717-1722.
(48) Lewis, F. D.; Cohen, B. E. *J. Phys. Chem* 1994, *98*, 10591-10597.
(49) Swinnen, A. M.; Van der Auweraer, M.; De Schryver, F. C. *J. Photochem.* 1985, *28*, 315-327.
(50) Masaki, S.; Okada, T.; Mataga, N.; Sakata, Y.; Misumi, S. *Bull. Chem. Soc. Jpn.* 1976, *49*, 1277-1283.
(51) Mataga, N.; Miyasaka, H. *Adv. Chem. Phys.* 1999, *107*, 431-496.
(52) Mataga, N.; Okada, T.; Yamamoto, N. *Chem. Phys. Lett.* 1967, *1*, 119-121.
(53) Chandross, E. A.; Thomas, H. T. *Chem. Phys. Lett.* 1971, *9*, 393-395.
(54) Taylor, G. N.; Chandross, E. A.; Schiebel, A. H. *J. Am. Chem. Soc.* 1974, *96*, 26932697.
(55) Ide, R.; Sakata, Y.; Misumi, S. *J. Chem. Soc.* 1972, 1009.
(56) Horner, M. G.; Larson, J. R. *J. Photochem. Photobiol., A* 1990, *55*, 145-155.
(57) Tong, G.; Lawlor, J. M.; Tregear, G. W.; Haralambidis, J. *J. Am. Chem. Soc.* 1995, *117*, 12151-12158.

(58) Balakin, K. V.; Korshun, V. A.; Prokhorenko, I. A.; Maleev, A. D.; Kudelina, I. A.; Gontarev, S. V.; Berlin, Y. A. *Russ. J. Bioorg. Chem.* 1997, *23*, 33-41.
(59) Lewis, F. D.; Zhang, Y.; Letsinger, R. L. *J. Am. Chem. Soc.* 1997, *119*, 5451-5452.
(60) Kostenko, E.; Dobrikov, M.; Pyshnyi, D.; Petyuk, V.; Komarova, N.; Vlassov, V.; Zenkova, M. *Nucleic Acids Res.* 2001, *29*, 3611-3620.
(61) Balakin, K. V.; Korshun, V. A.; Mikhelev, I. I.; Maleev, A. D.; Malakhov, A. D.; Prokhorenko, I. A.; Berlin, Y. A. *Biosens. Bioelectron.* 1998, *13*, 771-778.
(62) Yamana, K.; Takei, M.; Nakano, H. *Tet. Lett.* 1997, *38*, 6051-6054.
(63) Koval, V. V.; Lakteva, N. A.; Karnaukhova, S. L.; Fedorova, O. S. *J. Biomol. Struct. Func.* 1999, *17*, 259-265.
(64) Colocci, N.; Dervan, P. B. *J. Am. Chem. Soc.* 1995, *117*, 4781-4787.
(65) Lane, M. J.; Paner, T.; kashkin, I.; Faldasz, B. D.; Li, B.; Gallo, F. J.; Benight, A. S. *Nucleic Acids Res.* 1997, *25*, 611-616.
(66) Adeenah-Zadah, A.; Knorre, D. G.; Fedorova, O. S. *Journal of Biomolecular Structure and Function* 1997, *15*, 369.
(67) O'Meara, D.; Nilsson, P.; Nygren, P. A.; Uhlen, M.; Lundeberg, J. *Anal. Biochem.* 1998, *255*, 195-203.
(68) O'Meara, D.; Yun, Z.; Sonnerborg, A.; Lundeberg, J. *J. Clin. Microbiol.* 1998, *36*, 2454-2459.
(69) Blomstergren, A.; O'Meara, D.; Lukacs, M.; Uhlen, M.; Lundeberg, J. *BioTechniques* 2000, *29*, 352-363.
(70) Dobrikov, M.; Bichenkova, E. V.; Douglas, K. T.; Gainutdinov, T. I.; Vlassov, V. *J. Biomol. Struct. Func.* 1999, *17*, 213-221.
(71) Dobrikov, M.; Gainutdinov, T. I.; Vlassov, V. *Nucleosides Nucleotides* 1999, *18*, 1517-1518.
(72) Dobrikov, M. *Russian Chemical Reviews* 1999, *68*, 967-982.
(73) Dobrikov, M.; Gaidamakov, S. A.; Gainutdinov, T. I.; Koshkin, A. A.; Vlassov, V. *Antisense Nucleic Acid Drug Dev.* 1997, *7*, 309-317.
(74) Fedorova, O. S.; Koval, V. V.; Karnaukhova, S. L.; Dobrikov, M.; Vlassov, V.; Knorre, D. G. *Mol. Biol.* 2000, *34*, 814-822.
(75) Landegren, U.; Kaiser, R.; Sanders, J.; Hood, L. *Science* 1988, *241*, 1077-1079.
(76) Carr, F. J. EP0246864. 25-11-1987.
(77) Cruickshank, K. A., Morrison, L. E., and Royer, G. P. (EP0324616). 19-7-1989.
(78) Shabarova, Z. A.; Merenkova, I. N.; Oretskaya, T. S.; Sokolova, N. I.; Skripkin, E. A.; Alekseeva, E. V.; Balakin, A. G.; Bogdanov, A. A. *Nucleic Acids Res.* 1991, *19*, 4247-4251.
(79) Fedorova, O. S.; Gottikin, M. B.; Oretskaya, T. S.; Shabarova, Z. A. *Nucleosides Nucleotides* 1996, *30*, 348-352.
(80) Sokolova, N. I.; Ashirbekova, D. T.; Dolinnaya, N. G.; Shabarova, Z. A. *FEBS Lett.* 1988, *232*, 153-155.
(81) Kabilov, M. R.; Pyshnyi, D.; Dymshits, G. M.; Gashnikova, N. M.; Pokrovskii, A. G.; Zarytova, V. F.; Ivanova, E. M. *Mol. Biol.* 2002, *36*, 424-431.
(82) Chen, X.; Zehnbauer, B.; Gnirke, A.; Kwok, P. Y. *Proc. Natl. Acad. Sci. USA.* 1997, *94*, 10756-10761.
(83) Chen, X.; Kwok, P. Y. *Nucleic Acids Res.* 1997, *25*, 347-353.
(84) Chen, X.; Kwok, P. Y. *Genetic Analysis: Biomol. Eng.* 1999, *14*, 157-163.
(85) Seife, C. *Science* 2002, *297*, 1462.
(86) Cao, Y.; Jin, R.; Mirkin, C. A. *Science* 2002, *297*, 1536-1539.
(87) Park, S. J.; Taton, T. A.; Mirkin, C. A. *Science* 2002, *295*, 1503-1506.
(88) Naesby, M. (EP0897991). 24-2-1999.

(89) Castro, A.; Williams, J. G. K. *Anal. Chem.* 1997, *69*, 3915-3920.
(90) Heller, M. J., Morrison, L. E., Prevatt, W. D., and Atkin, C. Light Emitting Polynucleotide Hybridisation Diagnostic Method. 1983 Patent No.070685.
(91) Oser, A.; Valet, G. *Angew. Chem. Int .Ed.* 1990, *29*, 1167-1169.
(92) Ebata, K.; Masuko, M.; Ohtani, H.; Kashiwasake-Jibu, M. *Photochem. Photobiol.* 1995, *62*, 836-839.
(93) Ebata, K.; Masuko, M.; Ohtani, H.; Kashiwasake-Jibu, M. *Nucleic Acid Symp. Ser.* 1995, *34*, 187-188.
(94) Masuko, M.; Ohtani, H.; Ebata, K.; Shimadzu, A. *Nucleic Acids Res.* 1998, *26*, 5409-5416.
(95) Paris, P. L.; Langenhan, J. M.; Kool, E. T. *Nucleic Acids Res.* 1998, *26*, 3789-3793.
(96) Rehm, D. *S. Naturfarsch* 1970, *25*, 1442-1447.
(97) Birks, J. B. Excimers; In *Photophysics of Aromatic Molecules*; Wiley-Interscience: London, 1970; pp 301-370.
(98) Drew, H. R.; Dickerson, R. E. *J. Mol. Biol.* 1981, *151*, 535-556.
(99) Dickerson, R. E.; Drew, H. R.; Conner, B. N.; Wing, R. M.; Fratini, A. V.; Kopka, M. L. *Science* 1982, *216*, 475-484.
(100) Bichenkova, E. V.; Marks, D.; Dobrikov, M.; Vlassov, V.; Morris, G. A.; Douglas, K. T. *J. Biomol. Struct. Func.* 1999, *17*, 193-221.
(101) Bichenkova, E. V.; Marks, D.; Lokhov, S. G.; Dobrikov, M.; Vlassov, V.; Douglas, K. T. *J. Biomol. Struct. Funct.* 1997, *15*, 307-320.
(102) Roll, C.; Ketterie, C.; Faibis, V.; Fazakerley, G. V.; Boulard, Y. *Biochemistry* 1998, *37*, 4059-4070.
(103) Bellio-Mills, J.; Cooper, J. P.; Hagerman, P. J. *Biochemistry* 1994, *33*, 1797-1803.
(104) Aymani, J.; Coll, M.; Van Der Marel, G. A.; Van Boom, J. H.; Wang, A. H. J.; Rich, A. *Proc. Natl. Acad. Sci. USA.* 1990, *87*, 2526-2530.
(105) Pieters, J. M. L.; Mans, R. M. W.; Van Den Elst, H.; Van Der Marel, G. A.; Van Boom, J. H.; Altona, C. *Nucleic Acids Res.*1989, *17*, 4551-4565.
(106) Fedoroff, O. Y.; Salazar, M.; Reid, B. R. *J. Mol. Biol.* 1993, *233*, 509-523.
(107) Spiess, A. N.; Ivell, R. *Anal. Biochem.* 2002, *301*, 168-174.
(108) Chakrabarti, R.; Schutt, C. E. *Gene* 2001, *274*, 293-298.
(109) Koshkin, A. A.; Nielsen, P.; Meldgaard, M.; Rajwanshi, V. K.; Singh, S. K.; Wengel, J. *J. Am. Chem. Soc.* 1998, *120*, 13252-13253.
(110) Nauck, M.; Wieland, H.; Marz, W. *Clin. Chem. Lab. Med.* 2000, *38*, 667-672.
(111) Hirs, C. H. W. *Methods Enzymol.* 1967, *11*, 806-819.
(112) Fedorova, O. S.; Nevinsky, G. A.; Koval, V. V.; Ishchenko, A. A.; Vasilenko, N. L.; Douglas, K. T. *Biochemistry* 2002, *41*, 1520-1528.
(113) Diakou, A.; Dovas, C. I. *Anal. Biochem.* 2001, *288*, 195-200.
(114) Seto, D. *Nucleic Acids Res.* 1990, *18*, 5905-5906.
(115) Ngugen, A. *Mayo. Clin. Proc.* 2000, *75*, 595-604.
(116) Birks, J. B. *Rep. Prog. Phys.* 1975, *38*, 904-974.
(117) Lianos, P.; Georghiou, S. *Photochem. Photobiol.* 1979, *29*, 13-21.
(118) Manoharan, M.; Tivel, K. L.; Zhao, M.; Nafisi, K.; Netzel, T. L. *J. Phys. Chem* 1995, *99*, 17461-17472.
(119) Geacintov, N. E.; Prusik, T.; Khosrofian, J. M. *J. Am. Chem. Soc.* 1976, *98*, 6444-6452.
(120) O'Conner, D.; Shafirovich, V. Y.; Geacintov, N. E. *J. Phys. Chem* 1994, *98*, 9831-9839.
(121) Intergrated DNA Technologies. OligoAnalyzer. (3.0). 2000.
(122) Mann, J. S.; Shibata, Y.; Meehan, T. *Bioconjugate Chem.* 1992, *3*, 554-558.

(123) Lindberg, P.; Roeraade, J. *J. Liquid Chromatogr. Related Technol.* 1999, *22*, 307-321.
(124) Castanheira, E. M. S.; Martinho, J. M. G. *Chem. Phys. Lett.* 1991, *185*, 319-323.
(125) Castanheira, E. M. S.; Martinho, J. M. G. *J. Photochem. Photobiol., A* 1994, *80*, 151-156.
(126) Suppan, P. *J. Photochem. Photobiol.; A* 1990, *50*, 293-330.
(127) Ivanov, V. I.; Minchenkova, L. E.; Minyat, E. E.; Frank-Kamenetskii, M. D.; Schyolkina, A. K. *J. Mol .Biol.* 1974, *87*, 817-833.
(128) Zimmerman, S. B.; Pheifer, B. H. *J. Mol. Biol.* 1979, *135*, 1023-1027.
(129) Malenkov, G. *FEBS Lett.* 1975, *51*, 38-42.
(130) Lan, T.; McLaughlin, L. W. *Biochemistry* 2001, *40*, 968-976.
(131) Charney, E.; Chen, H. H. *Proc. Natl. Acad. Sci. USA.* 1987, *84*, 1546-1549.
(132) Leslie, A. G. W.; Arnott, S.; Chandrasekaran, R.; Ratliff, R. L. *J. Mol. Biol.* 1980, *143*, 49-72.
(133) Arnott, S.; Chandrasekaran, R.; Millane, R. P.; Park, H. *J. Mol .Biol.* 1986, *188*, 631-640.
(134) Reid, D. G.; Salisbury, S. A.; Brown, T.; Williams, D. H.; Vasseur, J. J.; Rayner, B.; Imbach, J. L. *Eur. Biophys .J.* 1983, *135*, 307-314.
(135) Zimmerman, S. B.; Pheifer, B. H. *Proc .Natl .Acad. Sci .USA.* 1981, *78*, 78-82.
(136) Sonnichsen, F. D.; Van Eyk, J. E.; Hodges, R. S.; Sykes, B. D. *Biochemistry* 1992, *31*, 8790-8798.
(137) Gast, K.; Siemer, A.; Zirwer, D.; Damashun, G. *Eur. Biophys. J.* 2001, *30*, 273-283.
(138) Buck, M. *Q. Rev. Biophys.* 1998, *31*, 297-355.
(139) Luo, P.; Baldwin, R. L. *Biochemistry* 1997, *36*, 8413-8421.
(140) Nelson, J. W.; Kallenbach, N. R. *Biochemistry* 1989, *28*, 5256-5261.
(141) Chitra, R.; Smith, P. E. *J. Chem. Phys.* 2001, *114*, 426-435.
(142) Blanco, F. J.; Jimenez, M. A.; Pineda, A.; Rico, M.; Santoro, J.; Nieto, J. L. *Biochemistry* 1994, *33*, 6004-6014.
(143) Ramirez-Alvarado, M.; Blanco, F. J.; Serrano, L. *Nat. Struct. Biol.* 1996, *3*, 604-612.
(144) Ptitsyn, O. B. *FEBS Lett.*1981, *131*, 197-202.
(145) Caldwell, R. A.; Creed, D.; DeMarco, D. C.; Melton, L. A.; Ohta, H.; Wine, P. H. *J. Am .Chem. Soc.* 1980, *102*, 2369-2377.
(146) Turpin. *Photochem. Photobiol.* 1990, *51*, 519-525.
(147) Lewis, F. D.; Zhang, B. W.; Liu, X.; Xu, N.; Letsinger, R. L. *J. Phys. Chem* 1999, *103*, 2570-2578.
(148) Lewis, F. D. *J. Am. Chem .Soc.* 1997, *119*.
(149) Yamana, K.; Nunota, K.; Nakano, H.; Sangen, O. *Tet. Lett.* 1994, *35*, 2555-2558.
(150) Koenig, P.; Reines, S. A.; Cantor, C. R. *Biopolymers* 1977, *16*, 2231-2242.
(151) Cox, G. S.; Turro, N. J.; Yang, N. C.; Chen, M. J. *J. Am. Chem. Soc.* 1984, *106*, 422-424.
(152) Douglas, K. T. and Bichenkova, E. V. US19990467015 19991220(US6475730). 2002.
(153) Nielsen, C. B.; Singh, S. K.; Wengel, J.; Jacobsen, J. P. *J. Biomol. Struct. Dyn.* 1999, *17*, 175-191.
(154) Egli, M.; Minasov, G.; Teplova, M.; Kumar, R.; Wengel, J. *Chem. Commun.* 2001, 651-652.